

2023

## Investigating the Impact of Demographic Factors on Contactless Fingerprint Interoperability

Aeddon David Berti

West Virginia University, adb0068@mix.wvu.edu

Follow this and additional works at: <https://researchrepository.wvu.edu/etd>



Part of the [Other Electrical and Computer Engineering Commons](#)

---

### Recommended Citation

Berti, Aeddon David, "Investigating the Impact of Demographic Factors on Contactless Fingerprint Interoperability" (2023). *Graduate Theses, Dissertations, and Problem Reports*. 11852.

<https://researchrepository.wvu.edu/etd/11852>

This Thesis is protected by copyright and/or related rights. It has been brought to you by the The Research Repository @ WVU with permission from the rights-holder(s). You are free to use this Thesis in any way that is permitted by the copyright and related rights legislation that applies to your use. For other uses you must obtain permission from the rights-holder(s) directly, unless additional rights are indicated by a Creative Commons license in the record and/ or on the work itself. This Thesis has been accepted for inclusion in WVU Graduate Theses, Dissertations, and Problem Reports collection by an authorized administrator of The Research Repository @ WVU. For more information, please contact [researchrepository@mail.wvu.edu](mailto:researchrepository@mail.wvu.edu).

# Investigating the Impact of Demographic Factors on Contactless Fingerprint Interoperability

Aeddon Berti

Thesis submitted to the  
Benjamin M. Statler College of Engineering and Mineral Resources  
at West Virginia University  
in partial fulfillment of the requirements  
for the degree of

Master of Science in  
Electrical Engineering

Jeremy Dawson, Ph.D., Chair

Nasser Nasrabadi, Ph.D.

Matthew Valenti, Ph.D.

Lane Department of Computer Science and Electrical Engineering

Morgantown, West Virginia

2023

Keywords: Fingerprint, Contact, Contactless, Fingerphoto, Interoperability, Melanin, Erythema, Ethnicity, Demographic, Bias

Copyright ©2023 Aeddon Berti

## ABSTRACT

### Investigating the Impact of Demographic Factors on Contactless Fingerprint Interoperability

Aeddon Berti

Improvements in contactless fingerprinting have resulted in contactless fingerprints becoming a faster and more convenient alternative to contact fingerprints. The interoperability between contactless fingerprints and contact fingerprints and how demographic factors can change interoperability has been challenging since COVID-19; the need for hygienic alternatives has only grown because of the sudden focus during the pandemic. Past work has shown issues with the interoperability of contactless prints from kiosk devices and phone fingerprint collection apps. Demographic bias in photography for facial recognition could affect photographed fingerprints. The paper focuses on evaluating match performance between contact and contactless fingerprints and evaluating match score bias based on five skin demographics; melanin, erythema, and the three measurements of the CIELab color space. The interoperability of three fingerprint matchers was tested. The best and worst Area Under the Curve (AUC) and Equal Error Rate (EER) values for the best-performing matcher were an AUC of 0.99398 and 0.97873 and an EER of 0.03016 and 0.07555, respectively, while the best contactless AUC and EER were 0.99337 and 0.03387 indicating that contactless match performance can be as good as contact fingerprints depending on the device. In contrast, the best and worst AUC and EER for the cellphone contactless fingerprints were an AUC of 0.96812 and 0.85772 and an EER of 0.08699 and 0.22130, falling short of the lowest performing contact fingerprints. Demographic analysis was on the top two of the three matchers based on the top one percent of non-match scores. Resulting efforts found matcher-specific bias for melanin showing specific ranges affected by low and high melanin values. While higher levels of erythema and general redness of the skin improved performance. Higher lightness values showed a decreased performance in the top-performing matcher.

# Acknowledgements

I would like to give my deepest thanks to my academic and research advisor Dr. Jeremy Dawson for allowing me the opportunity to work under him as an undergraduate student worker initially and then to continue to mentor me as a graduate research assistant. Additionally, I would like to extend my gratitude to my committee members, Dr. Nasser Nasrabadi and Dr. Matthew Valenti. Dr. Nasrabadi has pushed me to value and take pride in my work rather than simply doing the job. Dr. Valenti, for introducing me to many of the principles of biometrics I've used during my research.

I would also like to extend my gratitude to a past colleague, John McCauley, who had previously worked for Dr. Jeremy Dawson as a graduate research assistant and served as a mentor before he graduated, preparing me for my roles and responsibilities.

I would like to thank my Mother, Rhonda Hilt, and Father, Dr. William Berti, for supporting me through any hardships that befell me. Without them, my accomplishments would not have been possible, especially when my health took a turn for the worse in my second semester.

Last but not least, I would like to thank my friends and coworkers for supporting my life and work during my five years attending West Virginia University.



# Table of Contents

<b>Acknowledgements</b> .....	<b>iii</b>
<b>Table of Contents</b> .....	<b>iv</b>
<b>List of Figures</b> .....	<b>vi</b>
<b>List of Tables</b> .....	<b>xvii</b>
<b>List of Equations</b> .....	<b>xviii</b>
<b>Chapter 1: Introduction</b> .....	<b>1</b>
1.1 Summary.....	1
1.2 History.....	1
1.3 Motivation.....	2
1.4 Previous Work.....	3
1.5 Goals and Impact of the Research .....	7
1.6 Organization of the Thesis .....	8
<b>Chapter 2: Technical Information and Theory</b> .....	<b>11</b>
2.1 Fingerprint Hardware Collection Methods .....	11
2.1.1 Light Emitting Sensor LES.....	11
2.1.2 Structured Light .....	13
2.1.3 Frustrated Total Internal Reflection (FTIR).....	14
2.1.4 Polarized Reflected Light .....	15
2.2 Matching and Recognition.....	16
2.2.1 Fingerprint Minutiae .....	16
2.2.2 Fingerprint Matching .....	18
2.2.3 Bozorth3.....	21
2.3 Metrics .....	22
2.3.1 Performance FMR FNMR .....	22
2.3.2 ROC AUC .....	23
2.3.3 DET EER .....	24
2.3.4 99 <sup>th</sup> Percentile Non-Mated Score Differential Performance .....	25
2.3.5 NIST Fingerprint Image Quality.....	26
2.3.6 Skin Reflectance .....	27
<b>Chapter 3: Dataset</b> .....	<b>29</b>

3.1 Data Collection .....	29
3.2 Description of the Dataset.....	31
<b>Chapter 4: Experiments .....</b>	<b>43</b>
4.1 Matching Experiment Organization.....	43
4.2 Results.....	45
4.2.1 Matcher AUC and EER values .....	45
4.2.2 Matcher ROC and DET Curves .....	50
4.2.3 Genuine Match Score Comparison .....	80
4.2.4 NFIQ2 Quality Score Distributions .....	92
4.2.5 NFIQ2 Quality Score VS Genuine Match Score .....	100
4.2.6 Melanin raw match score distribution.....	122
4.2.7 Skin Reflectance VS 99 <sup>th</sup> Percentile Non-Mated Match Scores .....	124
<b>Chapter 5: Summary and Conclusion.....</b>	<b>210</b>
5.1 Contact Fingerprints.....	210
5.2 Contactless Fingerprints.....	210
5.3 Cellphone Fingerprints.....	211
5.4 Melanin Analysis .....	212
5.5 Lightness Analysis .....	213
5.6 Erythema and Red-Green Spectrum Analysis.....	214
5.7 Blue-Yellow Spectrum Analysis .....	215
5.8 Bozorth3.....	215
5.9 Concluding Thoughts.....	216
5.10 Future Work .....	218
<b>References .....</b>	<b>219</b>

# List of Figures

Figure 1 underside of the LES film showing the blue glow of the luminescent LES [22].....	12
Figure 2 ridge extraction from an optical sensor and LES of a finger marked with black ink [22] .....	13
Figure 3 (a) graphically illustrates 3D fingerprint data (b) graphically illustrates 2D fingerprint data [25] .....	14
Figure 4 FTIR-based fingerprint sensor operation [26].....	15
Figure 5 The most common minutiae types [32] .....	17
Figure 6 Spurious minutiae and missing genuine minutiae. (a) Impression 1 (I1); (b) Impression 2 (I2); (c) Mosaiced image. [33] .....	17
Figure 7 (a) Original Fingerprint (b) Binarized image [35].....	19
Figure 8 (a) Binarized Fingerprint (b) Image after thinning [35] .....	19
Figure 9 Minutiae matching using distance [26] .....	20
Figure 10 Typical minutiae matching algorithm [36] .....	21
Figure 11 Example ROC curve.....	24
Figure 12 Example DET curve .....	25
Figure 13 General distribution diagram of imposter scores and genuine scores showing additional information describing the classification of the FMR and FNMR for a declared threshold [44].	26
Figure 14 a representation of L*a*b* color space using a 3D plot [45].....	28
Figure 15 Collection Process and Organization.....	30
Figure 16 distribution of participants by ethnicity.....	32
Figure 17 distribution of participants by age .....	33
Figure 18 distribution of participants by gender and ethnicity .....	34
Figure 19 Dataset ethnicity distribution by melanin value .....	38
Figure 20 Dataset ethnicity distribution by erythema value .....	38
Figure 21 Dataset ethnicity distribution by L* value.....	39
Figure 22 Dataset ethnicity distribution by a* value .....	39
Figure 23 Dataset ethnicity distribution by b* value .....	40
Figure 24 Innovatrics ROC curve Gemalto and Morpho vs Kojak. ....	50
Figure 25 Innovatrics DET curve Gemalto and Morpho vs Kojak.....	51
Figure 26 Innovatrics ROC curve S20 Operational Sciometrics and Veridium vs Kojak. ....	52
Figure 27 Innovatrics DET curve S20 Operational Sciometrics and Veridium vs Kojak.....	53
Figure 28 Innovatrics ROC curve S20 Controlled Sciometrics and Veridium vs Kojak.....	54

Figure 29 Innovatrics DET curve S20 Controlled Sciometrics and Veridium vs Kojak. ....	55
Figure 30 Innovatrics ROC curve S21 Operational Sciometrics and Veridium vs Kojak. ....	56
Figure 31 Innovatrics DET curve S21 Operational Sciometrics and Veridium vs Kojak.....	57
Figure 32 Innovatrics ROC curve S21 Controlled Sciometrics and Veridium vs Kojak.....	58
Figure 33 Innovatrics DET curve S21 Controlled Sciometrics and Veridium vs Kojak. ....	59
Figure 34 VeriFinger ROC curve Gemalto and Morpho vs Kojak. ....	60
Figure 35 Figure 26 VeriFinger DET curve Gemalto and Morpho vs Kojak. ....	61
Figure 36 VeriFinger ROC curve S20 Operational Sciometrics and Veridium vs Kojak. ....	62
Figure 37 VeriFinger DET curve S20 Operational Sciometrics and Veridium vs Kojak.....	63
Figure 38 VeriFinger ROC curve S20 Controlled Sciometrics and Veridium vs Kojak.....	64
Figure 39 VeriFinger DET curve S20 Controlled Sciometrics and Veridium vs Kojak. ....	65
Figure 40 VeriFinger ROC curve S21 Operational Sciometrics and Veridium vs Kojak. ....	66
Figure 41 VeriFinger DET curve S21 Operational Sciometrics and Veridium vs Kojak.....	67
Figure 42 VeriFinger ROC curve S21 Controlled Sciometrics and Veridium vs Kojak.....	68
Figure 43 VeriFinger DET curve S21 Controlled Sciometrics and Veridium vs Kojak. ....	69
Figure 44 Bozorth3 ROC curve Gemalto and Morpho vs Kojak. ....	70
Figure 45 Bozorth3 DET curve Gemalto and Morpho vs Kojak.....	71
Figure 46 Bozorth3 ROC curve S20 Operational Sciometrics and Veridium vs Kojak. ....	72
Figure 47 Bozorth3 DET curve S20 Operational Sciometrics and Veridium vs Kojak.....	73
Figure 48 Bozorth3 ROC curve S20 Controlled Sciometrics and Veridium vs Kojak. ....	74
Figure 49 Bozorth3 DET curve S20 Controlled Sciometrics and Veridium vs Kojak. ....	75
Figure 50 Bozorth3 ROC curve S21 Operational Sciometrics and Veridium vs Kojak. ....	76
Figure 51 Bozorth3 DET curve S21 Operational Sciometrics and Veridium vs Kojak.....	77
Figure 52 Bozorth3 ROC curve S21 Controlled Sciometrics and Veridium vs Kojak. ....	78
Figure 53 Bozorth3 DET curve S21 Controlled Sciometrics and Veridium vs Kojak. ....	79
Figure 54 Innovatrics match score comparison for contact sets compared to baseline. ....	80
Figure 55 Innovatrics match score comparison for contactless sets compared to baseline. ....	81
Figure 56 Innovatrics match score comparison for S20 sets from both cellphone applications in both settings compared to baseline. ....	82
Figure 57 Innovatrics match score comparison for S21 sets from both cellphone applications in both settings compared to baseline. ....	83
Figure 58 VeriFinger match score comparison for contact sets compared to baseline. ....	84
Figure 59 VeriFinger match score comparison for contactless sets compared to baseline. ....	85
Figure 60 VeriFinger match score comparison for S20 sets from both cellphone applications in both settings compared to baseline. ....	86

Figure 61 VeriFinger match score comparison for S21 sets from both cellphone applications in both settings compared to baseline. ....	87
Figure 62 Bozorth3 match score comparison for contact sets compared to baseline. ....	88
Figure 63 Bozorth3 match score comparison for contactless sets compared to baseline. ....	89
Figure 64 Bozorth3 match score comparison for S20 sets from both cellphone applications in both settings compared to baseline. ....	90
Figure 65 Bozorth3 match score comparison for S21 sets from both cellphone applications in both settings compared to baseline. ....	91
Figure 66 NFIQ2 score distribution for Kojak Slap fingerprints.....	92
Figure 67 NFIQ2 score distribution for Kojak Roll fingerprints.....	93
Figure 68 NFIQ2 score distribution for Guardian Slap fingerprints.....	93
Figure 69 NFIQ2 score distribution for Guardian Roll fingerprints.....	94
Figure 70 NFIQ2 score distribution for MorphoWave fingerprints.....	94
Figure 71 NFIQ2 score distribution for Gemalto fingerprints.....	95
Figure 72 NFIQ2 score distribution for S20 Sciometrics Stand fingerprints. ....	95
Figure 73 NFIQ2 score distribution for S20 Veridium Stand fingerprints. ....	96
Figure 74 NFIQ2 score distribution for S20 Sciometrics Op fingerprints.....	96
Figure 75 NFIQ2 score distribution for S20 Veridium Op fingerprints.....	97
Figure 76 NFIQ2 score distribution for S21 Sciometrics Stand fingerprints. ....	97
Figure 77 NFIQ2 score distribution for S21 Veridium Stand fingerprints. ....	98
Figure 78 NFIQ2 score distribution for S21 Sciometrics Op fingerprints.....	98
Figure 79 NFIQ2 score distribution for S21 Veridium Op fingerprints.....	99
Figure 80 Kojak Roll NFIQ2 rounded quality score vs Innovatrics match score.....	100
Figure 81 Guardian Slap NFIQ2 rounded quality score vs Innovatrics match score. ....	101
Figure 82 Guardian Roll NFIQ2 rounded quality score vs Innovatrics match score.....	101
Figure 83 Gemalto NFIQ2 rounded quality score vs Innovatrics match score.....	102
Figure 84 MorphoWave NFIQ2 rounded quality score vs Innovatrics match score. ....	102
Figure 85 S20 Sciometrics Stand NFIQ2 rounded quality score vs Innovatrics match score. ...	103
Figure 86 S20 Sciometrics Op NFIQ2 rounded quality score vs Innovatrics match score. ....	103
Figure 87 S20 Veridium Stand NFIQ2 rounded quality score vs Innovatrics match score. ....	104
Figure 88 S20 Veridium Op NFIQ2 rounded quality score vs Innovatrics match score. ....	104
Figure 89 S21 Sciometrics Stand NFIQ2 rounded quality score vs Innovatrics match score. ...	105
Figure 90 S21 Sciometrics Op NFIQ2 rounded quality score vs Innovatrics match score. ....	105
Figure 91 S21 Veridium Stand NFIQ2 rounded quality score vs Innovatrics match score. ....	106
Figure 92 S21 Veridium Op NFIQ2 rounded quality score vs Innovatrics match score. ....	106

Figure 93 Kojak Roll NFIQ2 rounded quality score vs VeriFinger match score.....	108
Figure 94 Guardian Slap NFIQ2 rounded quality score vs VeriFinger match score. ....	108
Figure 95 Guardian Roll NFIQ2 rounded quality score vs VeriFinger match score.....	109
Figure 96 Gemalto NFIQ2 rounded quality score vs VeriFinger match score.....	109
Figure 97 MorphoWave NFIQ2 rounded quality score vs VeriFinger match score. ....	110
Figure 98 S20 Sciometrics Stand NFIQ2 rounded quality score vs VeriFinger match score. ....	110
Figure 99 S20 Sciometrics Op NFIQ2 rounded quality score vs VeriFinger match score. ....	111
Figure 100 S20 Veridium Stand NFIQ2 rounded quality score vs VeriFinger match score. ....	111
Figure 101 S20 Veridium Op NFIQ2 rounded quality score vs VeriFinger match score. ....	112
Figure 102 S21 Sciometrics Stand NFIQ2 rounded quality score vs VeriFinger match score. ...	112
Figure 103 S21 Sciometrics Op NFIQ2 rounded quality score vs VeriFinger match score. ....	113
Figure 104 S21 Veridium Stand NFIQ2 rounded quality score vs VeriFinger match score. ....	113
Figure 105 S21 Veridium Op NFIQ2 rounded quality score vs VeriFinger match score. ....	114
Figure 106 Kojak Roll NFIQ2 rounded quality score vs Bozorth3 match score.....	115
Figure 107 Guardian Slap NFIQ2 rounded quality score vs Bozorth3 match score. ....	116
Figure 108 Guardian Roll NFIQ2 rounded quality score vs Bozorth3 match score.....	116
Figure 109 Gemalto NFIQ2 rounded quality score vs Bozorth3 match score.....	117
Figure 110 MorphoWave NFIQ2 rounded quality score vs Bozorth3 match score.....	117
Figure 111 S20 Sciometrics Stand NFIQ2 rounded quality score vs Bozorth3 match score.....	118
Figure 112 S20 Sciometrics Op NFIQ2 rounded quality score vs Bozorth3 match score.....	118
Figure 113 S20 Veridium Stand NFIQ2 rounded quality score vs Bozorth3 match score. ....	119
Figure 114 S20 Veridium Op NFIQ2 rounded quality score vs Bozorth3 match score.....	119
Figure 115 S21 Sciometrics Stand NFIQ2 rounded quality score vs Bozorth3 match score. ....	120
Figure 116 S21 Sciometrics Op NFIQ2 rounded quality score vs Bozorth3 match score.....	120
Figure 117 S21 Veridium Stand NFIQ2 rounded quality score vs Bozorth3 match score. ....	121
Figure 118 S21 Veridium Op NFIQ2 rounded quality score vs Bozorth3 match score.....	121
Figure 119 Innovatrics match scores binned into melanin ranges for Guardian Slap (Baseline). .....	122
Figure 120 Innovatrics match scores binned into melanin ranges for S20 Sciometrics Op. ....	123
Figure 121 Innovatrics match scores binned into melanin ranges for S20 Veridium Op. ....	123
Figure 122 Innovatrics 99th non-match percentile binned into melanin ranges for Kojak Roll.	124
Figure 123 Innovatrics 99th non-match percentile binned into melanin ranges for Guardian Slap (Baseline). ....	125
Figure 124 Innovatrics 99th non-match percentile binned into melanin ranges for Guardian Roll. .....	125

Figure 125 Innovatrics 99th non-match percentile binned into melanin ranges for Gemalto. ...	126
Figure 126 Innovatrics 99th non-match percentile binned into melanin ranges for MorphoWave. .....	126
Figure 127 Innovatrics 99th non-match percentile binned into melanin ranges for S20 Sciometrics Stand.....	127
Figure 128 Innovatrics 99th non-match percentile binned into melanin ranges for S20 Sciometrics Op.....	127
Figure 129 Innovatrics 99th non-match percentile binned into melanin ranges for S20 Veridium Stand. ....	128
Figure 130 Innovatrics 99th non-match percentile binned into melanin ranges for S20 Veridium Op.....	128
Figure 131 Innovatrics 99th non-match percentile binned into melanin ranges for S21 Sciometrics Stand.....	129
Figure 132 Innovatrics 99th non-match percentile binned into melanin ranges for S21 Sciometrics Op.....	129
Figure 133 Innovatrics 99th non-match percentile binned into melanin ranges for S21 Veridium Stand. ....	130
Figure 134 Innovatrics 99th non-match percentile binned into melanin ranges for S21 Veridium Op.....	130
Figure 135 VeriFinger 99th non-match percentile binned into melanin ranges for Kojak Roll.	131
Figure 136 VeriFinger 99th non-match percentile binned into melanin ranges for Guardian Slap. .....	132
Figure 137 VeriFinger 99th non-match percentile binned into melanin ranges for Guardian Roll. .....	132
Figure 138 VeriFinger 99th non-match percentile binned into melanin ranges for Gemalto. ....	133
Figure 139 VeriFinger 99th non-match percentile binned into melanin ranges for MorphoWave. .....	133
Figure 140 VeriFinger 99th non-match percentile binned into melanin ranges for S20 Sciometrics Stand. ....	134
Figure 141 VeriFinger 99th non-match percentile binned into melanin ranges for S20 Sciometrics Op.....	134
Figure 142 VeriFinger 99th non-match percentile binned into melanin ranges for S20 Veridium Stand. ....	135
Figure 143 VeriFinger 99th non-match percentile binned into melanin ranges for S20 Veridium Op.....	135
Figure 144 VeriFinger 99th non-match percentile binned into melanin ranges for S21 Sciometrics Stand. ....	136
Figure 145 VeriFinger 99th non-match percentile binned into melanin ranges for S21 Sciometrics Op.....	136

Figure 146 VeriFinger 99th non-match percentile binned into melanin ranges for S21 Veridium Stand. ....	137
Figure 147 VeriFinger 99th non-match percentile binned into melanin ranges for S21 Veridium Op.....	137
Figure 148 Bozorth3 99th non-match percentile binned into melanin ranges for Kojak Roll. ..	139
Figure 149 Bozorth3 99th non-match percentile binned into melanin ranges for Guardian Slap (Baseline). ....	139
Figure 150 Bozorth3 99th non-match percentile binned into melanin ranges for Guardian Roll. ....	140
Figure 151 Bozorth3 99th non-match percentile binned into melanin ranges for Gemalto. ....	140
Figure 152 Bozorth3 99th non-match percentile binned into melanin ranges for MorphoWave. ....	141
Figure 153 Bozorth3 99th non-match percentile binned into melanin ranges for S20 Sciometrics Stand. ....	141
Figure 154 Bozorth3 99th non-match percentile binned into melanin ranges for S20 Sciometrics Op.....	142
Figure 155 Bozorth3 99th non-match percentile binned into melanin ranges for S20 Veridium Stand. ....	142
Figure 156 Bozorth3 99th non-match percentile binned into melanin ranges for S20 Veridium Op.....	143
Figure 157 Bozorth3 99th non-match percentile binned into melanin ranges for S21 Sciometrics Stand. ....	143
Figure 158 Bozorth3 99th non-match percentile binned into melanin ranges for S21 Sciometrics Op.....	144
Figure 159 Bozorth3 99th non-match percentile binned into melanin ranges for S21 Veridium Stand. ....	144
Figure 160 Bozorth3 99th non-match percentile binned into melanin ranges for S21 Veridium Op.....	145
Figure 161 Innovatrics 99th non-match percentile binned into erythema ranges for Kojak Roll. ....	146
Figure 162 Innovatrics 99th non-match percentile binned into erythema ranges for Guardian Slap (Baseline). ....	147
Figure 163 Innovatrics 99th non-match percentile binned into erythema ranges for Guardian Roll.....	147
Figure 164 Innovatrics 99th non-match percentile binned into erythema ranges for Gemalto. .	148
Figure 165 Innovatrics 99th non-match percentile binned into erythema ranges for MorphoWave. ....	148
Figure 166 Innovatrics 99th non-match percentile binned into erythema ranges for S20 Sciometrics Stand.....	149



Figure 167 Innovatrics 99th non-match percentile binned into erythema ranges for S20 Sciometrics Op.....	149
Figure 168 Innovatrics 99th non-match percentile binned into erythema ranges for S20 Veridium Stand. ....	150
Figure 169 Innovatrics 99th non-match percentile binned into erythema ranges for S20 Veridium Op.....	150
Figure 170 Innovatrics 99th non-match percentile binned into erythema ranges for S21 Sciometrics Stand.....	151
Figure 171 Innovatrics 99th non-match percentile binned into erythema ranges for S21 Sciometrics Op.....	151
Figure 172 Innovatrics 99th non-match percentile binned into erythema ranges for S21 Veridium Stand. ....	152
Figure 173 Innovatrics 99th non-match percentile binned into erythema ranges for S21 Veridium Op.....	152
Figure 174 VeriFinger 99th non-match percentile binned into erythema ranges for Kojak Roll. .....	153
Figure 175 VeriFinger 99th non-match percentile binned into erythema ranges for Guardian Slap. .....	154
Figure 176 VeriFinger 99th non-match percentile binned into erythema ranges for Guardian Roll. .....	154
Figure 177 VeriFinger 99th non-match percentile binned into erythema ranges for Gemalto. ..	155
Figure 178 VeriFinger 99th non-match percentile binned into erythema ranges for MorphoWave. .....	155
Figure 179 VeriFinger 99th non-match percentile binned into erythema ranges for S20 Sciometrics Stand.....	156
Figure 180 VeriFinger 99th non-match percentile binned into erythema ranges for S20 Sciometrics Op.....	156
Figure 181 VeriFinger 99th non-match percentile binned into erythema ranges for S20 Veridium Stand. ....	157
Figure 182 VeriFinger 99th non-match percentile binned into erythema ranges for S20 Veridium Op.....	157
Figure 183 VeriFinger 99th non-match percentile binned into erythema ranges for S21 Sciometrics Stand.....	158
Figure 184 VeriFinger 99th non-match percentile binned into erythema ranges for S21 Sciometrics Op.....	158
Figure 185 VeriFinger 99th non-match percentile binned into erythema ranges for S21 Veridium Stand. ....	159
Figure 186 VeriFinger 99th non-match percentile binned into erythema ranges for S21 Veridium Op.....	159

Figure 187 Bozorth3 99th non-match percentile binned into erythema ranges for Kojak Roll.	160
Figure 188 Bozorth3 99th non-match percentile binned into erythema ranges for Guardian Slap (Baseline).	161
Figure 189 Bozorth3 99th non-match percentile binned into erythema ranges for Guardian Roll.	161
Figure 190 Bozorth3 99th non-match percentile binned into erythema ranges for Gemalto. ....	162
Figure 191 Bozorth3 99th non-match percentile binned into erythema ranges for MorphoWave.	162
Figure 192 Bozorth3 99th non-match percentile binned into erythema ranges for S20 Sciometrics Stand.	163
Figure 193 Bozorth3 99th non-match percentile binned into erythema ranges for S20 Sciometrics Op.	163
Figure 194 Bozorth3 99th non-match percentile binned into erythema ranges for S20 Veridium Stand.	164
Figure 195 Bozorth3 99th non-match percentile binned into erythema ranges for S20 Veridium Op.	164
Figure 196 Bozorth3 99th non-match percentile binned into erythema ranges for S21 Sciometrics Stand.	165
Figure 197 Bozorth3 99th non-match percentile binned into erythema ranges for S21 Sciometrics Op.	165
Figure 198 Bozorth3 99th non-match percentile binned into erythema ranges for S21 Veridium Stand.	166
Figure 199 Bozorth3 99th non-match percentile binned into erythema ranges for S21 Veridium Op.	166
Figure 200 Innovatrics 99th non-match percentile binned lightness ranges Kojak Roll.	167
Figure 201 Innovatrics 99th non-match percentile binned lightness ranges Guardian Slap (Baseline).	168
Figure 202 Innovatrics 99th non-match percentile binned lightness ranges Guardian Roll.	168
Figure 203 Innovatrics 99th non-match percentile binned lightness ranges Gemalto.	169
Figure 204 Innovatrics 99th non-match percentile binned lightness ranges MorphoWave.	169
Figure 205 Innovatrics 99th non-match percentile binned lightness ranges S20 Sciometrics Stand.	170
Figure 206 Innovatrics 99th non-match percentile binned lightness ranges S20 Sciometrics Op.	170
Figure 207 Innovatrics 99th non-match percentile binned lightness ranges S20 Veridium Stand.	171
Figure 208 Innovatrics 99th non-match percentile binned lightness ranges S20 Veridium Op.	171

Figure 209 Innovatrics 99th non-match percentile binned lightness ranges S21 Sciometrics Stand. ....	172
Figure 210 Innovatrics 99th non-match percentile binned lightness ranges S21 Sciometrics Op. ....	172
Figure 211 Innovatrics 99th non-match percentile binned lightness ranges S21 Veridium Stand. ....	173
Figure 212 Innovatrics 99th non-match percentile binned lightness ranges S21 Veridium Op..	173
Figure 213 VeriFinger 99th non-match percentile binned lightness ranges Kojak Roll. ....	174
Figure 214 VeriFinger 99th non-match percentile binned lightness ranges Guardian Slap. ....	175
Figure 215 VeriFinger 99th non-match percentile binned lightness ranges Guardian Roll. ....	175
Figure 216 VeriFinger 99th non-match percentile binned lightness ranges Gemalto. ....	176
Figure 217 VeriFinger 99th non-match percentile binned lightness ranges MorphoWave. ....	176
Figure 218 VeriFinger 99th non-match percentile binned lightness ranges S20 Sciometrics Stand. ....	177
Figure 219 VeriFinger 99th non-match percentile binned lightness ranges S20 Sciometrics Op. ....	177
Figure 220 VeriFinger 99th non-match percentile binned lightness ranges S20 Veridium Stand. ....	178
Figure 221 VeriFinger 99th non-match percentile binned lightness ranges S20 Veridium Op..	178
Figure 222 VeriFinger 99th non-match percentile binned lightness ranges S21 Sciometrics Stand. ....	179
Figure 223 VeriFinger 99th non-match percentile binned lightness ranges S21 Sciometrics Op. ....	179
Figure 224 VeriFinger 99th non-match percentile binned lightness ranges S21 Veridium Stand. ....	180
Figure 225 VeriFinger 99th non-match percentile binned lightness ranges S21 Veridium Op..	180
Figure 226 Innovatrics 99th non-match percentile binned red-green ranges Kojak Roll. ....	181
Figure 227 Innovatrics 99th non-match percentile binned red-green ranges Guardian Slap (Baseline). ....	182
Figure 228 Innovatrics 99th non-match percentile binned red-green ranges Guardian Roll. ....	182
Figure 229 Innovatrics 99th non-match percentile binned red-green ranges Gemalto. ....	183
Figure 230 Innovatrics 99th non-match percentile binned red-green ranges MorphoWave. ....	183
Figure 231 Innovatrics 99th non-match percentile binned red-green ranges S20 Sciometrics Stand. ....	184
Figure 232 Innovatrics 99th non-match percentile binned red-green ranges S20 Sciometrics Op. ....	184
Figure 233 Innovatrics 99th non-match percentile binned red-green ranges S20 Veridium Stand. ....	185

Figure 234 Innovatrics 99th non-match percentile binned red-green ranges S20 Veridium Op.	185
Figure 235 Innovatrics 99th non-match percentile binned red-green ranges S21 Sciometrics Stand. ....	186
Figure 236 Innovatrics 99th non-match percentile binned red-green ranges S21 Sciometrics Op. ....	186
Figure 237 Innovatrics 99th non-match percentile binned red-green ranges S21 Veridium Stand. ....	187
Figure 238 Innovatrics 99th non-match percentile binned red-green ranges S21 Veridium Op.	187
Figure 239 VeriFinger 99th non-match percentile binned red-green ranges Kojak Roll.....	188
Figure 240 VeriFinger 99th non-match percentile binned red-green ranges Guardian Slap. ....	189
Figure 241 VeriFinger 99th non-match percentile binned red-green ranges Guardian Roll.....	189
Figure 242 VeriFinger 99th non-match percentile binned red-green ranges Gemalto.....	190
Figure 243 VeriFinger 99th non-match percentile binned red-green ranges MorphoWave.....	190
Figure 244 VeriFinger 99th non-match percentile binned red-green ranges S20 Sciometrics Stand. ....	191
Figure 245 VeriFinger 99th non-match percentile binned red-green ranges S20 Sciometrics Op. ....	191
Figure 246 VeriFinger 99th non-match percentile binned red-green ranges S20 Veridium Stand. ....	192
Figure 247 VeriFinger 99th non-match percentile binned red-green ranges S20 Veridium Op.	192
Figure 248 VeriFinger 99th non-match percentile binned red-green ranges S21 Sciometrics Stand. ....	193
Figure 249 VeriFinger 99th non-match percentile binned red-green ranges S21 Sciometrics Op. ....	193
Figure 250 VeriFinger 99th non-match percentile binned red-green ranges S21 Veridium Stand. ....	194
Figure 251 VeriFinger 99th non-match percentile binned red-green ranges S21 Veridium Op.	194
Figure 252 Innovatrics 99th non-match percentile binned blue-yellow ranges Kojak Roll. ....	195
Figure 253 Innovatrics 99th non-match percentile binned blue-yellow ranges Guardian Slap (Baseline). ....	196
Figure 254 Innovatrics 99th non-match percentile binned blue-yellow ranges Guardian Roll..	196
Figure 255 Innovatrics 99th non-match percentile binned blue-yellow ranges Gemalto. ....	197
Figure 256 Innovatrics 99th non-match percentile binned blue-yellow ranges MorphoWave...	197
Figure 257 Innovatrics 99th non-match percentile binned blue-yellow ranges S20 Sciometrics Stand. ....	198
Figure 258 Innovatrics 99th non-match percentile binned blue-yellow ranges S20 Sciometrics Op.....	198

Figure 259 Innovatrics 99th non-match percentile binned blue-yellow ranges S20 Veridium Stand. ....	199
Figure 260 Innovatrics 99th non-match percentile binned blue-yellow ranges S20 Veridium Op. ....	199
Figure 261 Innovatrics 99th non-match percentile binned blue-yellow ranges S21 Sciometrics Stand. ....	200
Figure 262 Innovatrics 99th non-match percentile binned blue-yellow ranges S21 Sciometrics Op. ....	200
Figure 263 Innovatrics 99th non-match percentile binned blue-yellow ranges S21 Veridium Stand. ....	201
Figure 264 Innovatrics 99th non-match percentile binned blue-yellow ranges S21 Veridium Op. ....	201
Figure 265 VeriFinger 99th non-match percentile binned blue-yellow ranges Kojak Roll. ....	202
Figure 266 VeriFinger 99th non-match percentile binned blue-yellow ranges Guardian Slap...	203
Figure 267 VeriFinger 99th non-match percentile binned blue-yellow ranges Guardian Roll...	203
Figure 268 VeriFinger 99th non-match percentile binned blue-yellow ranges Gemalto. ....	204
Figure 269 VeriFinger 99th non-match percentile binned blue-yellow ranges MorphoWave....	204
Figure 270 VeriFinger 99th non-match percentile binned blue-yellow ranges S20 Sciometrics Stand. ....	205
Figure 271 VeriFinger 99th non-match percentile binned blue-yellow ranges S20 Sciometrics Op. ....	205
Figure 272 VeriFinger 99th non-match percentile binned blue-yellow ranges S20 Veridium Stand. ....	206
Figure 273 VeriFinger 99th non-match percentile binned blue-yellow ranges S20 Veridium Op. ....	206
Figure 274 VeriFinger 99th non-match percentile binned blue-yellow ranges S21 Sciometrics Stand. ....	207
Figure 275 VeriFinger 99th non-match percentile binned blue-yellow ranges S21 Sciometrics Op. ....	207
Figure 276 VeriFinger 99th non-match percentile binned blue-yellow ranges S21 Veridium Stand. ....	208
Figure 277 VeriFinger 99th non-match percentile binned blue-yellow ranges S21 Veridium Op. ....	208

# List of Tables

Table 1 skin reflectance ranges by self-reported ethnicity using CIELab color space with Melanin and Erythema .....	36
Table 2 skin reflectance mean/median by self-reported ethnicity using CIELab color space with Melanin and Erythema .....	37
Table 3 Example fingerprints for each device and setting.....	41
Table 4 Dataset Composition .....	42
Table 5 Area Under the Curve values for all datasets and matchers.....	45
Table 6 Innovatrics EER for each dataset and FNMR@FMR ratios.....	47
Table 7 VeriFinger EER for each dataset and FNMR@FMR ratios.....	48
Table 8 Bozorth3 EER for each dataset and FNMR@FMR ratios.....	49

# List of Equations

Equation 1 (a) the integral to calculate the FNRM (b) the integral to calculate the FMR.....	22
Equation 2 Simplified explanation of (a) FNMR equation and (b) FMR equation .....	22

# Chapter 1: Introduction

## 1.1 Summary

The human body has many identifiable characteristics—some obvious things like hair color, eye color, and height. In contrast, some are hard to see, like iris texture, fingerprints, and human bioluminescence. All human characteristics are considered biometrics, though different biometrics are valued highly over others based on seven characteristics: universality, uniqueness, permanence, collectability, performance, acceptability, and circumvention. Fingerprints excel at each of these categories, so we use fingerprints daily to secure our identity and data. Though everyone is different, some people are older, and some have lighter skin tones. These differences are demographic features, and their impact on the interoperability of fingerprint identification is not a new issue, though, with the rapid changes and adoption of new fingerprint technologies such as non-contact fingerprinting and using cellphone cameras to record fingerprints. Continued efforts must be made to verify the interoperability for both existing datasets containing legacy modalities that are no longer commonly used, such as ink fingerprints and plain impression digital fingerprints, which are the currently favored modality, and additional efforts need to be made to make sure all demographics perform equally, so all individuals are treated fair when fingerprints are used.

## 1.2 History

The earliest government dataset in the US was in 1903 when New York state implemented the American Classification System leading to the fingerprinting of all criminals within the state; in 1904 the US Government began collecting fingerprints starting with the Leavenworth Federal Prison [1]. Only recently, in the last twenty years, has digital fingerprinting



become standardized, with the FBI only releasing image quality specifications for scanning and capturing digital fingerprints before 2010. The specifications outline the minimum capture sizes a fingerprint should be and supply a table of minimum modulation a bar target scanner should have for 500 and 1000 pixels per inch (PPI) [2]. Scanners could now be certified for converting physical copies of ink fingerprints to a digital format with minimal loss. The minimum modulation standard has continued to be used even outside the initial purpose. It is now applied to cameras to capture images of existing contact fingerprints and non-contact fingerprints since no new standard has been set in place. The ability to extract fingerprints from digital fingerphotos has become a reality, with smartphone multi-modal biometric capture platforms replacing traditional kiosk-style sensor devices.

## 1.3 Motivation

Non-contact devices in all forms offer a high-throughput, hygienic means of capturing fingerprints when compared to traditional methods, such as contact devices requiring the subject to come in contact with the sensor leaving behind, at best, oil and residue from their skin that will need to be removed by the operator to prevent any interference with the capture of later prints and at worst any contact can introduce pathogens that both the operator and later subjects could come in contact with. Additionally, with the advent of improved cameras in cellphones, contactless recording extends the benefits to allow highly mobile working environments such as law enforcement to travel with suitable devices for recording fingerprints through the implementation of applications that use the camera to record and segment fingerphotos that can then be stored for later ridge extraction or the ridge extraction can be immediately processed by the application leaving a final output that can be immediately used. These cellphone applications can also retain the ability to control and quality check fingerprints during recording to guarantee

a minimum level of fingerprint quality. The applications also can guide the operator to position the camera optimally before capture, minimizing the amount of training needed to operate the device.

However, the differences in the capture process itself introduce interoperability issues. Specifically, the contact-based capture methods (livescan, ink & paper) used to compile the majority of legacy fingerprint datasets cause elastic deformation. At the same time, fingerphotos often have significant photometric distortion, nonuniform focus, and motion blur [3]. Additional polarity inversions that appear during processing occur since contactless fingerprints do not have a pressure-based measurement reading, whereas, for most contact sensors, darker prints usually indicate more pressure. Leading to extracted fingerprints from fingerphotos having inverted ridges occur in parts of the print. This thesis will present an analysis of the interoperability of fingerprints from digital contact sensors and non-contact fingerprints recorded using kiosk and cellphone-based sensors.

## 1.4 Previous Work

Most of the previous works on improving interoperability between contact and contactless fingerprints have focused on addressing the challenge by developing new matching and comparison schemes, such as imparting the elastic deformation in contact prints onto contactless prints to counteract perspective distortions [4], In this work, they ultimately applied three different warping models and achieved a noticeable improvement in matching performance on their dataset. Another group implementing specialized convolutional neural networks (CNN) focused on distortion correction to correct rotations in non-contact fingerprints as part of the postprocessing for a mobile application designed for fingerprint acquisition [5]. Outside of best

practices, studies have been performed to evaluate and improve the matching interoperability of contact to contactless fingerprints using different types of convolutional neural network (CNN) models. An attempt at improving interoperability without adding distortion implemented a network using an attention module with Siamese architecture for detecting minutiae by looking at certain regions of a fingerprint that have little to no distortion while ignoring regions prone to distortion where minutiae from contact fingerprints would not line up with non-contact fingerprints [6]. Improvements were seen on two tested datasets compared to a consumer off-the-shelf (COTS) matcher and another Siamese network. A second application of a CNN Siamese network was reported to attempt matching between contact fingerprints and contactless fingerphotos by incorporating contextual information learned by the network for the minutiae feature correspondence [7]. Achieving improvement based on two datasets when compared to both a deformation correction model and a minutiae matcher based on the equal error rate and rank one accuracy.

The US National Institute for Standards and Technology (NIST) has released a document on the guidance of evaluating contactless fingerprints [3] and an additional document directly on the interoperability of contactless-to-contact fingerprints [8]. Direct evaluation of contactless fingerprint quality can be shown by using contrast measurements, through the usage of signal-to-noise ratio, and sample rate measured by pixels per inch (PPI) of individual fingerprints [3]. The NIST interoperability report extends much of the guidance to include the comparison of contact and contactless images by suggesting fair metrics that can be used to directly compare the different types of prints to gather a quality assessment of the fingerprints by scoring differences in the minutiae [8]. Additionally, NIST has a publicly available quality assessment tool NFIQ 2.0, calibrated against finger comparison performance to help evaluate how suitable the

fingerprint capture would be for recognition [3]. NFIQ 2.0 is an open-source software designed as an improved version of NIST's previous version NFIQ. Improvements are in the overall computational complexity allowing support for quality assessment on mobile platforms and changes to the quality scoring system from 0-100 instead of 1-5 to align with the international biometric sample quality standard [9]. Ideally, the higher quality scores an image is given should correspond with the operational recognition performance, though it should be noted that this tool was developed for contact-based fingerprints and may not be directly applicable to fingerprints extracted from fingerphotos as shown later in this thesis contactless fingerprint images score lower on average than the same subjects contact fingerprint image even when the score is comparable between contactless and contact fingerprints from the same subject.

Differential performance of biometric approaches between various ages, gender, and ethnic demographics is a current area of concern in the field. Facial recognition and how it relates to fingerprints helps illustrate this bias. For example, as part of maintaining equitable performance across all members of a specific population, the impacts of how demographic underrepresentation in a dataset can lead to differences in facial recognition accuracy must be understood (see, e.g., [10], [11], [12], [13], [14], [15], [16]). In [12], a facial recognition experiment that considered skin reflectance found that lower reflectance values corresponding with darker skin tones had lower average comparison scores than higher reflectance values corresponding with lighter skin tones. When comparing two systems, one using a stationary image and one using an in-motion image, the reflectance net effect improvement between the in-movement and stationary image showed the most significant improvement in low reflectance subjects, with the lowest scores ending up higher than the highest scores in the worse of the two systems, additionally suggesting the importance of having controlled data of high quality

significantly reducing demographic concerns. A different work attempting to remove female characteristics from fingerprints for de-identification to reduce unauthorized disclosure [17] showed differences in male and female energy concentrations at select frequency bands. Because contactless fingerprints are often captured using photographic methods, the same differential performance challenges impacting facial recognition may also negatively impact contactless fingerprint interoperability with legacy contact-based galleries. A past colleague presented the work in [18] that evaluated the effect of melanin values on comparison scores from fingerprints captured using cellphones. It showed no perceivable impact on match scores. As mentioned earlier, limited data was available when the research was undertaken. The data had fewer subjects and fewer modalities tested, and specific demographics were underrepresented in the dataset population. The study in [16] also tested the relationship between demographic bias and fingerprint quality, showing no correlation. The study used an optical contact fingerprint reader and bases the conclusion of no correlation on image quality of fingerprints being uncorrelated with any specific skin features. The study, however, did not observe differences in match performance. The study limited its scope only to contact fingerprints leaving the need of additional work on other modalities using other acquisition technologies or additional work on a controlled environment to obtain the best quality image. However, a different study [19] tested differential performance using a COTS fingerprint matcher and a neural network matcher using contact fingerprints. The results showed that performance varied on both matchers based on self-reported ethnicity. The COTS matcher had a higher average performance and showed little evidence of bias. However, the neural network had poorer performance and showed some trend between demographics leading the researchers to suggest that external factors can significantly impact a specific group's performance. This suggests that in a controlled environment,

demographic factors are minimized. However, once the quality of data drops or if entries in the dataset are incorrect, then demographic trends will arise, leading to more significant decreases in the performance of some groups over others. This decrease in performance is similar to what was observed in [12] when facial recognition was tested using two different systems of varying quality. In [20], match performance for different ethnicities and ages was evaluated, showing that performance varied based on ethnicity. Caucasians had a higher accuracy for fingerprints from right index fingers than non-Caucasians, while exhibiting lower accuracy for right thumbs. When considering different age ranges, [20] found that, as age increased, so did accuracy. The study presented in [21] showed the opposite; a decrease in match performance with age when attempting to match fingerprints taken from the same individual over at least five years.

## 1.5 Goals and Impact of the Research

This thesis's significant focus areas serve to expand and continue previous efforts on the interoperability of demographic features. The contributions of the resulting research effort are the quantification of the comparison score interoperability of four contactless fingerprint modalities in a new contactless dataset - two datasets from kiosk-style devices, and two datasets from mobile phone applications, each recorded twice on different phone models for a total of six contactless fingerprint datasets. An exploration of the effect of skin pigmentation measured by skin reflectance on the comparison interoperability of contact and contactless fingerprints, with a specific focus on different components of skin color, consisting of measurements of melanin erythema and values of the CIELAB color space. To report the interoperability differences shown between the modalities with an evaluation of overlap of fingerprint comparison based on self-reported ethnicity and quantitative measurement of skin reflectance to demonstrate the importance of expanding feature groups past sex and ethnicity and instead use measured values

taken from existing biometric information or taken at the time of collection. Additionally, combining the analysis of quality scores from NFIQ2 and match scores with different demographics to observe if high match scores trend with high-quality scores and specific demographics and the inverse. If successful, this thesis will impact the recording of demographics showing that using skin reflectance instead of self-reported ethnicities allows for better analysis of specific ranges. Additionally, using different fingerprinting platforms and fingerprint-matching systems will show demographic interoperability concerns that require further development and research to represent all demographic groups fairly. The most important application of this work will be as a benchmark for the current state of interoperability between commonly used contact fingerprinting platforms, newly used contactless platforms, and newly introduced fingerphoto cellphone applications.

## 1.6 Organization of the Thesis

Chapter one introduces the thesis and the basis for this work, providing an overview of the history of fingerprint databases and why interoperability is essential, along with the previous work in analyzing interoperability and demographics. Additionally, the motivations of the thesis are outlined, along with the goals and potential impact of the research.

Chapter two outlines the technical information explored in this thesis. The technology used in each fingerprint sensor in the dataset is introduced and explained to show the different techniques deployed for devices labeled under the same type of fingerprint. How fingerprint matching is performed and what fingerprint details are observed when matching. Each metric used to analyze the results of the matching experiments is detailed in calculating the metric and

the critical information the metric conveys. Lastly, the skin reflectance measurements and details of the specific color space are explained.

Chapter three describes the data collection that took place to collect the fingerprint data used in this thesis. The details of individual stations and the organization of devices are explained to show the process of a participant coming through the collection with specific details describing the cellphone applications used to record fingerprints.

Chapter four elaborates on the dataset outlining the type of fingerprints each device recorded and the breakdown of demographic information. The demographic information is broken down into self-reported information and the skin reflectance ranges of each ethnicity. Additionally, the number of participants for each ethnicity and gender is available.

Chapter five details the different matchers tested along with any version details for each of the matchers; details of the dataset used for each are outlined, with the same gallery dataset used for all matchers. Lastly, the following section will give an overview of how the results will be compiled and any additional analyses will be made.

Chapter six contains the results of the matching experiment organized by type of figure and matcher used. Descriptions of the information shown follow each set of figures containing critical information. The first, second, and third subsections contain results from only the matchers, subsections four and five contain the quality score results, and subsection six contains the skin reflectance results.

Chapter seven is the concluding discussion summarizing the findings from chapter six and elaborating on important information shown in the results. Subsections one through six summarize the results explaining any findings from each type of fingerprint or important



information seen for melanin and erythema skin reflectance measurements. Subsections seven and eight summarize the concluded results from earlier in the section stating the significance of the findings and introducing any future work that could be done to continue the thesis.

# Chapter 2: Technical Information and Theory

## 2.1 Fingerprint Hardware Collection Methods

### 2.1.1 Light Emitting Sensor LES

A Light Emitting Sensor (LES) is a multilayer film that gives off luminescence narrow wavelength light when a conductive material comes in contact with the film [22] [23]. The multilayer LES consists of a top protective layer, a phosphor layer, and an Indium Tin Oxide Electrode layer [22]. When a finger contacts the LES, the phosphor particles align with the ridges of the skin, causing a circuit to be formed across the film producing light that traces the finger's ridges at the point of contact on the underside of the LES [22]. A camera below the LES then records the illumination produced, and an example of the light the LES produces can be seen in Figure 1. A significant benefit of LES devices is the ability to record fingerprints when markings are on the skin, such as skin color blemishes and staining, which is shown in Figure 2. LES devices also resist other environmental factors such as direct sunlight, heat, cold, dry skin, and wet skin [22] [23].



*Figure 1 underside of the LES film showing the blue glow of the luminescent LES [22]*

Black Mark on Finger  
on Optical Scanner



Black Mark on Finger  
on LES



*Figure 2 ridge extraction from an optical sensor and LES of a finger marked with black ink [22]*

## 2.1.2 Structured Light

Structured Light is commonly used for contactless fingerprint acquisition. One or more projectors are used to project a pattern of light into a volume designated for a hand or finger to be placed in, and one or more cameras then records images of the light projected in the volume [24]. When using multiple cameras at different angles to record the pattern projected, the resulting images can be reconstructed into a 3D or hybrid 2-D model of the object [25]. The texture of the fingerprint is then represented as part of the reconstruction. It can be separated from the full model as an extracted fingerprint without numerical measurements of the ridge height [25]. Figure 4(a) below shows the projected pattern on the finger creating the 3D

representation and the deformation of the projected pattern, which is how the captured images correlate the individual 2D images into the 3D representation shown. Figure 4(b) shows the 2D fingerprint data of the 3D representation.

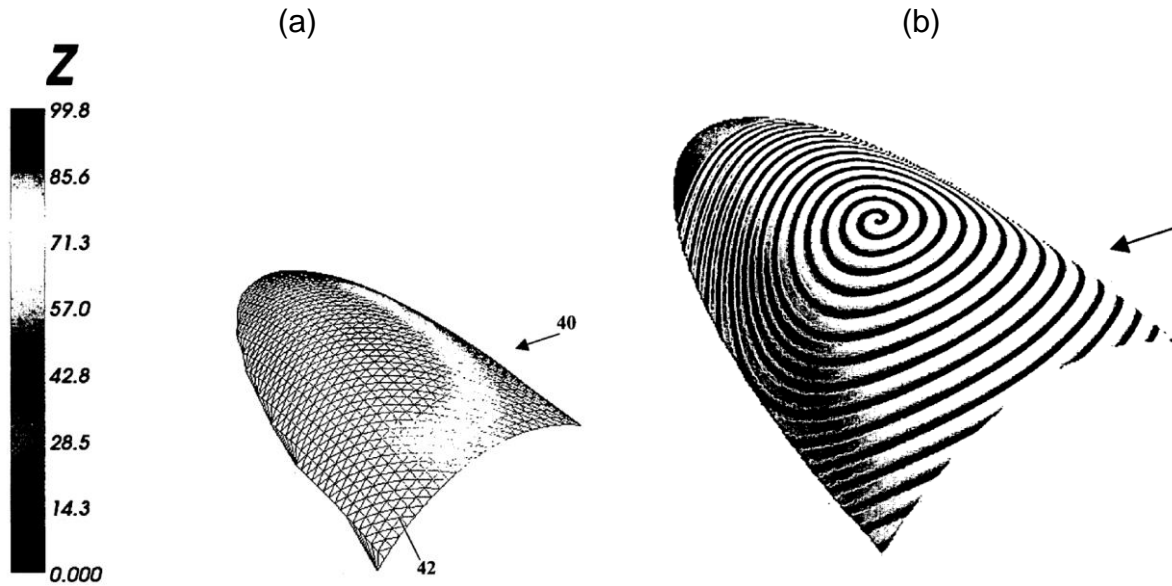


Figure 3 (a) graphically illustrates 3D fingerprint data (b) graphically illustrates 2D fingerprint data [25]

### 2.1.3 Frustrated Total Internal Reflection (FTIR)

Frustrated Total Internal Reflection is an optical sensor type and is the oldest and most used live-scan acquisition technique [26]. FTIR passes light through a clear prism or platen [26] [27]. The light is reflected off the finger in contact with the prism or platen. The image sensor then receives the reflected light; an example using a prism is shown below in Figure 4. The resulting image is an extraction of the fingerprint, with ridges that scatter the light and appear black in the final image. The valleys are not in contact with the prism leading the light to be reflected and continue to the sensor to appear white in the image. The receiving image sensor is either a Charge Coupled Device (CCD) or Complementary Metal Oxide Semiconductor (CMOS)

image sensor that both convert photons from the reflected light into electrons that can be interpreted into the resulting image with CMOS and CCD having different benefits over each other based on the application [28].

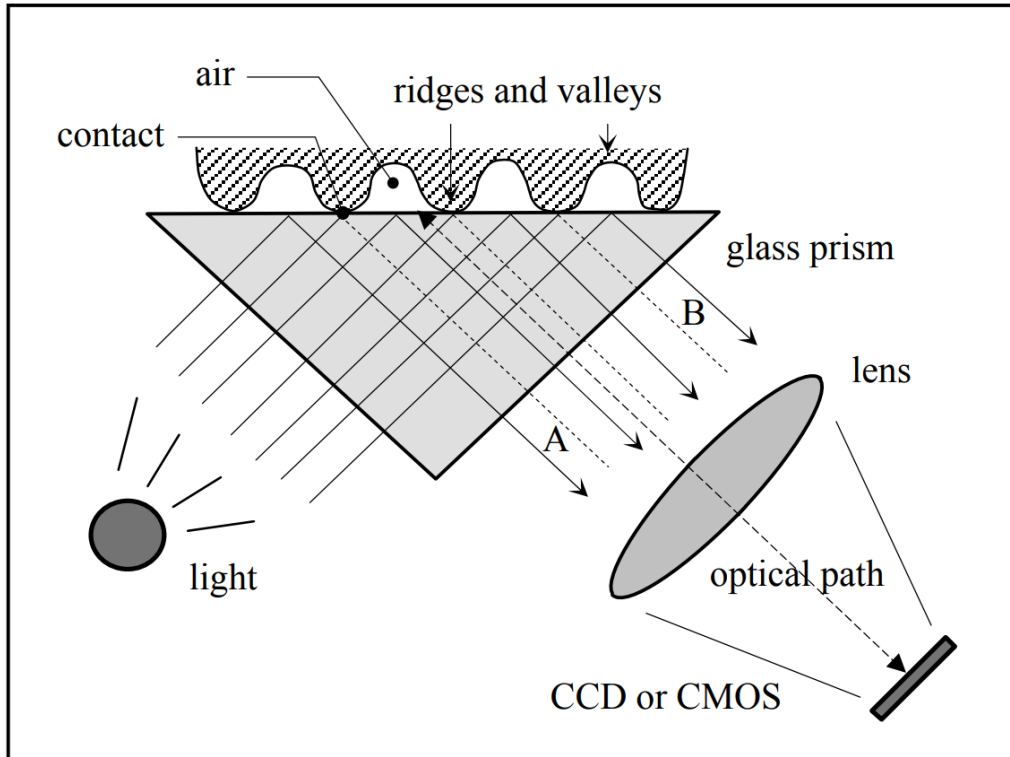


Figure 4 FTIR-based fingerprint sensor operation [26]

## 2.1.4 Polarized Reflected Light

Polarized Reflected Light is a method for capturing contactless fingerprints where a light source is used to illuminate and reflect light from a finger; the reflected light is then passed through a liquid crystal panel (LCP) and birefringent element before reaching the image capture device [29]. The resulting capture comprises multiple images of different rotations and polarization orientations which can be reconstructed into a simulated rolled fingerprint [29]. The fingerprint's depth and structural features are calculated using a depth-from-focus algorithm that

estimates the 3D surface from a set of multiple images using differences in the depth of focus [29] [30]. The resulting calculations can create a 2D fingerprint representation from the simulated rolled fingerprint.

## 2.2 Matching and Recognition

### 2.2.1 Fingerprint Minutiae

Fingerprints consist of ridges and valleys that can be categorized into patterns such as whirls, loops, and arches, further classified as level 1 feature extraction [31]. Level 2 feature extraction involves looking closer there are discontinuities in the ridges that can be classified and mapped as minutiae points [31] [32]. The individual classification of minutiae points is based on the shape of the ridge, and whether it is ending or splitting common types of minutiae are shown in Figure 5 below. When working with minutiae, two other factors that can hurt the performance of a fingerprint are missing minutiae, which can occur when the same fingerprint is recorded multiple times at different positions and angles or if the print was a single static impression and not a roll [33]. Missing minutiae can be mitigated by combining multiple captures from the same finger to create a composite image through mosaicing [33]. Spurious minutiae are the other factor that can occur, and is when the extraction method picks up or creates artifacts in the fingerprint, creating points that appear to be minutia that does not exist in the original fingerprint [34]. Figure 6 shows both examples of minutiae failing to be detected and spurious minutiae being detected as genuine minutiae; the combined occurrence of both will lower the match performance of a genuine pair.








	Termination
	Bifurcation
	Lake
	Independent ridge
	Point or island
	Spur
	Crossover

Figure 5 The most common minutiae types [32]

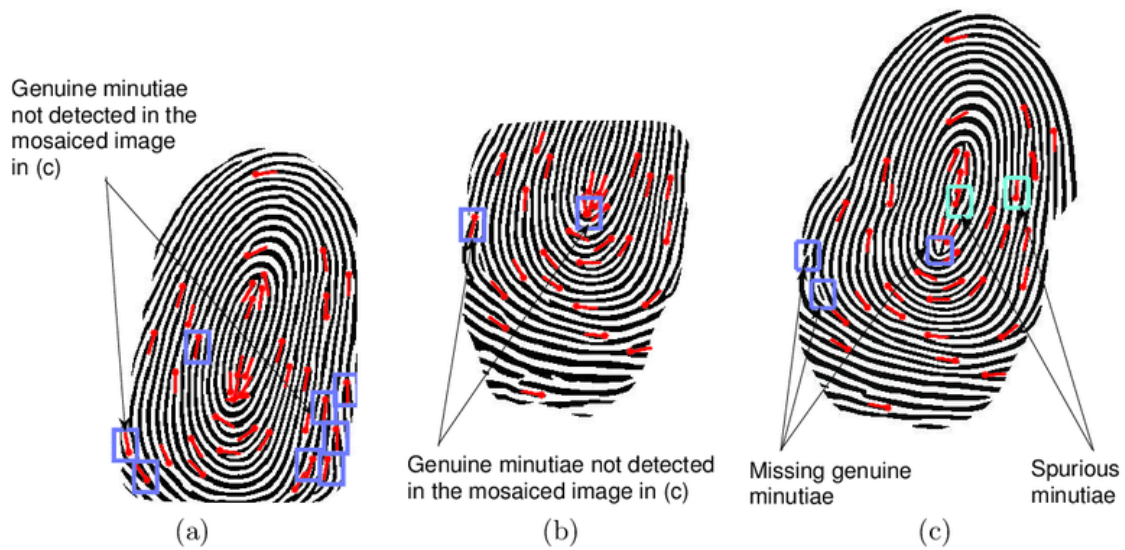


Figure 6 Spurious minutiae and missing genuine minutiae. (a) Impression 1 (I1); (b) Impression 2 (I2); (c) Mosaiced image. [33]



## 2.2.2 Fingerprint Matching

Fingerprint matching compares two or more fingerprints through correlation, minutiae, and non-minutiae features [26]. Correlation-based matching compares two superimposed fingerprints by aligning the two prints at corresponding pixels using different displacements and rotations. Meanwhile, minutiae matching attempts to create pairs of minutiae points between the different fingerprints [26]. Feature-based extraction is readily used when one or both fingerprints being compared are low-quality, and the minutiae cannot be readily extracted. Instead, the print's more prominent features and patterns are used to compare the prints [26].

Before matching many fingerprints, matching systems must preprocess the fingerprint images to be compared. The original images are usually in grayscale and are converted into a binarized version through binarization that reduces the range of all pixels below a threshold to 0 for valleys and values above the threshold to 1 for ridges [35]. Additionally, preprocessing could include block filtering to reduce the thickness of the ridge lines to only a single pixel to improve the extraction of the minutiae points [35]. Figure 7 below shows an example of a fingerprint before and after binarization. The most significant changes can be seen along the edge of the print, with some ridges being removed while others are darkened. Figure 8 continues the processing and shows the same fingerprint in Figure 7(b) with the additional application of block filtering.



Figure 7 (a) Original Fingerprint (b) Binarized image [35].



Figure 8 (a) Binarized Fingerprint (b) Image after thinning [35]

Minutiae matching is the most common and well-known fingerprint-matching method [26]. Each of the matchers used in this thesis uses minutiae matching as the primary method of quantifying the similarities of fingerprints. A standard method of minutiae matching assigns each minutiae point a location value based on the points' location in the image and an angle [26]. Minutiae points are then compared between the fingerprint images based on the location and rotation differences, and points that fall within a defined tolerance are considered pairs [26]. A similar method defines a search distance around the minutiae points of one fingerprint's minutiae

template. As long as only a single minutiae from the compared minutiae template falls within the area, then the points can be compared as seen in Figure 9,  $m_1$  and  $m_2''$  failed to match while all other points had a pair, though  $m_3$  and  $m_6''$  failed due to the significant difference in angle. A similarity score is produced from the comparison, with a simple similarity score being from the number of successful minutiae pairs compared to half the total number of minutiae points [26]. Generalized minutiae matching pipeline that shows the pairing and discrimination of minutiae points is shown in Figure 10.

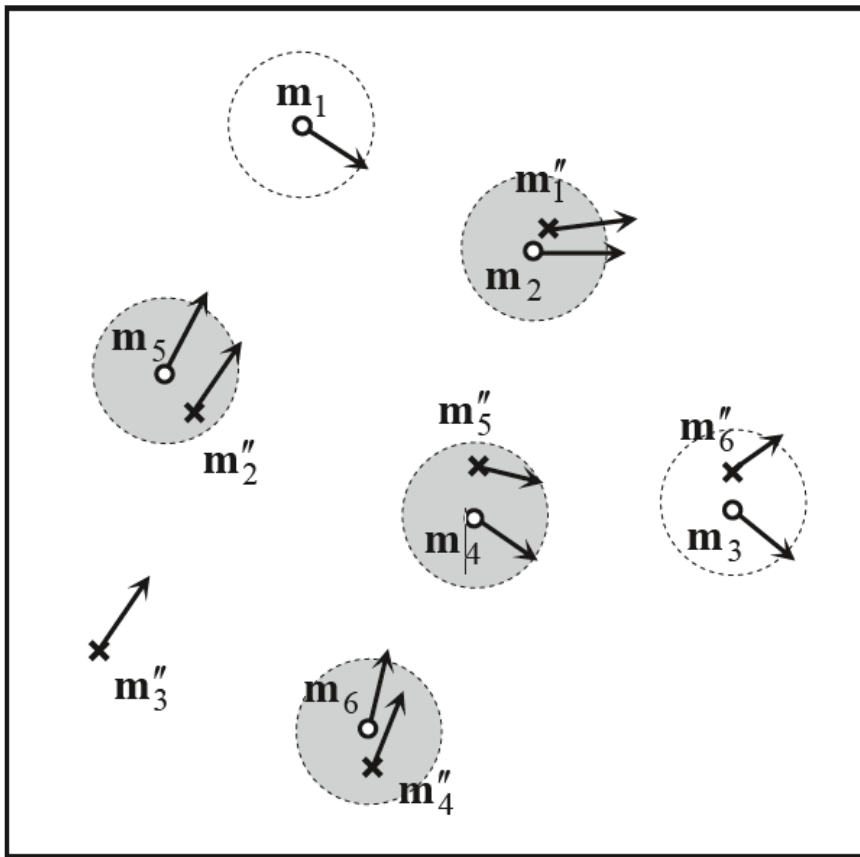


Figure 9 Minutiae matching using distance [26]

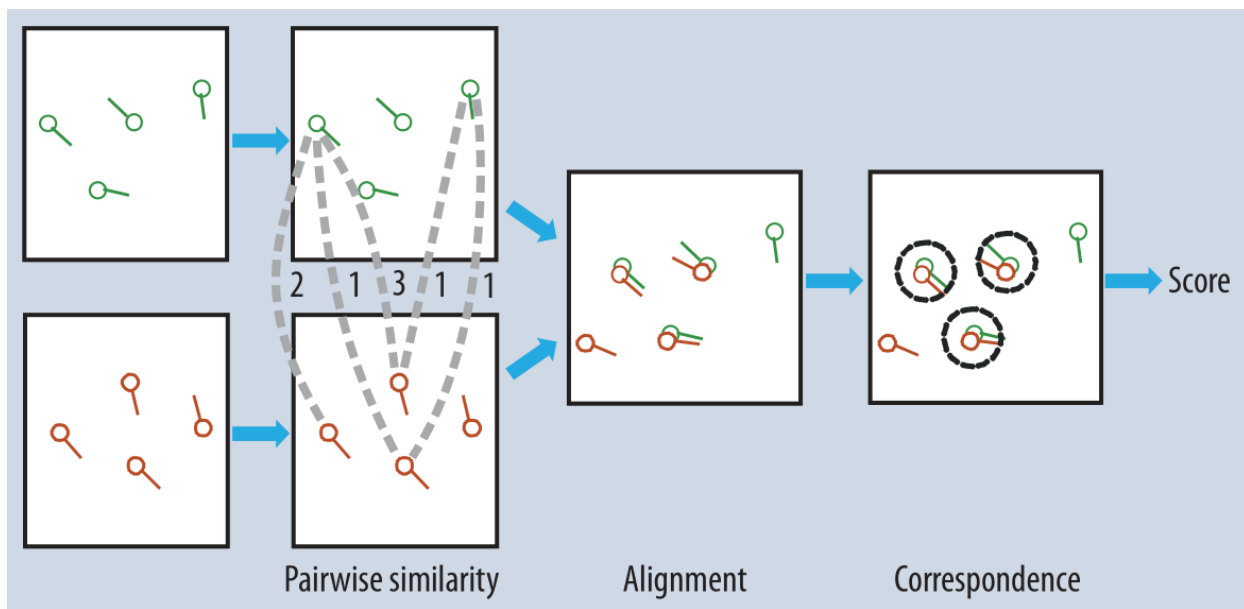


Figure 10 Typical minutiae matching algorithm [36]

### 2.2.3 Bozorth3

The Bozorth3 matcher is an open-source fingerprint matcher from NIST through their NBIS software package [37]. The Bozorth3 matcher performs minutiae comparisons from already enrolled fingerprints processed using the included MINDTCT software [37]. MINDTCT extracts minutiae point coordinates and exports a corresponding file containing the locations of the detected minutiae as a list of raw values. Bozorth3 is a publicly available version of NIST's internal matching algorithm called Bozorth98 and is functionally identical [37]. Bozorth3 is rotation and translation invariant and only uses the minutiae points for matching based on preprocessing from MINDTCT, assigning each minutiae point an  $(x, y)$  value and an orientation value 't' [37].

## 2.3 Metrics

### 2.3.1 Performance FMR FNMR

The performance of a dataset can be measured using the similarity scores generated by comparing each fingerprint in one set- such as comparing a probe set to each image in a gallery set. The two types of errors that a matcher can have been False Match Rate (FMR) when an image is matched to an imposter and False Nonmatch Rate (FNMR) when the image fails to match the genuine image [36]. FMR and FNMR are defined by a threshold set before measuring performance, with any similarity score falling above the threshold classifying as a match and scores below are nonmatches; the matches are then categorized into whether they match was correctly identified, and in the case of being incorrectly identified the match adds to the FMR [36]. Similarly, if a nonmatch was incorrectly identified, then the nonmatch adds to the FNMR [26] [36]. Equation 1 shows both equations for calculating FNMR and FMR with (a) FNMR being a simple ratio of the total number of genuines rejected divided by the total genuines, and (b) FMR being the number of imposters accepted divided by the total imposters; a simplified version of the equations are shown in Equation 2.

*Equation 1 (a) the integral to calculate the FNMR (b) the integral to calculate the FMR*

$\text{FNMR} = \int_0^t p(s H_1)$	$\text{FMR} = \int_t^1 p(s H_0)$
$p(s H_1)$ is the probability of a false nonmatch (a)	$p(s H_0)$ is the probability of a false match (b)

*Equation 2 Simplified explanation of (a) FNMR equation and (b) FMR equation*

$\text{FNMR} = \frac{\text{Number of Genuines Rejected}}{\text{Total Genuines}}$	$\text{FMR} = \frac{\text{Number of Imposters Accepted}}{\text{Total Imposters}}$
<b>(a)</b>	<b>(b)</b>

## 2.3.2 ROC AUC

The Receiver Operating Characteristic Curve shows the relationship between the true accept rate (TAR), also referred to as sensitivity, and the FMR, also referred to as inverse specificity, with each point on the curve representing the TAR and FMR at a decision threshold [38]. ROC is further described by the area under the curve (AUC), representing a performance summary [38]. An AUC of 0.5 represents a random guess, while any value greater than 0.5 shows more than a random guess being made, with an AUC of 1.0 showing perfect performance [38] [39]. Similarly, a perfect ROC curve closely traces the left and top of the graph, while a system performing random guesses would be a 45-degree line across the center [38] [40]. An example ROC curve is shown below in Figure 11.

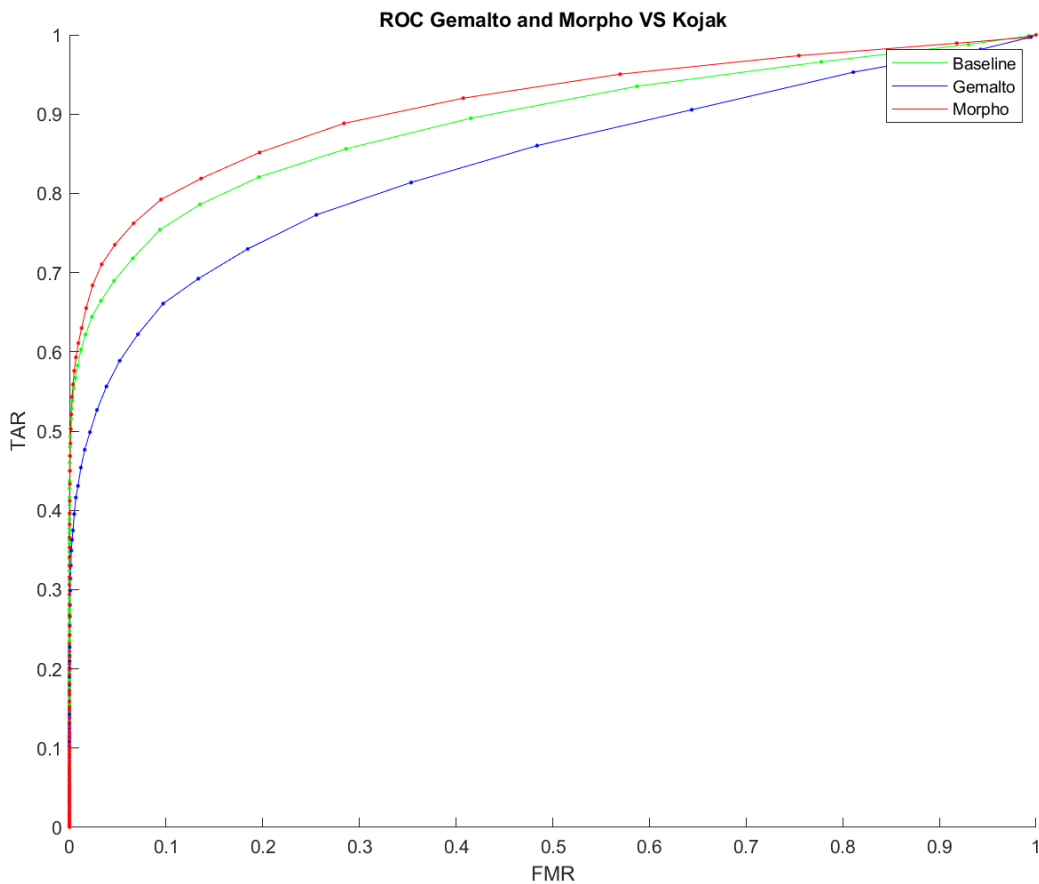


*Figure 11 Example ROC curve*

### 2.3.3 DET EER

The Detection Error Tradeoff (DET) Curve is a common way to represent the performance of biometric systems by showing the relationship between the false nonmatch rate (FNMR) and false match rate (FMR) [41] [42]. Like the ROC curve, each point on the graph represents the FNMR vs. the FMR at that threshold, with FNMR being the inverse of the true accept rate (TAR) [41]. The equal error rate (EER) helps describe the DET and is the location on the curve where the FNMR and FMR are equal; a lower EER generally shows a higher accuracy [43]. An example DET curve is shown below in Figure 12.

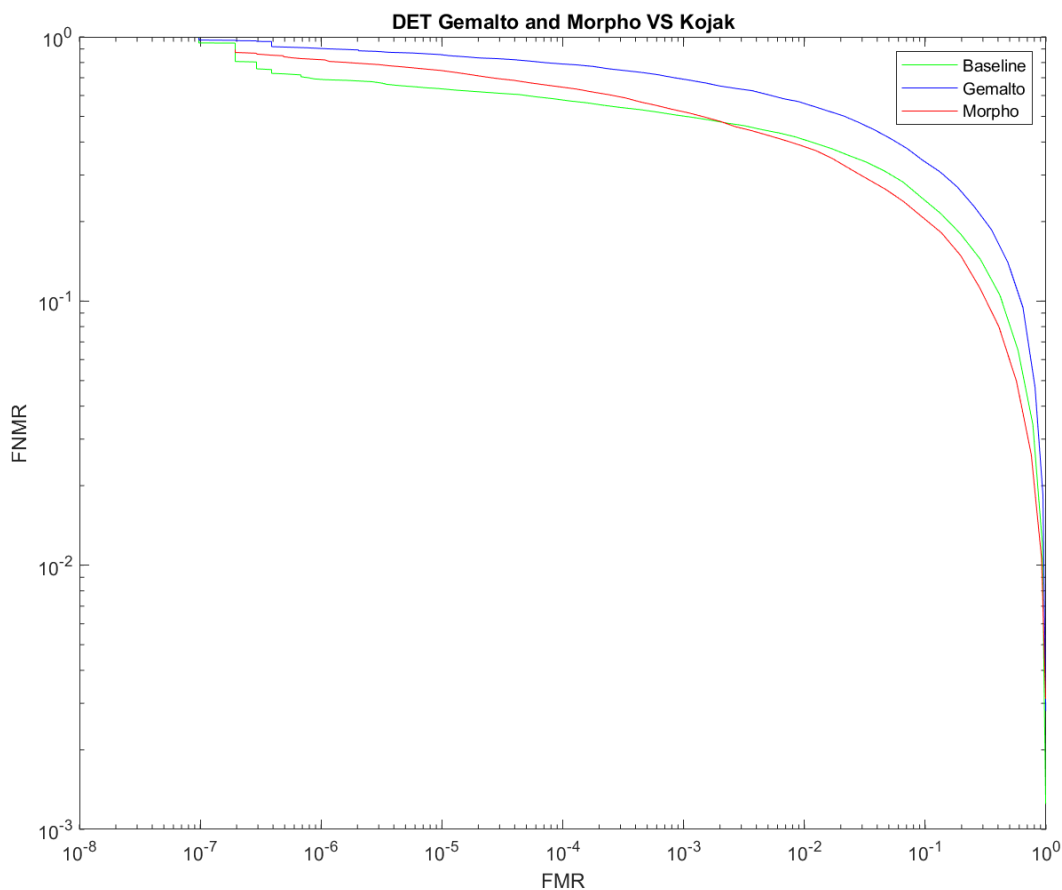


Figure 12 Example DET curve

### 2.3.4 99<sup>th</sup> Percentile Non-Mated Score Differential Performance

In *The Effect of Broad and Specific Demographic Homogeneity on the Imposter Distribution and False Match Rates in Face Recognition Algorithm Performance* [13], authors John J. Howard and Arun R. Vemury use Non-Mated match scores above a certain percentile to view the potential impact of demographic homogeneity on face recognition match performance [13]. The idea of the metric was to take the top 99<sup>th</sup> percentile of non-mated matches and separate them into different categories based on a mix of demographic factors being the same or different between the gallery and probe image [13]. The specific demographics used in the paper



were race, gender, and age; age was grouped by ten years, and if the non-mated match were less than ten years of the age difference, then the age would be counted as the same [13]. The reasoning behind limiting the non-mated scores to only a high percentile was based on the idea that the tails of the genuine and imposter distribution drive biometric error rates, with Figure 13 below showing a general diagram of score distributions for a matching experiment [13].

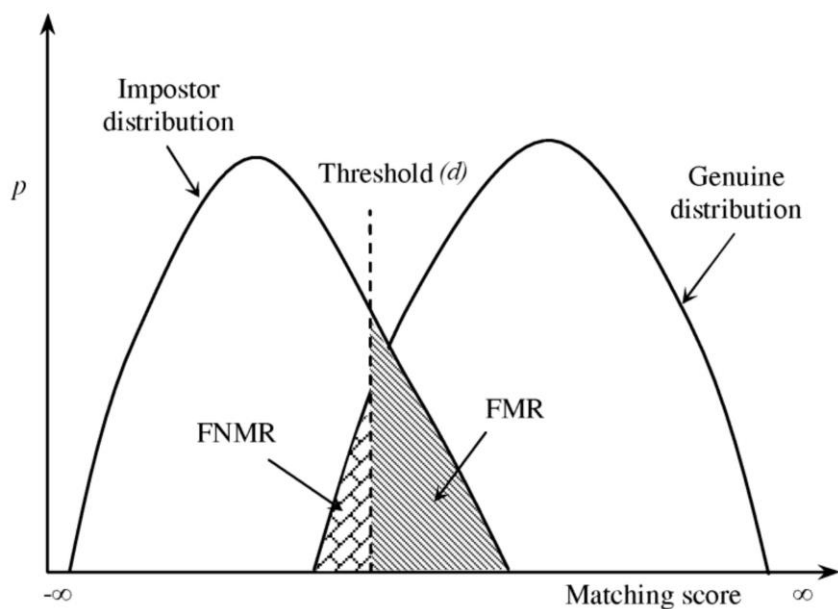


*Figure 13 General distribution diagram of imposter scores and genuine scores showing additional information describing the classification of the FMR and FNMR for a declared threshold [44]*

### 2.3.5 NIST Fingerprint Image Quality

The National Institute of Standards and Technology (NIST) released a fingerprint quality measurement software in 2004 called NIST Fingerprint Image Quality (NFIQ), with the most recent version being NFIQ2, released in 2014 [9]. NFIQ was designed to link the image quality score, or an image processed through the software to the expected match performance of the image [9]. The original NFIQ software releases a score for each image on a scale from 1-5, while

the new system NFIQ2 uses a 1-100 scoring system [9]. The image quality score generated by the software is created using random forest classification that was trained using a dataset of fingerprint images with either a high NFIQ 1.0 score or a low score [9]. Images processed through the network are given a probability multiplied by one hundred to generate the NFIQ2 quality score.

Additionally, NFIQ2 has a set of quality features to further describe the image by generating additional scores using local and global features of the fingerprint [9]. The intended goal of the algorithms is to generate quality scores on the local features of the fingerprint by dividing the fingerprint into smaller blocks that are each individually processed to determine a quality score of the global features [9]. NFIQ2 was designed to be used only on contact fingerprints; the extended application of NFIQ2 on contactless and cellphone fingerprints was not intended at the time of development though there is currently no newer version of NFIQ that is designed for contactless and cellphone fingerprint images.

### 2.3.6 Skin Reflectance

The skin reflectance measurement used in this thesis includes five values, melanin, erythema, and the CIELAB color space making up the last three values. CIELAB color space was created in 1976 by the International Commission on Illumination as a universal colorimetric reference system [45]. The CIELAB is measured in  $L^*a^*b^*$  with  $L^*$  representing the lightness,  $a^*$  representing an axis that extends from red to green, and  $b^*$  representing a third axis ranging from yellow to blue, as shown below in Figure 14 [45]. Melanin describes a group of molecules that function as a pigment found in skin and hair that acts as protection from ultraviolet radiation [46]. High levels of melanin are seen as darker skin, while lower levels are seen as pale skin.

Erythema is a visible redness of the skin caused by excess blood in the capillaries [47]. Higher erythema levels can easily be observed in paler skin but are still present in darker skin.

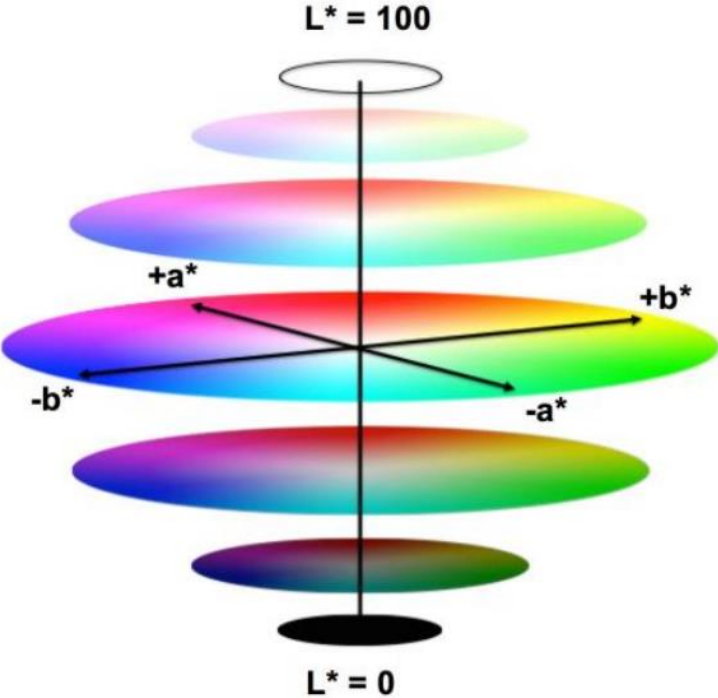


Figure 14 a representation of  $L^*a^*b^*$  color space using a 3D plot [45].

# Chapter 3: Dataset

## 3.1 Data Collection

For all experiments conducted as part of this thesis, the data was obtained from a previous data collection effort performed in the Biometrics Collection Lab under the Institutional IRB# 2001870127. The dataset was focused on collecting a wide variety of modalities, including contact fingerprints, contactless fingerprints, and finger photo contactless fingerprints taken using cellphone apps. The collection consisted of three locations, all in the same room; the first location was visited when the participant entered the room. The participants would go through consenting, and demographic information would additionally be collected that including age, gender, and ethnicity, along with being assigned a seven-digit random identification number that would be used to label all data collected during their participation in the collection. Additionally, each participant's palm and the back of their hand were scanned using the DSM III from Cortex technology to gather skin reflectance measurements. The second location had two stations, one for the contact fingerprint capture devices and the third for the two contactless fingerprint capture devices. The second location contained four stations. One station was for capturing the hand geometry of each participant's hands on both sides using a DSLR, followed by a station for capturing fingerphoto images of the participant's hands using the Galaxy S20 and S21. The next station was the controlled setting for Veridium's 4 Fingers TouchlessID system, and both phones were placed into a mount to record the fingerprints from the app. The fourth station was the controlled setting for Sciometric's Slapshot system for both cellphones. Both phone applications were then repeated in front of all the stations over the floor for both applications. A diagram of both images of the stations and the room is shown below in Figure 15.

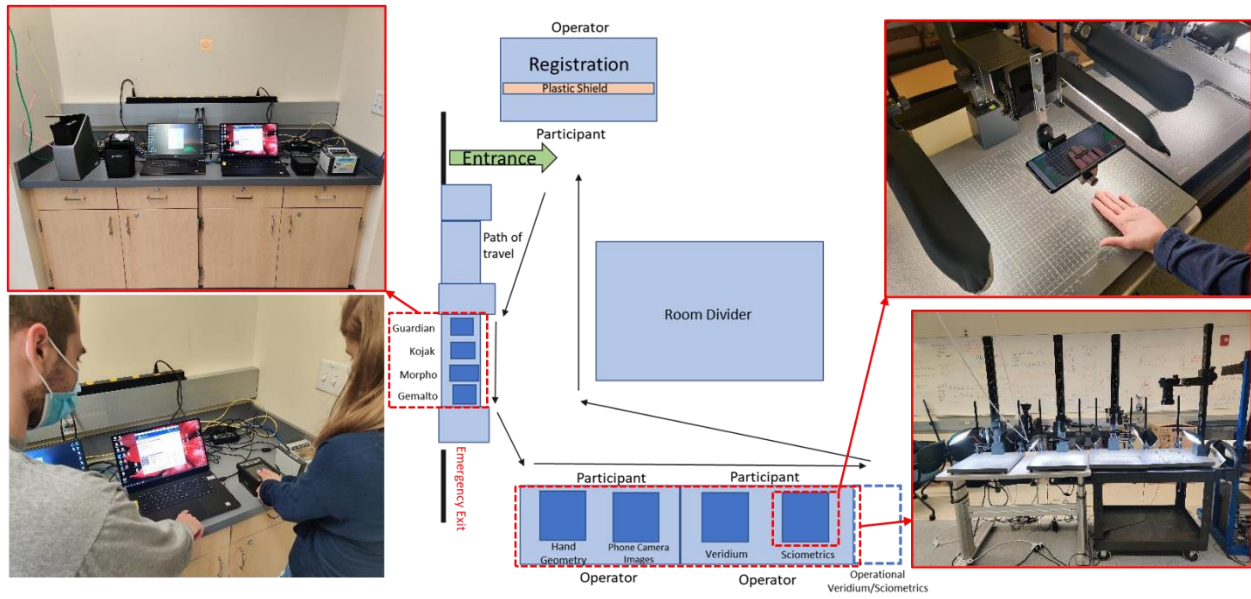


Figure 15 Collection Process and Organization

## 3.2 Description of the Dataset

The dataset includes 500 unique individuals with fingerprints provided across three major formats, contact fingerprints, contactless fingerprints, and fingerphoto fingerprints. For each modality, at least all eight fingers were recorded; thumbs were not recorded for all modalities. The contact fingerprints were taken on two separate devices, each capturing a rolled fingerprint set and a plain fingerprint set which will be referred to as Slap in the datasets. The first contact fingerprint device was the Crossmatch Guardian from Neurotechnology, an optical livescan device that uses frustrated total internal reflection (FTIR) for fingerprint capturing [48]. The second contact device was the Kojak from Integrated Biometrics which uses a Light Emitting Sensor (LES) thin-film transistor [49]. The contactless fingerprint sets from the dataset were captured using two separate devices, each collecting one set of the participant's fingers. The first device was an older model of Idemia's MorphoWave [50]. The second sensor was a contactless fingerprint sensor from Gemalto's Cogent Systems. Lastly, two fingerprint fingerphoto capturing applications were used and deployed on two cellphones. The first cellphone was the Galaxy S20, and the second was the Galaxy S21.

Additionally, cellphone recordings were taken in two scenarios, the first being a controlled well, illuminated environment with a controlled distance from the hand to the cellphone which will be referred to as the Stand setting, and the second was an 'in the wild' scenario that used room lighting with no controlled distance or background which will be referred to as the Operational setting or Op setting. The first application was Veridium's 4 Fingers TouchlessID system. The second application was Sciometric's Slapshot system. Each cellphone application performed its own 'black-box' processing, so the method of ridge

extraction from the original fingerphotos is unknown. A breakdown of the demographic information of the dataset is detailed below in Figure 16, Figure 17, and Figure 18.

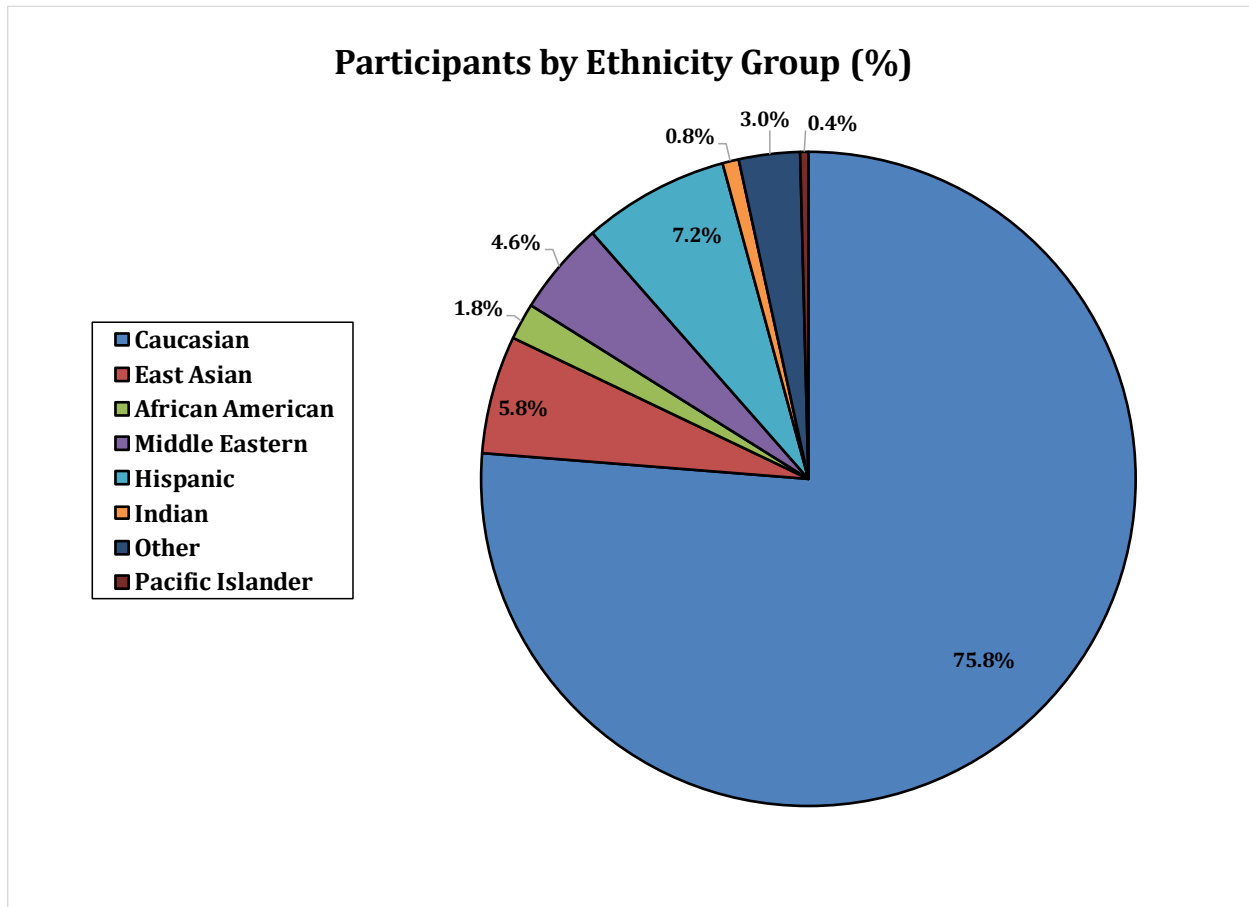


*Figure 16 distribution of participants by ethnicity*

**Participants by Age Group (%)**

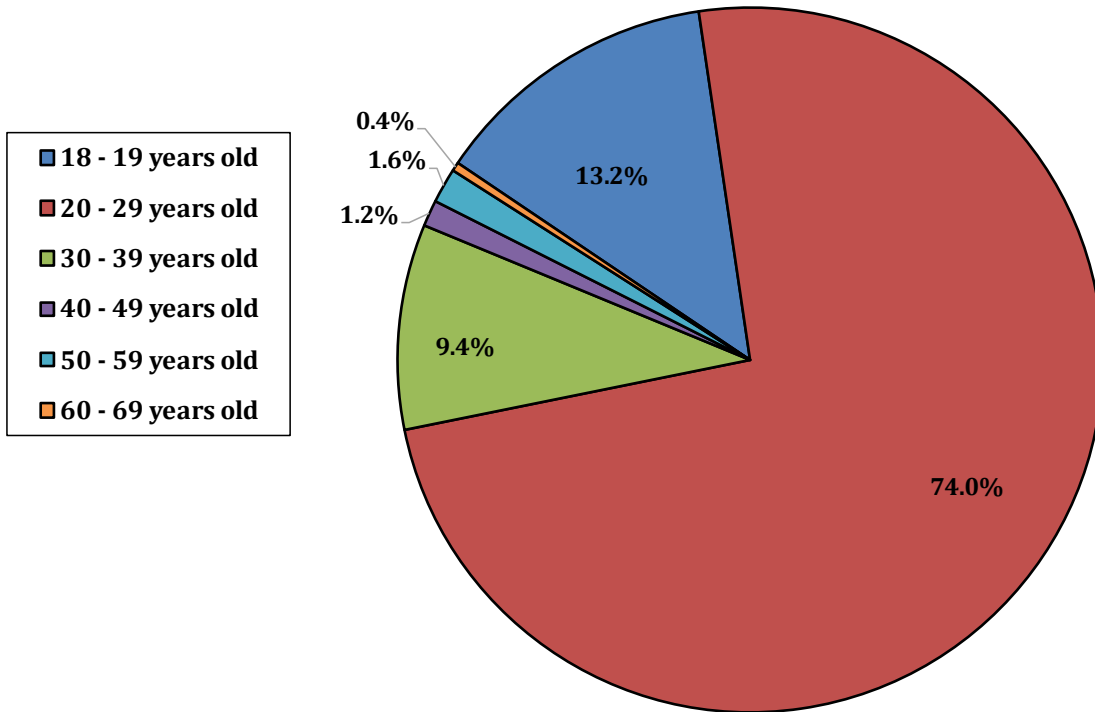


*Figure 17 distribution of participants by age*



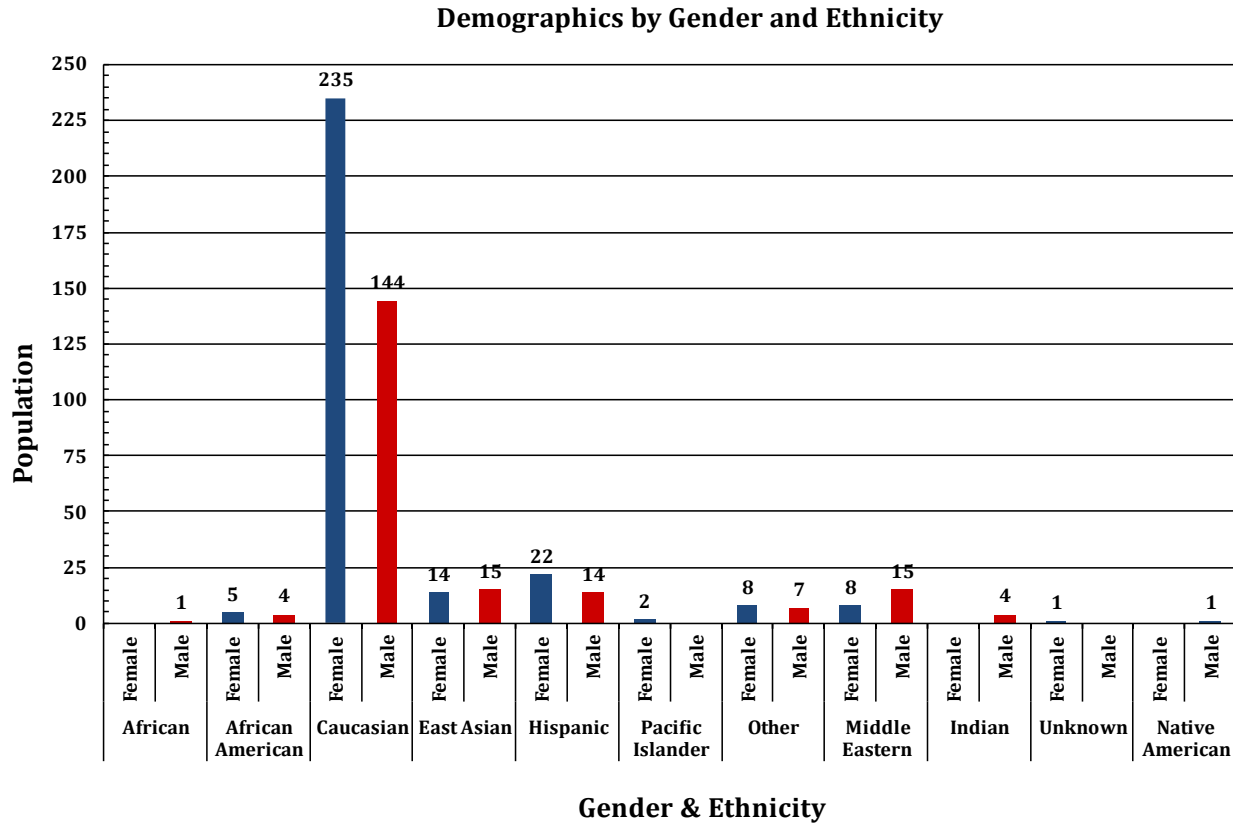


*Figure 18 distribution of participants by gender and ethnicity*

Additionally, measurements of the participant's skin color were taken using the Cortex Technology DSM III sensor for additional demographic metrics other than only self-reported information [51]. The skin reflectance recordings were measured in the CIEL\*a\*b\* color space with an additional Melanin and Erythema reading. In CIEL\*a\*b\* color space L\* is the measurement of perceptual light, and a\* and b\* are measurements for the red and green and blue and yellow axes, respectively [52]. The skin color ranges are also found below, listed in Table 1, and the mean and median values are listed in Table 2 by the self-reported ethnicity of the subject. Additionally, Figure 19 through Figure 23 show the distributions for each skin reflectance measurement as a set of boxplots—each category showing a different ethnicity. In total, there are

fourteen unique datasets. Four captures are from the contact fingerprint sensors, two datasets are plain fingerprints, and two are rolled fingerprints. Two captures are from contactless fingerprint sensors. Eight captures are from fingerphoto capturing cellphone applications, four are controlled settings, and four are operational settings. Of each of the four, two were taken on the Galaxy S20 and two on the S21, and each of the two captures was taken using different fingerphoto apps. Samples images from each of the devices are shown in Table 3. The dataset used for all experiments consisted of 3207 unique fingerprint images for each device; some fingerprints were removed before conducting experiments leading to a set smaller than the original dataset due to missing fingers from one set and the removal of that finger from each over set if no replacement could be found from suitable errors that were saved. Additionally, since some devices did not collect thumbprints, the experiment dataset consisted of fingerprints from only the four fingers on the left and right hands. Table 4 summarizes the dataset composition, including the number of sessions recorded on each device and whether the data was a rolled or slap fingerprint, the cellphone applications will be referred to by their company names, Sciometrics and Veridium, in the table.

Ethnicity	Melanin	Erythema	L*	a*	b*
African American 10	29.88 – 56.43	9.81 - 20.33	20.17 - 42.15	13.58 - 21.87	9.44 - 16.83
Caucasian 379	16.52 – 48.52	4.02 - 19.74	17.92 - 59.01	6.55 - 25.33	1.62 - 20.92
East Asian 27	27.57 – 47.41	8.78 - 15.99	25.5 - 44.8	11.59 - 21.45	10.69 - 15.4
Hispanic 34	23.86 – 38.52	7.74 - 18.23	30.24 - 47.64	11.64 - 22.1	9.35 - 16.87
Indian 5	30.52 – 49.69	10.66 - 17.17	23.63 - 39.8	14.28 - 18.26	10.61 - 17.28
Middle Eastern 25	23.64 – 41.44	9.47 - 16.84	32.01 - 46.81	13.77 - 23.62	8.61 - 21.03
Native American 1	29.73	12.08	41.12	17.73	15.04
Pacific Islander 2	29.87	8.57	43.41	12.71	11.25
Other 17	26.15 – 55.55	8.34 - 17.77	20.02 - 45.82	12.28 - 21.42	9.64 - 11.25
All 500	31 – 56.43	4.02 - 20.33	17.92 - 59.01	6.55 - 25.33	1.62 - 21.03

*Table 1 skin reflectance ranges by self-reported ethnicity using CIELab color space with Melanin and Erythema*

Ethnicity	Melanin	Erythema	L*	a*	b*
	Mean/Median	Mean/Median	Mean/Median	Mean/Median	Mean/Median
African American 10	37.68/ 34.14	14.45/13.47	33.81/36.13	17.30/18.18	13.94/14.66
Caucasian 379	29.04/28.44	10.32/10.08	43.28/43.91	15.25/15.15	12.18/11.93
East Asian 27	32.92/32.54	12.25/12.25	38.48/38.93	16.5/16.68	13.58/13.55
Hispanic 34	30.33/30.92	11.76/11.14	40.98/40.5	16.76/16.77	13.25/13.47
Indian 5	38.48/37.76	13.95/13.35	33.21/33.75	16.31/15.92	13.42/12.31
Middle Eastern 25	32.62/31.94	12.46/12.57	38.53/39.11	16.82/17.08	14.04/13.90
Native American 1	29.73/29.73	12.08/12.08	41.12/41.12	17.73/17.73	15.04/15.04
Pacific Islander 2	29.87/29.87	8.57/8.57	43.41/43.41	12.71/12.71	11.25/11.25
Other 17	37.54/33.64	13.92/13.94	34.3/36.83	17.01/17.67	13.15/13.09
All 500	30.1/29.18	10.88/10.73	42/42.44	15.62/15.59	12.52/12.36

*Table 2 skin reflectance mean/median by self-reported ethnicity using CIELab color space with Melanin and Erythema*

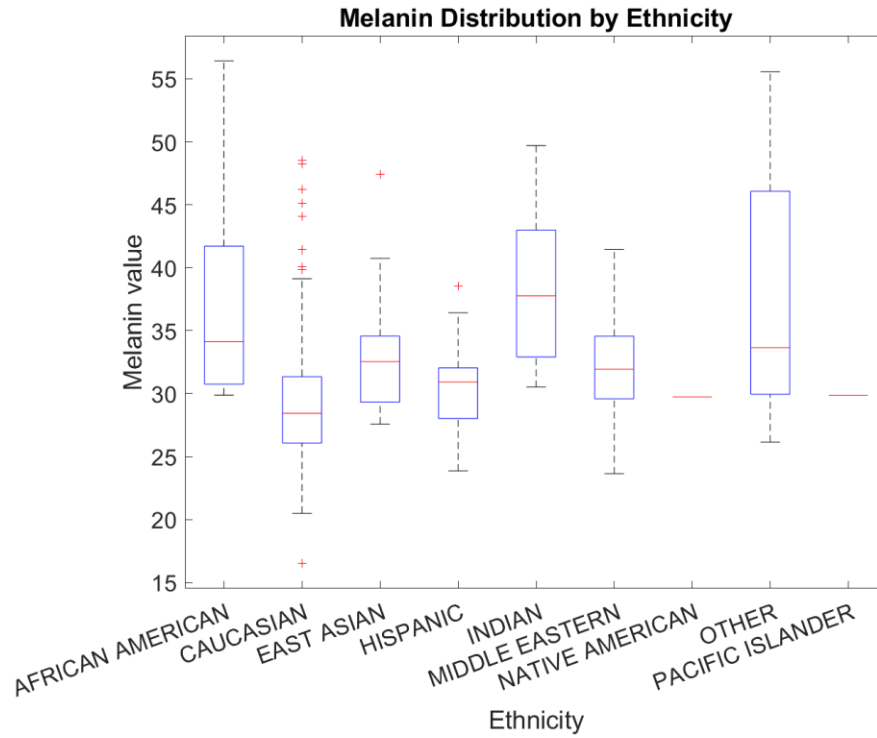


Figure 19 Dataset ethnicity distribution by melanin value

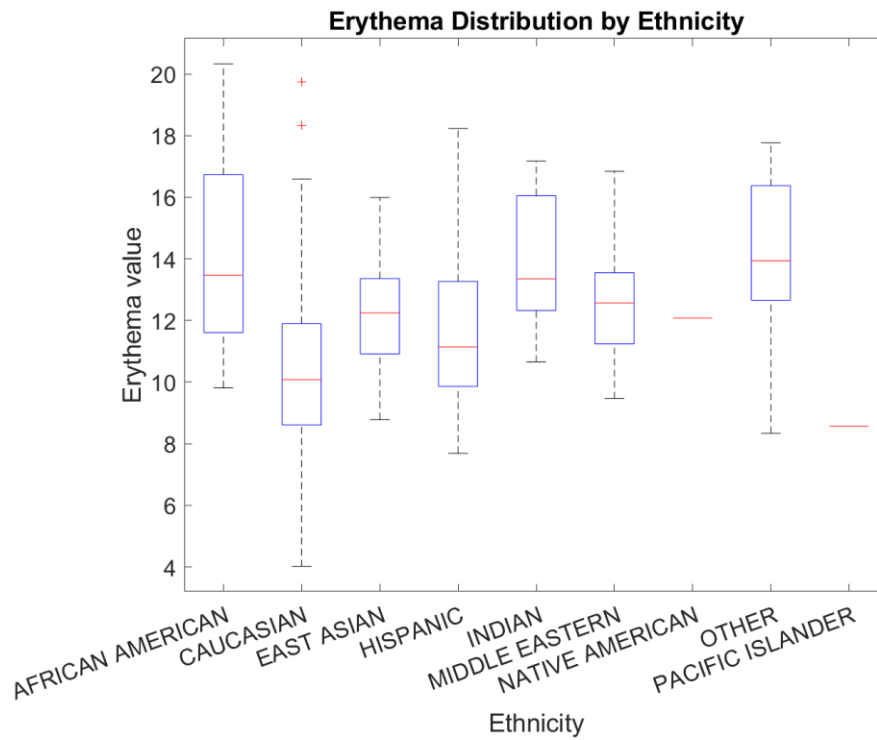


Figure 20 Dataset ethnicity distribution by erythema value

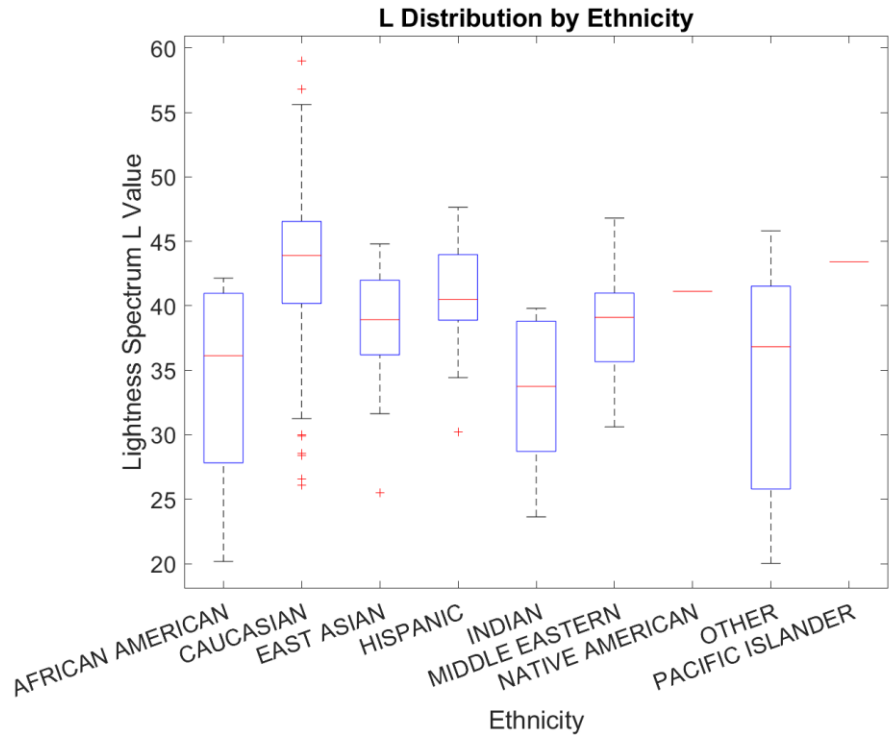


Figure 21 Dataset ethnicity distribution by  $L^*$  value

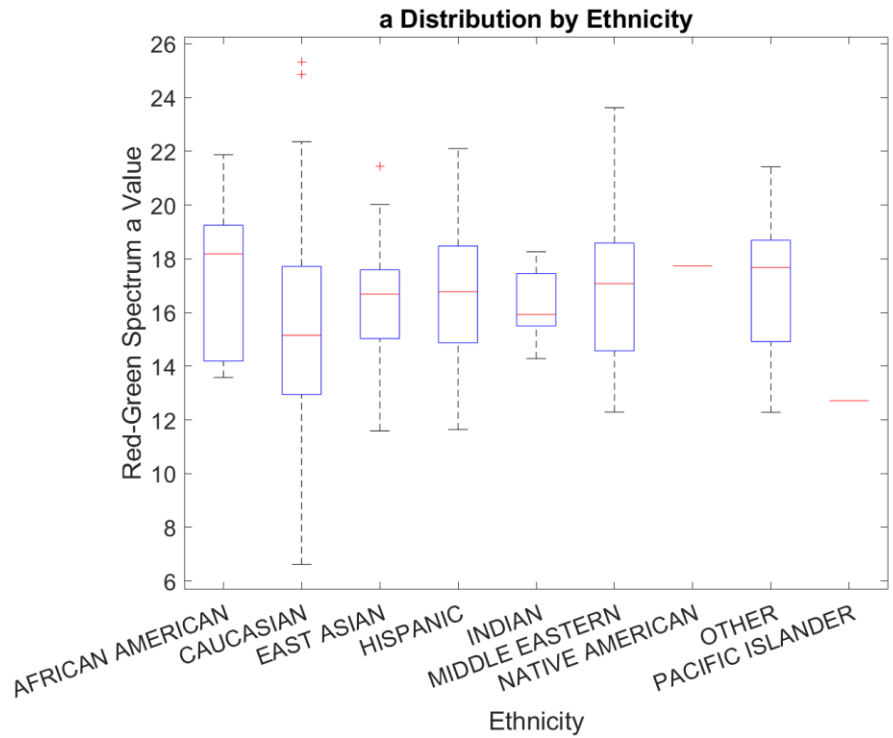


Figure 22 Dataset ethnicity distribution by  $a^*$  value

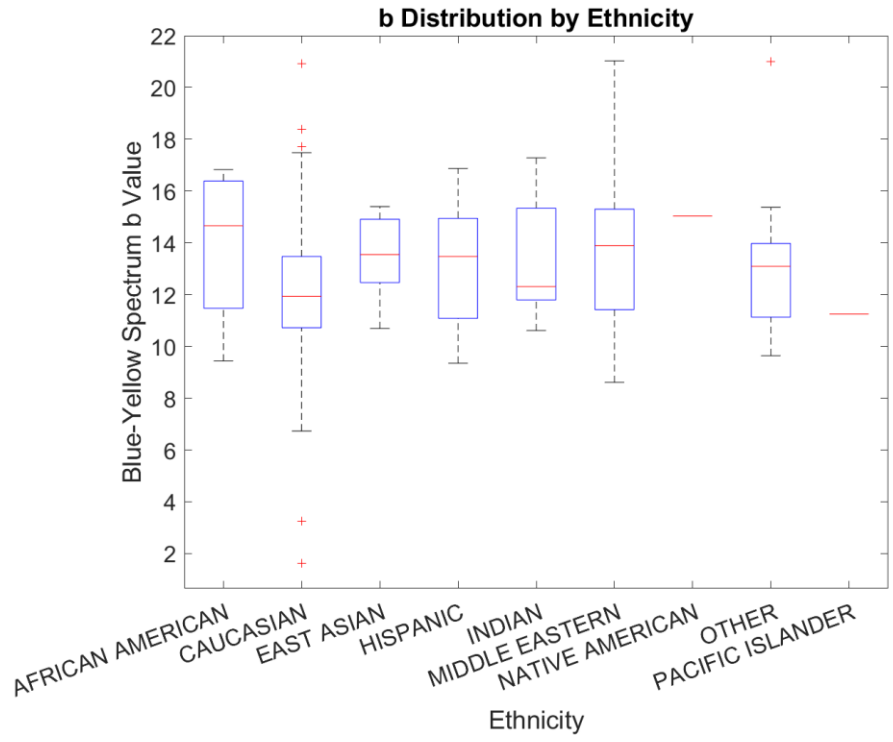
















Figure 23 Dataset ethnicity distribution by  $b^*$  value

				
Kojak Slap	Kojak Roll	Guardian Slap	Guardian Roll	Morpho
				
Gemalto	S20 Sciometrics Operational	S20 Sciometrics Controlled	S20 Veridium Operational	S20 Veridium Controlled
				
S21 Sciometrics Operational	S21 Sciometrics Controlled	S21 Veridium Operational	S21 Veridium Controlled	

*Table 3 Example fingerprints for each device and setting.*



<b>Device</b>	<b>Image Type</b>	<b>No. of Samples</b>	<b>No. of Sessions</b>	<b>Total Samples</b>
Kojak	Slaps & Rolls	2 slaps 2 thumbs 10 rolls	1	10000
Crossmatch Guardian	Slaps & Rolls	2 slaps 2 thumbs 10 rolls	1	10000
Morpho wave	Slaps	2 slaps 2 thumbs	2	10000
Cogent Gemalto	Slaps	2 slaps 2 thumbs	1	5000
S20 Controlled Sciometrics	Slaps	2 slaps	1	4000
S20 Controlled Veridium	Slaps	2 slaps	1	4000
S20 Operational Sciometrics	Slaps	2 slaps	1	4000
S20 Operational Veridium	Slaps	2 slaps	1	4000
S21 Controlled Sciometrics	Slaps	2 slaps	1	4000
S21 Controlled Veridium	Slaps	2 slaps	1	4000
S21 Operational Sciometrics	Slaps	2 slaps	1	4000
S21 Operational Veridium	Slaps	2 slaps	1	4000

*Table 4 Dataset Composition*

# Chapter 4: Experiments

## 4.1 Matching Experiment Organization

For the matching experiments, the baseline used is always the matching experiment between the Kojak Slap set as the gallery and the Guardian Slap set as the probe. In total there were three different consumer-off-the-shelf (COTS) matchers were used. The first is Innovatrics fingerprint matcher version 7.6.0.627. The second is VeriFinger 7.0. Both matchers are black-box systems, and the exact matching process is not readily known. The last matcher is the open-source, freely available Bozorth3 matcher from NIST's NBIS v5 software package [53]. Bozorth3 was added to the matcher list because it is widely available and free to use as part of NIST's NBIS package release. Including results from Bozorth3 will represent expected findings for those without access to a licensed matching system. Matchers were used as is, and no additional modifications were made to the data past the bare minimum required to enroll the fingerprints and have them recognized by the matchers. The dataset used for the VeriFinger matcher was a reduced size from the other matchers and consisted of 3069 instead of 3207. The lower number was due to rejections during enrollment, possibly caused by a partial print or an oddly small print that needed to meet minimum size requirements. The experiments were performed as one to all matches. Each fingerprint in the probe set was matched to every fingerprint in the gallery set, producing a matrix of size 3207 by 3207 for the Innovatrics and Bozorth3 matcher and 3069 by 3069 for the VeriFinger matcher for each of the experiments. Each matcher was run thirteen times, using one set as the gallery set and the other as probe sets. The gallery was always the plain set from the Kojak for all three matchers.

The results of the matchers are compiled into both a compilation of receiver operating characteristic (ROC) curves with area under the curve (AUC) values and detection error tradeoff (DET) curves with equal error (EER) rates and corresponding false nonmatch rate (FNMR) at a specific false match rate (FMR) ratio. Additional analysis of skin reflectance is reported based on each of the values recorded from the Cortex Technology DMS III. The Innovatrics, VeriFinger, and Bozorth3 results will have comparisons for the melanin and erythema distributions. The comparisons for the Innovatrics, and VeriFinger experiments will be included for the lightness, red-green, and blue-yellow measurements while further Bozorth3 comparisons will be left out due to low performance.

## 4.2 Results

### 4.2.1 Matcher AUC and EER values

Area Under the Curve values for all datasets and Matchers			
Dataset	Innovatrics	VeriFinger	Bozorth3
Kojak Roll	0.97873	0.95833	0.84301
Crossmatch Guardian Slap (baseline)	0.99398	0.98525	0.88952
Crossmatch Guardian Roll	0.99373	0.97987	0.87342
Morpho wave	0.99337	0.97872	0.91062
Cogent Gemalto	0.97004	0.94193	0.83604
S20 Stand Sciometrics	0.95612	0.93223	0.61369
S20 Stand Veridium	0.85772	0.79284	0.61506
S20 Op Sciometrics	0.96389	0.94041	0.64871
S20 Op Veridium	0.91314	0.85406	0.67909
S21 Stand Sciometrics	0.96521	0.93442	0.62395
S21 Stand Veridium	0.86963	0.80447	0.63403
S21 Op Sciometrics	0.96812	0.94231	0.66089
S21 Op Veridium	0.95066	0.89834	0.73301

*Table 5 Area Under the Curve values for all datasets and matchers.*

Based on the data shown in Table 5, the matchers can be divided by effectiveness.

Innovatrics performed the best (highest AUC values) across the board, with VeriFinger coming in second with a significant marginal drop in performance across all matching experiments, with an average drop in AUC of about 0.04. Bozorth3 had the lowest performance by a wide margin, with the contact and contactless matching experiments seeing a drop in AUC of more than 0.1. The cellphone apps had an even more significant drop exceeding 0.3 for more than half the

cellphone matching experiments. Looking between the different sets, the contact fingerprint experiments and contactless fingerprint experiments performed about equally for each matcher, with the Cogent Gemalto performing the lowest for all three matchers. Sciometrics consistently had a higher AUC for each experiment with a Veridium counterpart, except for the Bozorth3 experiments that experienced the reverse. The stand scenario in which the phones were placed in a controlled setting had similar results to the Op (Operational) setting for Sciometrics, though Veridium performed better in the Op setting compared to the Stand setting.

Innovatrics					
Dataset	EER	FNMR@FMR = 1:10	FNMR@FMR = 1:100	FNMR@FMR = 1:1000	FNMR@FMR = 1:1000
Kojak Roll	0.07555	0.12878	0.18896	0.27159	0.34768
Crossmatch Guardian Slap (baseline)	0.03016	0.04054	0.04989	0.06361	0.07671
Crossmatch Guardian Roll	0.03358	0.05176	0.06236	0.08045	0.10290
Morpho wave	0.03386	0.05426	0.07795	0.10196	0.14125
Cogent Gemalto	0.07873	0.13315	0.18959	0.24104	0.29498
S20 Stand Sciometrics	0.10719	0.20331	0.28594	0.36576	0.45401
S20 Stand Veridium	0.22130	0.46866	0.62738	0.73714	0.82569
S20 Op Sciometrics	0.09521	0.16807	0.24509	0.30683	0.37636
S20 Op Veridium	0.16990	0.33739	0.45494	0.53258	0.59900
S21 Stand Sciometrics	0.08876	0.16745	0.23137	0.29903	0.37917
S21 Stand Veridium	0.21473	0.41846	0.59713	0.69567	0.76582
S21 Op Sciometrics	0.08699	0.15341	0.21360	0.26879	0.32367
S21 Op Veridium	0.12350	0.23885	0.32180	0.39414	0.47646

*Table 6 Innovatrics EER for each dataset and FNMR@FMR ratios.*

VeriFinger					
Dataset	EER	FNMR@FMR = 1:10	FNMR@FMR = 1:100	FNMR@FMR = 1:1000	FNMR@FMR = 1:1000
Kojak Roll	0.06927	0.15249	0.15249	0.18508	0.21212
Crossmatch Guardian Slap (baseline)	0.03405	0.05148	0.05148	0.07071	0.07071
Crossmatch Guardian Roll	0.04431	0.06549	0.07136	0.08504	0.10101
Morpho wave	0.04379	0.06940	0.09254	0.11307	0.13685
Cogent Gemalto	0.10213	0.14109	0.17660	0.20984	0.24633
S20 Stand Sciometrics	0.11683	0.20137	0.26882	0.32095	0.38775
S20 Stand Veridium	0.27988	0.47638	0.58227	0.68068	0.75204
S20 Op Sciometrics	0.10865	0.17563	0.23623	0.28967	0.34604
S20 Op Veridium	0.21050	0.34148	0.44803	0.50081	0.56533
S21 Stand Sciometrics	0.10739	0.16976	0.22581	0.27403	0.34213
S21 Stand Veridium	0.27045	0.42457	0.55751	0.63245	0.70186
S21 Op Sciometrics	0.10596	0.15412	0.21180	0.25057	0.30531
S21 Op Veridium	0.14893	0.26197	0.32193	0.39557	0.43728

*Table 7 VeriFinger EER for each dataset and FNMR@FMR ratios.*

Bozorth3					
Dataset	EER	FNMR@FMR = 1:10	FNMR@FMR = 1:100	FNMR@FMR = 1:1000	FNMR@FMR = 1:1000
Kojak Roll	0.22956	0.43869	0.60094	0.70796	0.76849
Crossmatch Guardian Slap (baseline)	0.18777	0.33541	0.44587	0.51981	0.59314
Crossmatch Guardian Roll	0.20736	0.36630	0.47551	0.57379	0.64992
Morpho wave	0.15872	0.28955	0.44119	0.55008	0.65897
Cogent Gemalto	0.24130	0.44368	0.58378	0.71950	0.79906
S20 Stand Sciometrics	0.42503	0.77348	0.93541	0.98066	0.99251
S20 Stand Veridium	0.41902	0.80281	0.96193	0.99002	0.99532
S20 Op Sciometrics	0.39722	0.74228	0.90265	0.95913	0.98097
S20 Op Veridium	0.37634	0.73354	0.87363	0.92917	0.94758
S21 Stand Sciometrics	0.40929	0.78128	0.91825	0.97535	0.99158
S21 Stand Veridium	0.39799	0.78877	0.94883	0.98284	0.99126
S21 Op Sciometrics	0.39059	0.71950	0.87176	0.95070	0.97816
S21 Op Veridium	0.32732	0.63869	0.80624	0.88175	0.92605

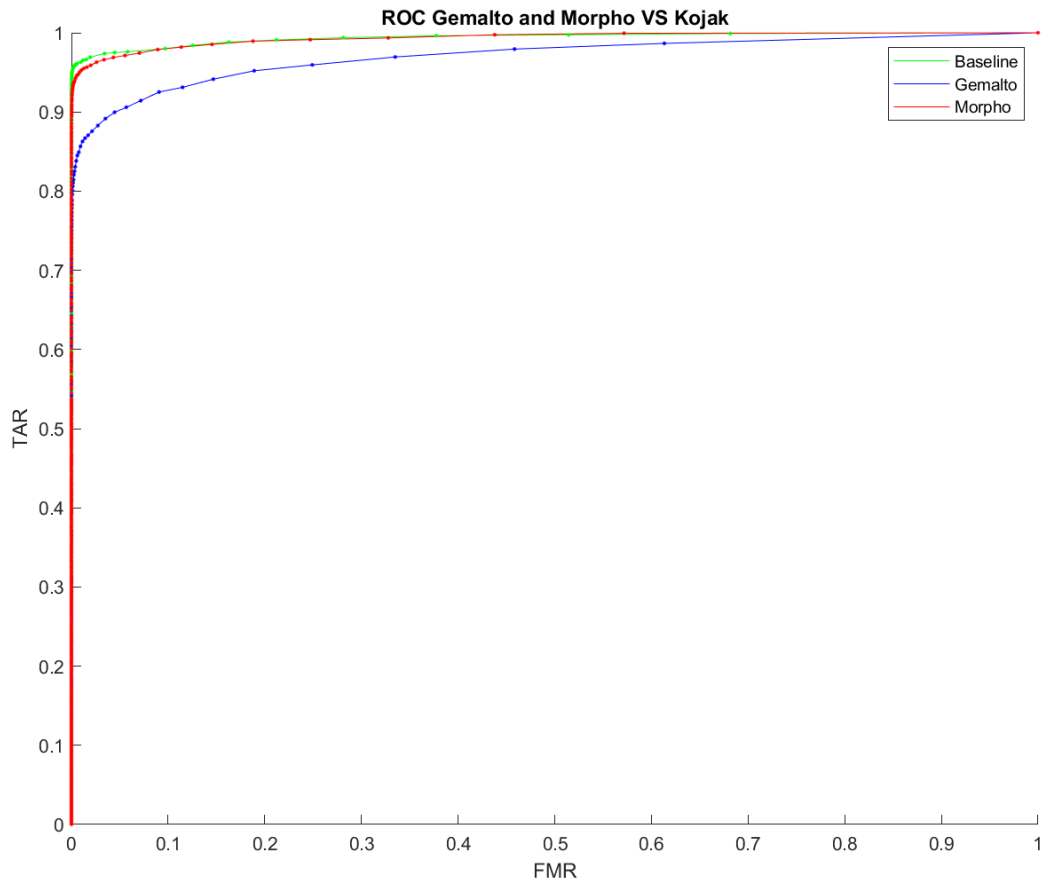
*Table 8 Bozorth3 EER for each dataset and FNMR@FMR ratios.*

Table 6, Table 7, and Table 8 show the Innovatrics, VeriFinger, and Bozorth3 results for both the EERs for each experiment and FNMR values for the corresponding FMR, respectively. With similar patterns as the AUC table, Innovatrics and VeriFinger performed about the same for EER results for each experiment, with Innovatrics having slightly lower EER values and higher FNMR ratio values for all experiments except for Kojak Roll. Bozorth3 again performed lower than the other two matchers, with the Sciometrics experiments having the highest EER values.



## 4.2.2 Matcher ROC and DET Curves

### 4.2.2.1 Innovatrics



*Figure 24 Innovatrics ROC curve Gemalto and Morpho vs Kojak.*

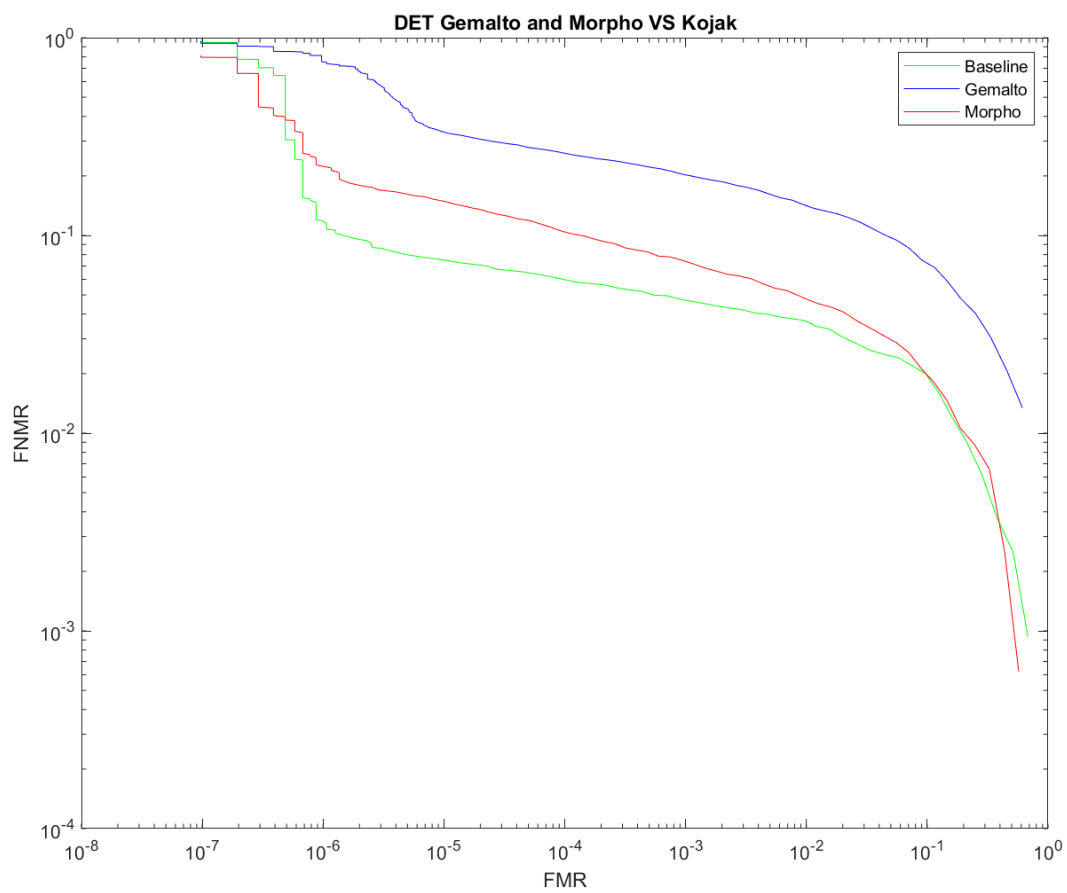


Figure 25 Innovatrics DET curve Gemalto and Morpho vs Kojak.

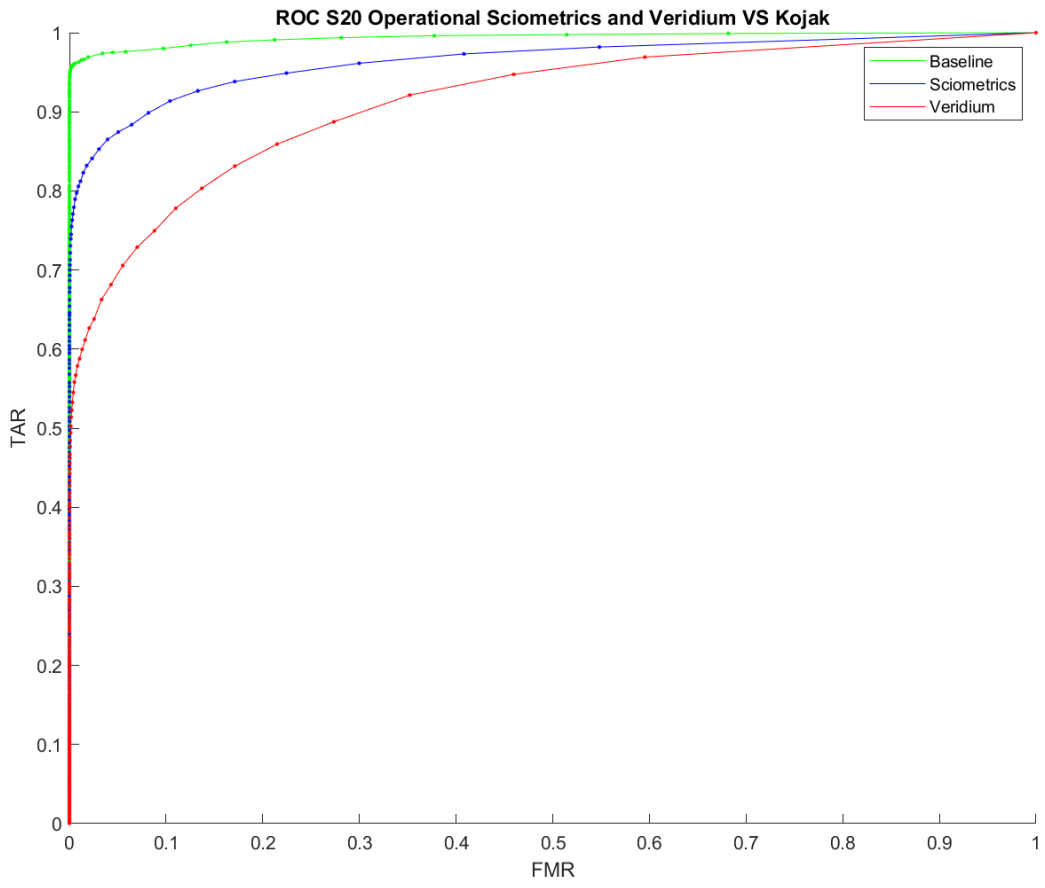


Figure 26 Innovatrics ROC curve S20 Operational Sciometrics and Veridium vs Kojak.

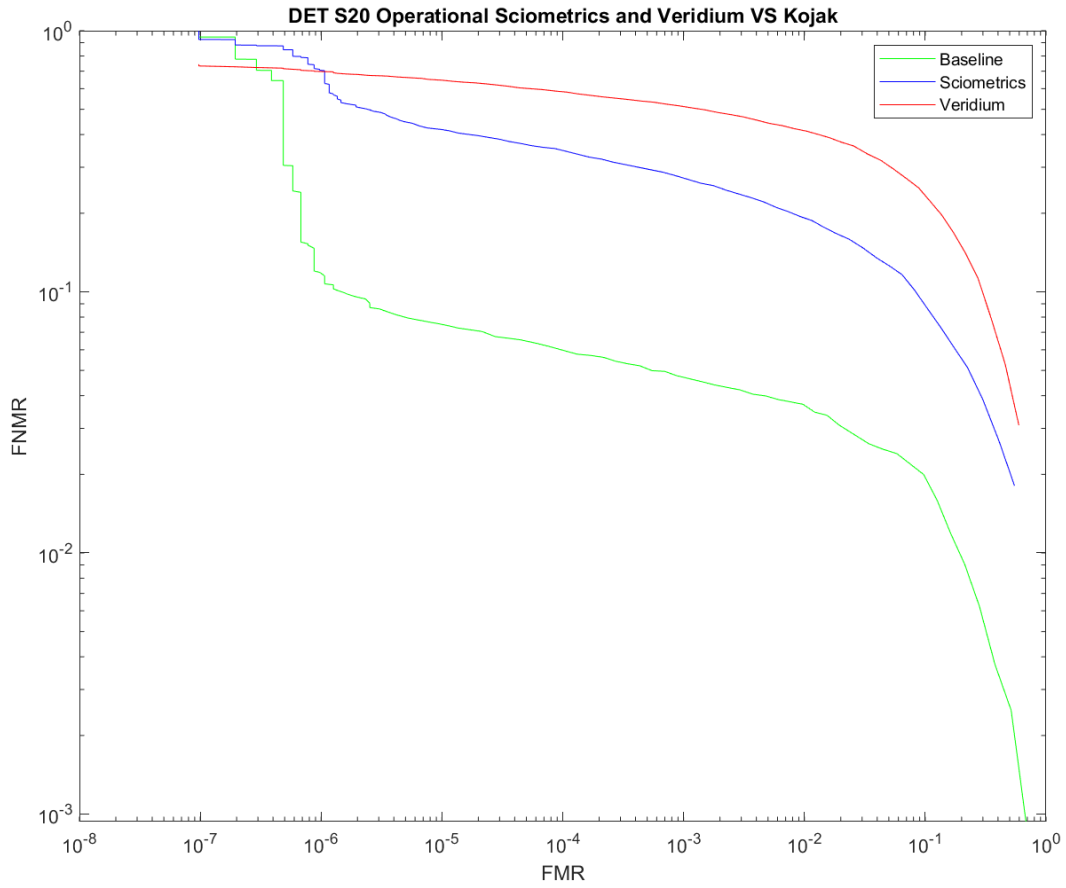


Figure 27 Innovatrics DET curve S20 Operational Sciometrics and Veridium vs Kojak.

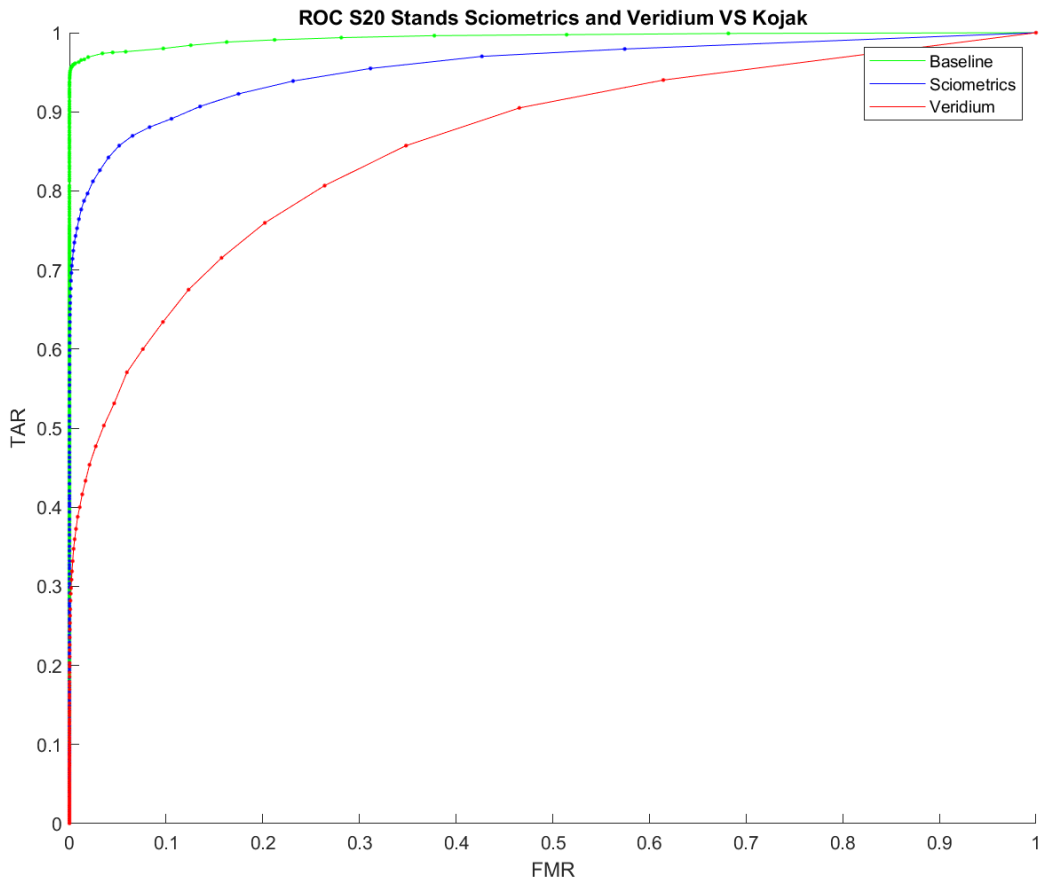


Figure 28 Innovatrix ROC curve S20 Controlled Sciometrics and Veridium vs Kojak.

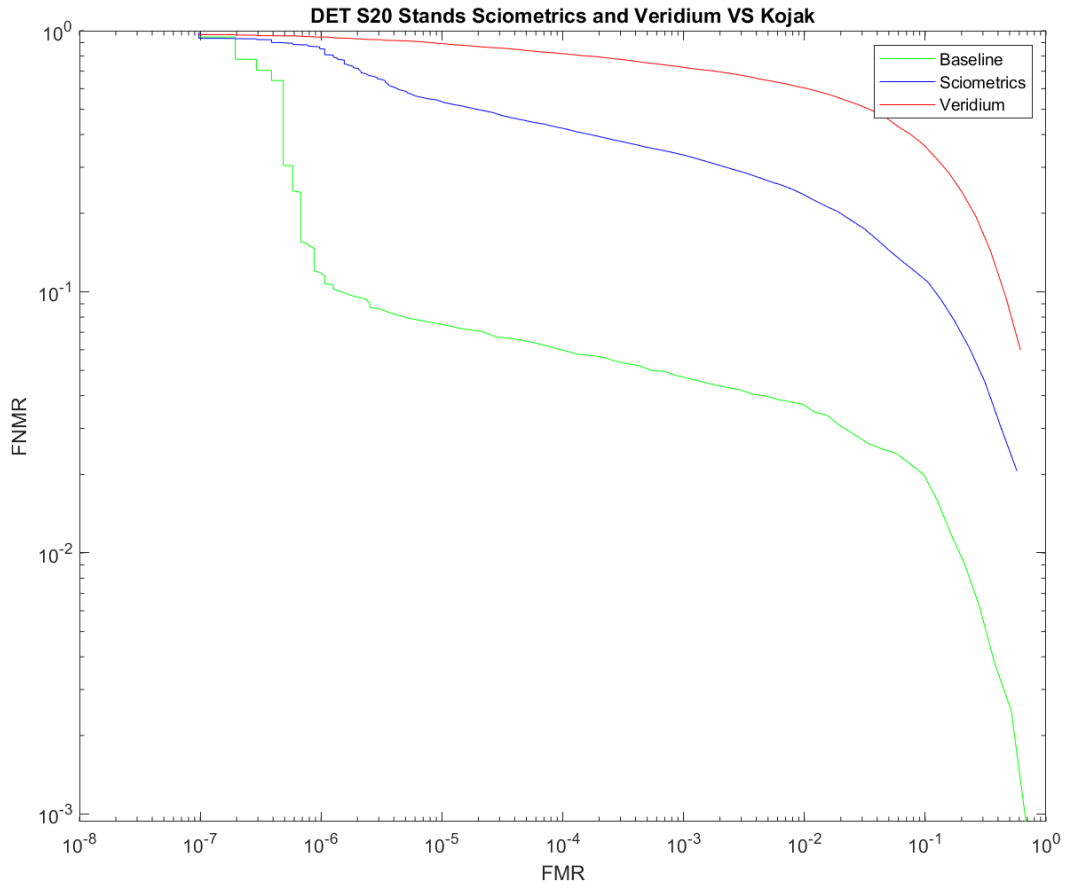


Figure 29 Innovatrics DET curve S20 Controlled Sciometrics and Veridium vs Kojak.

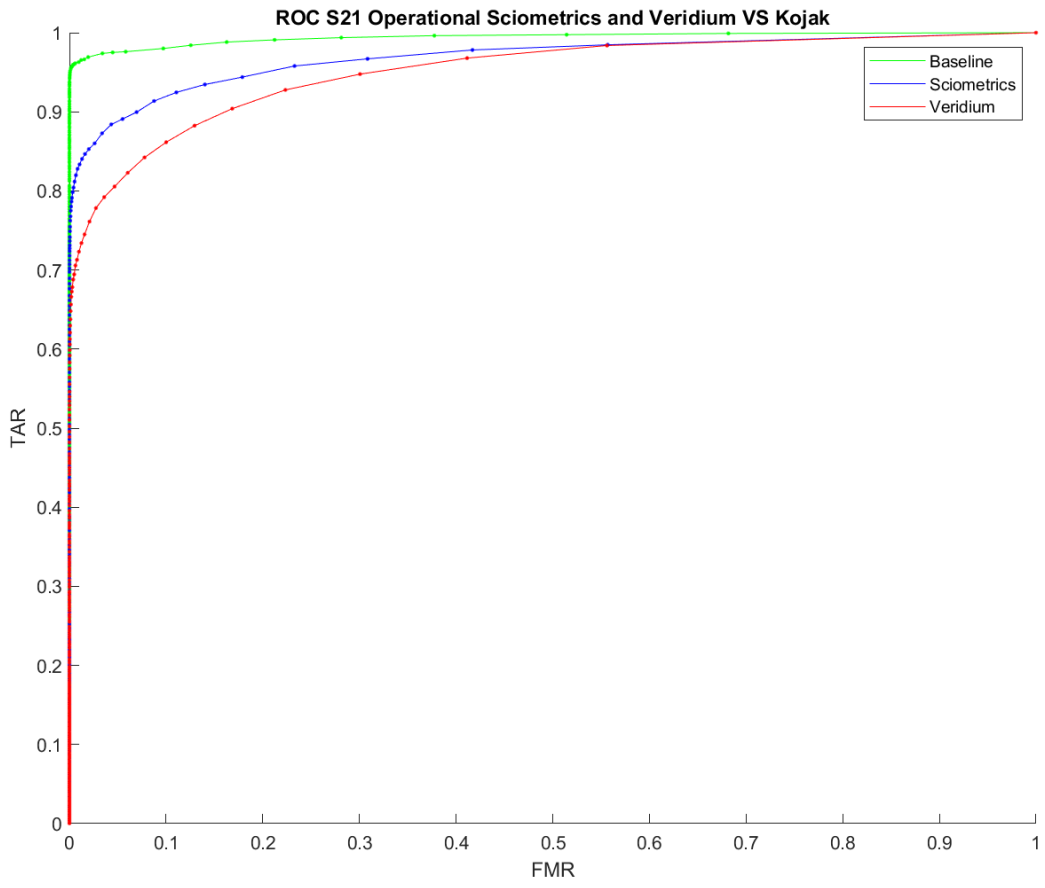


Figure 30 Innovatrics ROC curve S21 Operational Sciometrics and Veridium vs Kojak.

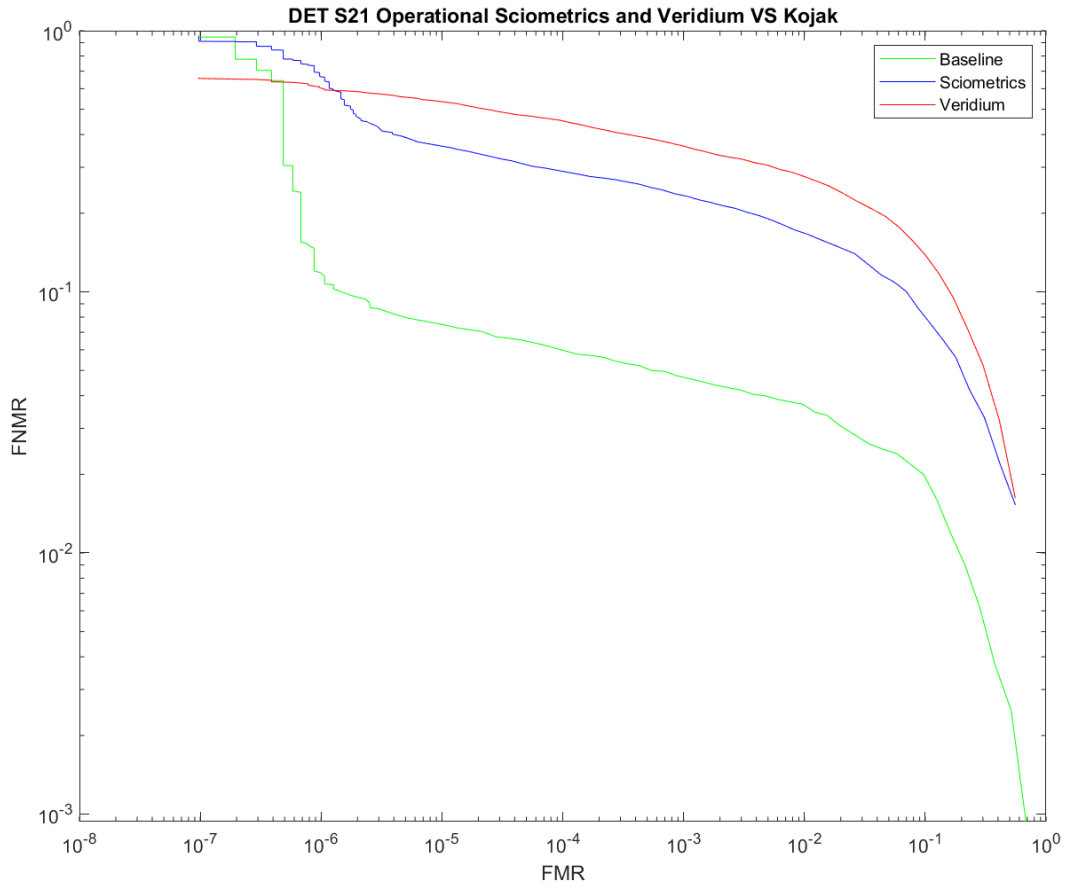


Figure 31 Innovatrics DET curve S21 Operational Sciometrics and Veridium vs Kojak.



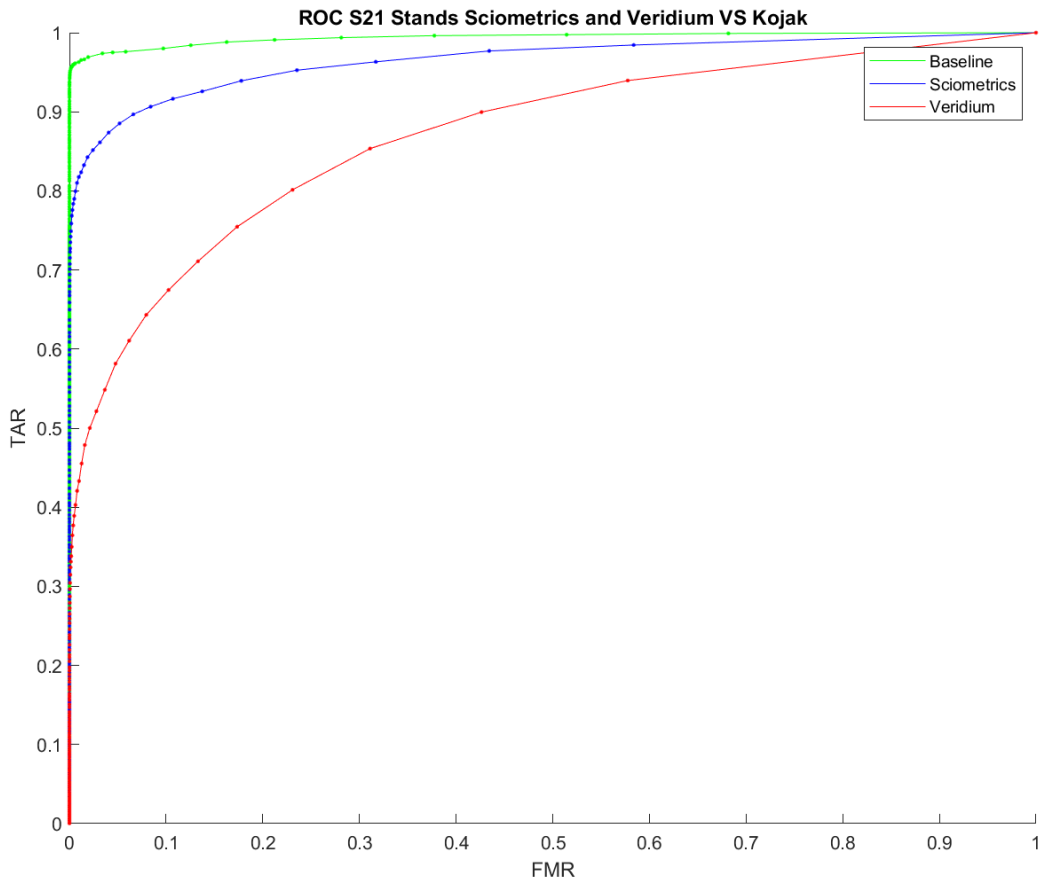


Figure 32 Innovatrix ROC curve S21 Controlled Sciometrics and Veridium vs Kojak.

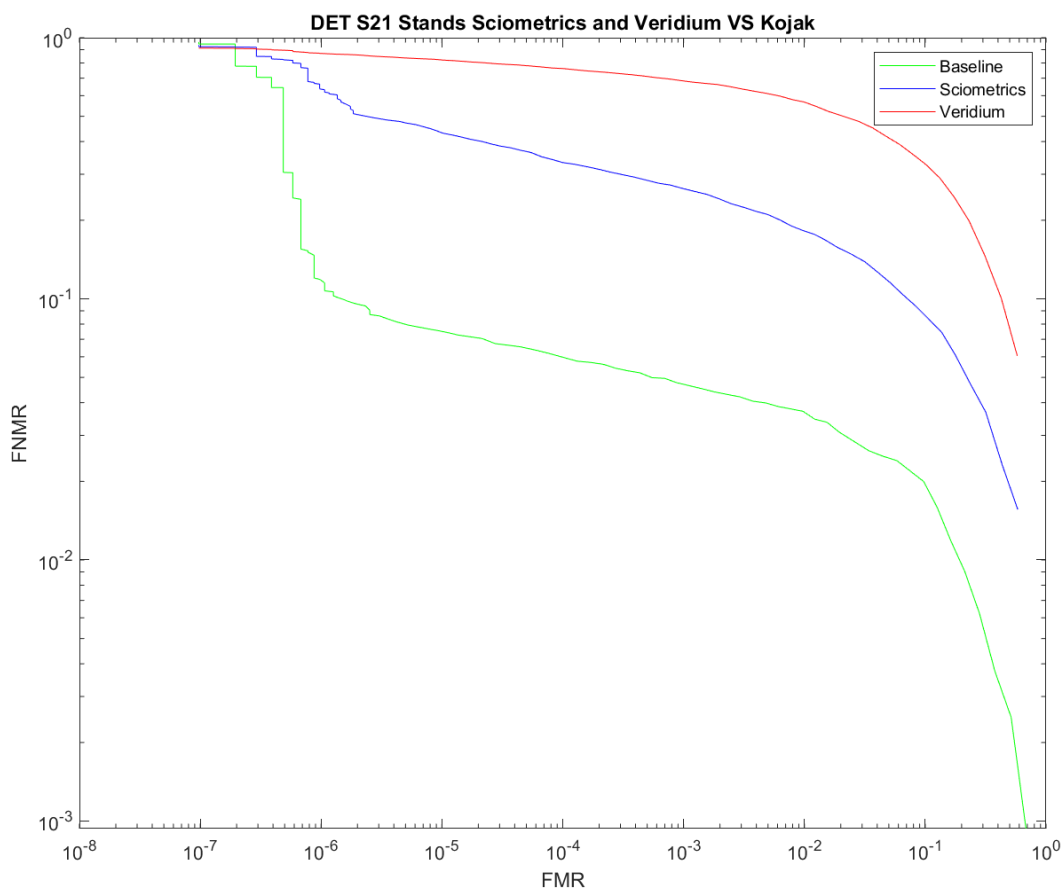


Figure 33 Innovatrics DET curve S21 Controlled Sciometrics and Veridium vs Kojak.

Figure 24 through Figure 33 show both the ROC and DET curves, respectively, for the Innovatrics matcher with the baseline experiment Guardian Slap vs. Kojak Slap always shown in green for each figure. The baseline and contactless ROC and DET in Figure 24, and Figure 25 show the MorphoWave experiment and baseline performed about the same, which is reflected by the AUC values recorded for each in Table 5. with the Gemalto ROC curve trending lower. The DET curves for the baseline and Morpho experiment in Figure 25 show the Morpho having a better initial error tradeoff. However, the baseline had a more significant total tradeoff in the first drop of the curve. In the Cellphone experiment ROC curves (Figure 26, Figure 28, Figure 30, Figure 32), the baseline consistently performed better, with the Veridium sets having the lowest

curve, and similar results are shown in the DET curves (Figure 27, Figure 29, Figure 31, and Figure 33) with Veridium having the lowest change in detection error.

#### 4.2.2.2 VeriFinger

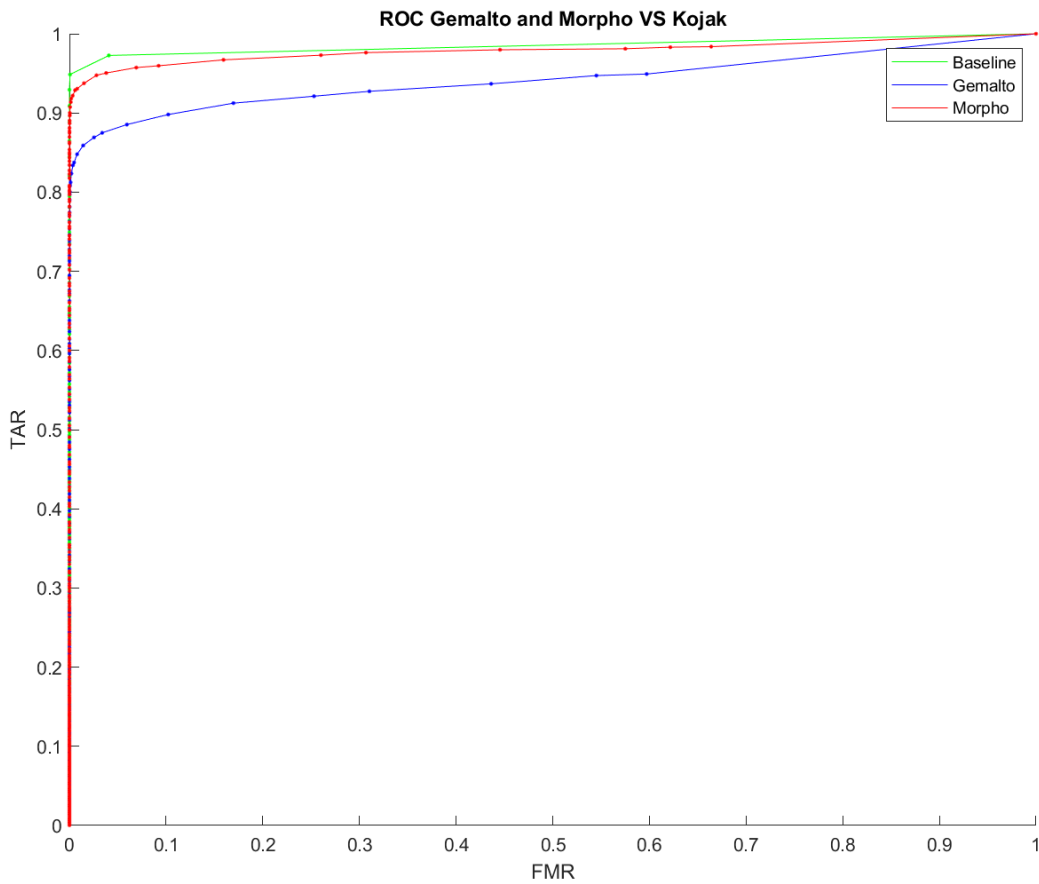


Figure 34 VeriFinger ROC curve Gemalto and Morpho vs Kojak.

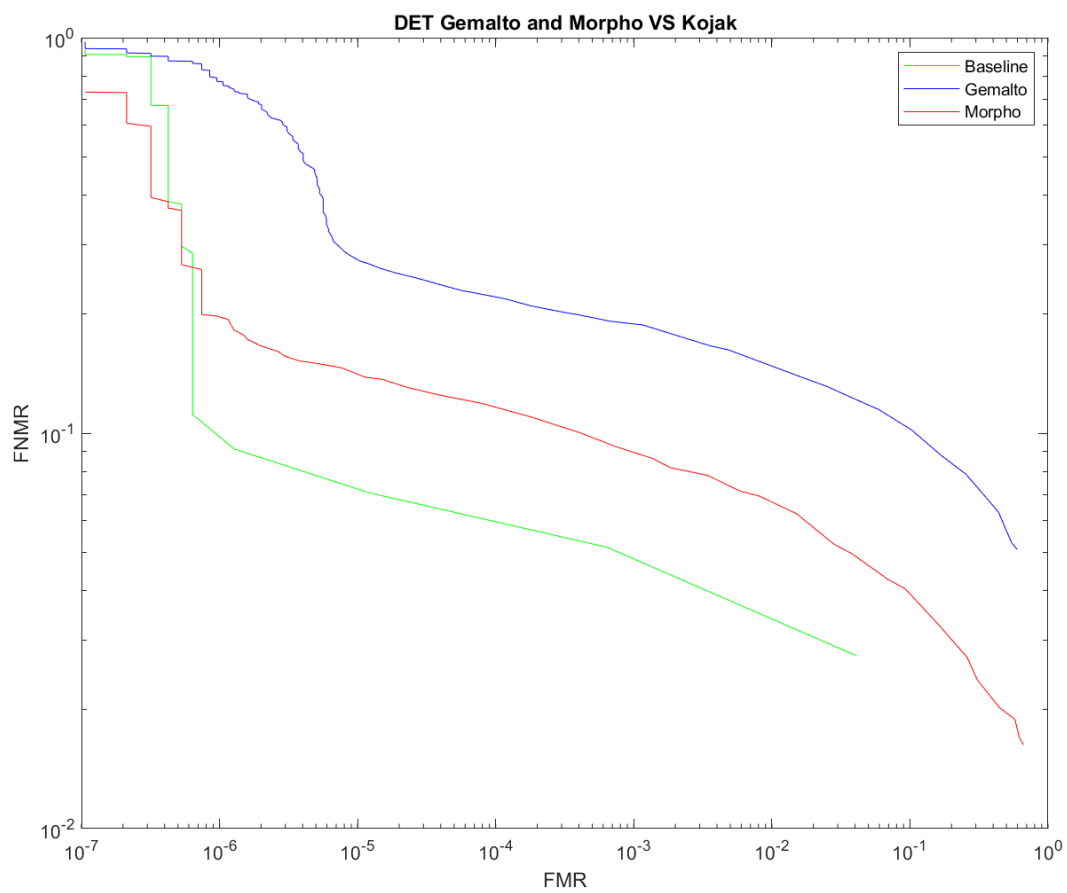


Figure 35 Figure 26 VeriFinger DET curve Gemalto and Morpho vs Kojak.

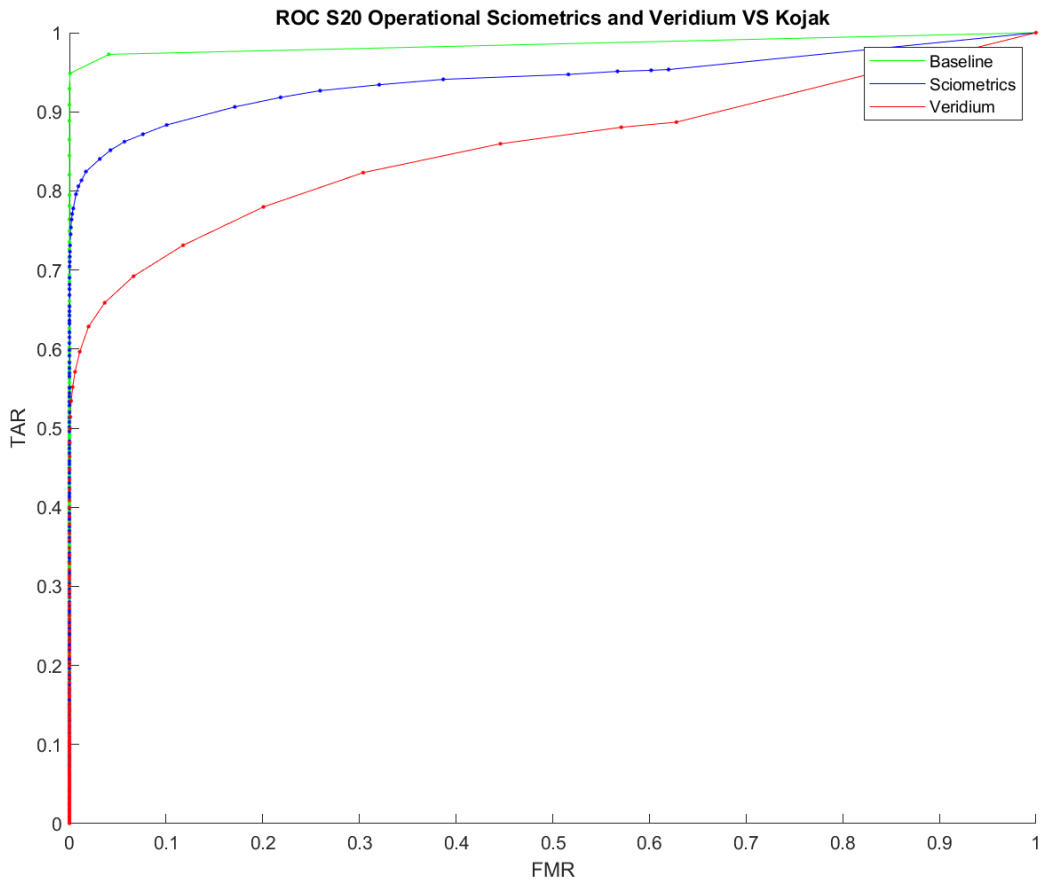


Figure 36 VeriFinger ROC curve S20 Operational Sciometrics and Veridium vs Kojak.

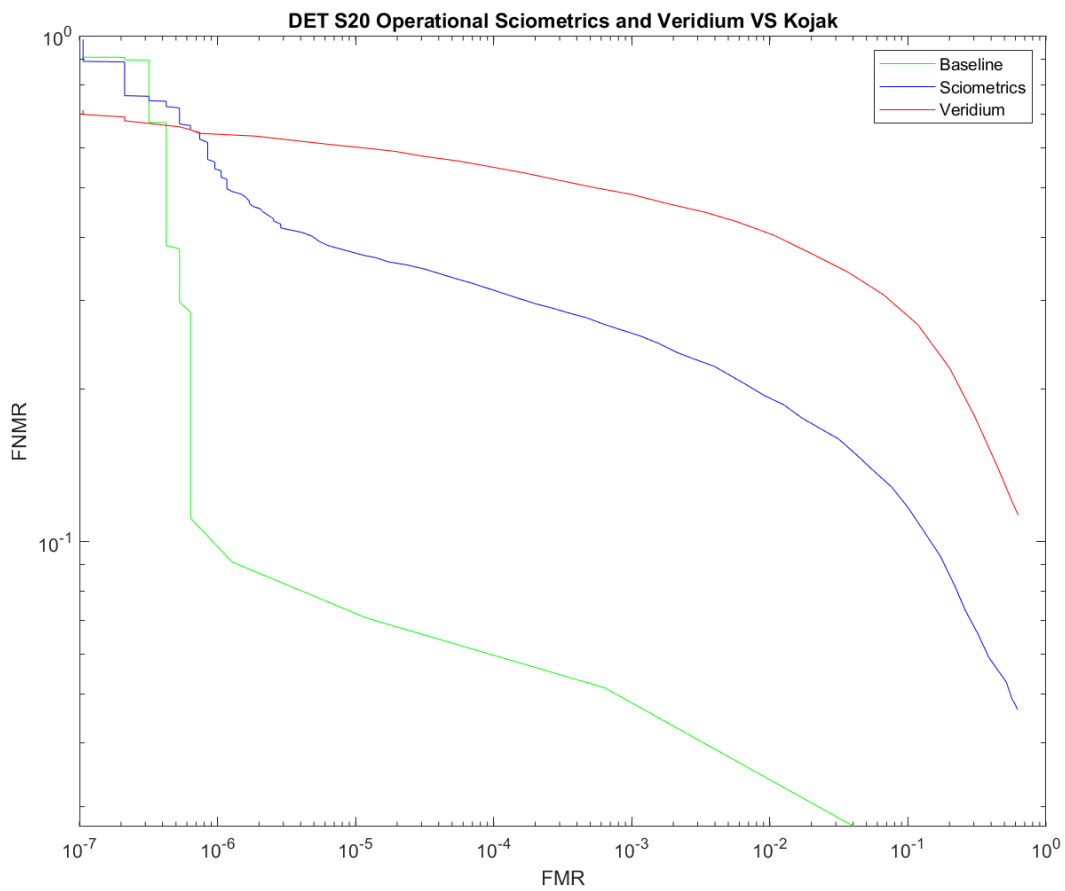


Figure 37 VeriFinger DET curve S20 Operational Sciometrics and Veridium vs Kojak.

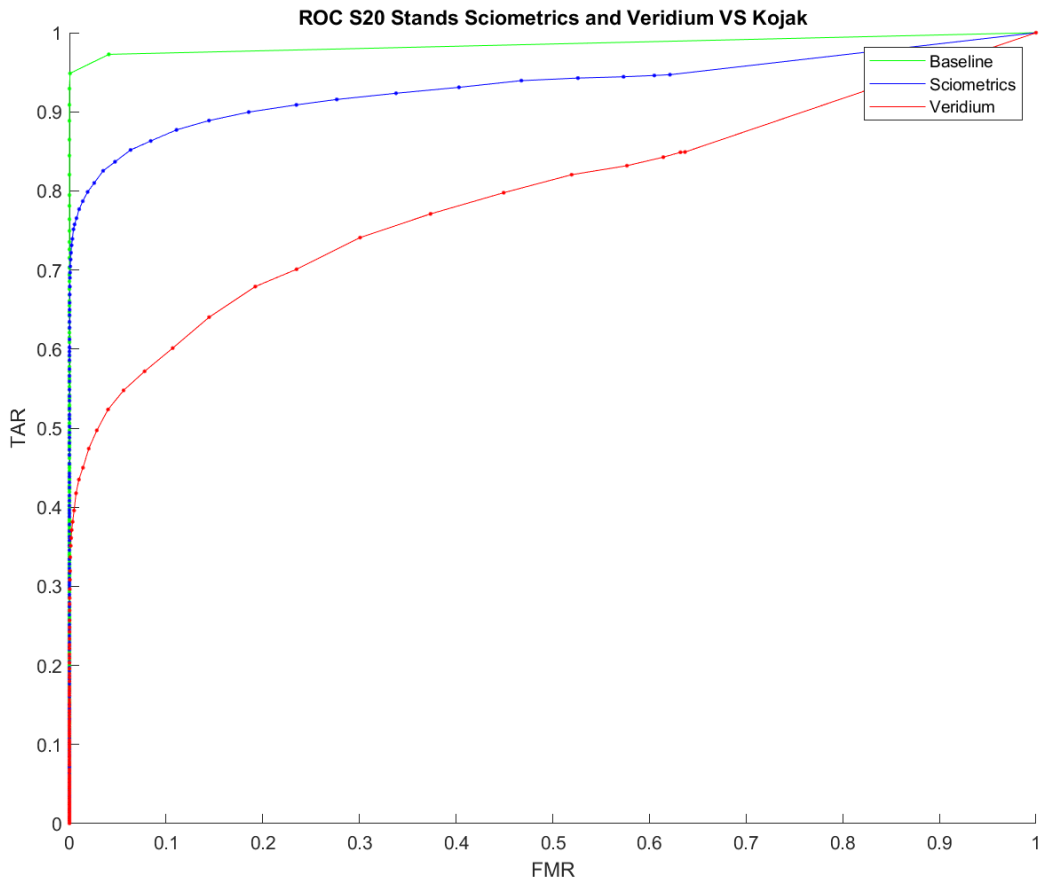


Figure 38 VeriFinger ROC curve S20 Controlled Sciometrics and Veridium vs Kojak.

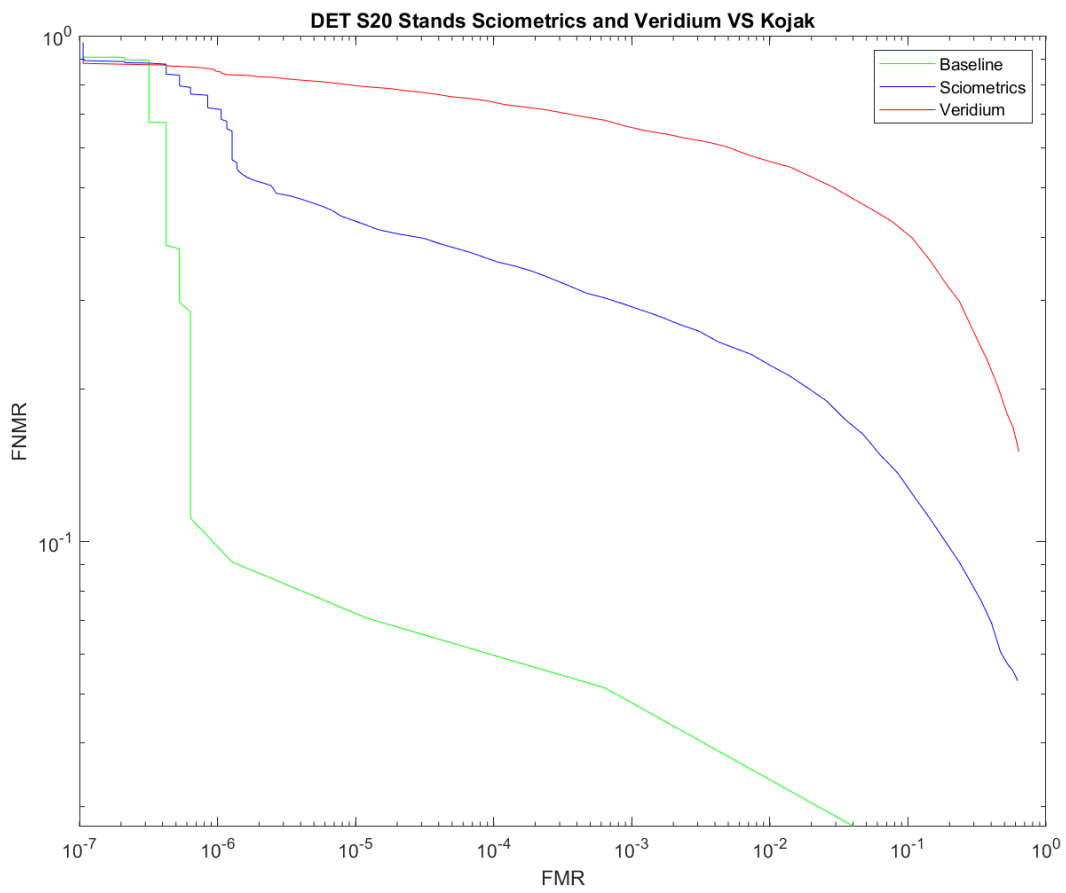


Figure 39 VeriFinger DET curve S20 Controlled Sciometrics and Veridium vs Kojak.



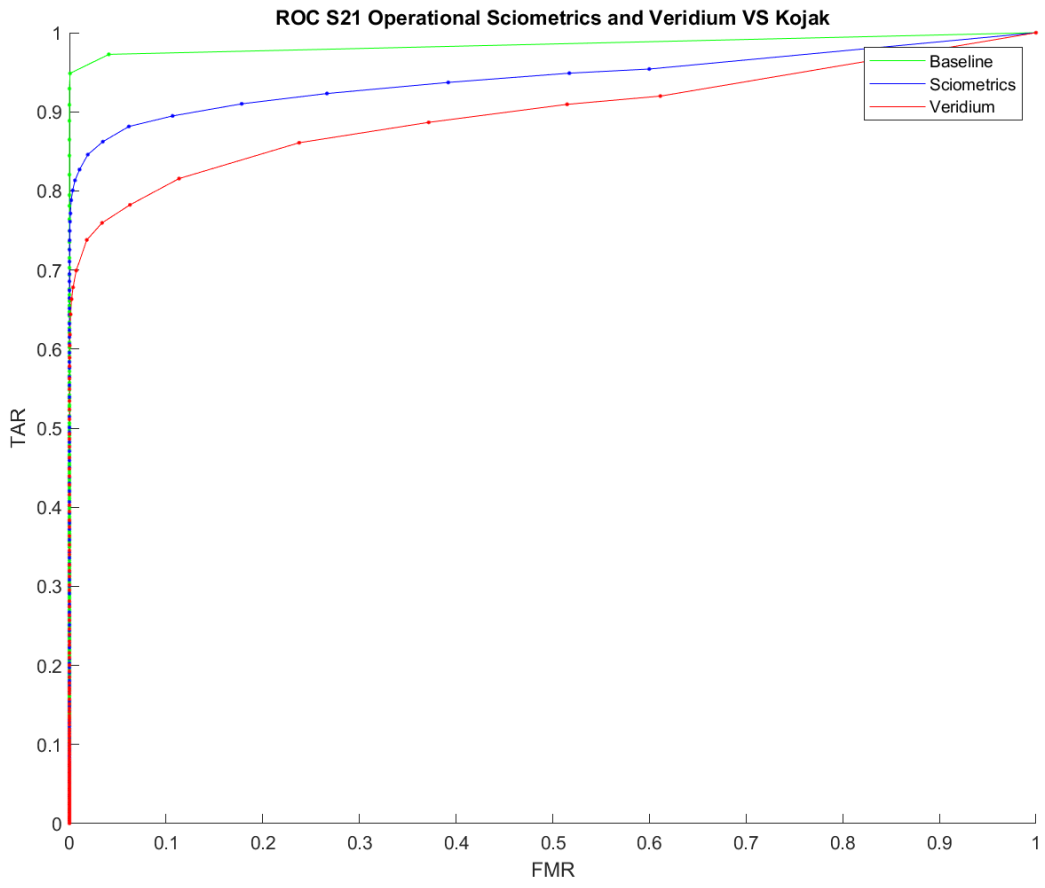


Figure 40 VeriFinger ROC curve S21 Operational Sciometrics and Veridium vs Kojak.

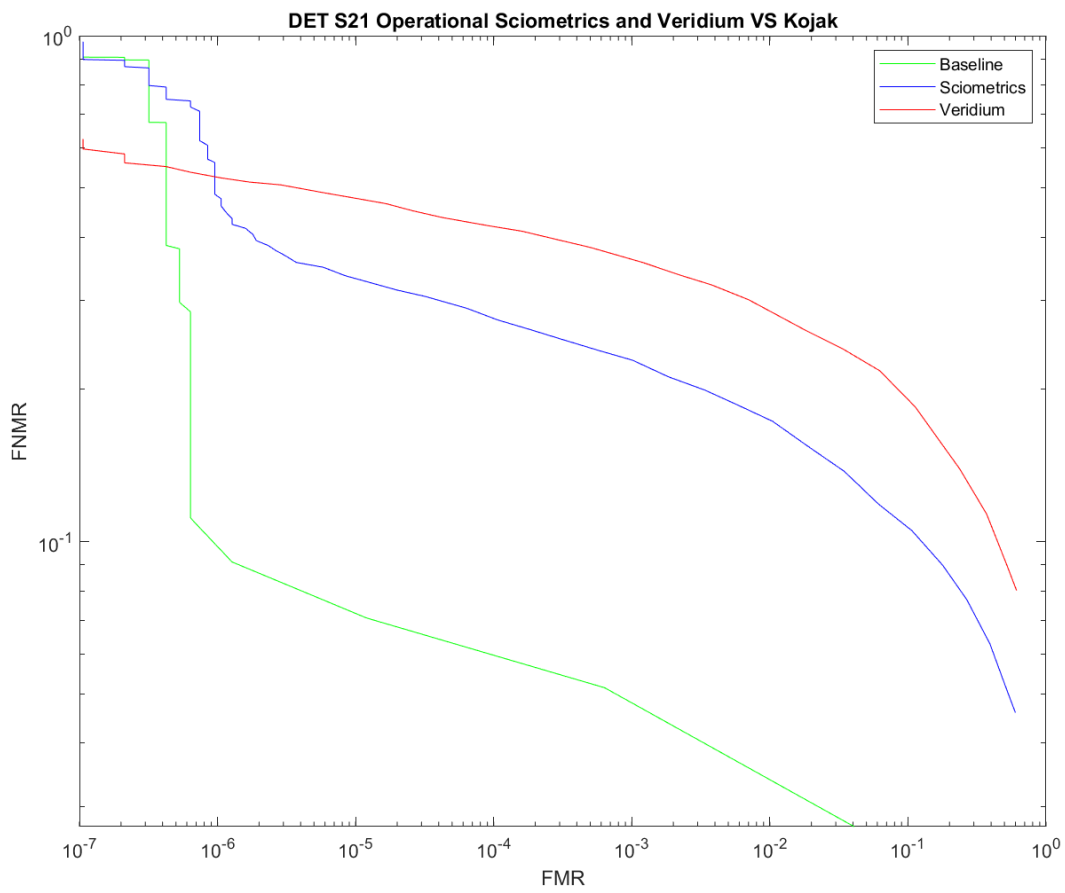


Figure 41 VeriFinger DET curve S21 Operational Sciometrics and Veridium vs Kojak.

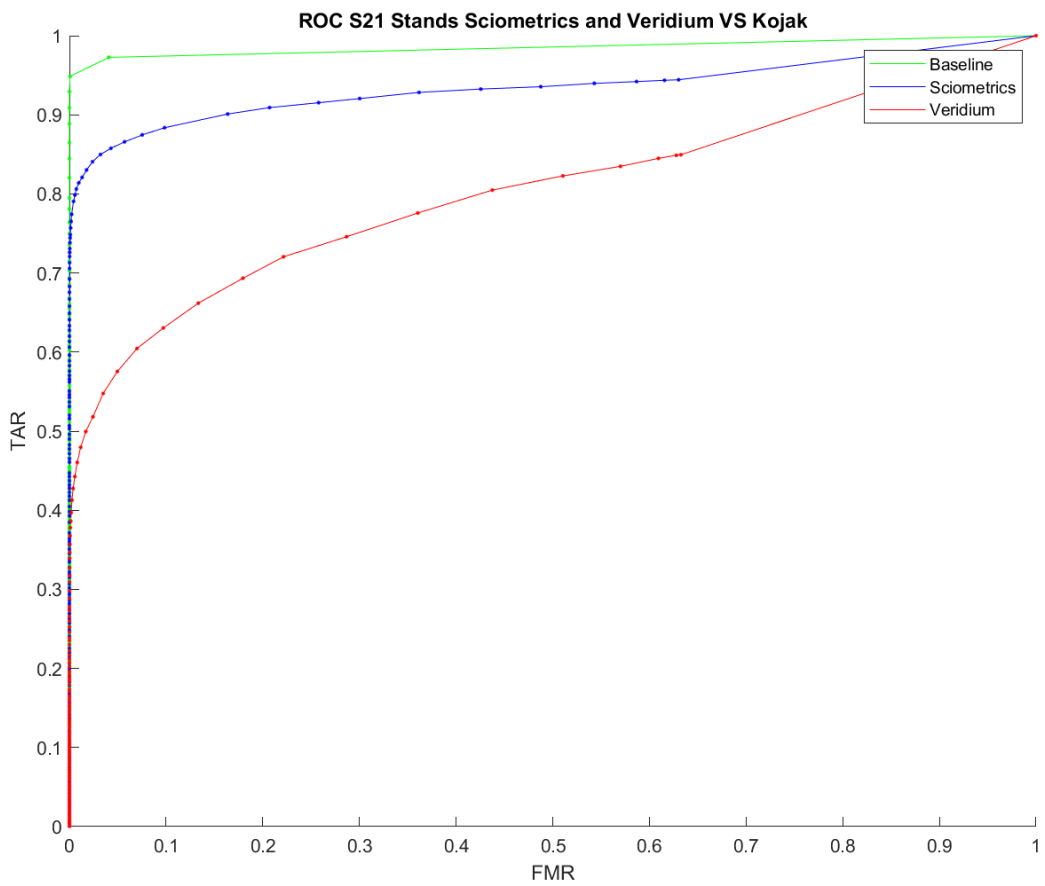


Figure 42 VeriFinger ROC curve S21 Controlled Sciometrics and Veridium vs Kojak.

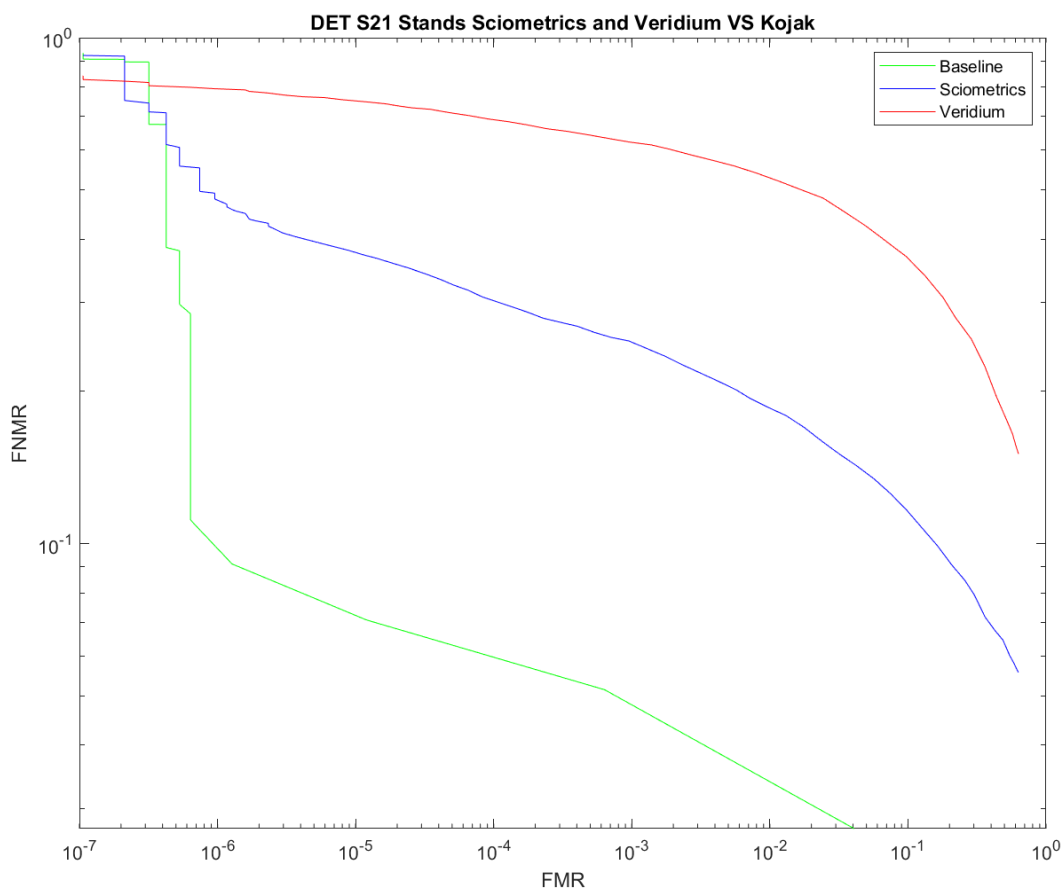


Figure 43 VeriFinger DET curve S21 Controlled Sciometrics and Veridium vs Kojak.

Figure 34 through Figure 43 show the ROC and DET curves for the VeriFinger matching experiments with similar results as the Innovatrics ROC and DET curves. Figure 34 shows the baseline experiment performing better than the MorphoWave compared to the similar curve in Figure 24, showing the Innovatrics results for the contactless experiments. The DET curves for the contactless experiments in Figure 35 show a sharper drop for the Morpho DET curve that outperforms the baseline before being overtaken again, similar to the Innovatrics Morpho DET curve. The VeriFinger cellphone experiments show results consistent with the reported AUC values in Table 5, and the Innovatrics experiments show the baseline always performing better.

Veridium has a lower ROC curve and less error tradeoff in the DET curve, with Sciometrics falling between the baseline and Veridium.

### 4.2.2.3 Bozorth3

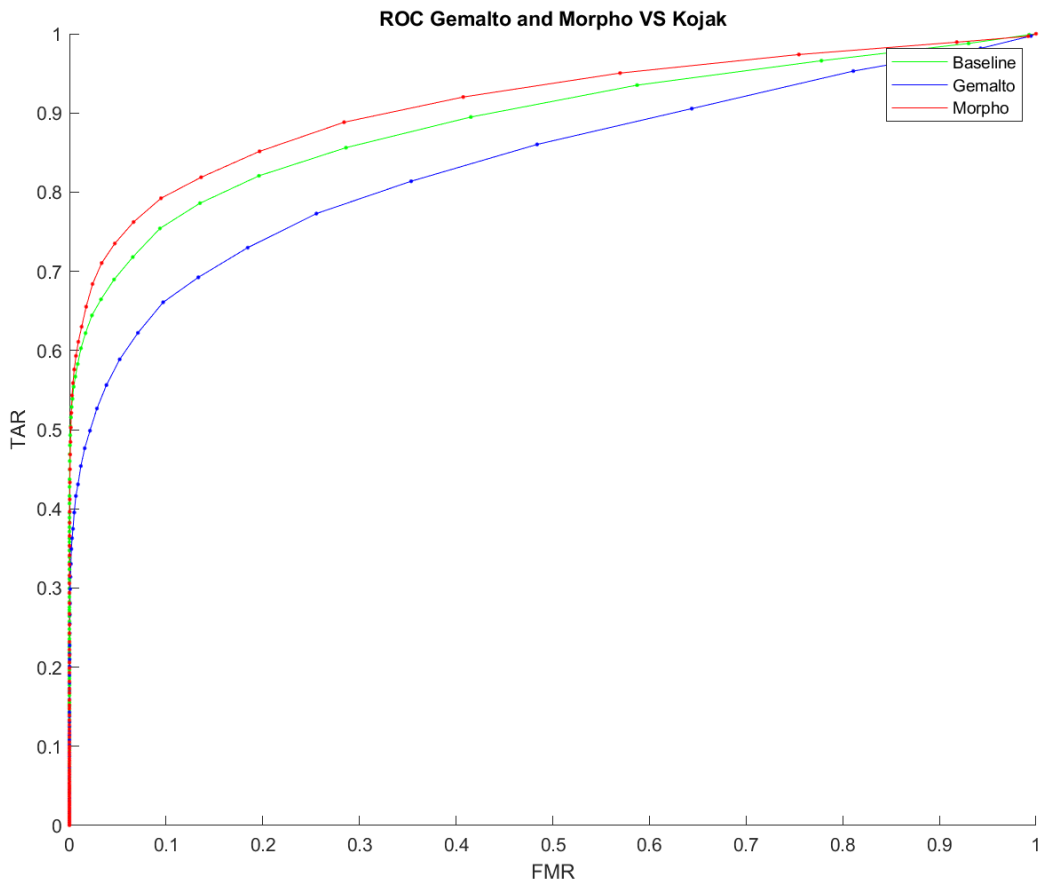


Figure 44 Bozorth3 ROC curve Gemalto and Morpho vs Kojak.

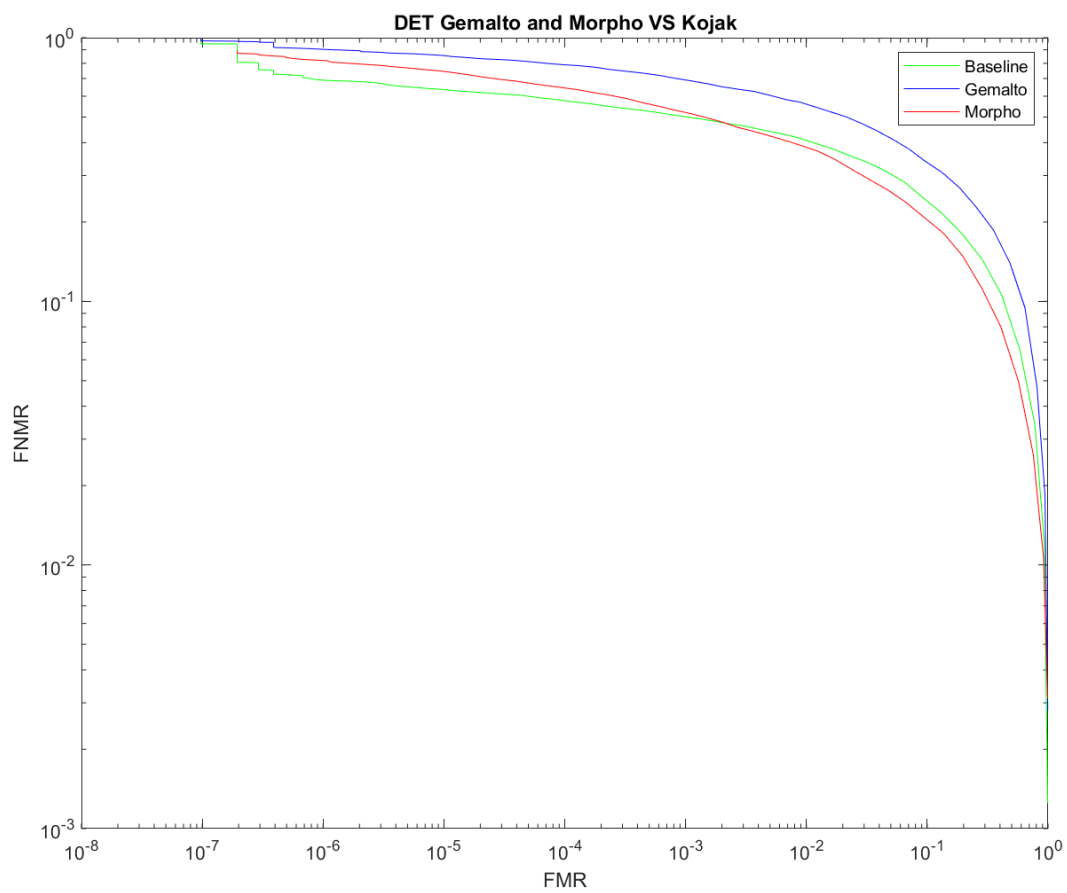


Figure 45 Bozorth3 DET curve Gemalto and Morpho vs Kojak.

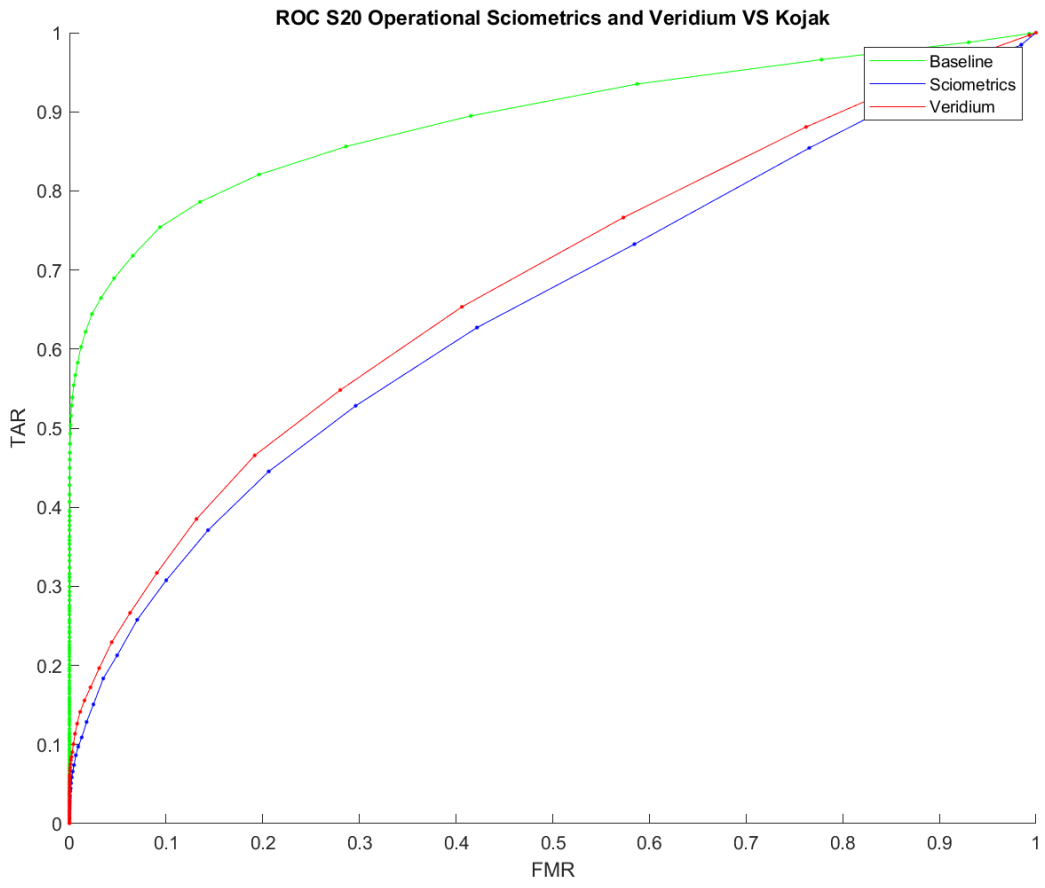


Figure 46 Bozorth3 ROC curve S20 Operational Sciometrics and Veridium vs Kojak.

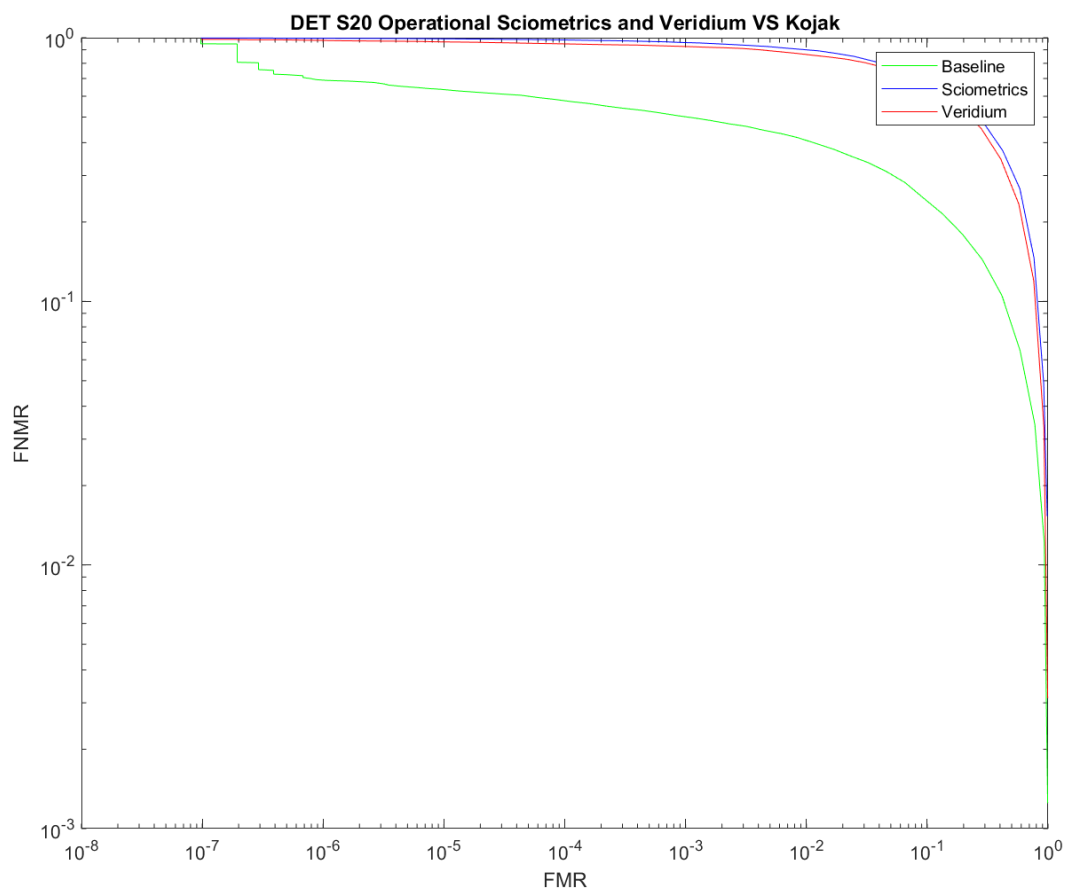


Figure 47 Bozorth3 DET curve S20 Operational Sciometrics and Veridium vs Kojak.



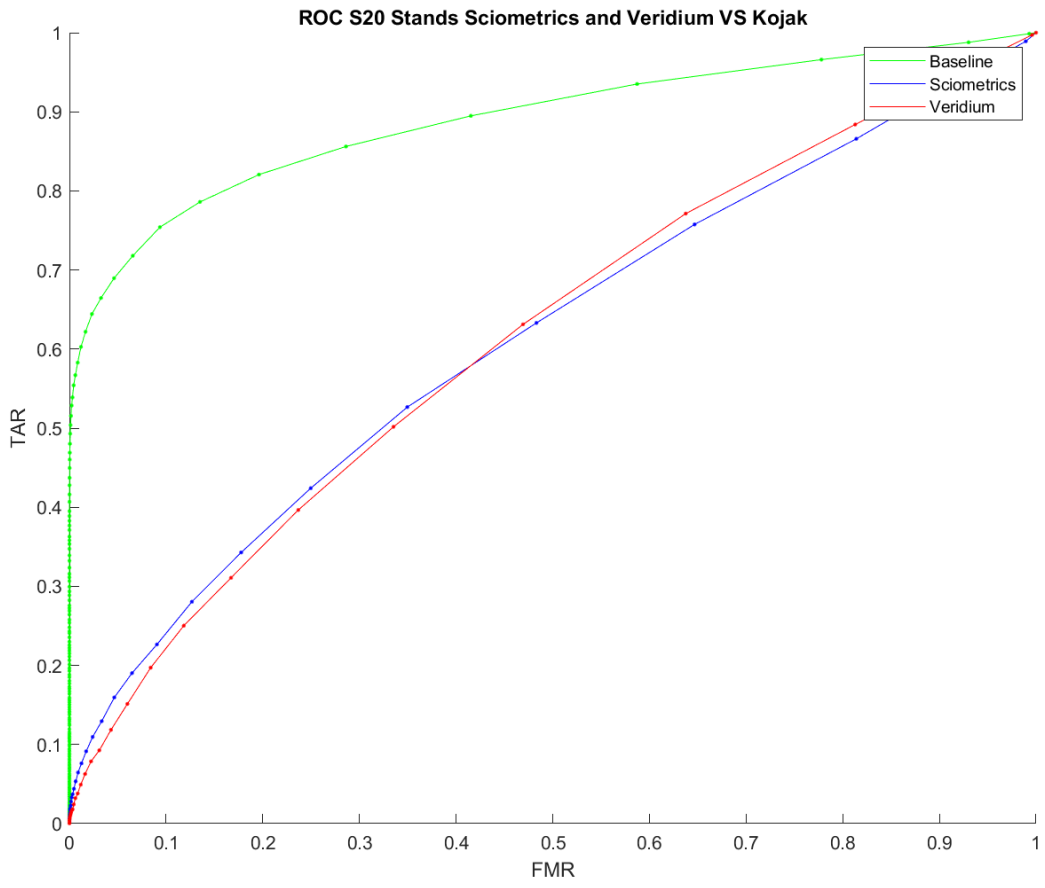


Figure 48 Bozorth3 ROC curve S20 Controlled Sciometrics and Veridium vs Kojak.

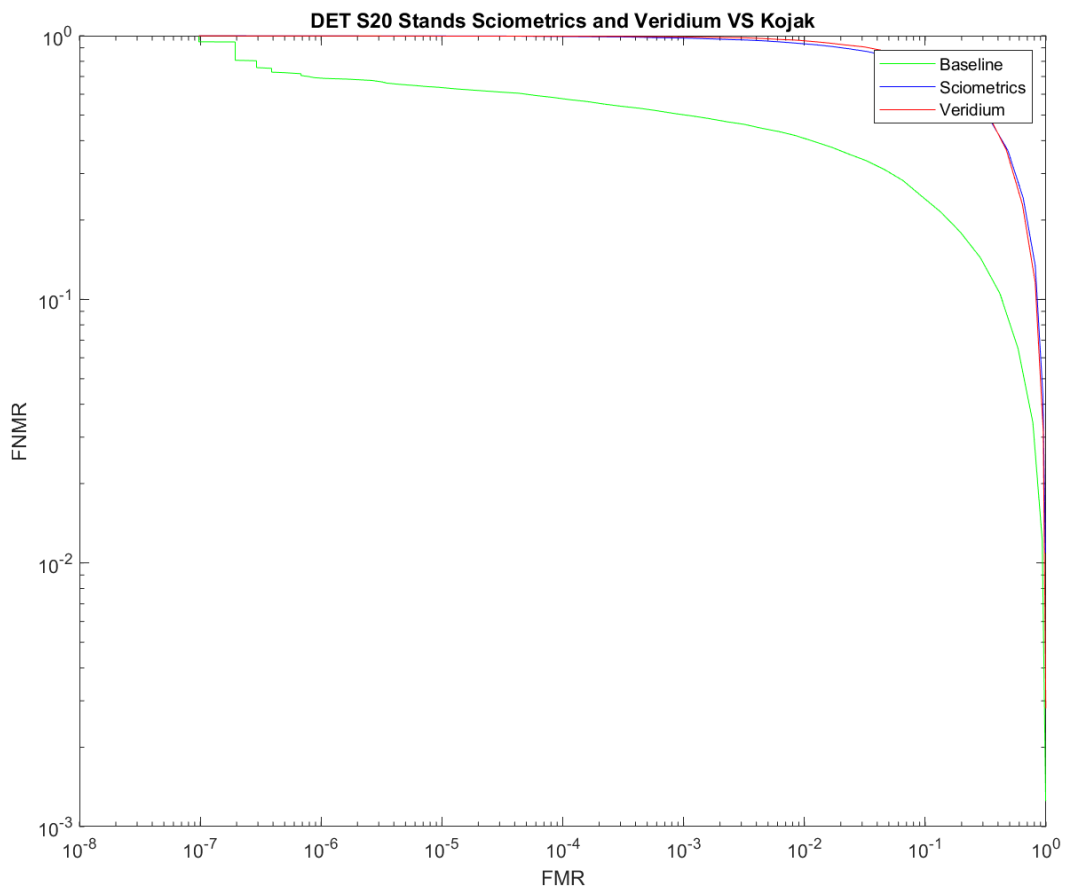


Figure 49 Bozorth3 DET curve S20 Controlled Sciometrics and Veridium vs Kojak.

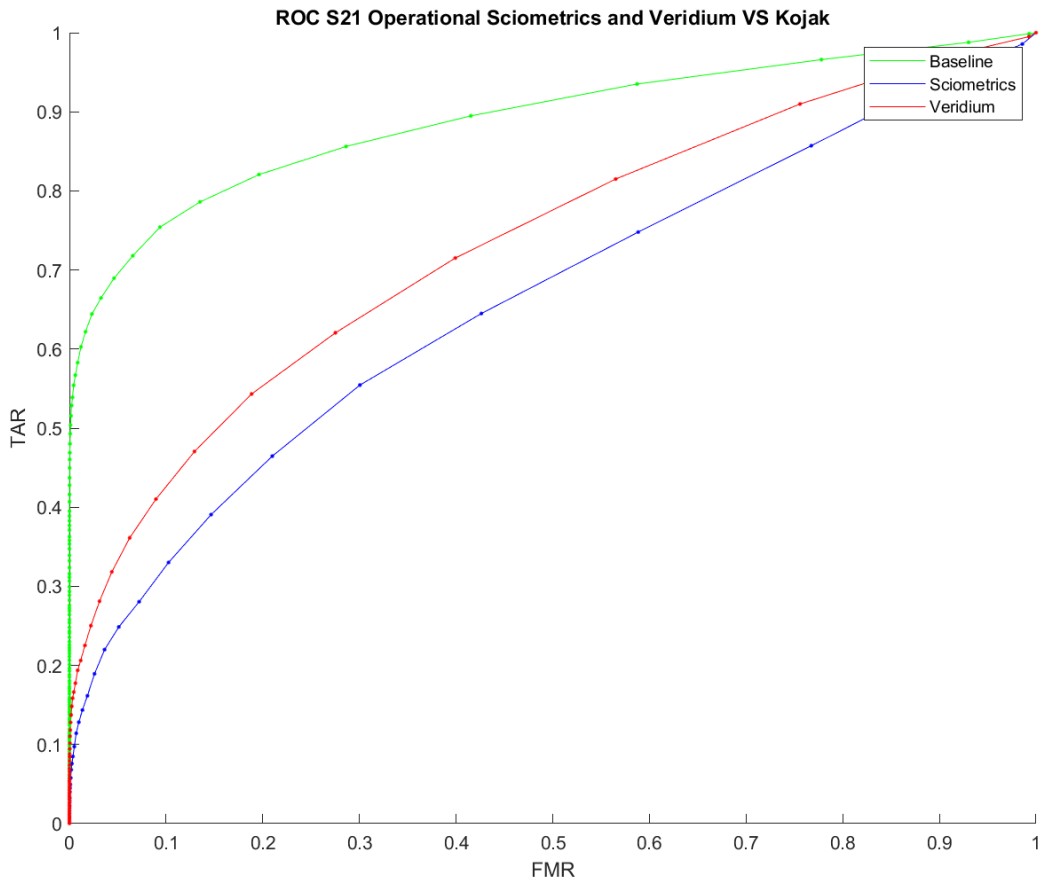


Figure 50 Bozorth3 ROC curve S21 Operational Sciometrics and Veridium vs Kojak.

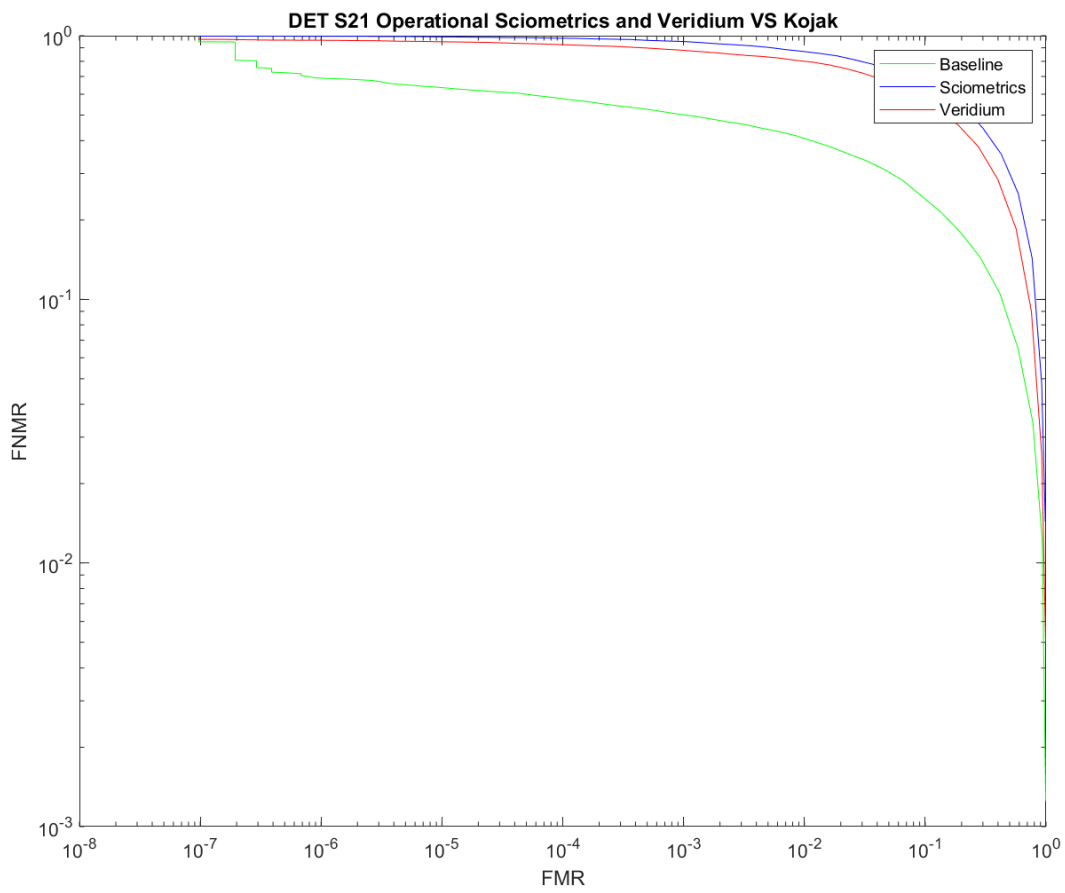


Figure 51 Bozorth3 DET curve S21 Operational Sciometrics and Veridium vs Kojak.

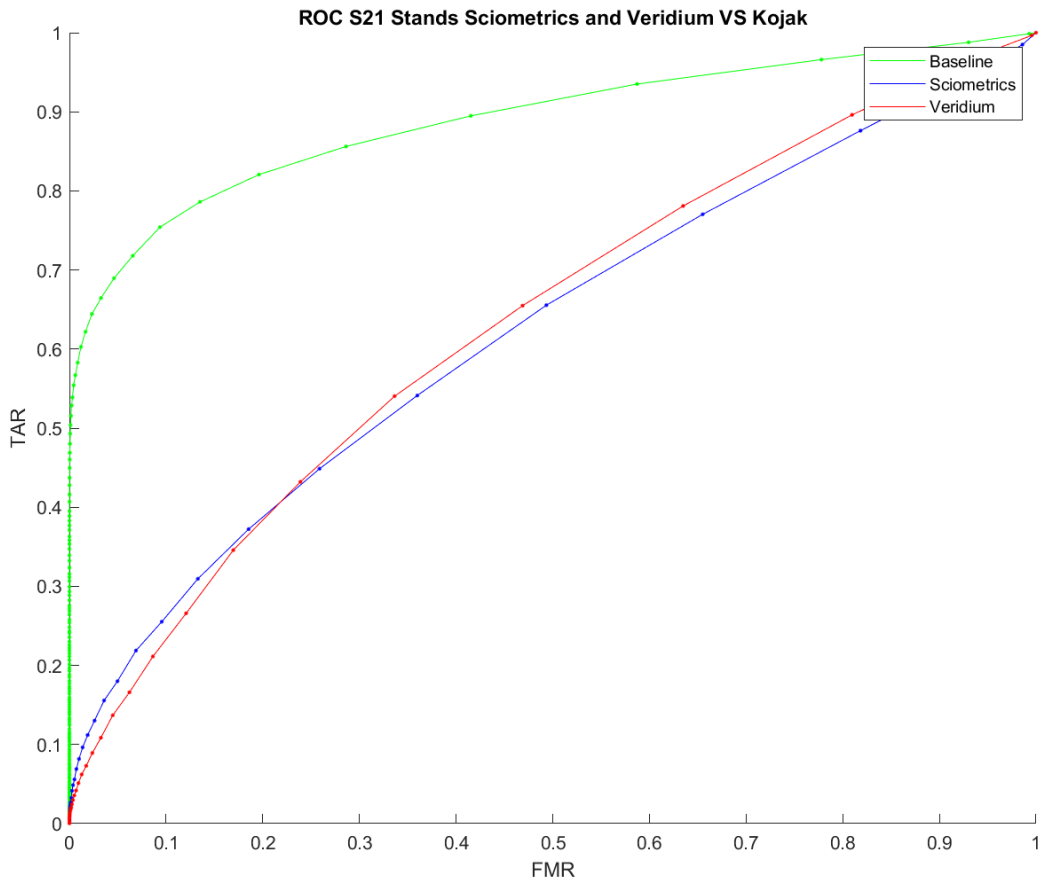
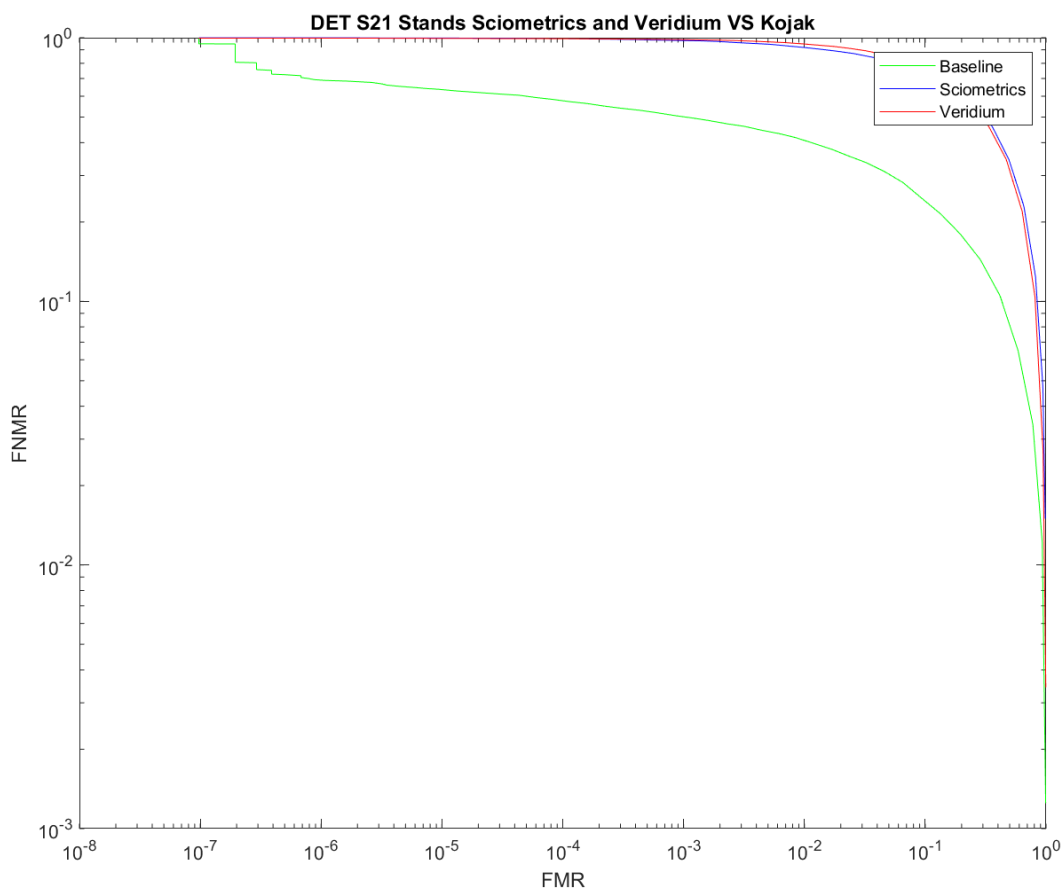


Figure 52 Bozorth3 ROC curve S21 Controlled Sciometrics and Veridium vs Kojak.



*Figure 53 Bozorth3 DET curve S21 Controlled Sciometrics and Veridium vs Kojak.*

Figure 44 through Figure 53 shows the ROC and DET curves for the Bozorth3 matching experiments. In Figure 44, the contactless experiments show the Morpho experiment performing better than the baseline throughout the curve, with Gemalto performing lower for the contactless experiments. The DET curves for the contactless experiments in Figure 45 show that the baseline had an initial drop in detection error over the Morpho experiment. However, the two performed comparably through the whole curve. The cellphone ROC curves show a curve approaching a straight diagonal for all experiments, with the S21 Operational Veridium in Figure 50 performing the best of all the Bozorth3 cellphone experiments.

## 4.2.3 Genuine Match Score Comparison

### 4.2.3.1 Innovatrics

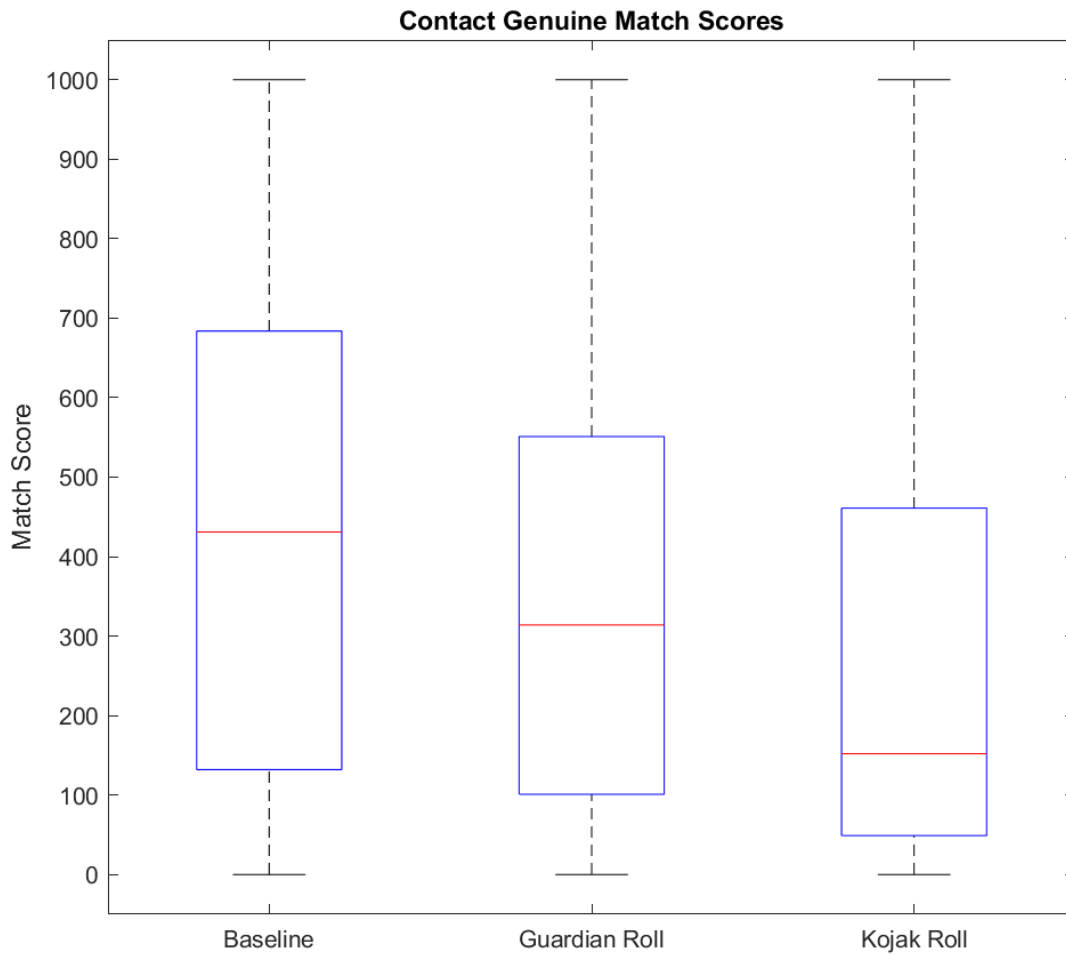


*Figure 54 Innovatrics match score comparison for contact sets compared to baseline.*

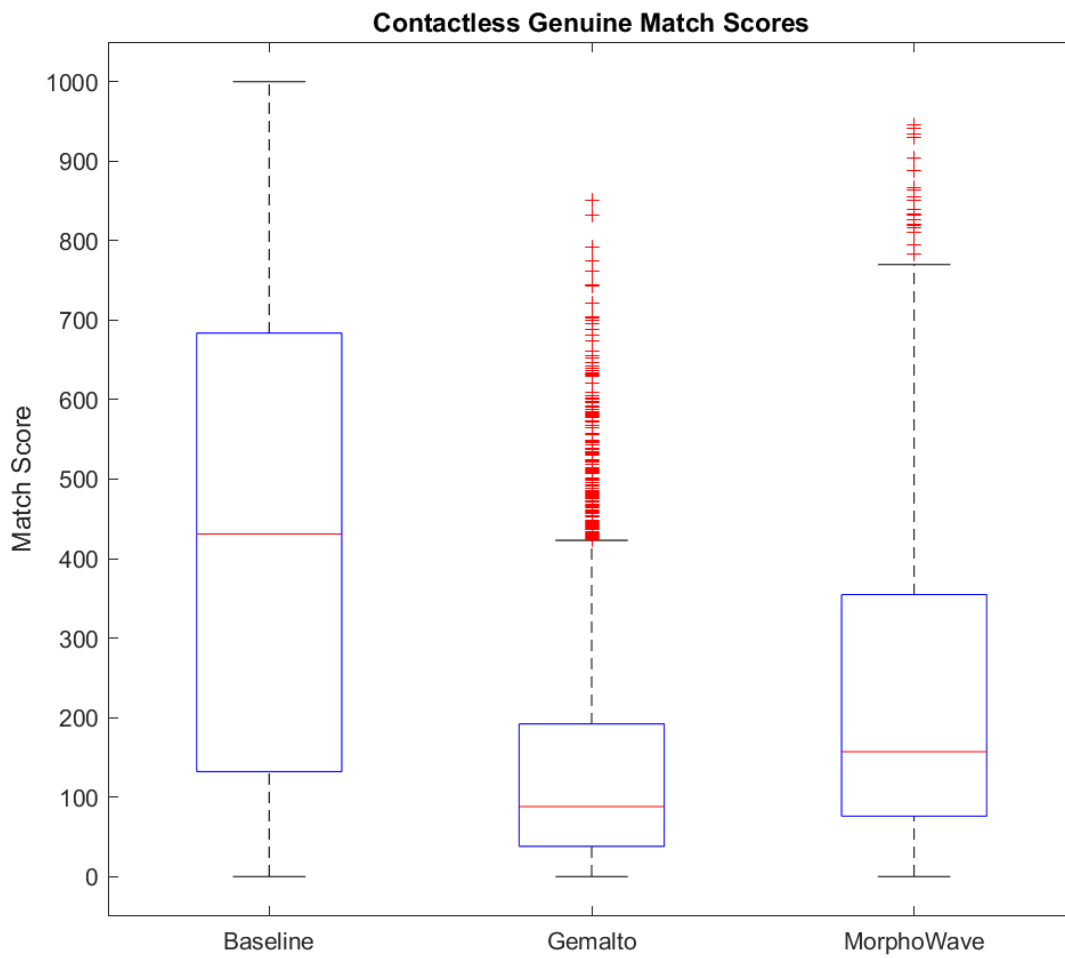


*Figure 55 Innovatrics match score comparison for contactless sets compared to baseline.*



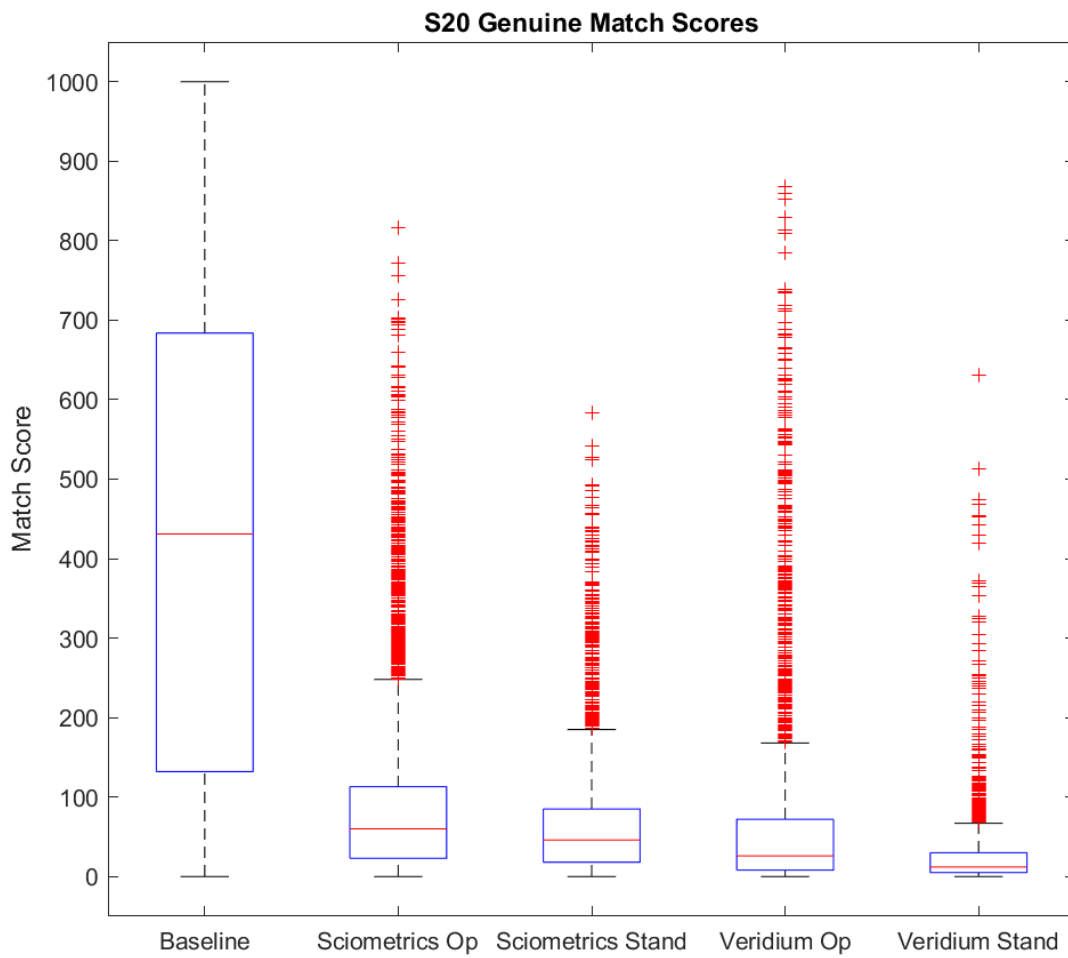


*Figure 56 Innovetrics match score comparison for S20 sets from both cellphone applications in both settings compared to baseline.*

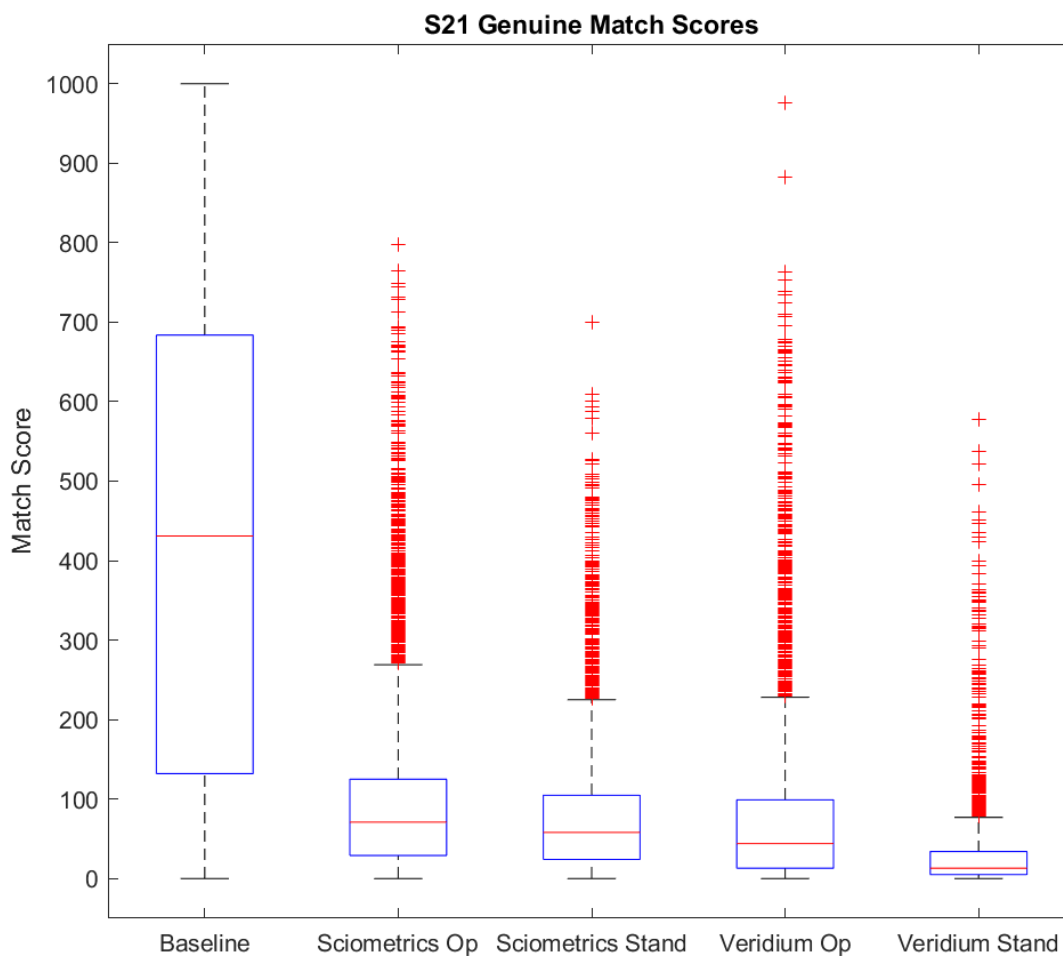


*Figure 57 Innovatrics match score comparison for S21 sets from both cellphone applications in both settings compared to baseline.*

The box plots in Figure 54 through Figure 57 show the distribution of the genuine match scores for each experiment for the Innovatrics matcher. Figure 54 shows that all contact fingerprint experiments have a higher median distribution, with the baseline performing the best with no outlier in any of the distributions. Figure 55 shows that the contactless genuine match distributions have a lower median, with the Gemalto experiment having a lower median and interquartile range. The cellphone distributions in Figure 56, and Figure 57 have very low medians and interquartile ranges compared to the baseline. All cellphone experiment

distributions have many outliers showing that most genuine matchers score around or below 100 for Innovatrics. At the same time, the possible range extends to 1000.

### 4.2.3.2 VeriFinger

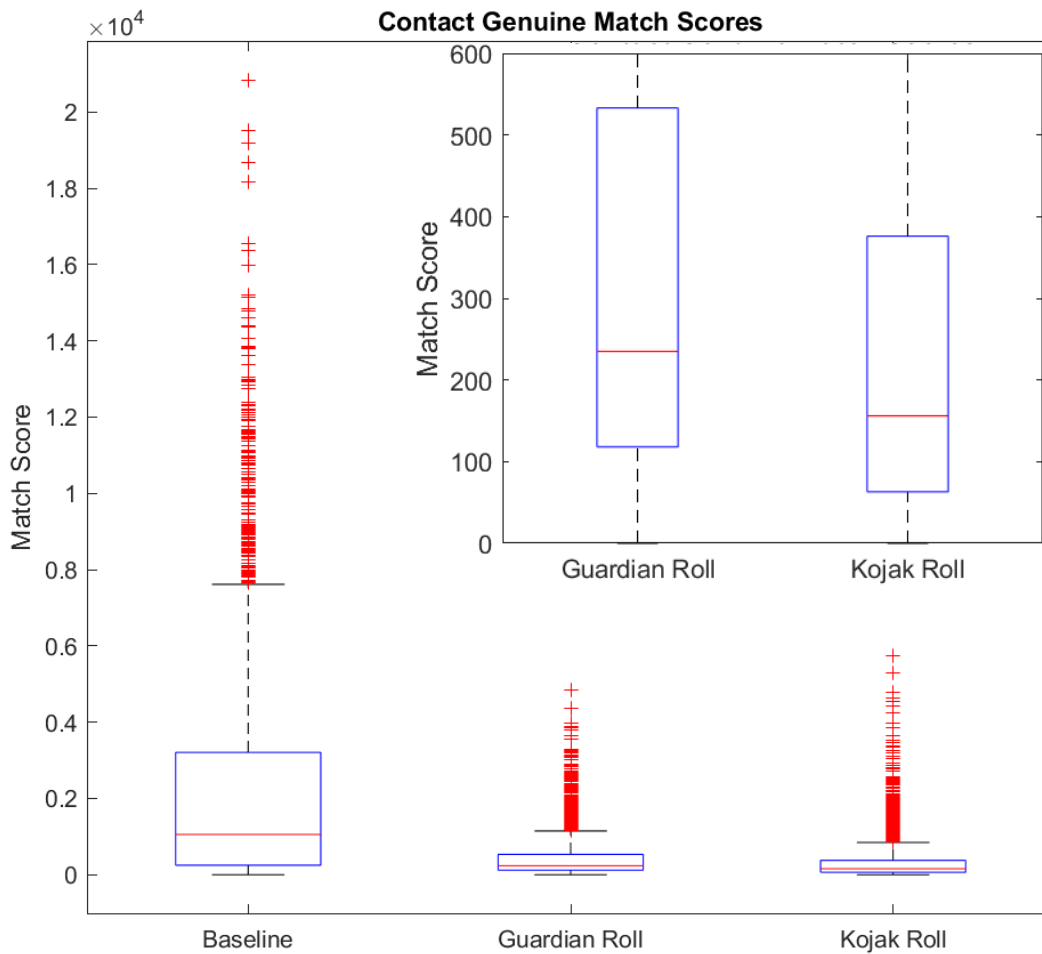


Figure 58 VeriFinger match score comparison for contact sets compared to baseline.

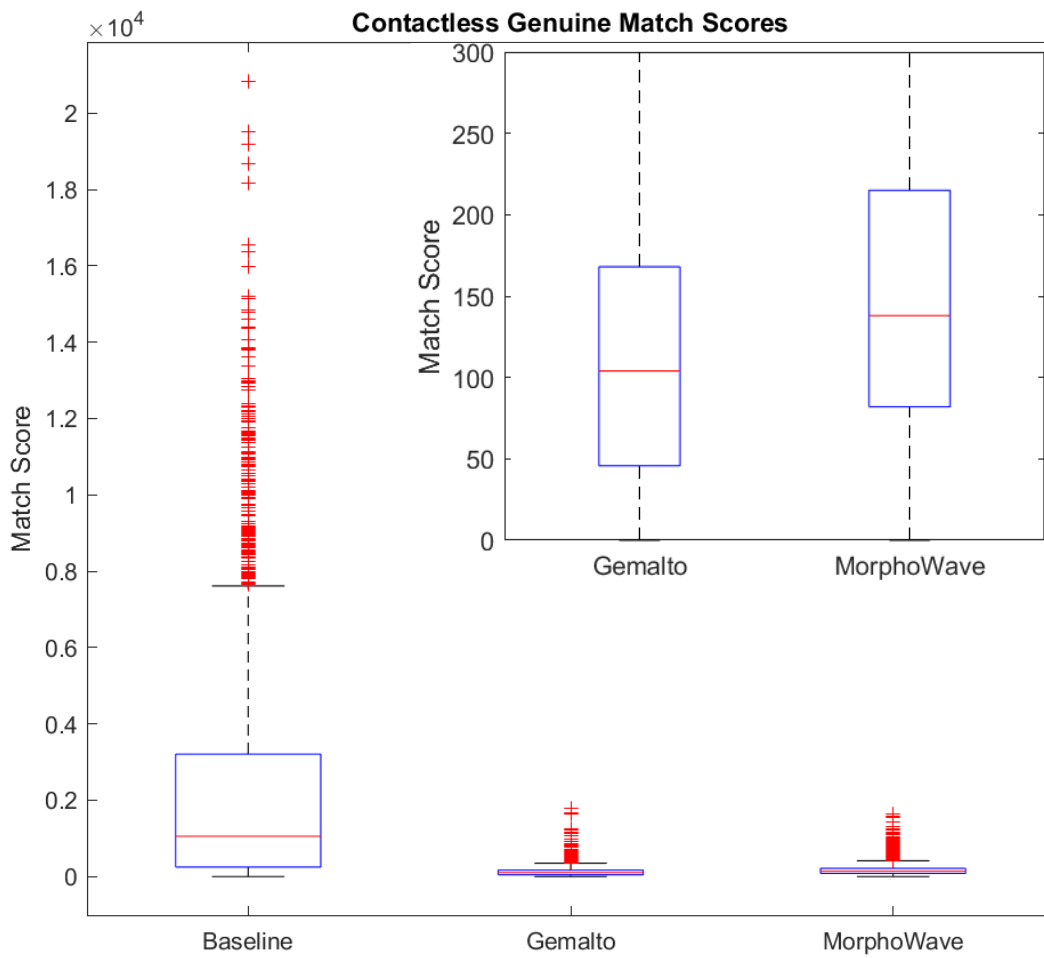


Figure 59 VeriFinger match score comparison for contactless sets compared to baseline.

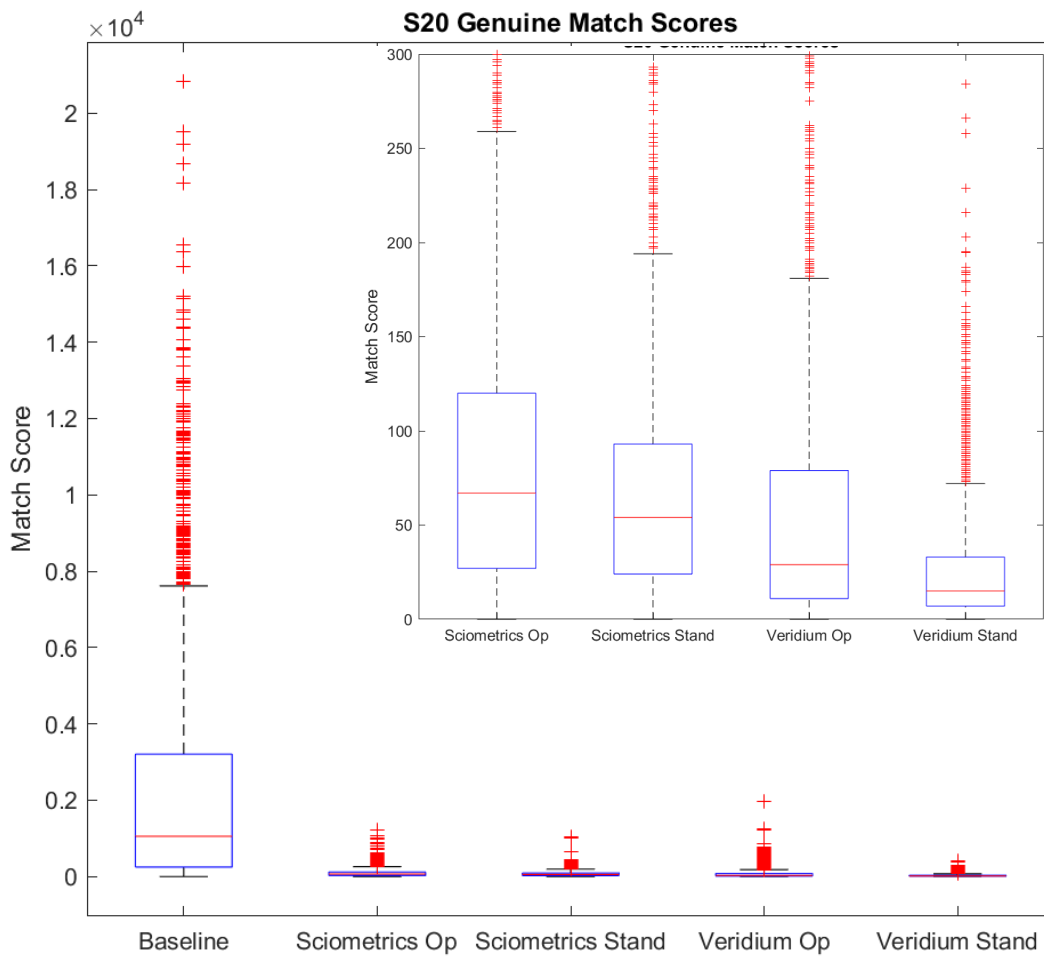


Figure 60 VeriFinger match score comparison for S20 sets from both cellphone applications in both settings compared to baseline.

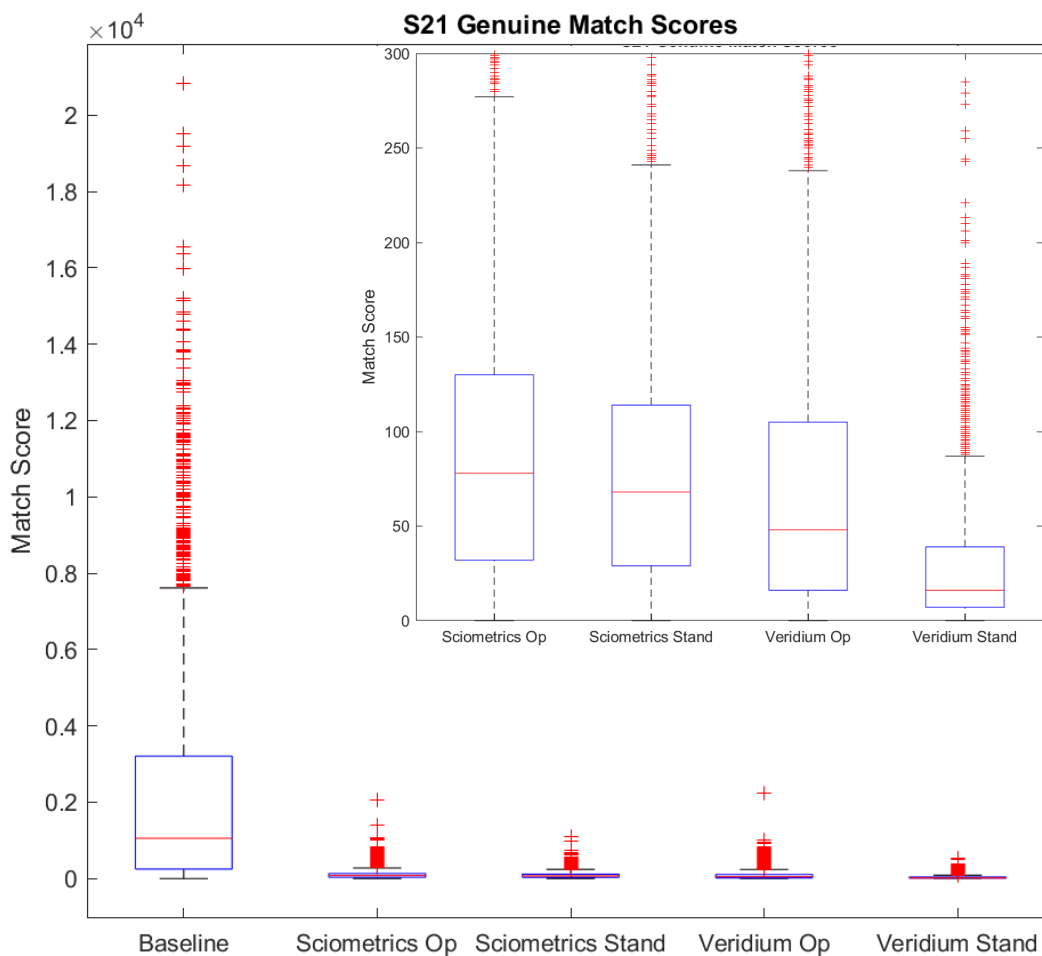


Figure 61 VeriFinger match score comparison for S21 sets from both cellphone applications in both settings compared to baseline.

The distributions for the VeriFinger genuine match experiments in Figure 58 through Figure 61 show many outliers for all experiments, including the baseline. The score range for VeriFinger is larger than Innovatrics at values greater than 20,000 being the upper limit; very few come close to a score of 600, with only the baseline consisting of Guardian Slap and Kojak Slap having a significant number exceeding a score of 600. The similar shape and size of the plain prints making up both the gallery and probe of the baseline are most likely performing exceptionally well for the VeriFinger matcher compared to all other sets. All other distributions

have very low medians with many outliers even within the baseline's interquartile and whisker range, with the contactless and cellphone experiments having particularly low scores. Even with low scores, VeriFinger did perform comparably to Innovatrics when looking at the AUC and DET values.

### 4.2.3.3 Bozorth3

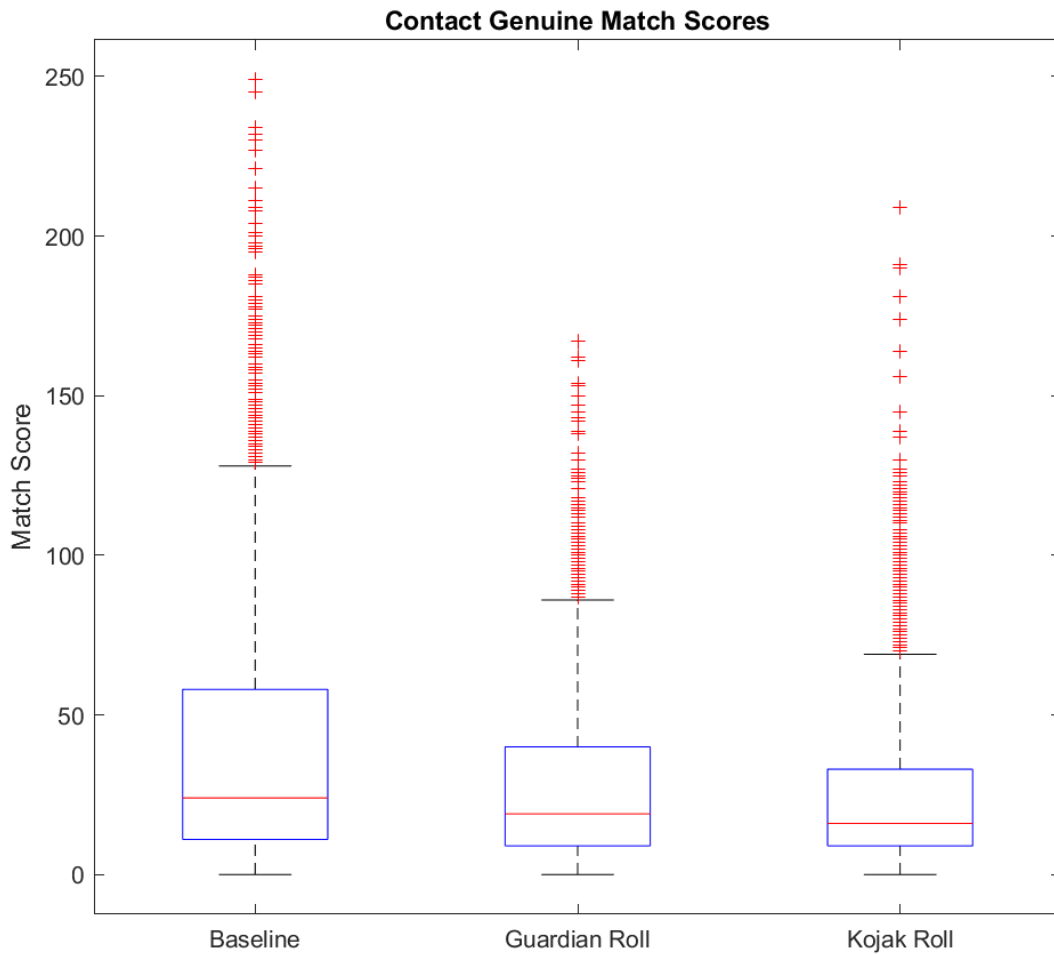


Figure 62 Bozorth3 match score comparison for contact sets compared to baseline.

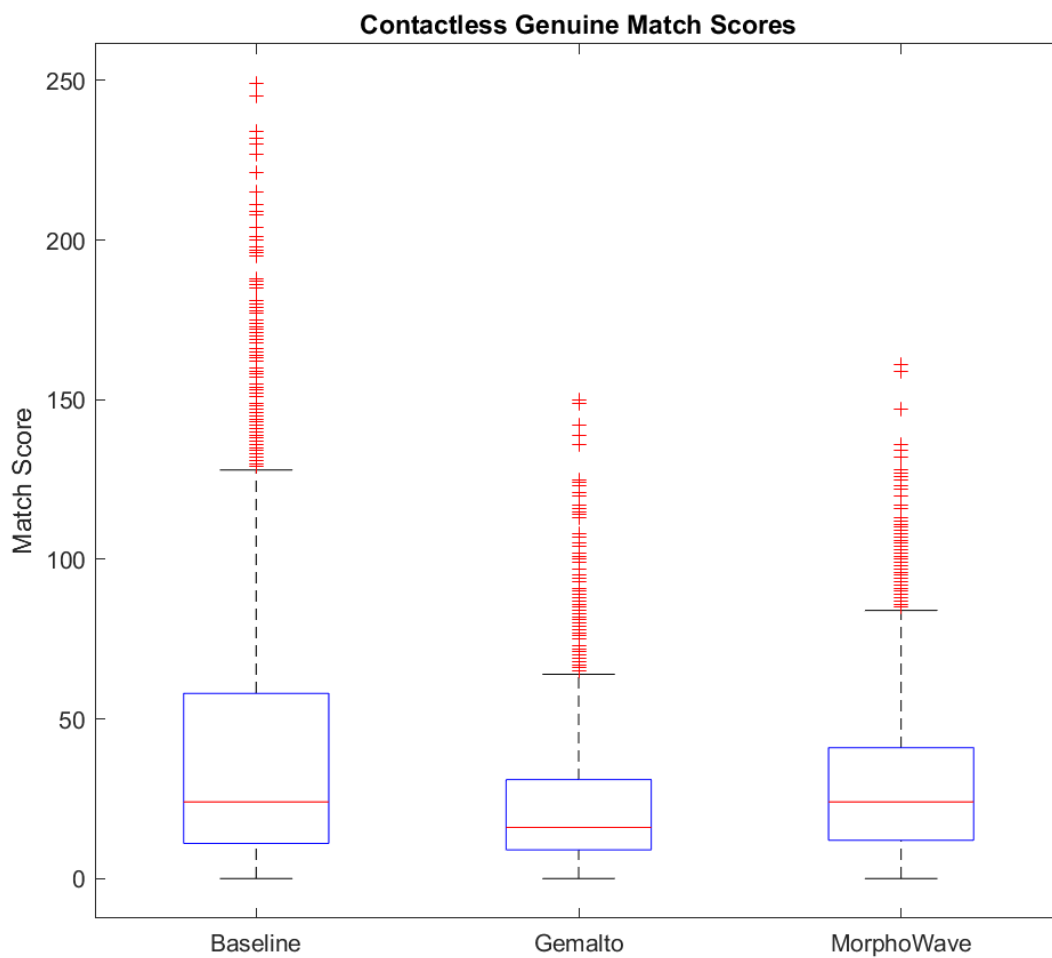


Figure 63 Bozorth3 match score comparison for contactless sets compared to baseline.



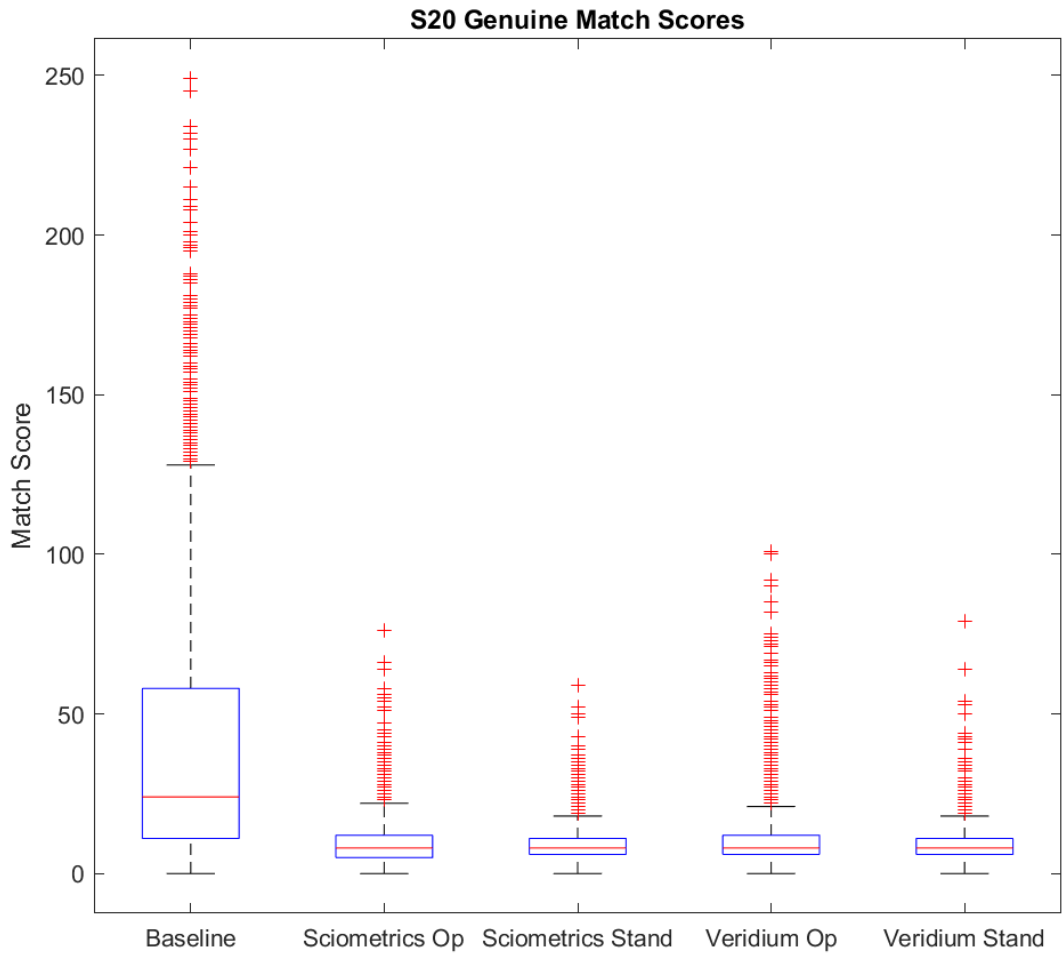
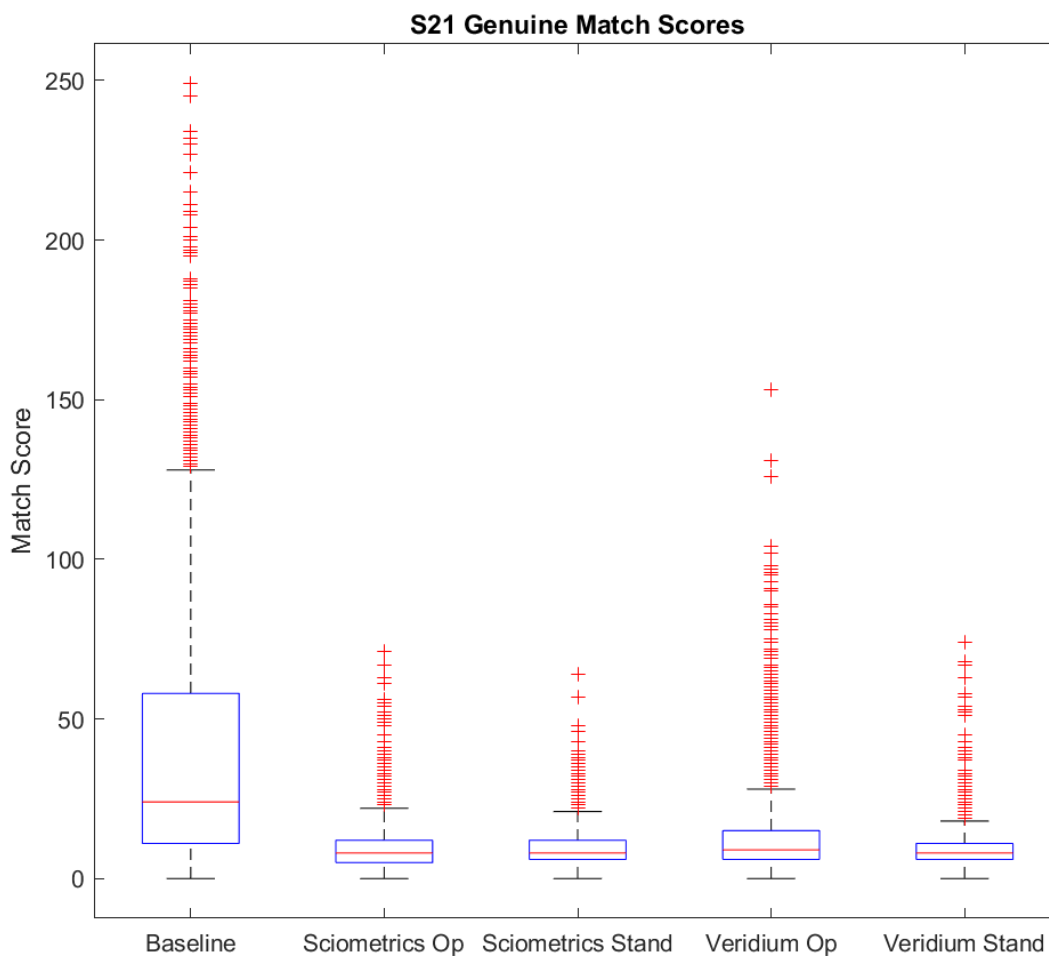


Figure 64 Bozorth3 match score comparison for S20 sets from both cellphone applications in both settings compared to baseline.



*Figure 65 Bozorth3 match score comparison for S21 sets from both cellphone applications in both settings compared to baseline.*

The Bozorth3 distributions for genuine match scores in Figure 62 through Figure 65 show a similar but far less extreme version of the VeriFinger distributions for the cellphone genuine matches, though the contactless and contact genuine matches are all comparable to the baseline. The contact and contactless genuine matches in Figure 62 and Figure 63, respectively, all have median distribution values around a score of 25, with the MorphoWave and Guardian Roll matches having the highest. However, all distributions, including the baseline, have significant outliers for Bozorth3's score range of at most 250. The cellphone distributions in Figure 64 and

Figure 65 all have a very low distribution, with the entire interquartile and whisker range of each cellphone distribution falling below the baseline’s median. Looking at the AUC values in Table 5 for the S20 and S21 Bozorth3 experiments, a low median, interquartile range, and whiskers were expected since Bozorth3 performed poorly, with only the S21 Operational Veridium experiment having an AUC above 0.7.

#### 4.2.4 NFIQ2 Quality Score Distributions

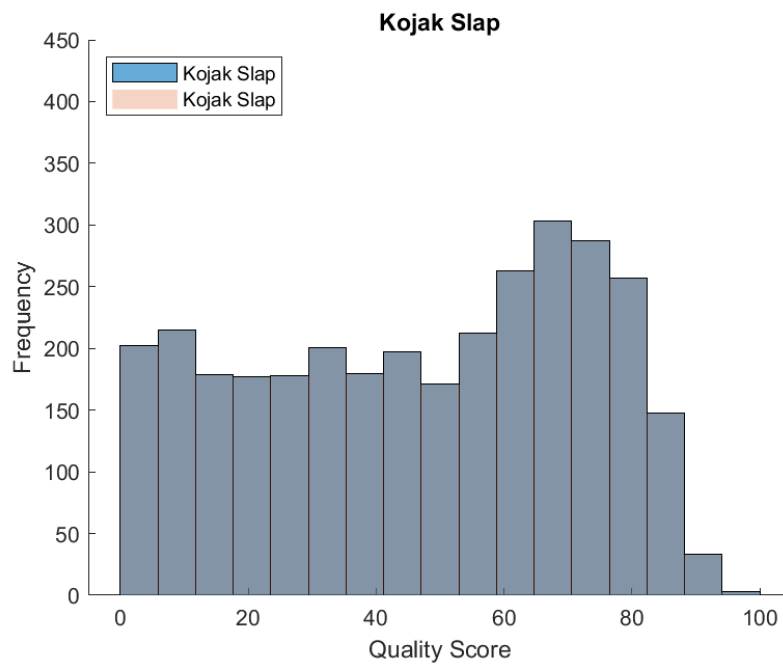


Figure 66 NFIQ2 score distribution for Kojak Slap fingerprints.

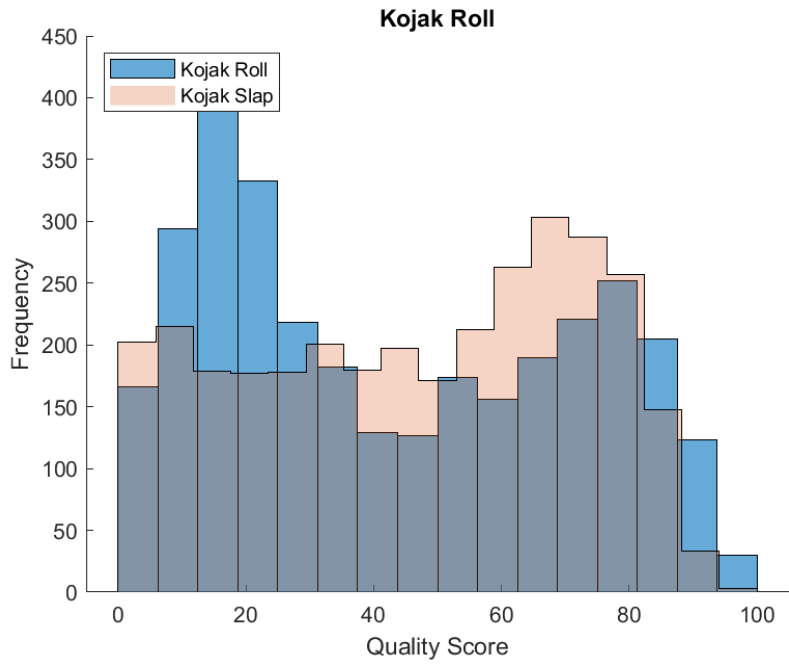


Figure 67 NFIQ2 score distribution for Kojak Roll fingerprints.

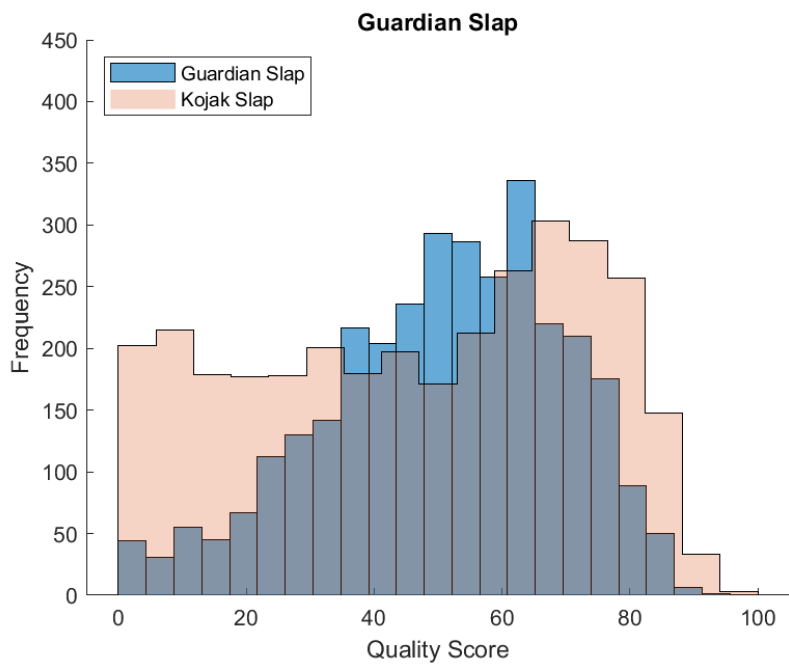


Figure 68 NFIQ2 score distribution for Guardian Slap fingerprints.

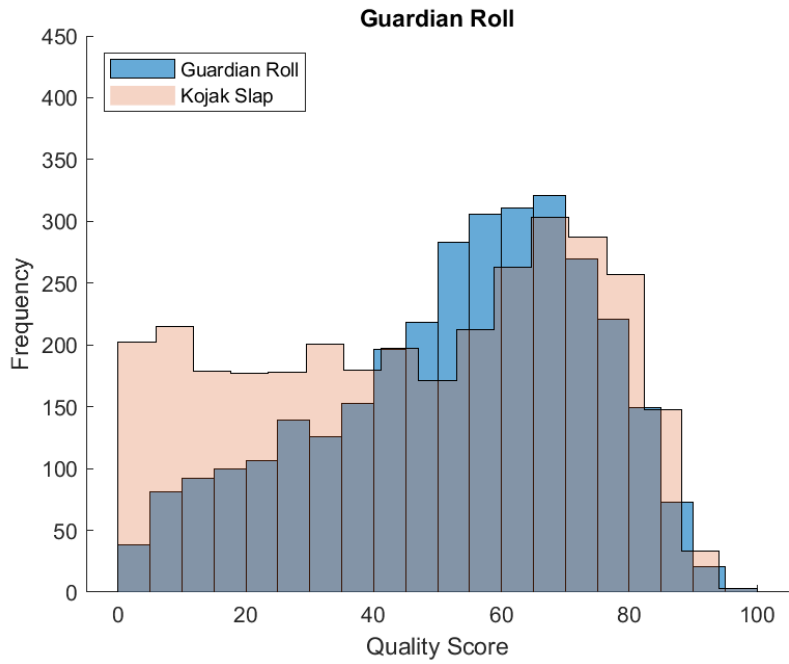


Figure 69 NFIQ2 score distribution for Guardian Roll fingerprints.

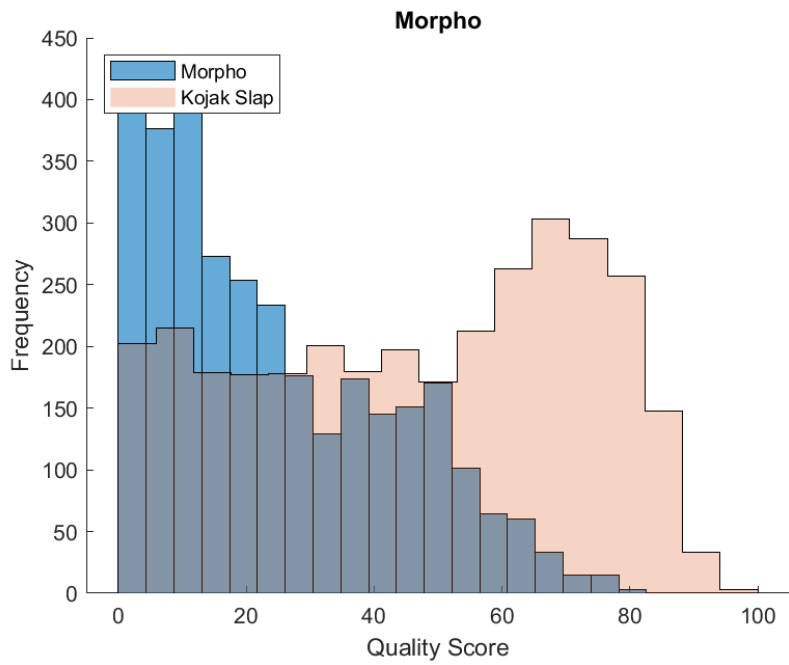


Figure 70 NFIQ2 score distribution for MorphoWave fingerprints.

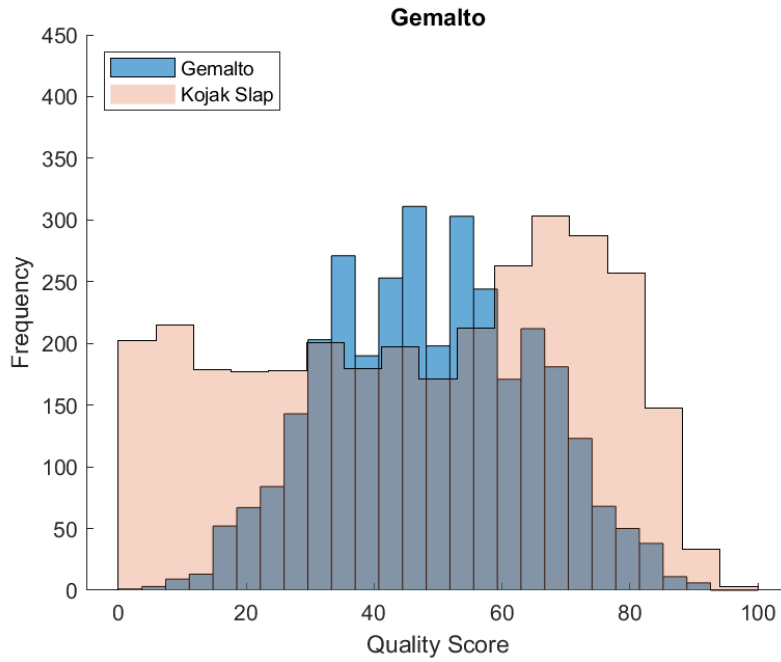


Figure 71 NFIQ2 score distribution for Gemalto fingerprints.

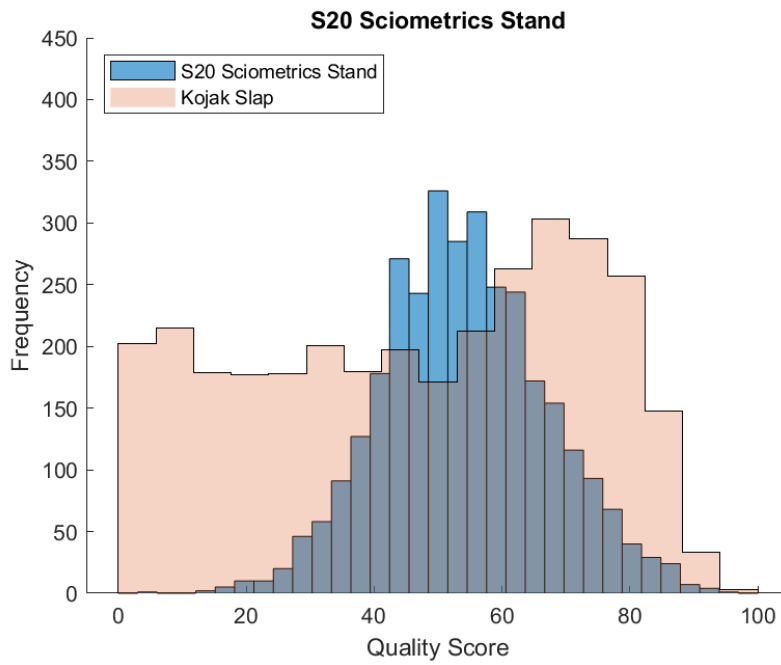


Figure 72 NFIQ2 score distribution for S20 Sciometrics Stand fingerprints.

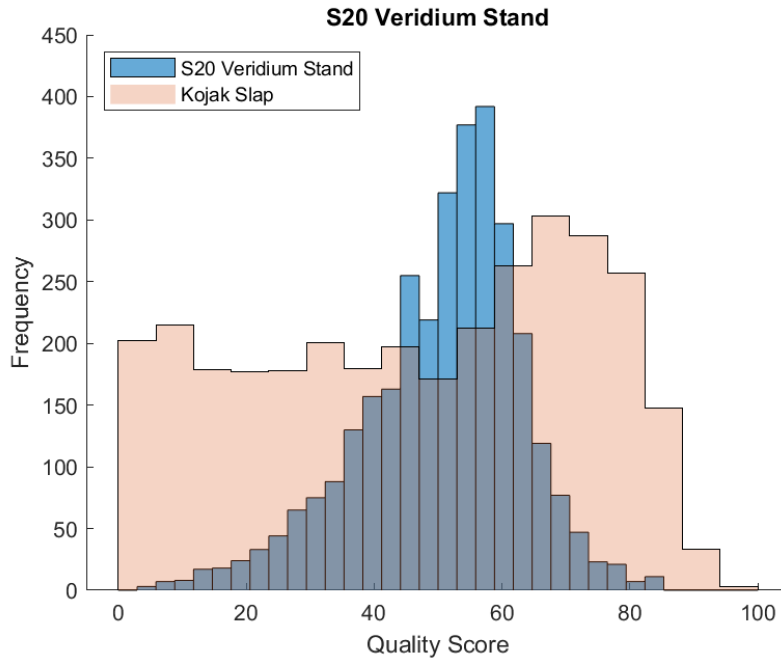


Figure 73 NFIQ2 score distribution for S20 Veridium Stand fingerprints.

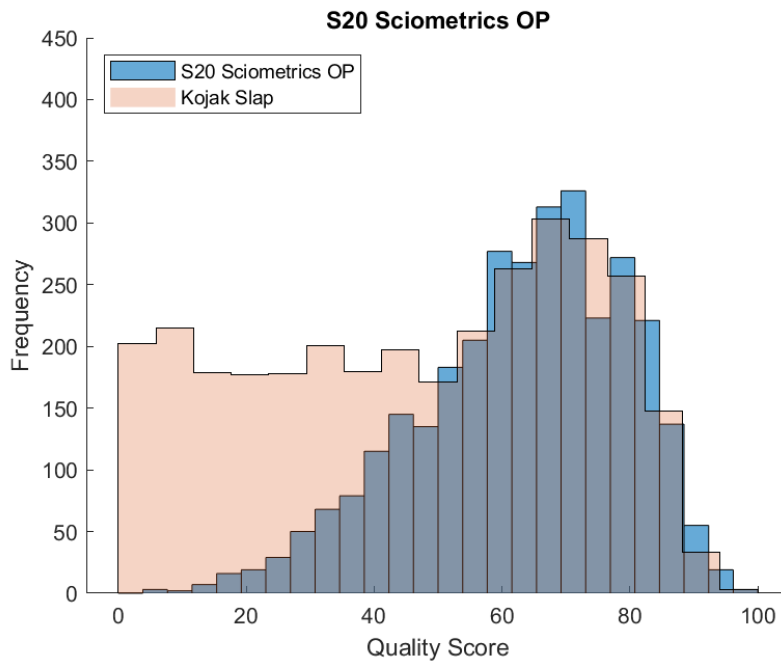


Figure 74 NFIQ2 score distribution for S20 Sciometrics Op fingerprints.

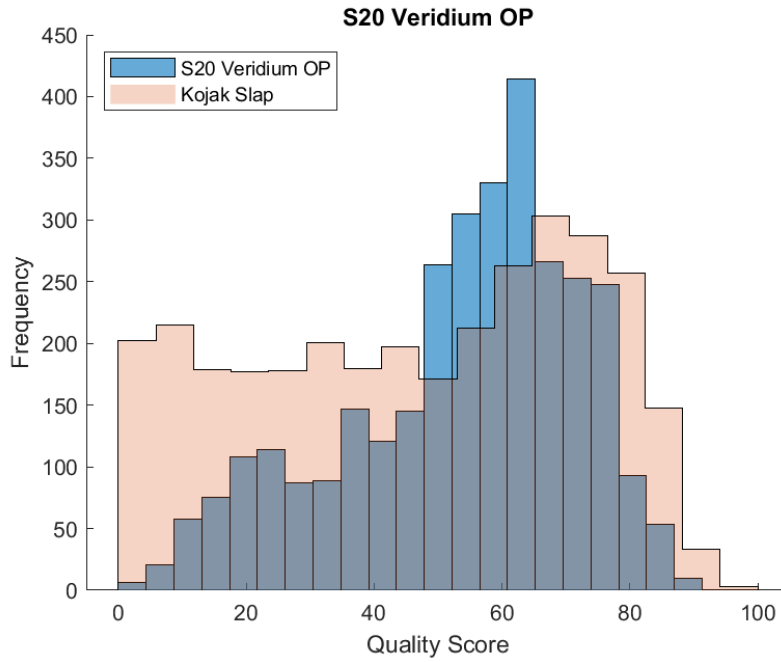


Figure 75 NFIQ2 score distribution for S20 Veridium Op fingerprints.

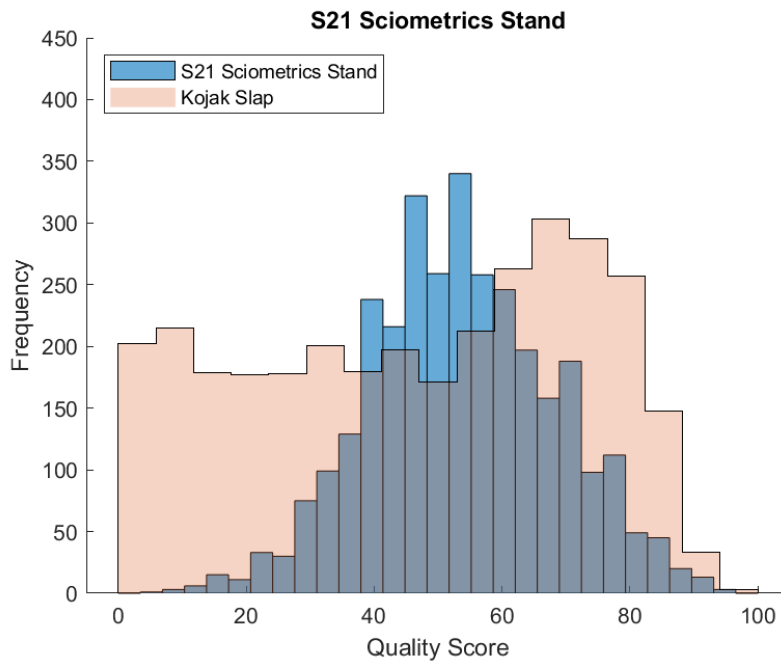


Figure 76 NFIQ2 score distribution for S21 Sciometrics Stand fingerprints.



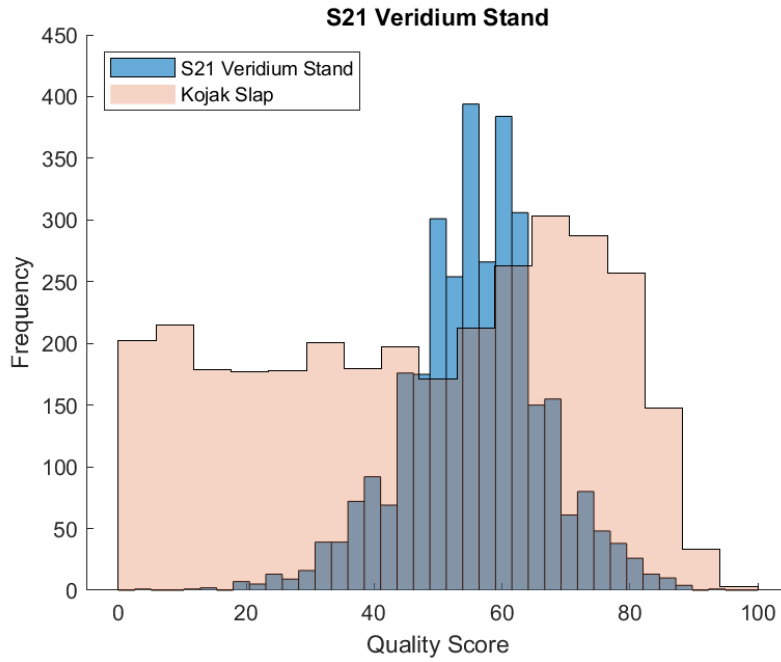


Figure 77 NFIQ2 score distribution for S21 Veridium Stand fingerprints.

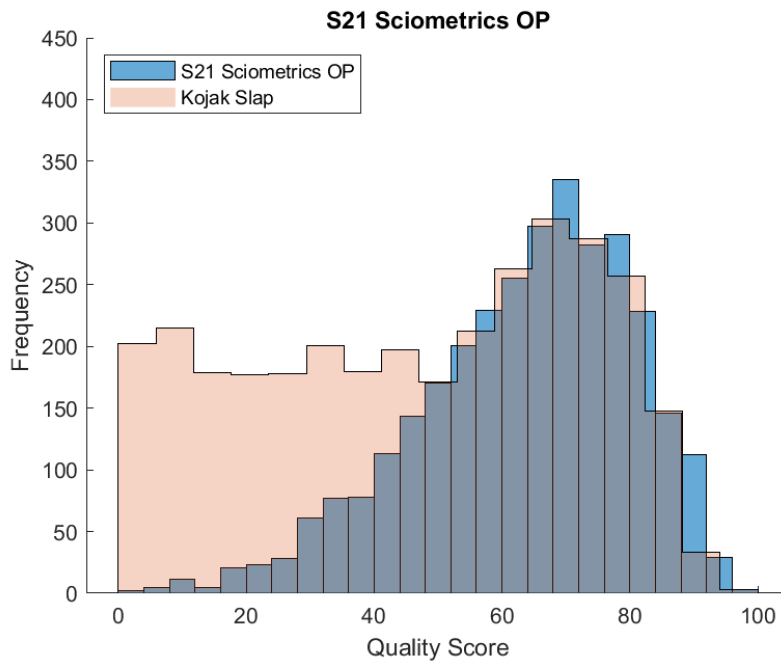
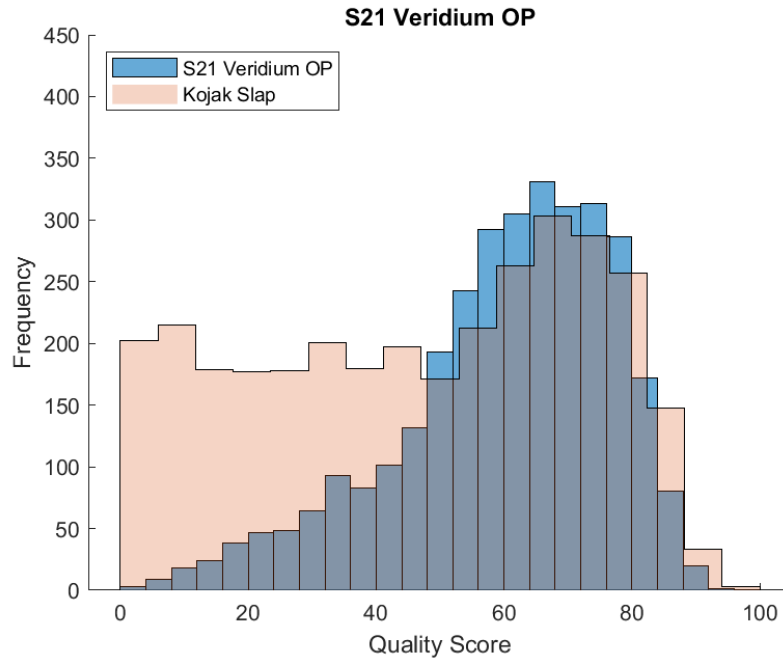


Figure 78 NFIQ2 score distribution for S21 Sciometrics Op fingerprints.



*Figure 79 NFIQ2 score distribution for S21 Veridium Op fingerprints.*

The NFIQ2 frequency distribution in Figure 66 through Figure 79 shows the concentration of quality scores for each fingerprint set since the purpose of generating the quality score of a fingerprint is to gauge an estimated match accuracy before using the fingerprint in a matching experiment. The baseline frequency distribution is shown in Figure 66, and a lower opacity baseline distribution appears in each figure to show comparison. Both guardian sets in Figure 68 and Figure 69 have similar distributions with a lower frequency of low-quality scores compared to the baseline. The Kojak Roll set in Figure 67 has a higher frequency of low-quality scores. The MorphoWave Frequency distribution in Figure 70 is the only distribution with a much higher frequency of low-quality scores. The Gemalto and all the cellphone distributions have a low frequency for low-quality scores and a higher frequency for high-quality scores as the baseline.

## 4.2.5 NFIQ2 Quality Score VS Genuine Match Score

### 4.2.5.1 Innovatrics

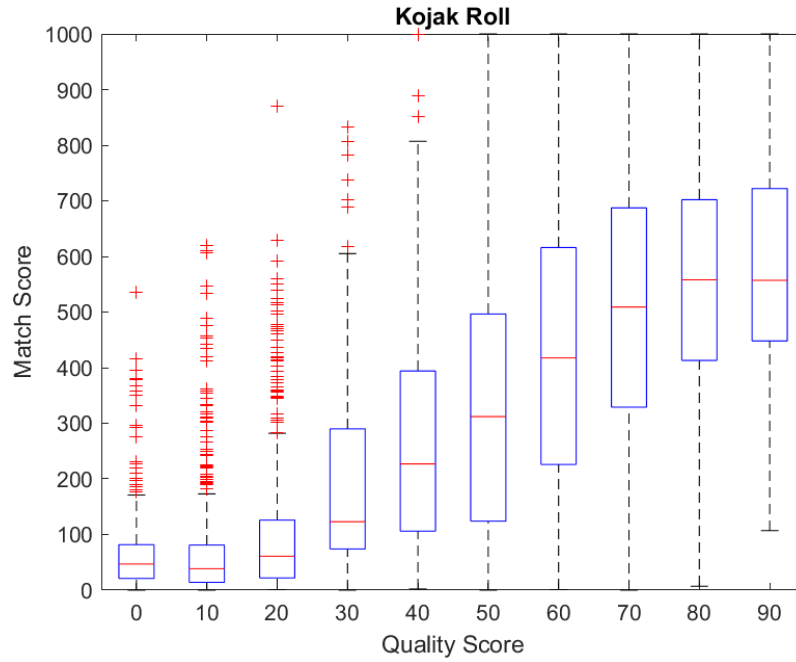


Figure 80 Kojak Roll NFIQ2 rounded quality score vs Innovatrics match score.

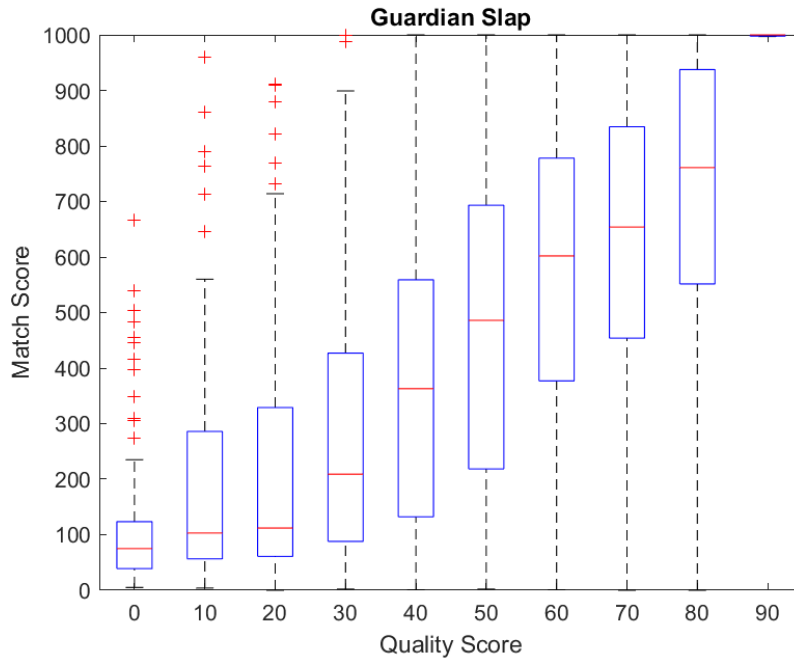


Figure 81 Guardian Slap NFIQ2 rounded quality score vs Innovatrics match score.

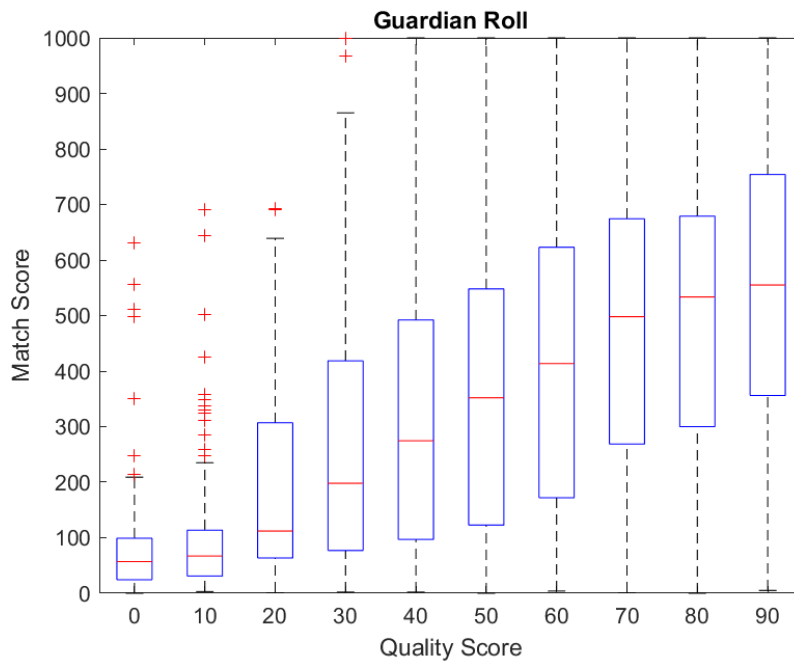


Figure 82 Guardian Roll NFIQ2 rounded quality score vs Innovatrics match score.

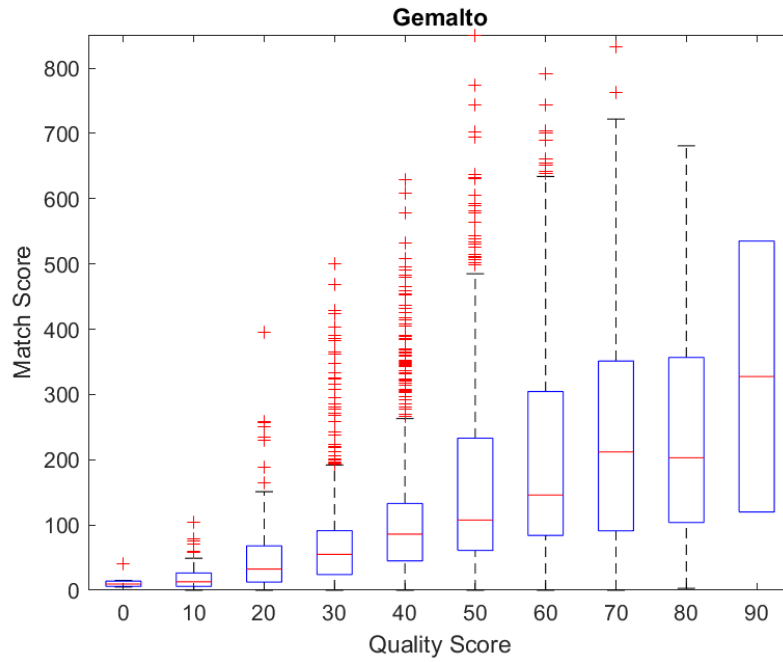


Figure 83 Gemalto NFIQ2 rounded quality score vs Innovatrics match score.

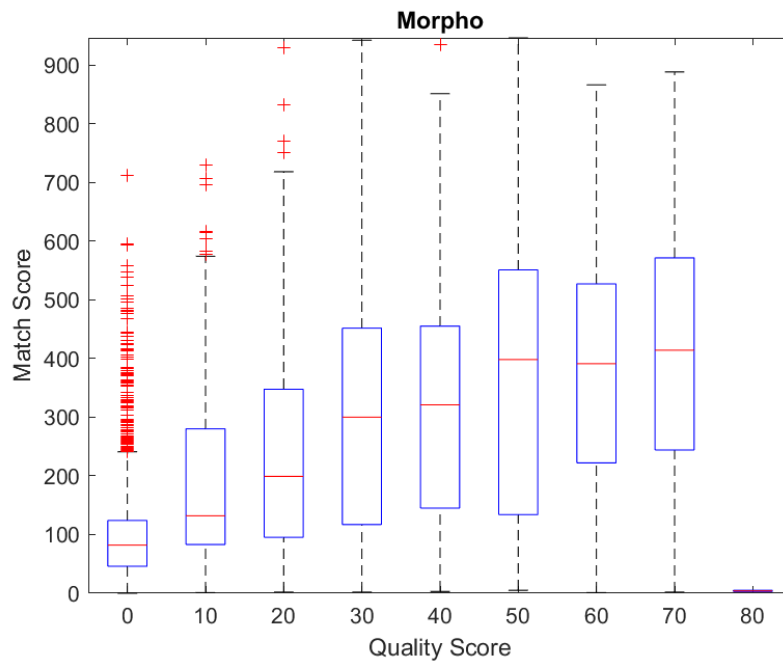


Figure 84 MorphoWave NFIQ2 rounded quality score vs Innovatrics match score.

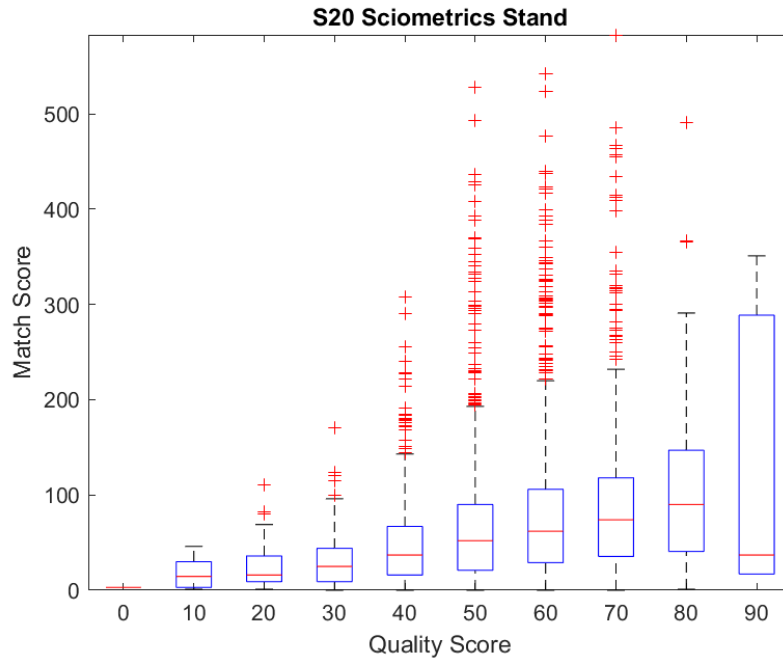


Figure 85 S20 Sciometrics Stand NFIQ2 rounded quality score vs Innovatrics match score.

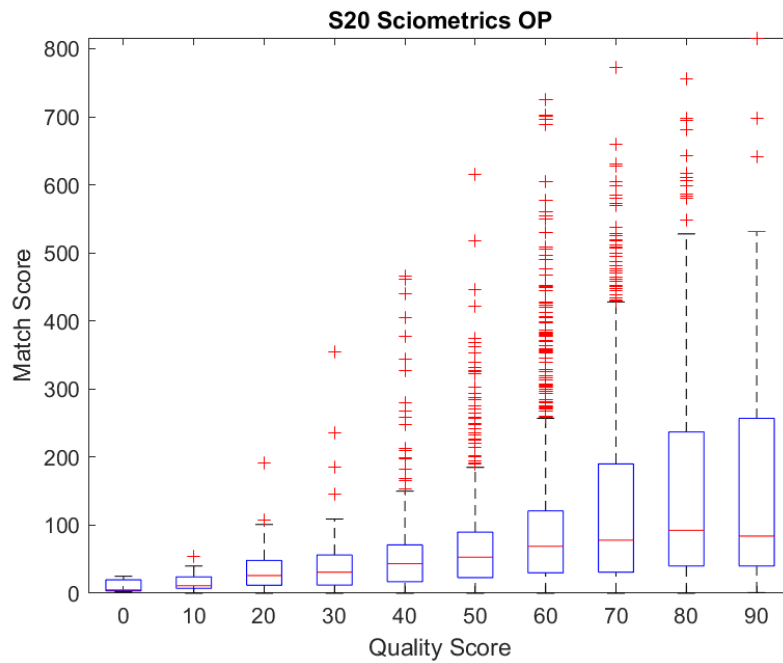


Figure 86 S20 Sciometrics Op NFIQ2 rounded quality score vs Innovatrics match score.

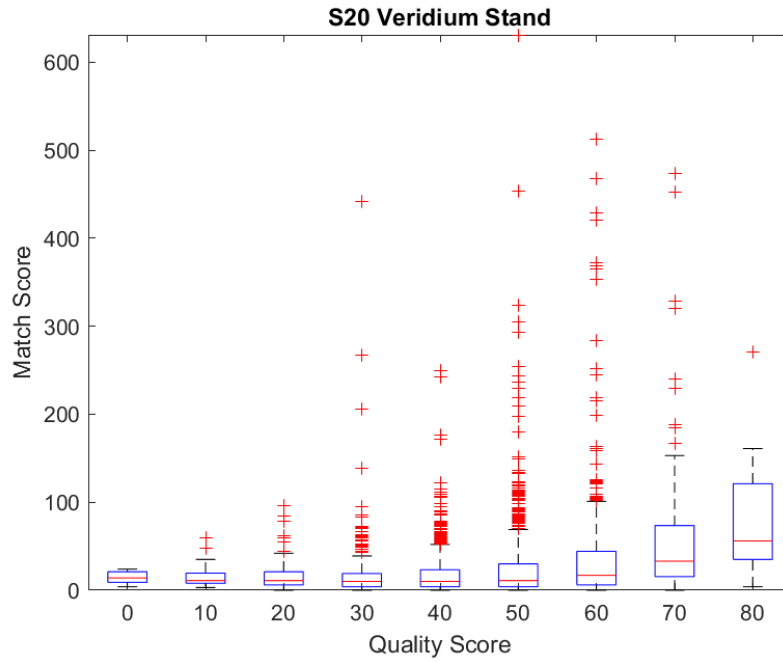


Figure 87 S20 Veridium Stand NFIQ2 rounded quality score vs Innovatrics match score.

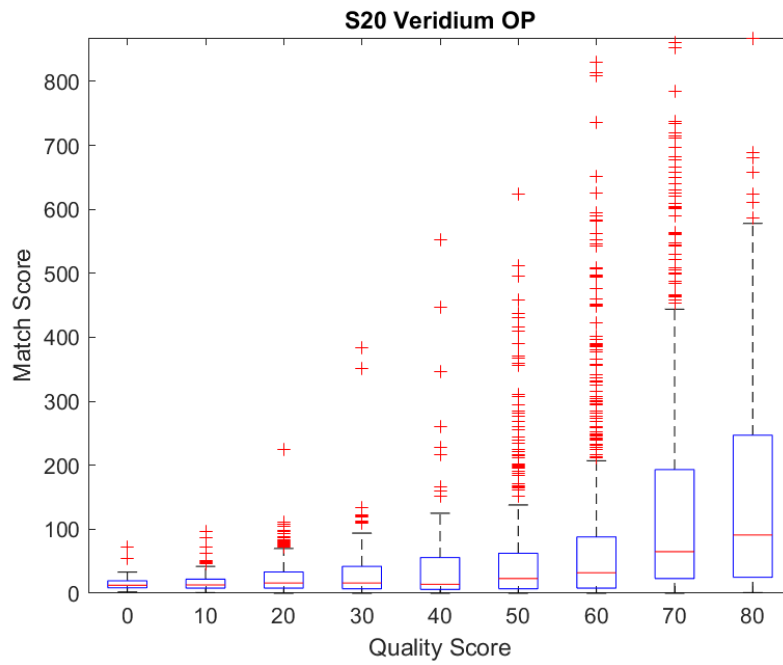


Figure 88 S20 Veridium Op NFIQ2 rounded quality score vs Innovatrics match score.

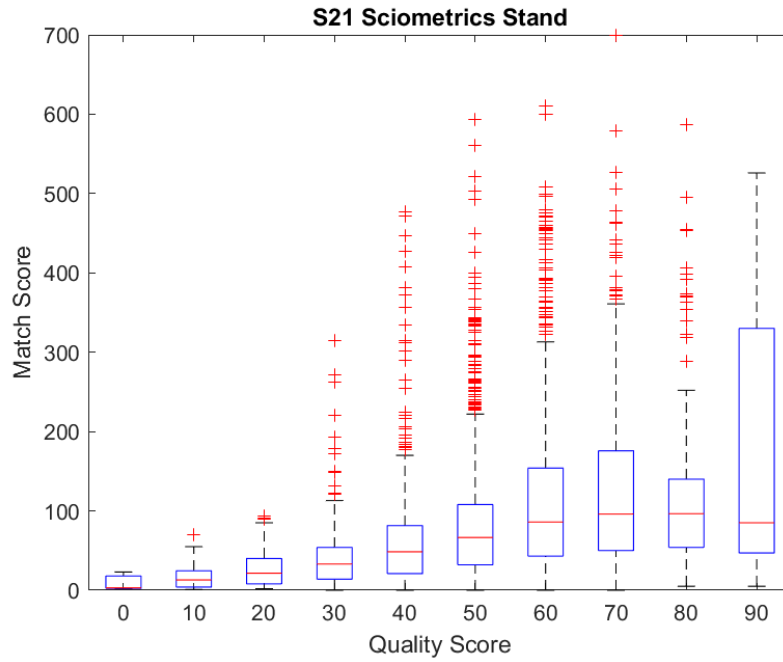


Figure 89 S21 Sciometrics Stand NFIQ2 rounded quality score vs Innovatrics match score.

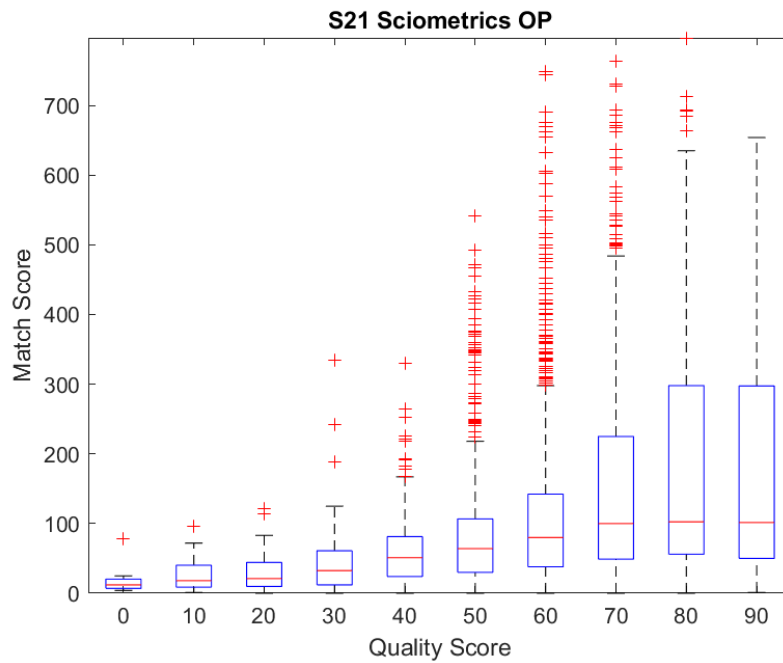


Figure 90 S21 Sciometrics Op NFIQ2 rounded quality score vs Innovatrics match score.



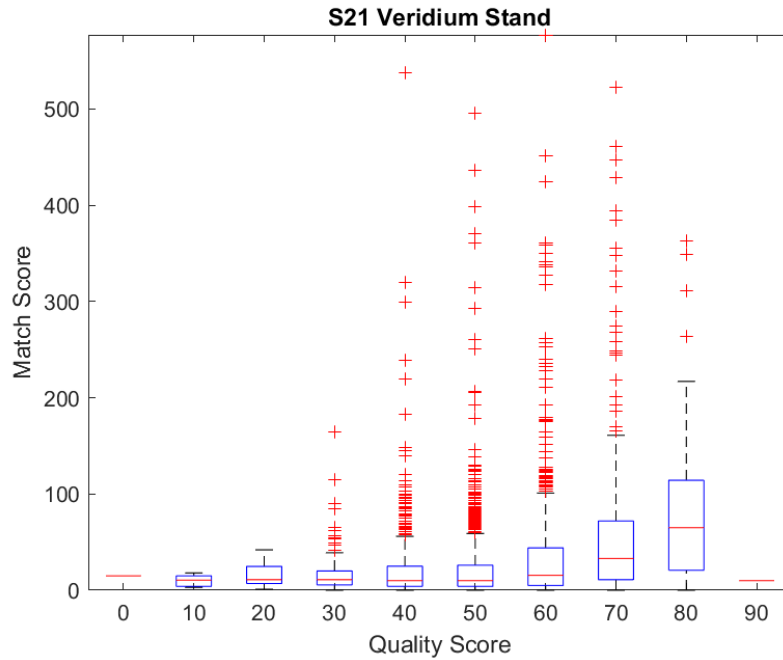


Figure 91 S21 Veridium Stand NFIQ2 rounded quality score vs Innovatrics match score.

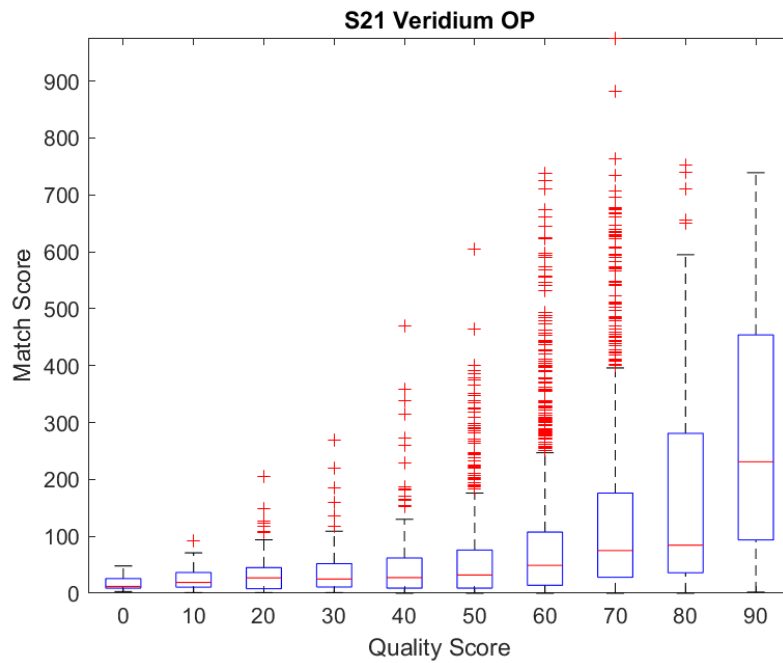


Figure 92 S21 Veridium Op NFIQ2 rounded quality score vs Innovatrics match score.

When compared to the Innovatrics matcher in Figure 80 through Figure 92, the quality scores show the expected outcome for all comparisons. As the quality score increases, so does

the match score. Each contact fingerprint set in Figure 80 through Figure 82 shows an ideal distribution with the interquartile ranges increasing with the median quality score. The contactless distributions in Figure 83 and Figure 84 are similar to the contact distributions, with the Gemalto distribution median gradually increasing with the quality score while the interquartile range increases, showing a rising but wider distribution of match scores for higher quality scores. The Gemalto distribution also has a significant number of outliers in the middle of the quality scores showing that the middle-quality fingerprints are matching better than expected. While the MorphoWave distribution shows a similar gradual increase as quality scores increase, there is also a large number of outliers within the lowest end of the quality scores showing a divergence from the goal of having quality scores represent expected match accuracy since all of the outliers matched exceptionally well when at the lowest quality. The cellphone distributions in Figure 85 through Figure 92 show another exception, unlike the MorphoWave. Similar to the Gemalto distribution, each cellphone distribution has many outliers in the upper half of the quality scores.

In contrast, interquartile ranges remain low compared to the Gemalto distribution and others. Many low match scores for higher qualities lead the distributions to remain low. However, the large number of outliers signifies that genuine matches with a higher score match much higher than expected when compared to other forms of fingerprints.

### 4.2.5.2 VeriFinger

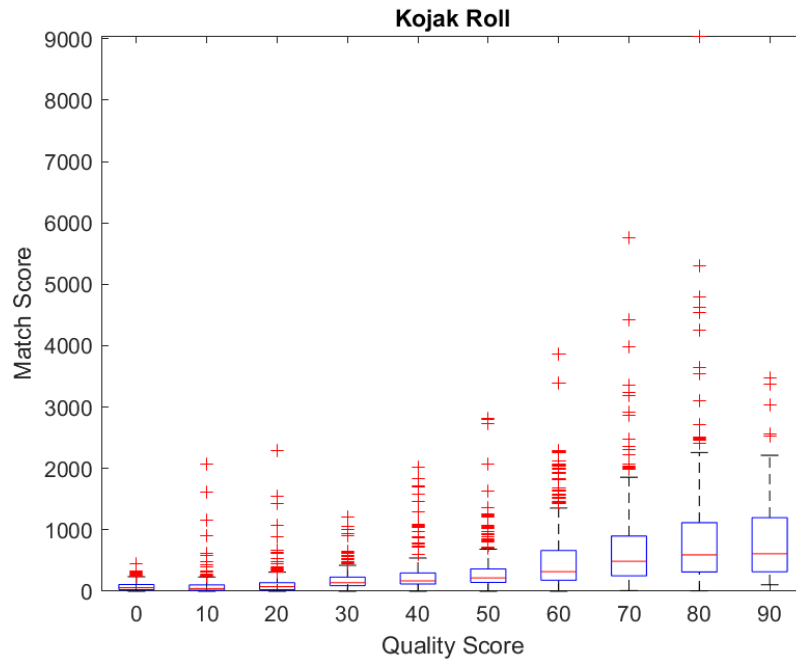


Figure 93 Kojak Roll NFIQ2 rounded quality score vs VeriFinger match score.

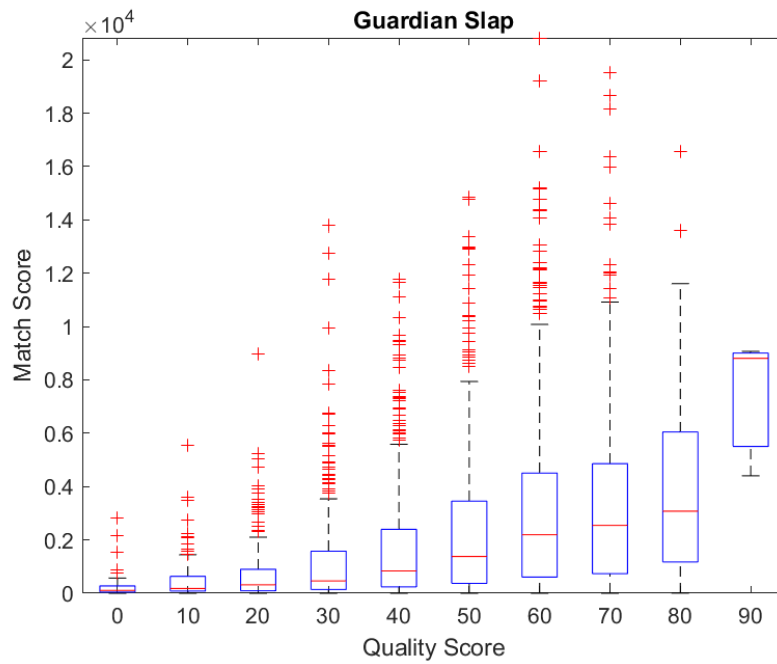


Figure 94 Guardian Slap NFIQ2 rounded quality score vs VeriFinger match score.

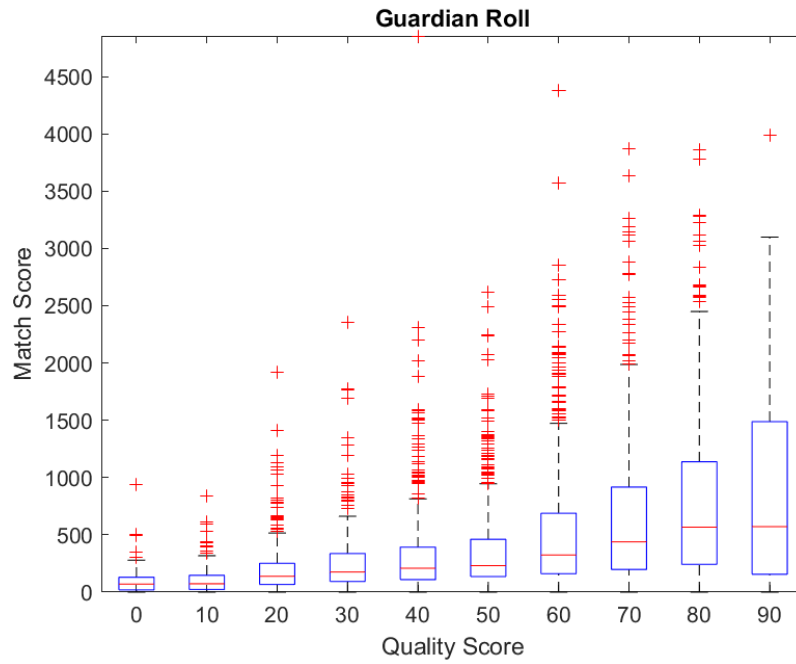


Figure 95 Guardian Roll NFIQ2 rounded quality score vs VeriFinger match score.

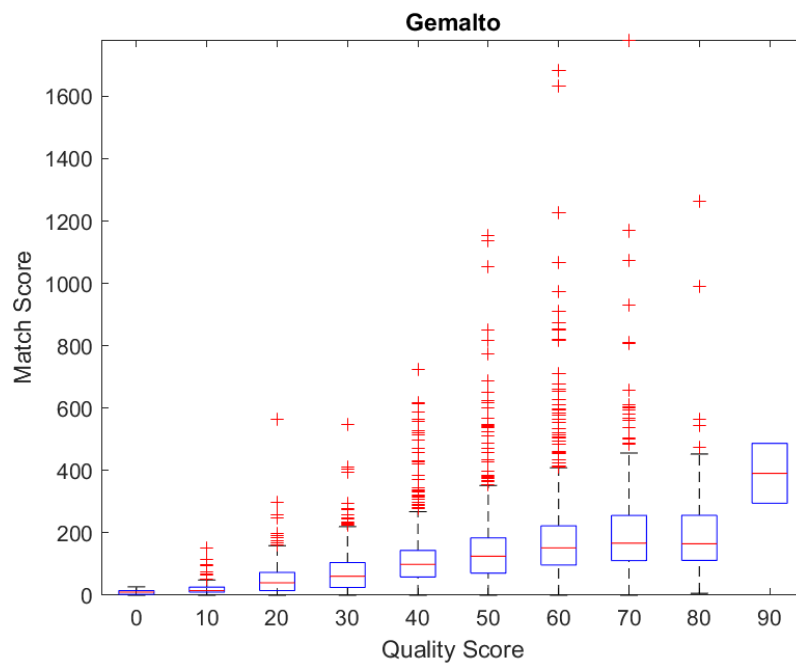


Figure 96 Gemalto NFIQ2 rounded quality score vs VeriFinger match score.

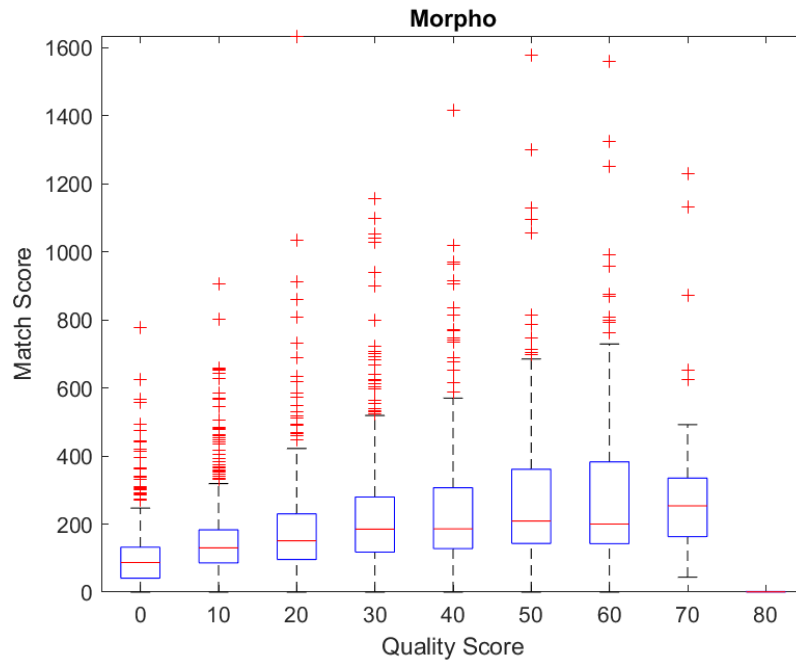


Figure 97 MorphoWave NFIQ2 rounded quality score vs VeriFinger match score.

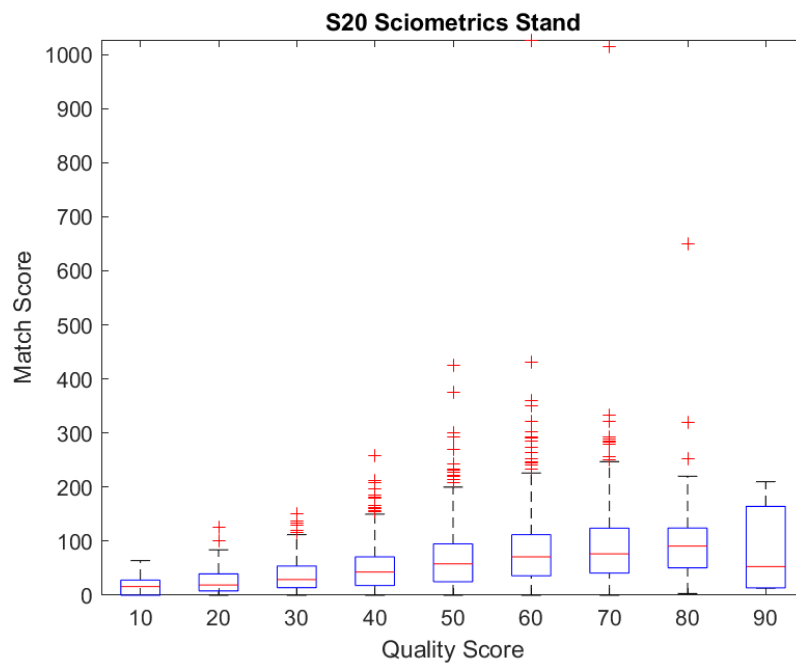


Figure 98 S20 Sciometrics Stand NFIQ2 rounded quality score vs VeriFinger match score.

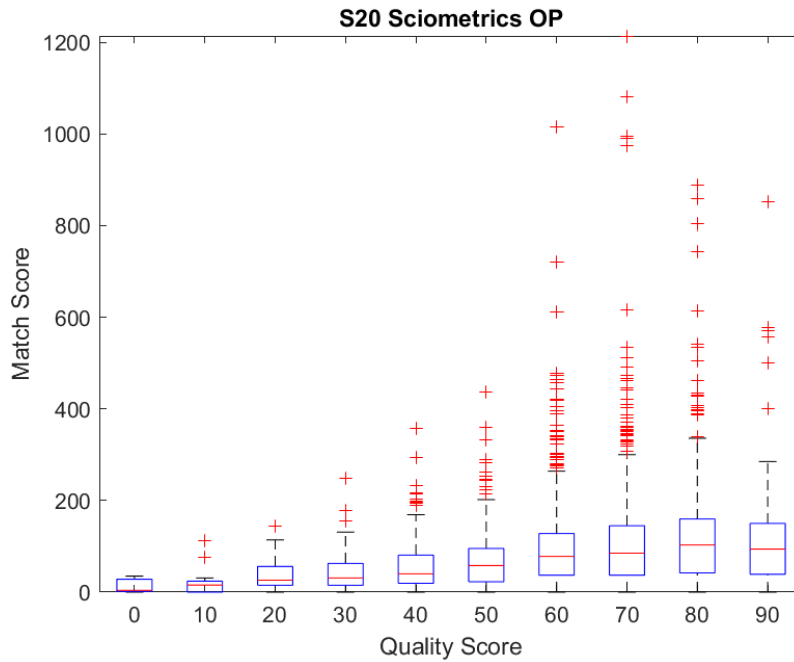


Figure 99 S20 Sciometrics Op NFIQ2 rounded quality score vs VeriFinger match score.

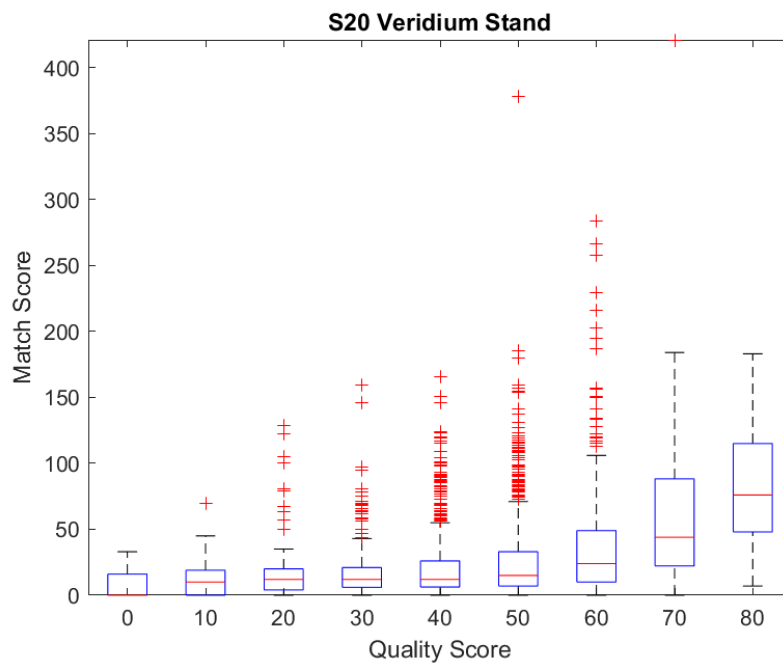


Figure 100 S20 Veridium Stand NFIQ2 rounded quality score vs VeriFinger match score.

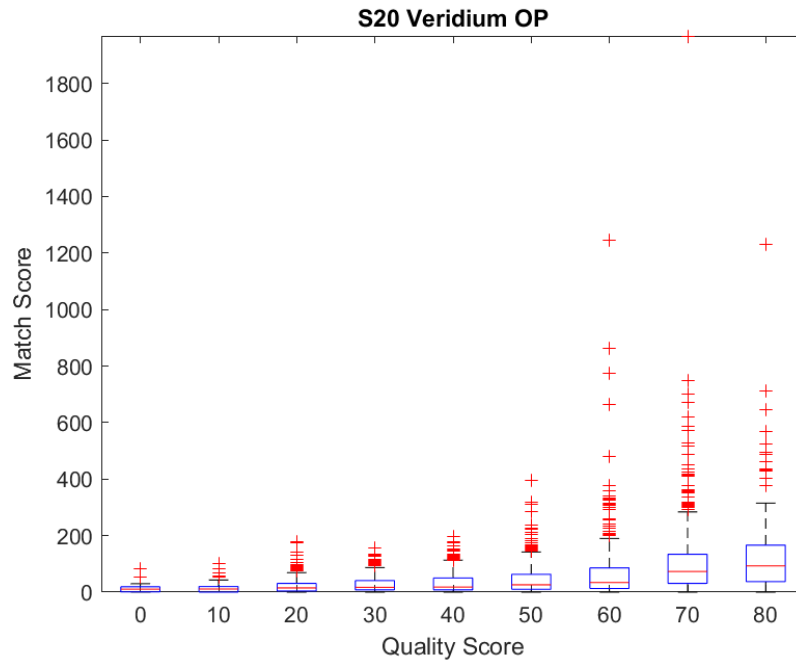


Figure 101 S20 Veridium Op NFIQ2 rounded quality score vs VeriFinger match score.

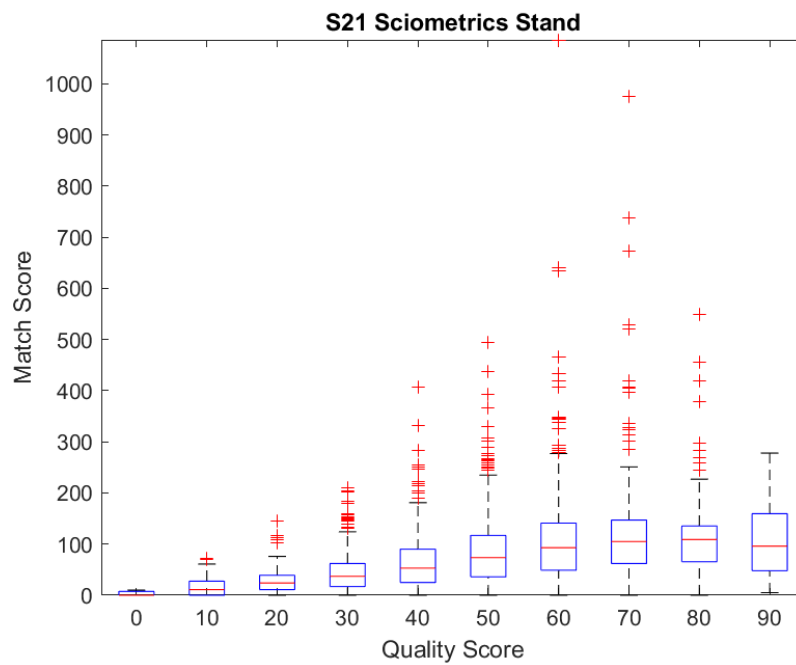


Figure 102 S21 Sciometrics Stand NFIQ2 rounded quality score vs VeriFinger match score.

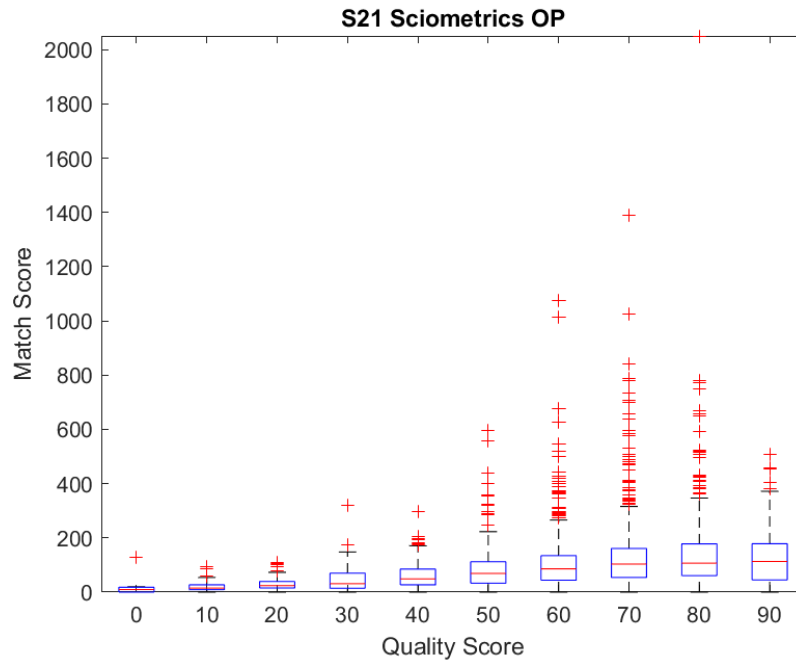


Figure 103 S21 Sciometrics Op NFIQ2 rounded quality score vs VeriFinger match score.

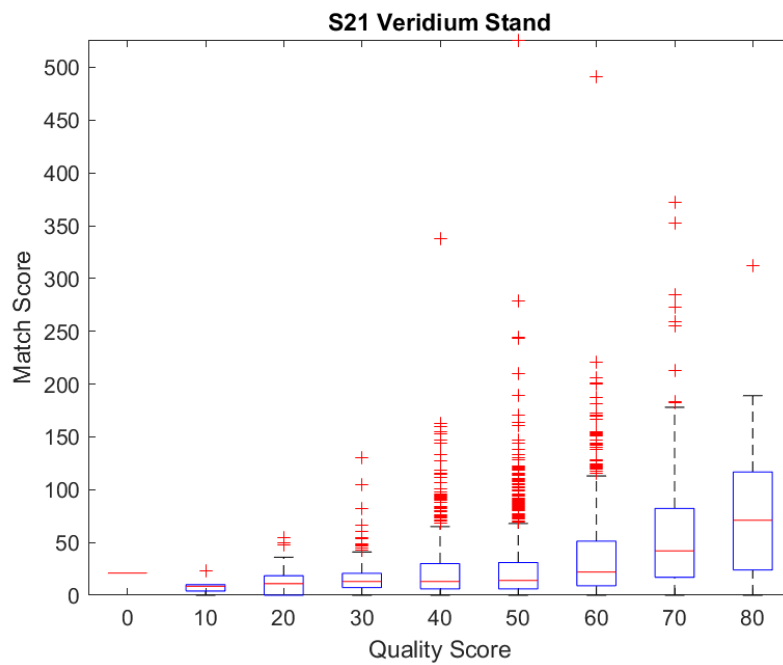


Figure 104 S21 Veridium Stand NFIQ2 rounded quality score vs VeriFinger match score.



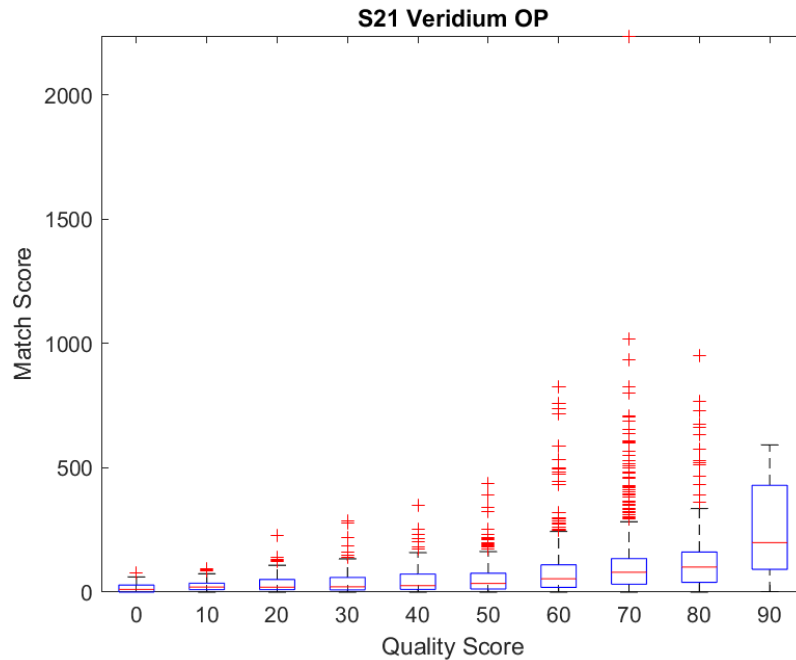


Figure 105 S21 Veridium Op NFIQ2 rounded quality score vs VeriFinger match score.

Comparing the VeriFinger results to the NFIQ2 rounded quality scores in the contact experiments in Figure 93 through Figure 95, the expected outcome is an increase in match performance as the quality score increases. Though VeriFinger uses a vast range for match scores that lead to an exponential scale between scores, with most scores performing in the lower range, many outliers appear due to the extreme margin for possible scores with all of the VeriFinger comparisons having a few outliers that have scores so high the rest of the scores are even further concentrated downward. The contactless comparisons in Figure 96, and Figure 97 both show an increase in the match score as the quality score increases. The median and interquartile gradually improve before rounding off at the top end of the quality scores. The Gemalto comparison has a jump in match performance at the 90-quality score bin. MorphoWave, on the other hand, has only a single score in the 80-quality bin and no scores in the 90-quality bin. The outliers in the Gemalto comparison are concentrated in the middle to the upper-quality range. At the same time, the MorphoWave has the majority of high match score outliers in the lower to middle-quality

range. In the cellphone comparisons shown in Figure 98 through Figure 105, the operational setting had a higher match score threshold than the stand set. When observed for the same device and setting, the Sciometrics application had a higher match score threshold than the Veridium comparisons. Most of the cellphone outliers for the Operational comparisons are in the upper range, and the Stand comparisons had most outliers in the middle range. Additionally, the Sciometrics comparisons generally had a gradual increase in median match score with a quality score that ended in a plateau at the highest quality. In contrast, the Veridium comparisons had a delayed increase in match scores. The lower and middle-quality scores had a low increase in the median match score before having a sharp increase in the upper-quality scores.

### 4.2.5.3 Bozorth3

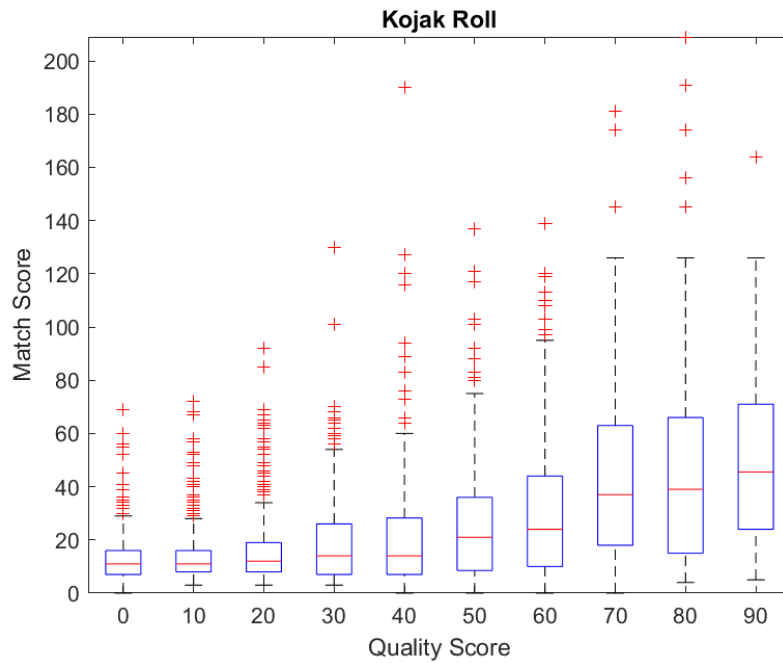


Figure 106 Kojak Roll NFIQ2 rounded quality score vs Bozorth3 match score.

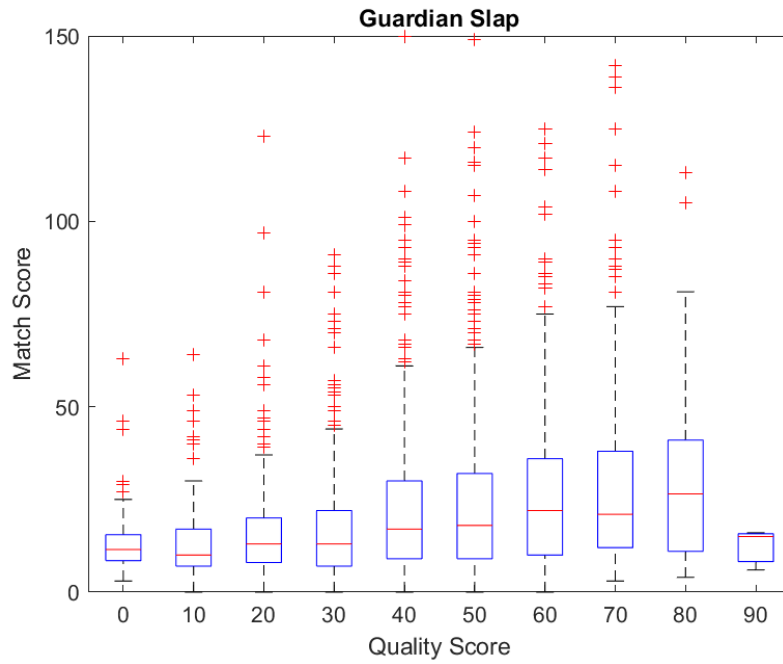


Figure 107 Guardian Slap NFIQ2 rounded quality score vs Bozorth3 match score.

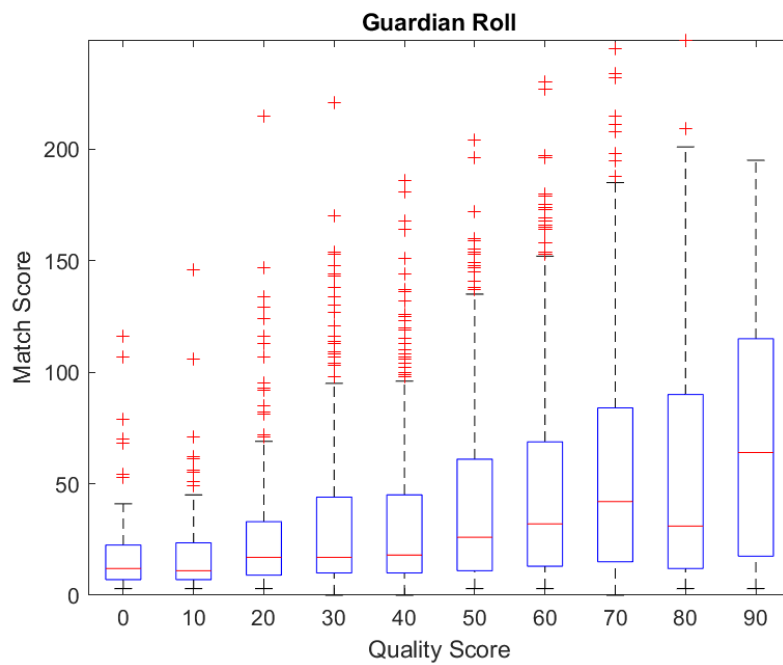


Figure 108 Guardian Roll NFIQ2 rounded quality score vs Bozorth3 match score.

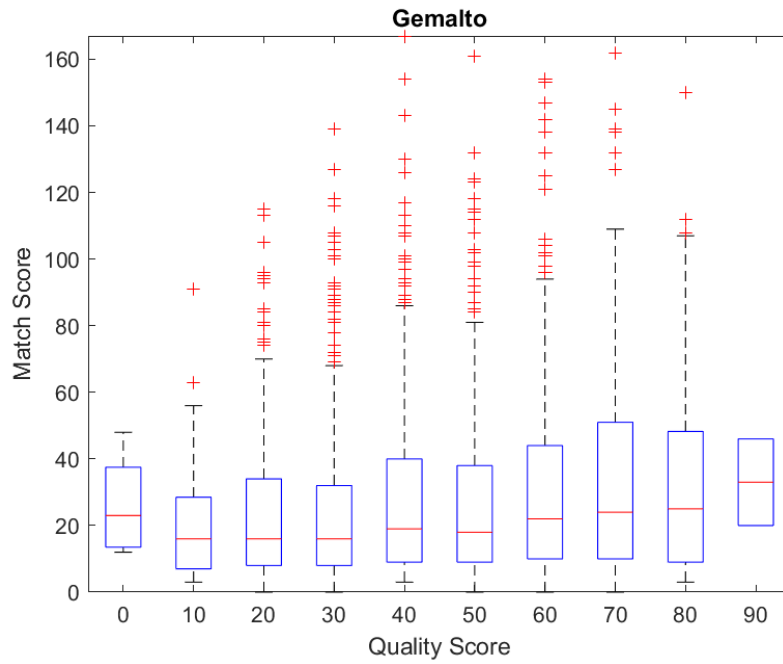


Figure 109 Gemalto NFIQ2 rounded quality score vs Bozorth3 match score.

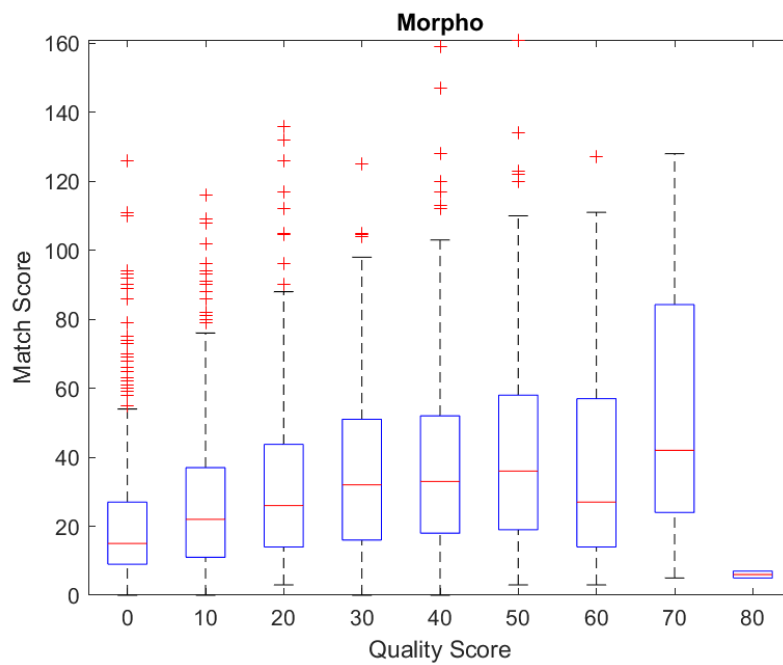


Figure 110 MorphoWave NFIQ2 rounded quality score vs Bozorth3 match score.

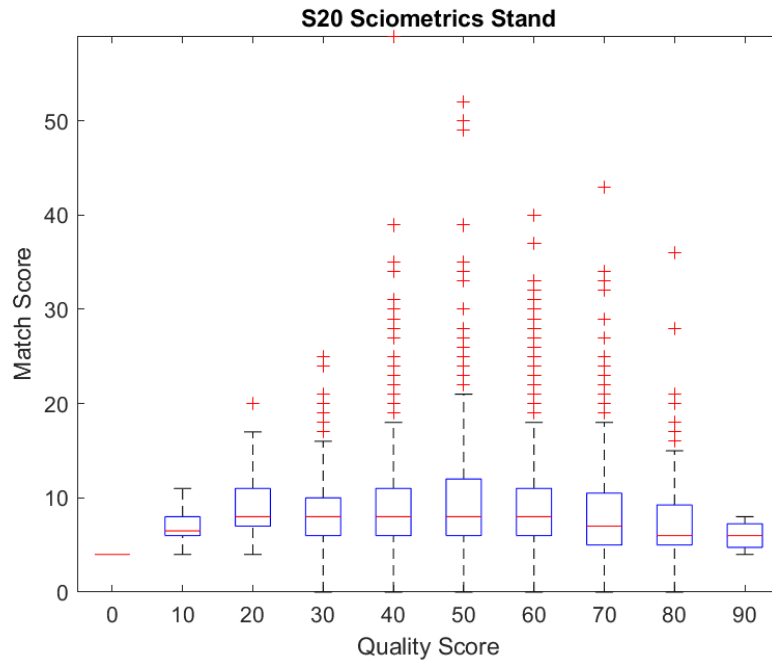


Figure 111 S20 Sciometrics Stand NFIQ2 rounded quality score vs Bozorth3 match score.

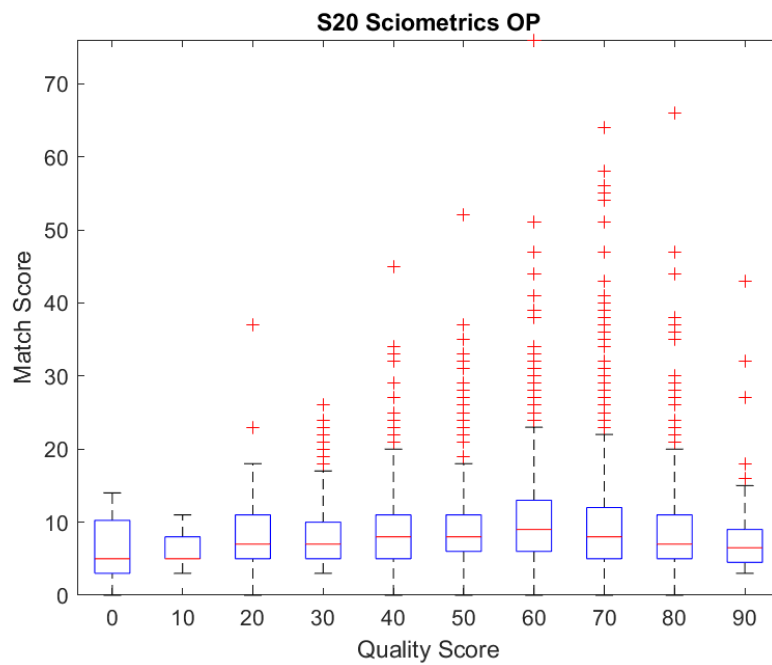


Figure 112 S20 Sciometrics Op NFIQ2 rounded quality score vs Bozorth3 match score.

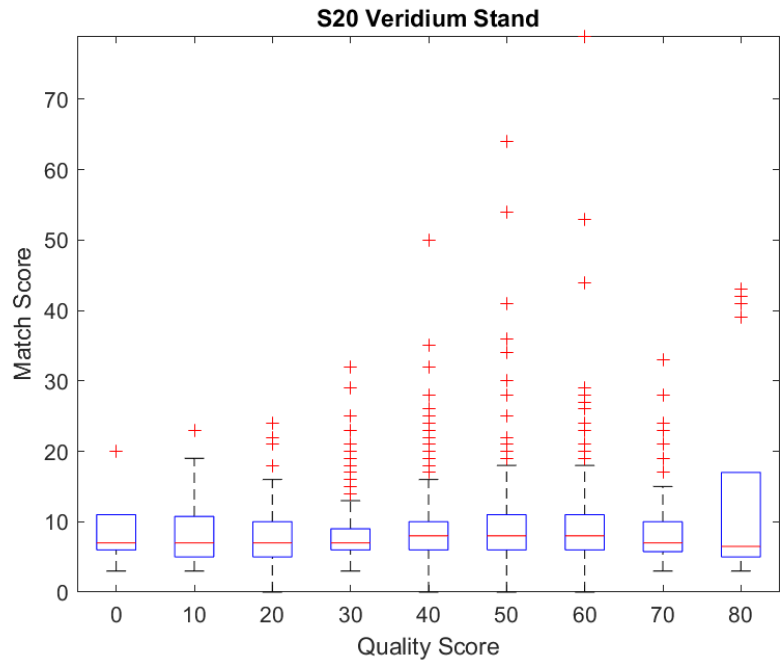


Figure 113 S20 Veridium Stand NFIQ2 rounded quality score vs Bozorth3 match score.

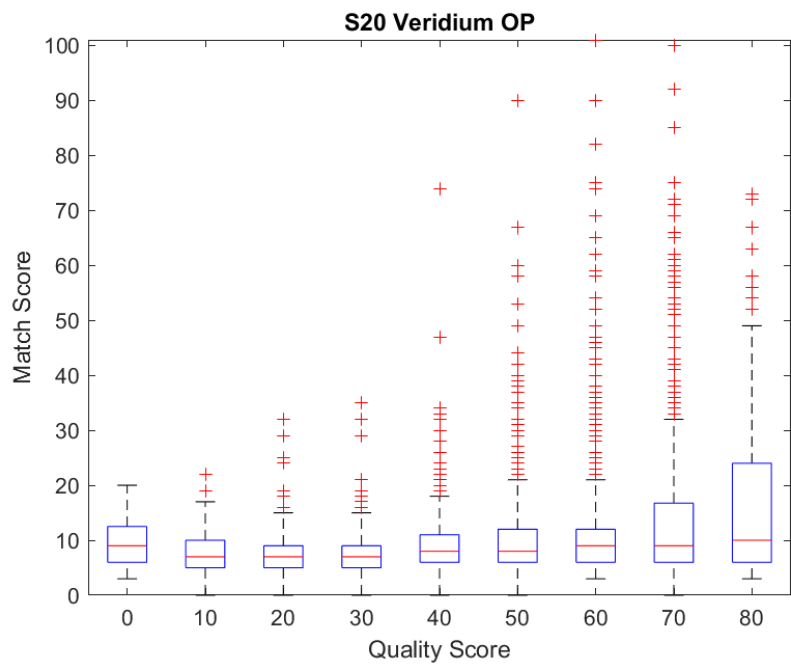


Figure 114 S20 Veridium Op NFIQ2 rounded quality score vs Bozorth3 match score.

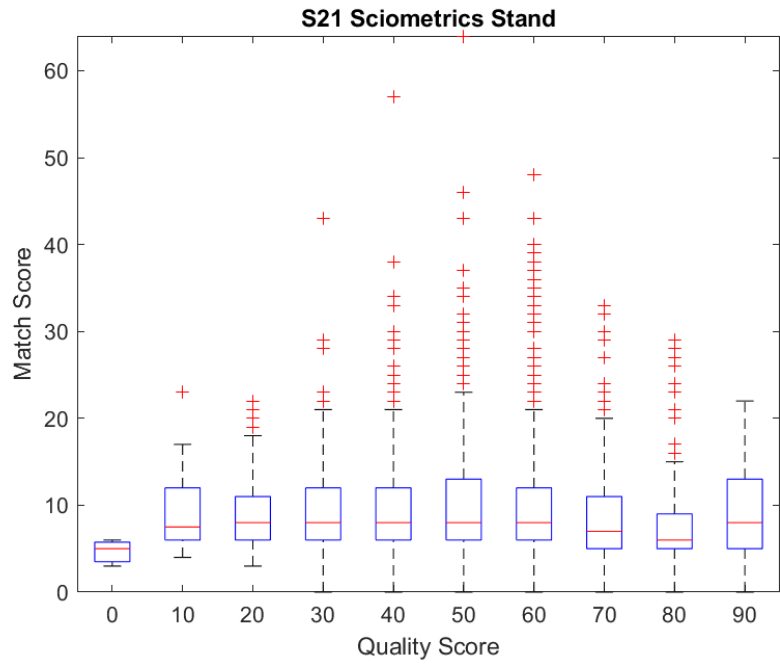


Figure 115 S21 Sciometrics Stand NFIQ2 rounded quality score vs Bozorth3 match score.

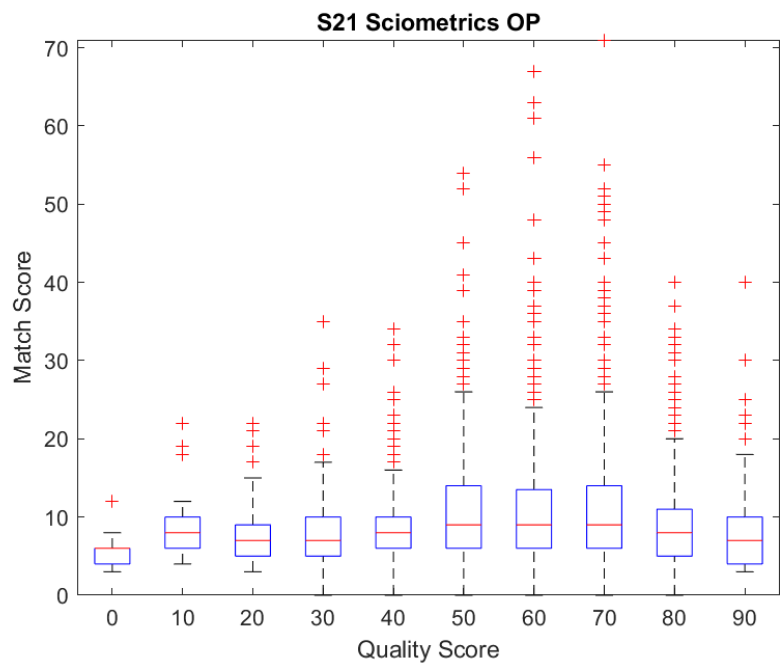


Figure 116 S21 Sciometrics Op NFIQ2 rounded quality score vs Bozorth3 match score.

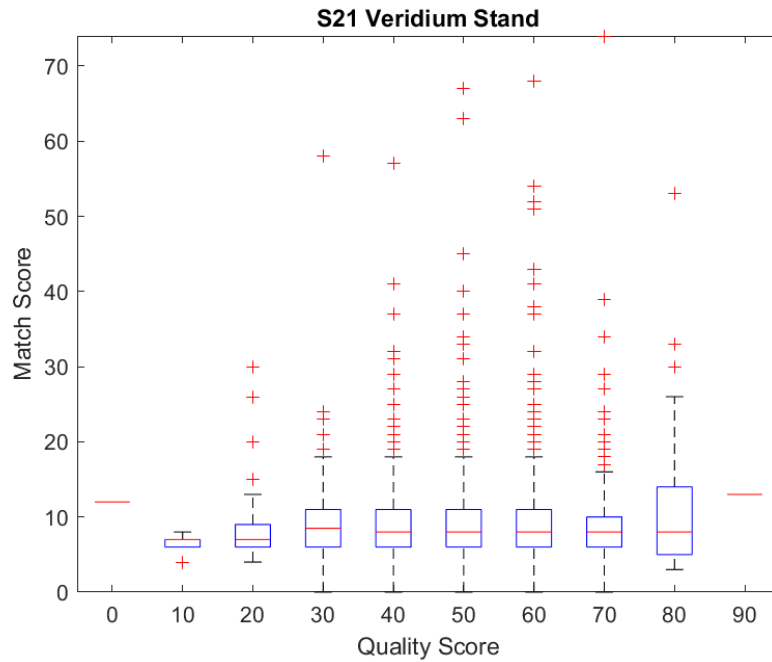


Figure 117 S21 Veridium Stand NFIQ2 rounded quality score vs Bozorth3 match score.

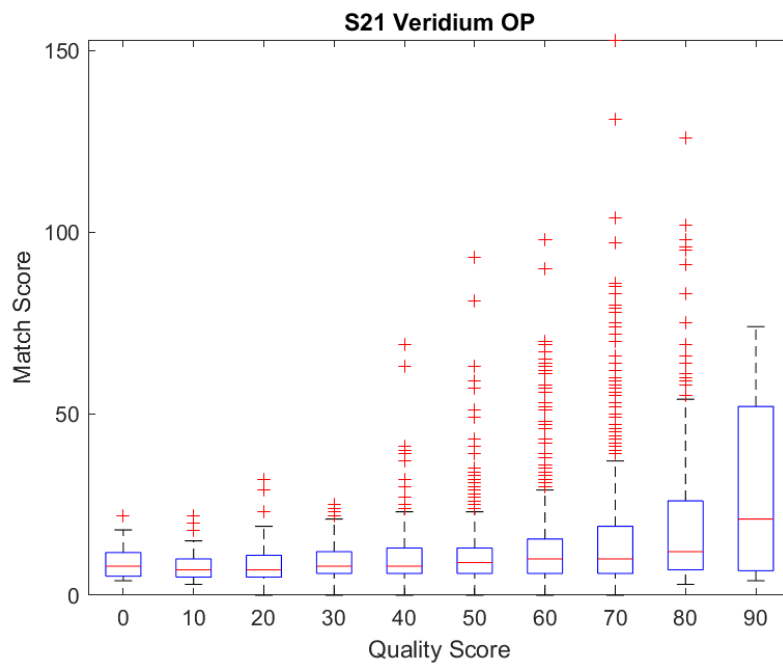


Figure 118 S21 Veridium Op NFIQ2 rounded quality score vs Bozorth3 match score.

For the Bozorth3's results for match score distribution by the quality score in Figure 106 through Figure 118, different patterns from the Innovatrics distributions are observed with the



contact distributions, including the baseline and contactless MorphoWave distribution in Figure 66 through Figure 70, showing the expected pattern seen in the Innovatrics distributions with the interquartile ranges and median scores increasing with the quality score. However, outliers are occurring in the middle-quality ranges, similar to what was seen in the Innovatrics cellphone distributions. The cellphone distributions for the Bozorth3 matcher shown in Figure 111 through Figure 118 have little to no correlation, which follows the performance of the Bozorth3 matcher since, for all cellphone experiments, the results were exceedingly poor. The Gemalto distribution fell between the cellphone distributions and contact distributions, showing little correlation between quality and score though the overall performance was better but still poor.

#### 4.2.6 Melanin raw match score distribution

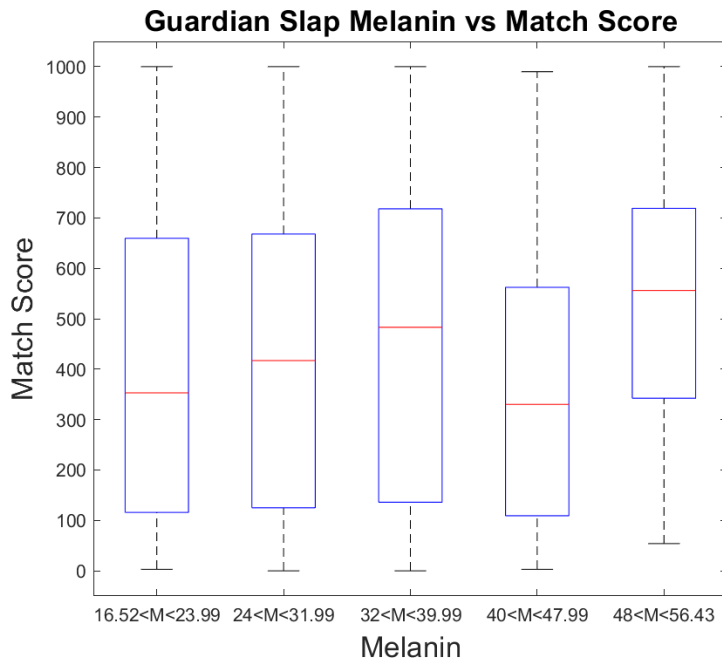


Figure 119 Innovatrics match scores binned into melanin ranges for Guardian Slap (Baseline).

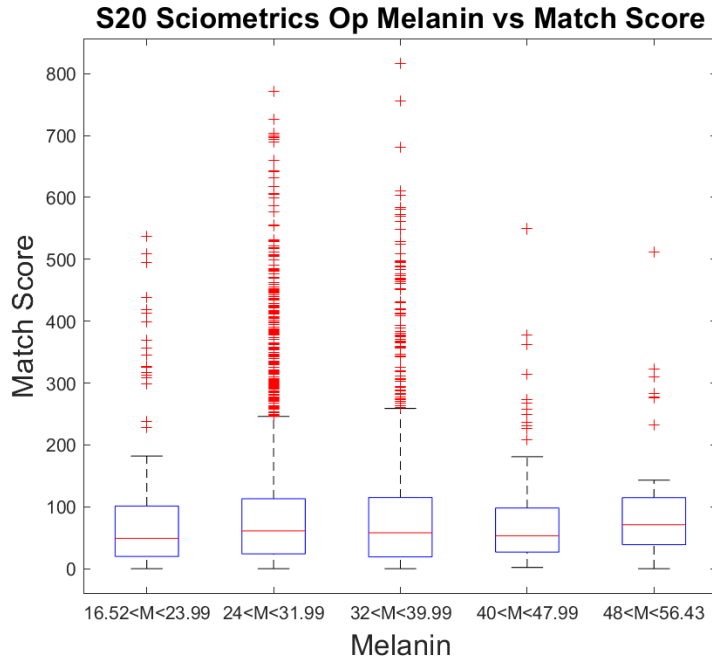


Figure 120 Innovatrics match scores binned into melanin ranges for S20 Sciometrics Op.

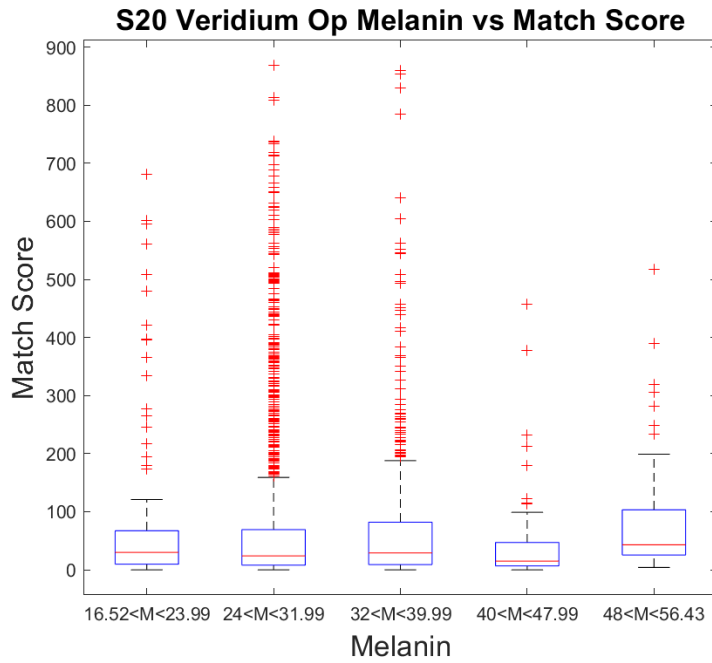


Figure 121 Innovatrics match scores binned into melanin ranges for S20 Veridium Op.

Figure 119, Figure 120, and Figure 121 are examples of the Innovatrics match scores binned into melanin ranges without any additional analysis. Figure 119 is the baseline performance and

shows vast interquartile ranges and whiskers that span most of the score ranges for all melanin values. Limited analysis can be drawn from the baseline because of these wide margins. Figure 120, and Figure 121 show the results for the S20 Sciometrics Op and S20 Veridium Op experiments; both have restricted bin ranges concentrated to the lowest score values. Additionally, both distributions have an uncountable number of outliers in the second and third bins. For the remaining demographic analysis, the 99<sup>th</sup> percentile non-match scores will be used instead to show the differences between the highest-scoring non-matches for each experiment.

## 4.2.7 Skin Reflectance VS 99<sup>th</sup> Percentile Non-Mated Match Scores

### 4.2.7.1 Melanin Distributions

#### 4.2.7.1.1 Innovatrics

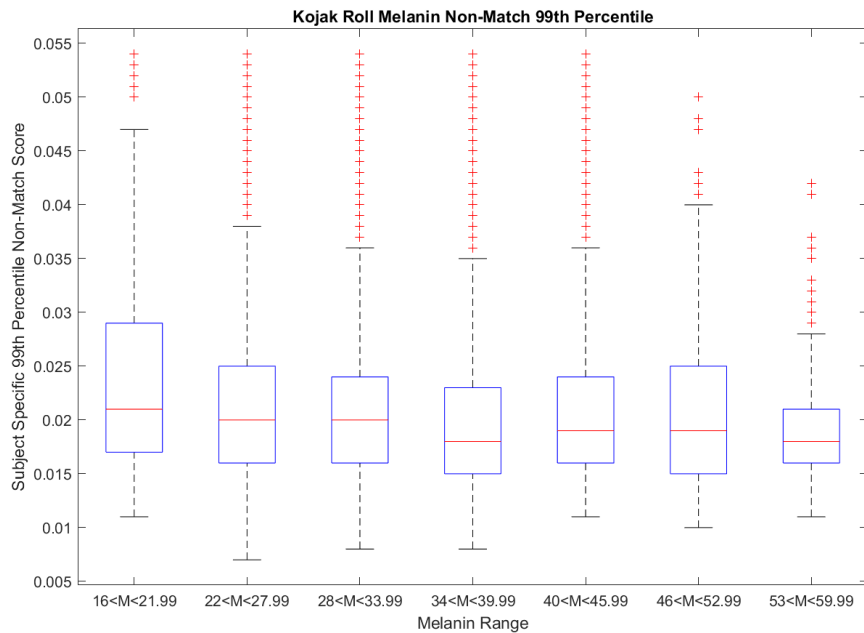


Figure 122 Innovatrics 99<sup>th</sup> non-match percentile binned into melanin ranges for Kojak Roll.

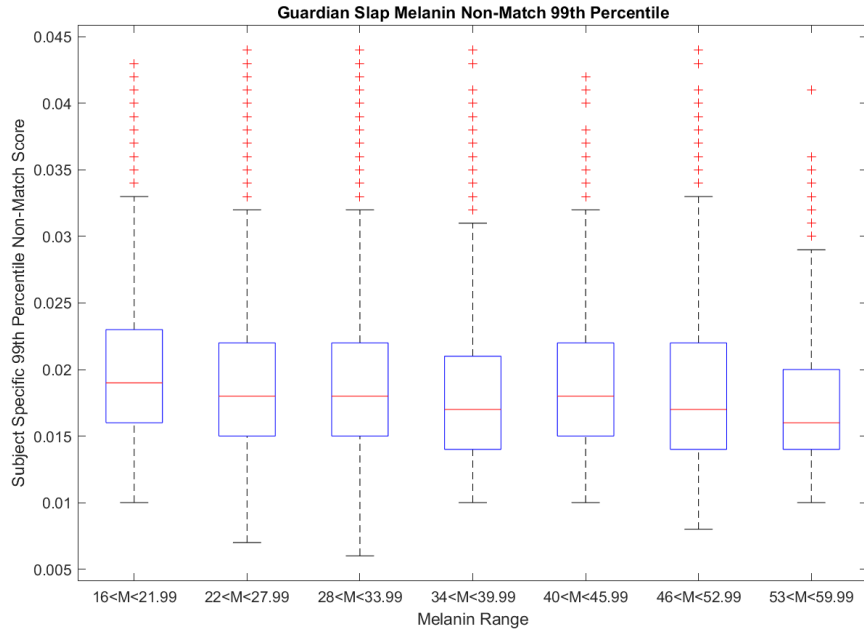


Figure 123 Innovatrics 99th non-match percentile binned into melanin ranges for Guardian Slap (Baseline).

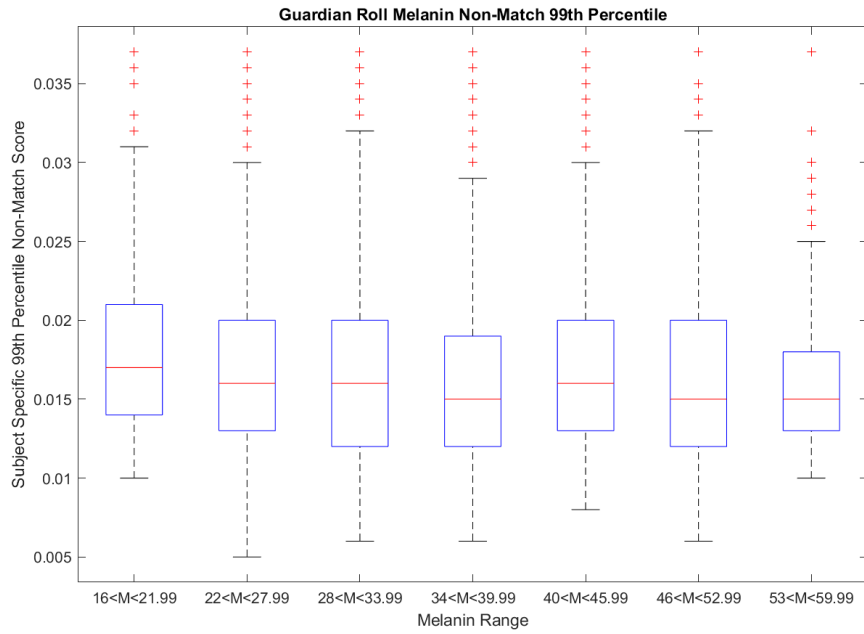


Figure 124 Innovatrics 99th non-match percentile binned into melanin ranges for Guardian Roll.

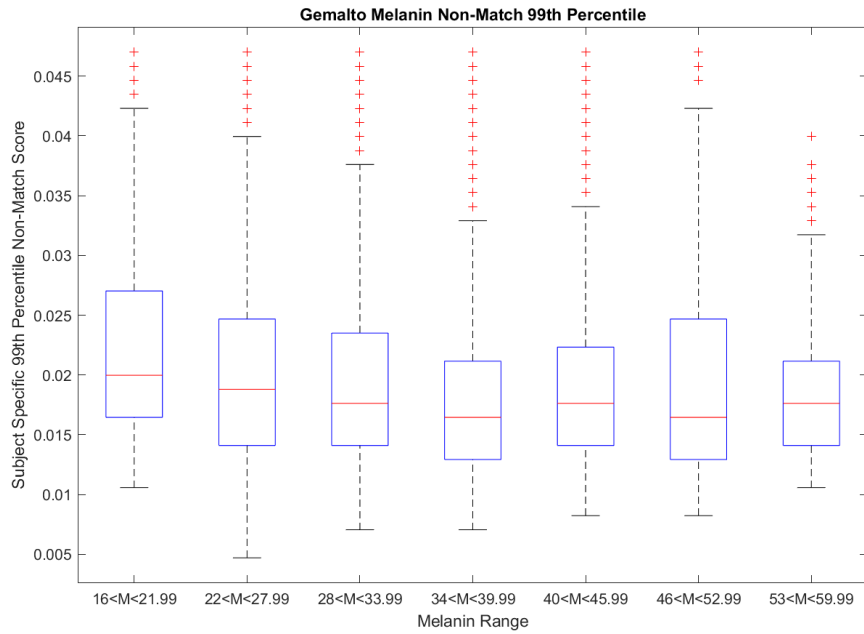


Figure 125 Innovatrics 99th non-match percentile binned into melanin ranges for Gemalto.

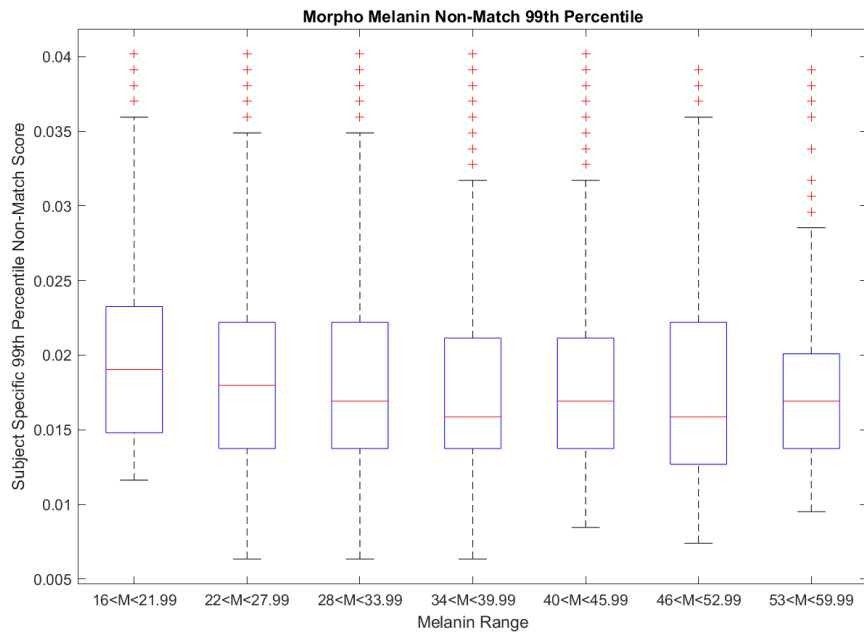


Figure 126 Innovatrics 99th non-match percentile binned into melanin ranges for MorphoWave.

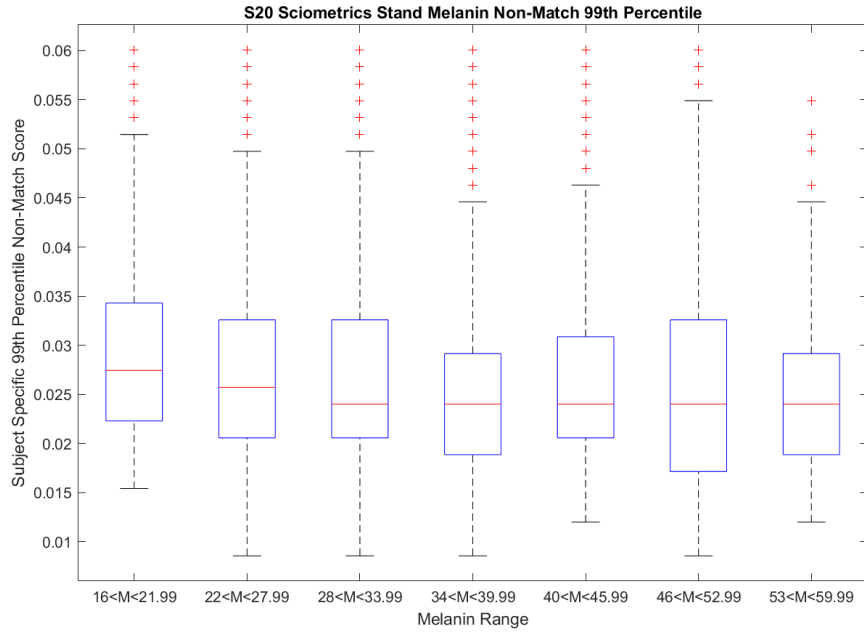


Figure 127 Innovatrics 99th non-match percentile binned into melanin ranges for S20 Sciometrics Stand.

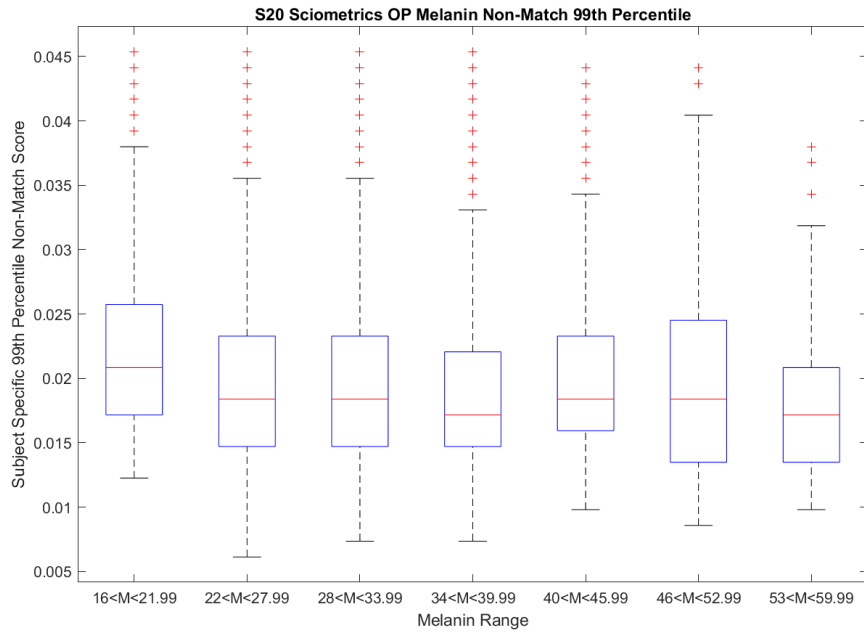


Figure 128 Innovatrics 99th non-match percentile binned into melanin ranges for S20 Sciometrics Op.

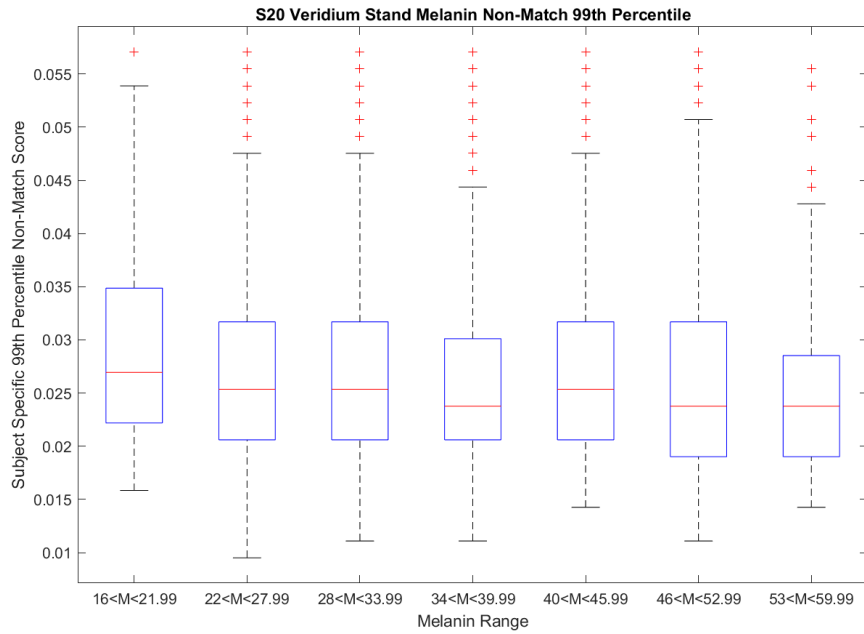


Figure 129 Innovetrics 99th non-match percentile binned into melanin ranges for S20 Veridium Stand.

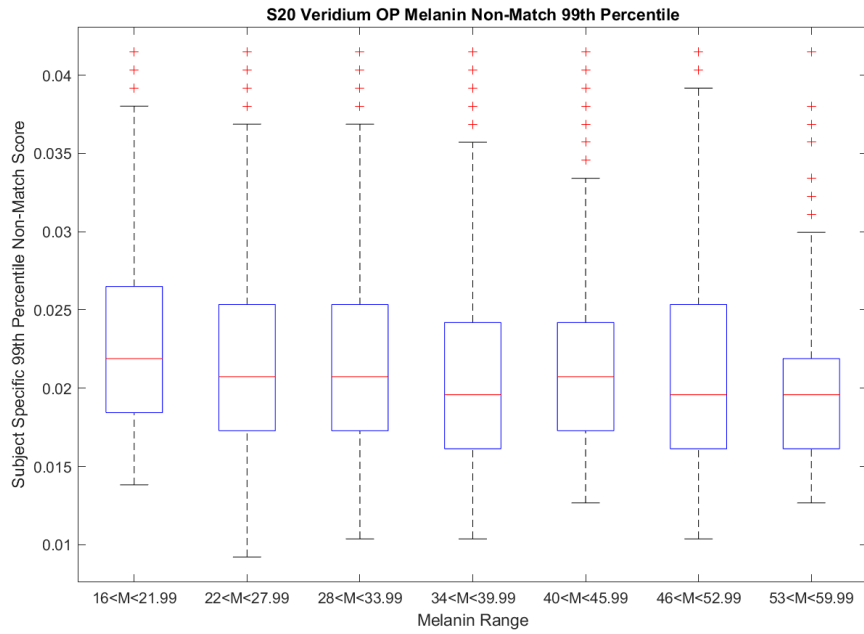


Figure 130 Innovetrics 99th non-match percentile binned into melanin ranges for S20 Veridium Op.

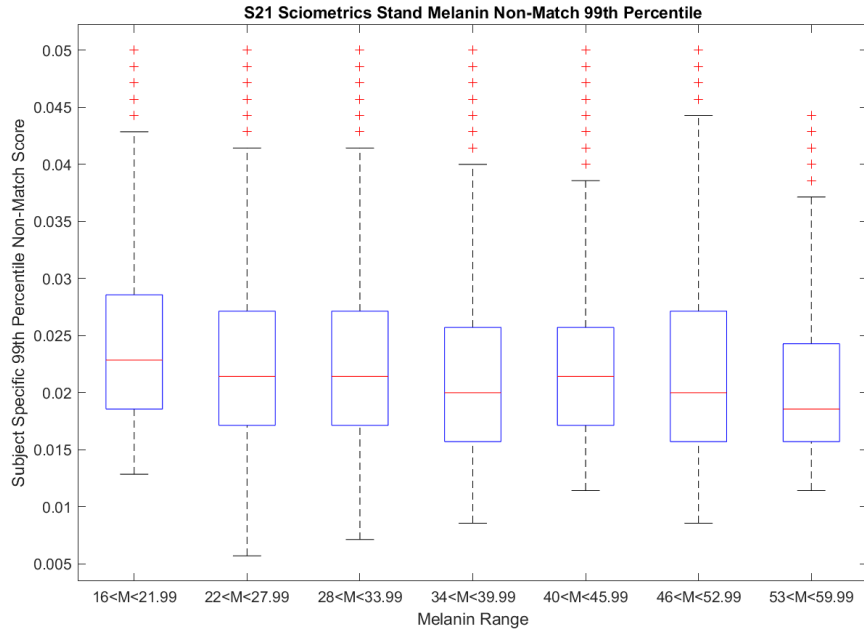


Figure 131 Innovatrics 99th non-match percentile binned into melanin ranges for S21 Sciometrics Stand.

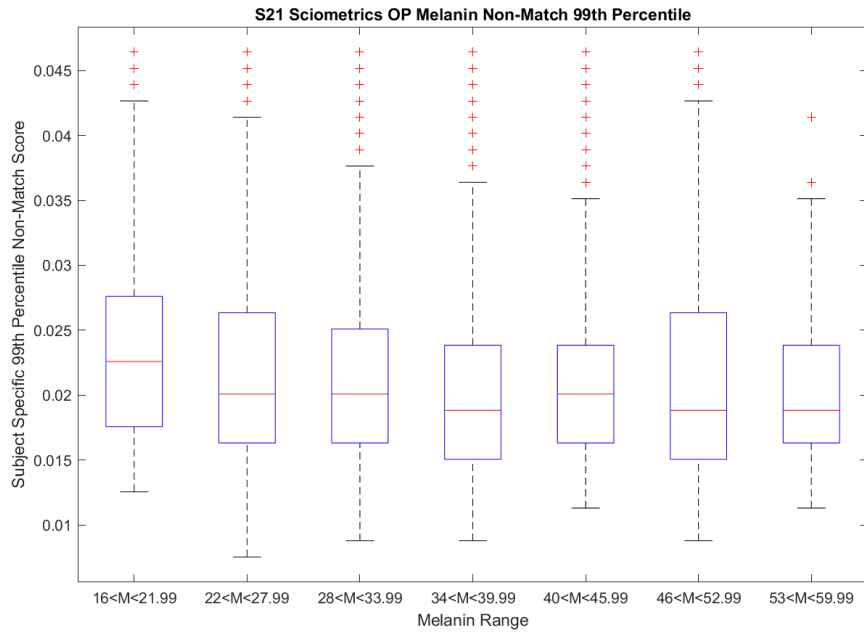


Figure 132 Innovatrics 99th non-match percentile binned into melanin ranges for S21 Sciometrics Op.



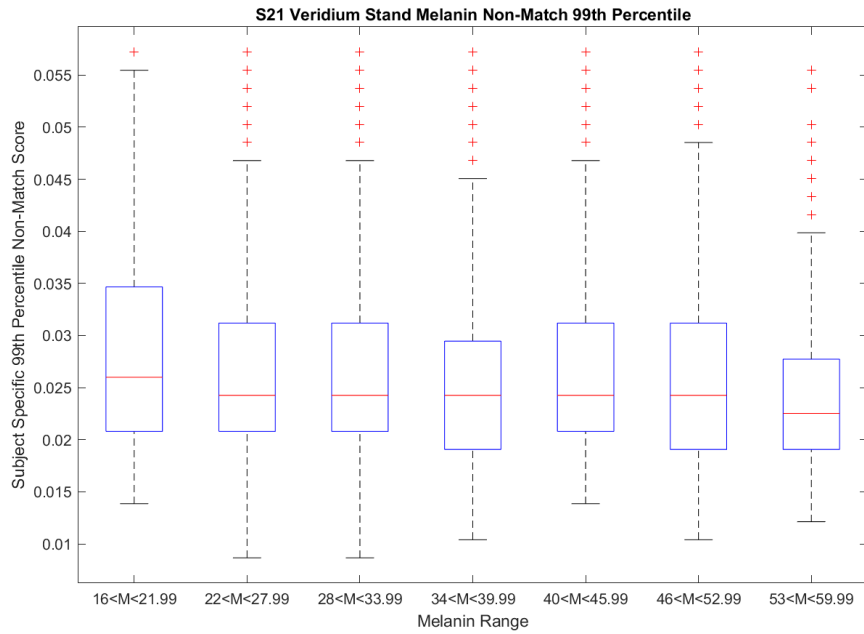


Figure 133 Innovetrics 99th non-match percentile binned into melanin ranges for S21 Veridium Stand.

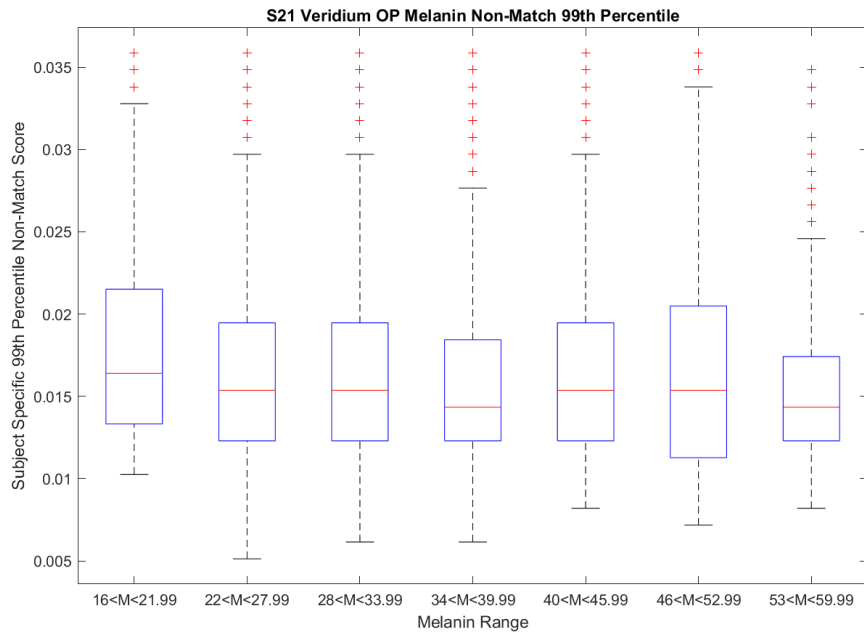


Figure 134 Innovetrics 99th non-match percentile binned into melanin ranges for S21 Veridium Op.

For the melanin distributions using the 99<sup>th</sup> percentile non-match scores, a higher median or interquartile would show worse performance since more non-match scores would be counted as matches for higher thresholds. In Figure 122 through Figure 134, the Innovatrics melanin distributions are shown with the lowest melanin bin having a higher value. Additionally, middle-range melanin bins for all distributions tend to have a lower interquartile range or, in some cases, a lower median than the upper and lower bins. Specifically, in Figure 125, the lower bins in the Gemalto distribution have a higher interquartile range and median. As the melanin increases, the median and range drop until the fourth bin; the following bins have a slightly higher interquartile range and median or stay steady. The same trend is seen to the same or a lesser degree in the other Innovatrics melanin distributions.

#### 4.2.7.1.2 VeriFinger

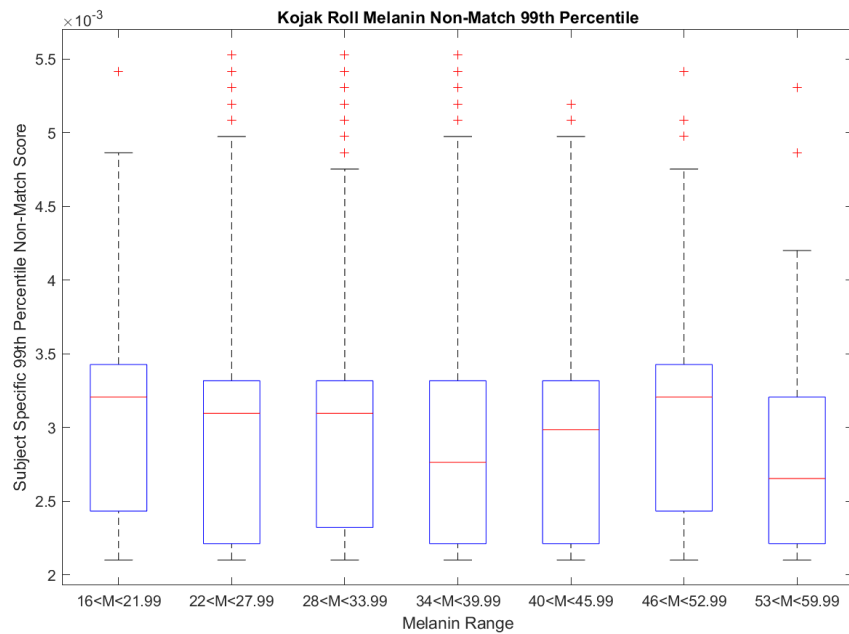


Figure 135 VeriFinger 99th non-match percentile binned into melanin ranges for Kojak Roll.

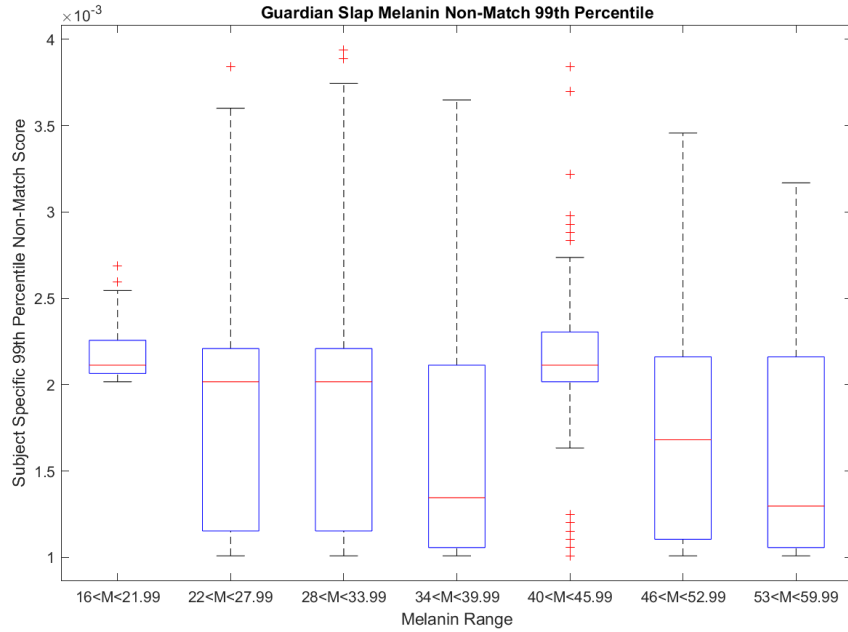


Figure 136 VeriFinger 99th non-match percentile binned into melanin ranges for Guardian Slap.

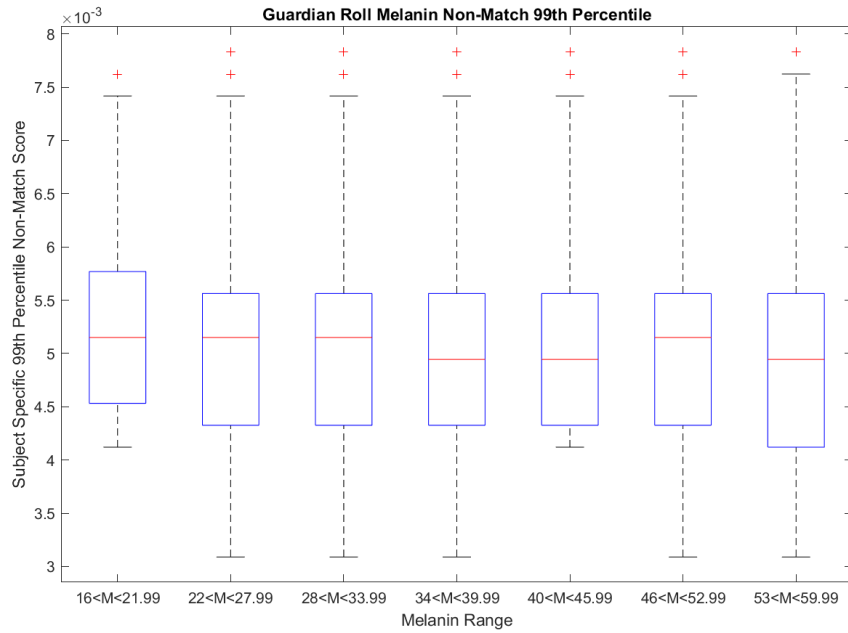


Figure 137 VeriFinger 99th non-match percentile binned into melanin ranges for Guardian Roll.

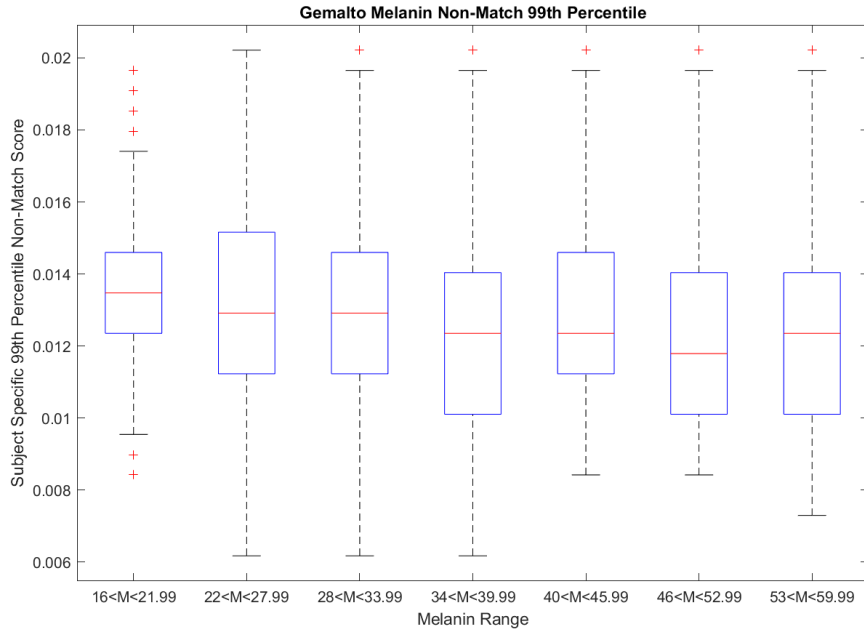


Figure 138 VeriFinger 99th non-match percentile binned into melanin ranges for Gemalto.

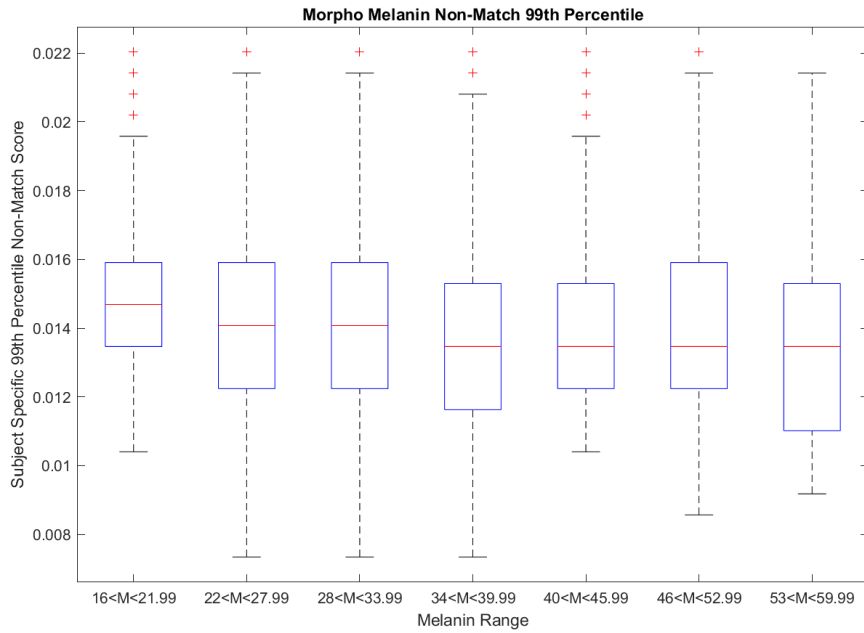


Figure 139 VeriFinger 99th non-match percentile binned into melanin ranges for MorphoWave.

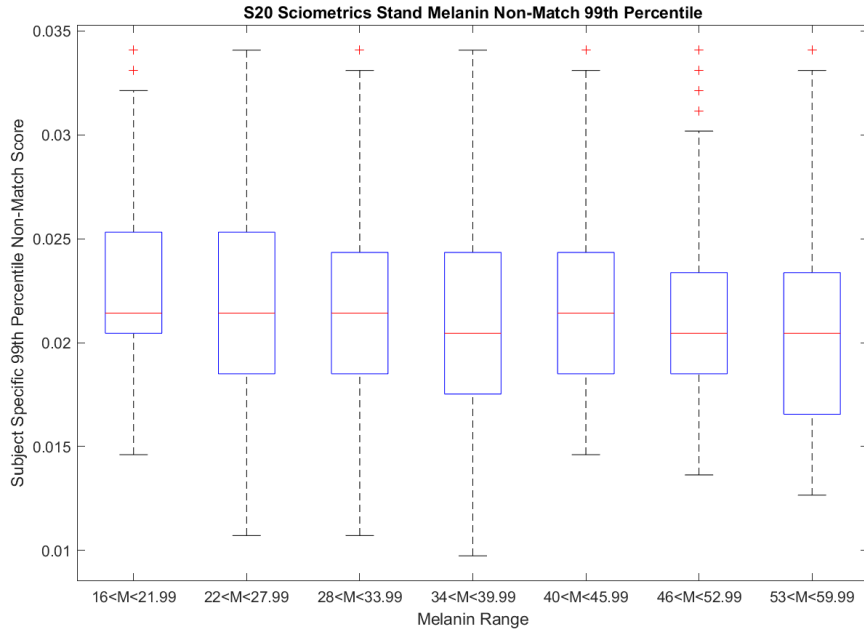


Figure 140 VeriFinger 99th non-match percentile binned into melanin ranges for S20 Sciometrics Stand.

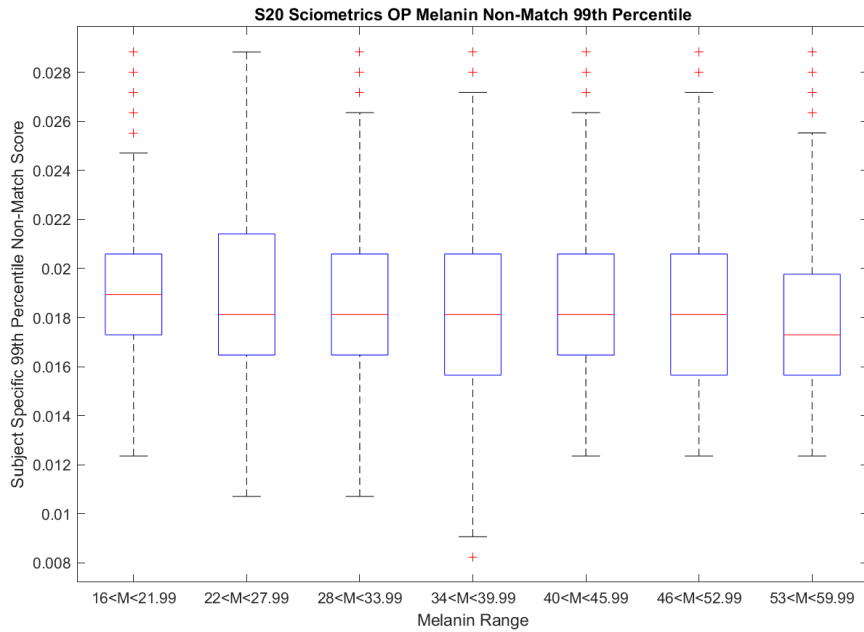


Figure 141 VeriFinger 99th non-match percentile binned into melanin ranges for S20 Sciometrics Op.

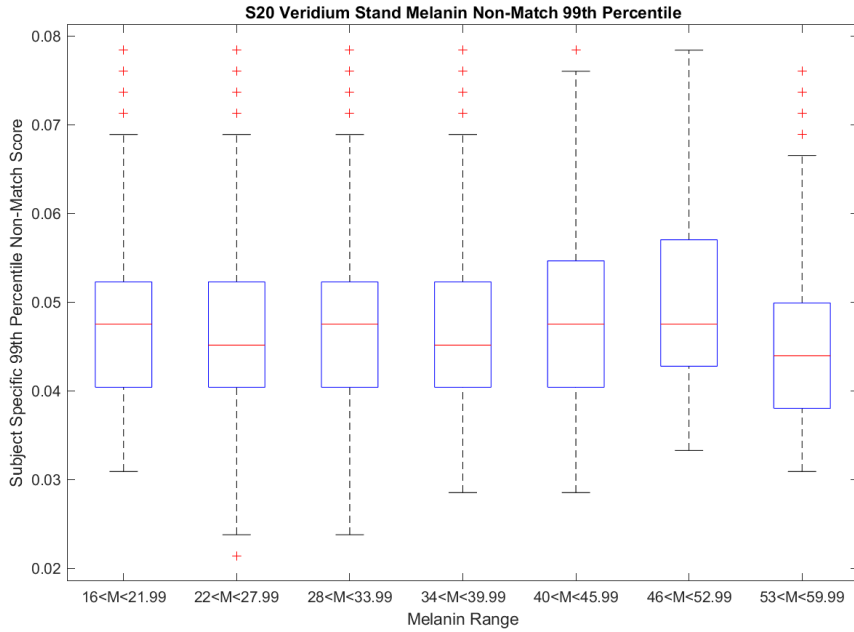


Figure 142 VeriFinger 99th non-match percentile binned into melanin ranges for S20 Veridium Stand.

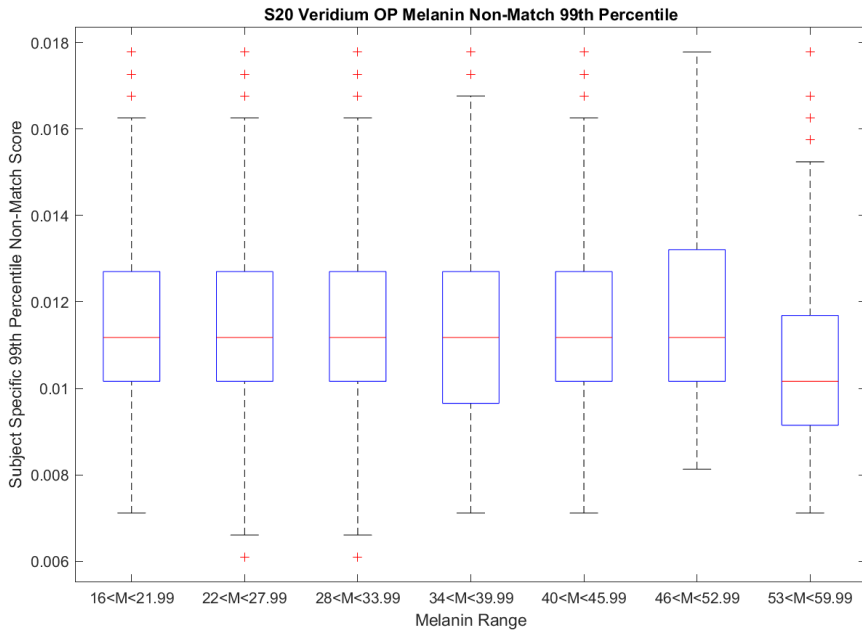


Figure 143 VeriFinger 99th non-match percentile binned into melanin ranges for S20 Veridium Op.

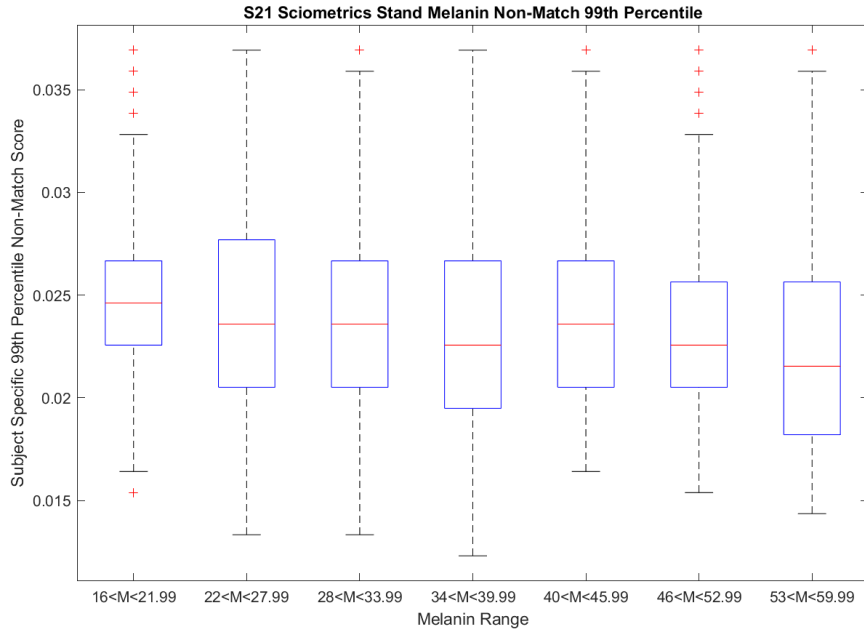


Figure 144 VeriFinger 99th non-match percentile binned into melanin ranges for S21 Sciometrics Stand.

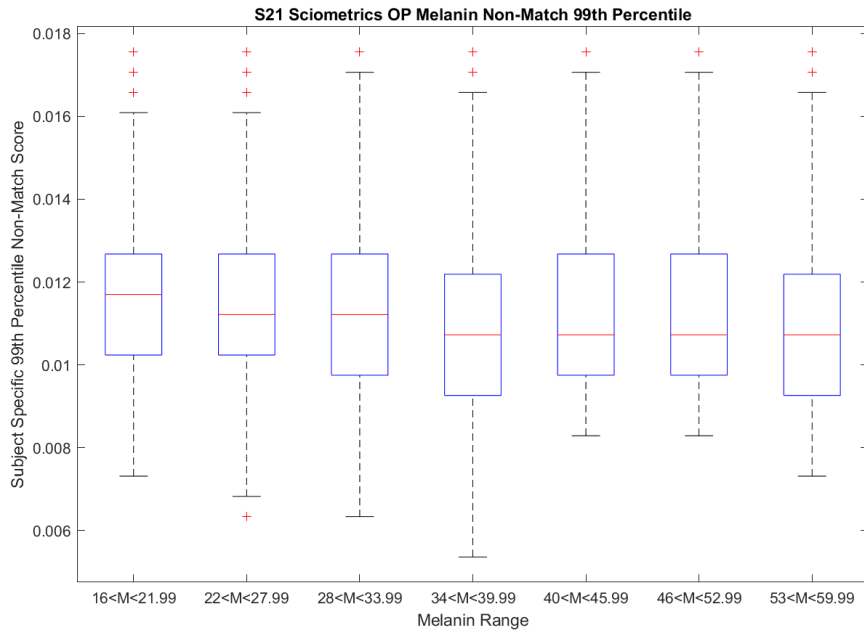


Figure 145 VeriFinger 99th non-match percentile binned into melanin ranges for S21 Sciometrics Op.

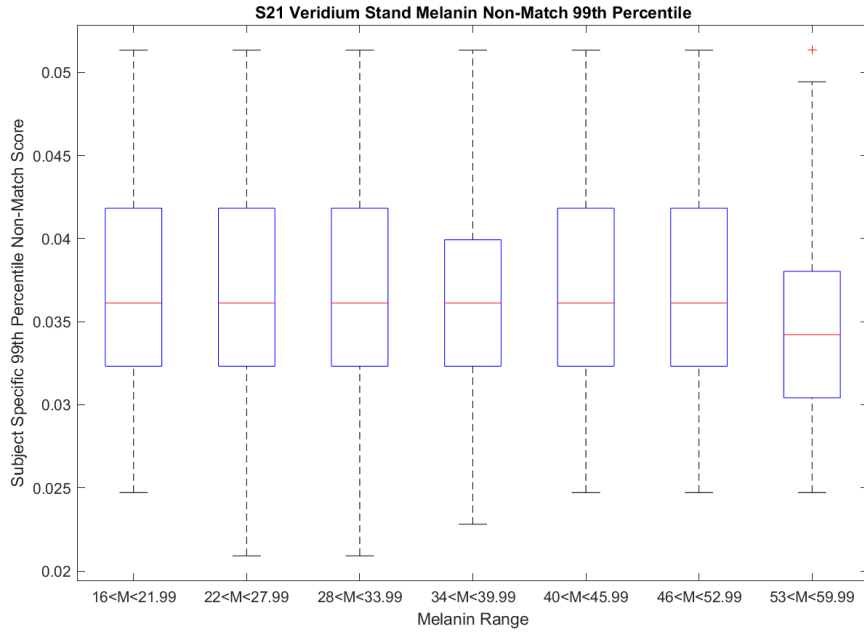


Figure 146 VeriFinger 99th non-match percentile binned into melanin ranges for S21 Veridium Stand.

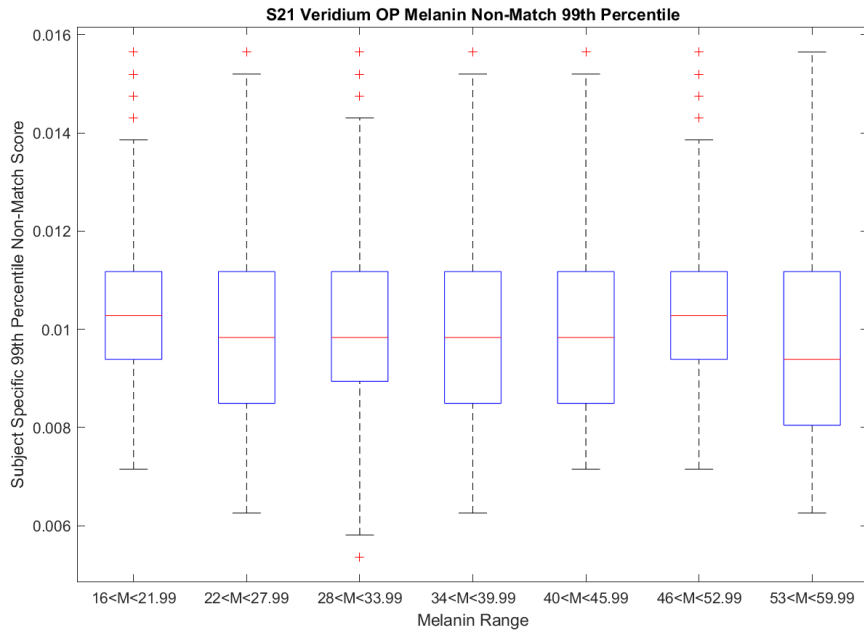


Figure 147 VeriFinger 99th non-match percentile binned into melanin ranges for S21 Veridium Op.



The 99<sup>th</sup> percentile non-match Kojak Roll distribution (Figure 135) shows generally consistent non-match score median and interquartile values with a drop in the median non-match score in the middle melanin range and highest bin. The Guardian Roll distribution (Figure 137) had a steady median and interquartile non-match score with a dip in the center and highest bin, similar to the Kojak Roll. The Guardian Slap distribution (Figure 136) showed different behavior from the other contact distributions with wide interquartile ranges for most bins except for the first and fifth bins. The medians were also higher and lower with no pattern. The range for the values in the Guardian Slap distribution is the lowest of all Melanin distributions for the VeriFinger matcher. Both contactless distributions shown in Figure 138 and Figure 139 have a slight trend in performance, with lower melanin bins having a higher median non-match score than higher melanin bins. For the cellphone distributions in Figure 140 through Figure 147, there is little significant information showing all distributions stay steady across all bins or have slight changes in the median non-match score value in a few bins with no trends other than the highest melanin bin usually having the lowest median non-match score. In contrast, the lowest melanin bin will have the highest median non-match score.

### 4.2.7.1.3 Bozorth3

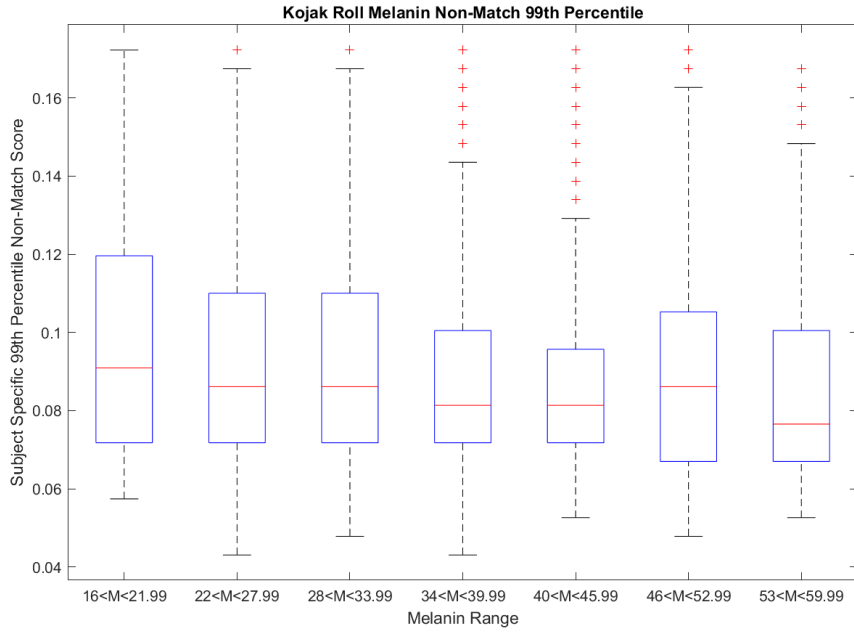


Figure 148 Bozorth3 99th non-match percentile binned into melanin ranges for Kojak Roll.

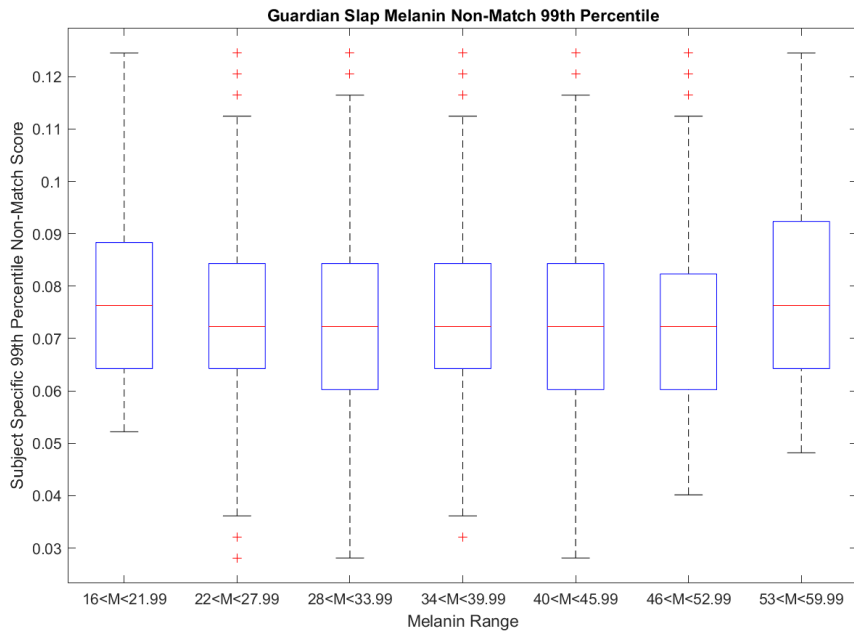


Figure 149 Bozorth3 99th non-match percentile binned into melanin ranges for Guardian Slap (Baseline).

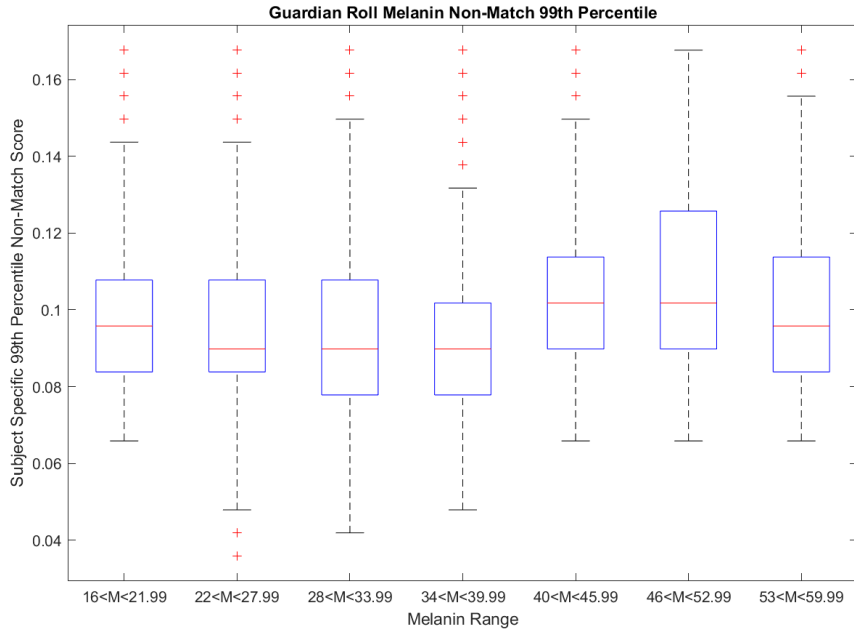


Figure 150 Bozorth3 99th non-match percentile binned into melanin ranges for Guardian Roll.

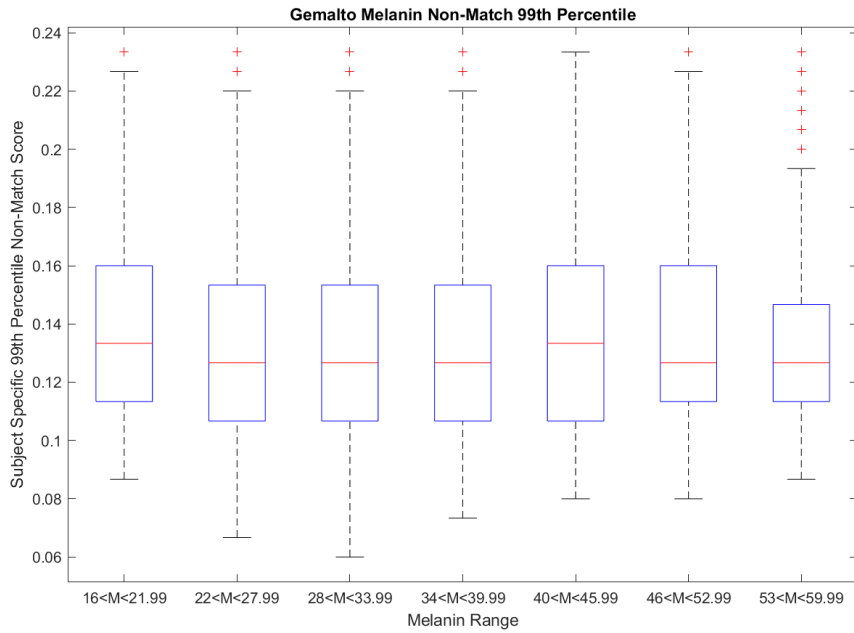


Figure 151 Bozorth3 99th non-match percentile binned into melanin ranges for Gemalto.

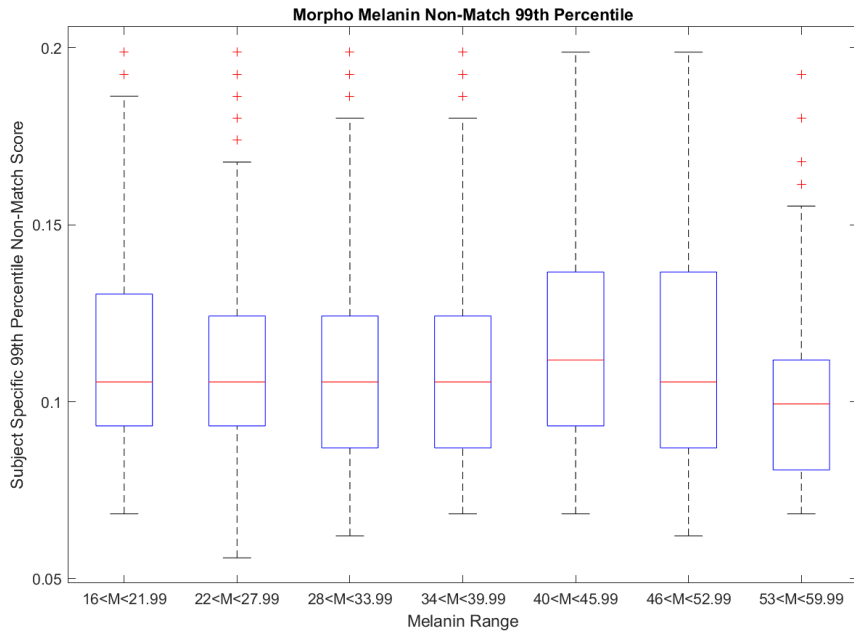


Figure 152 Bozorth3 99th non-match percentile binned into melanin ranges for MorphoWave.

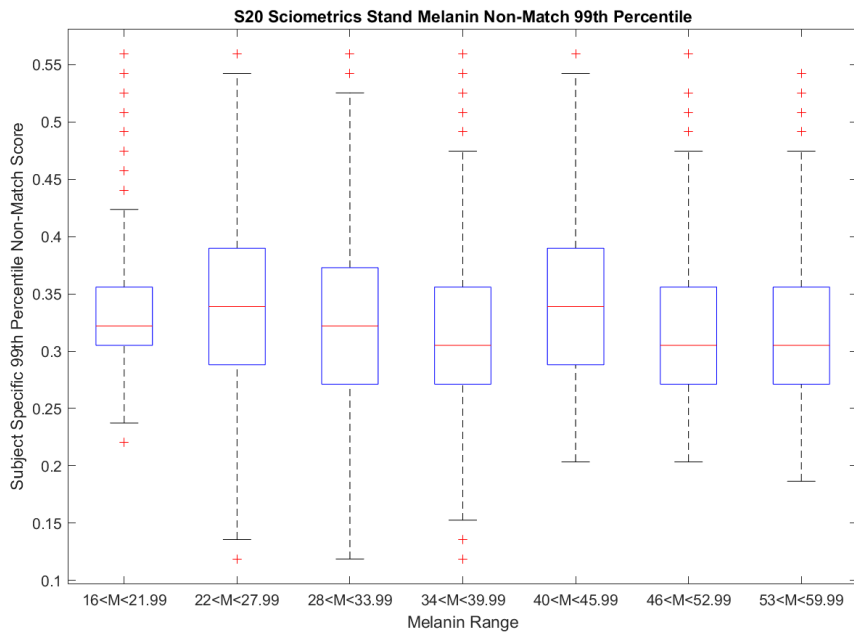


Figure 153 Bozorth3 99th non-match percentile binned into melanin ranges for S20 Sciometrics Stand.

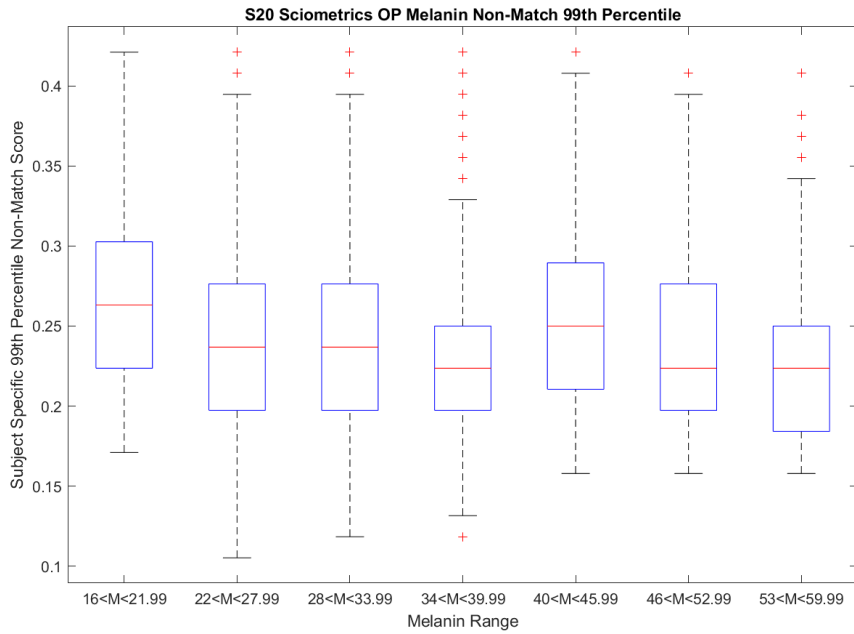


Figure 154 Bozorth3 99th non-match percentile binned into melanin ranges for S20 Sciometrics Op.

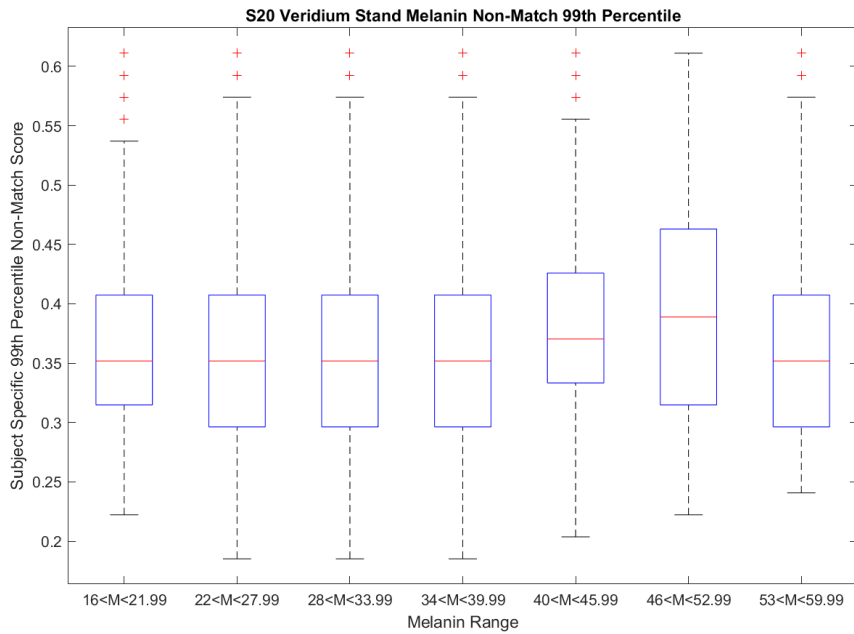


Figure 155 Bozorth3 99th non-match percentile binned into melanin ranges for S20 Veridium Stand.

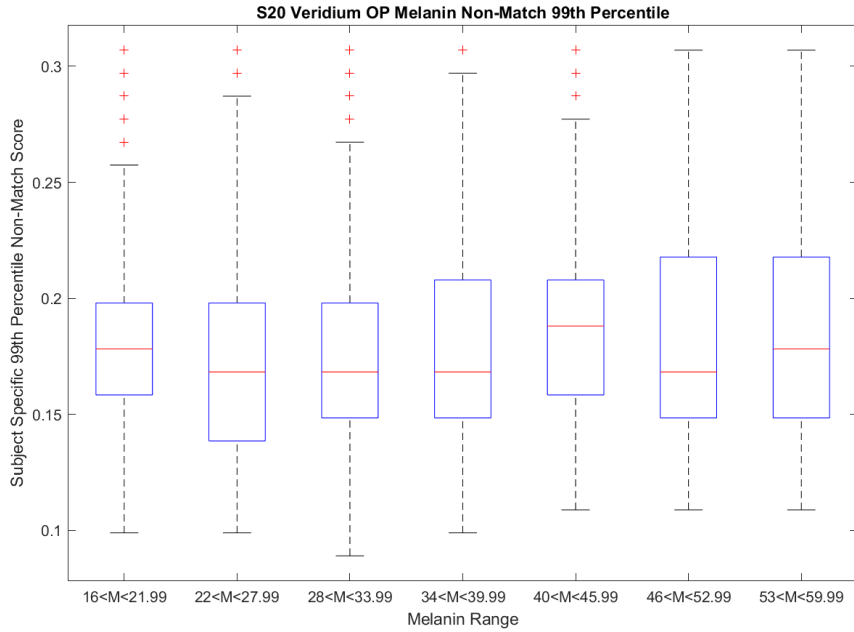


Figure 156 Bozorth3 99th non-match percentile binned into melanin ranges for S20 Veridium Op.

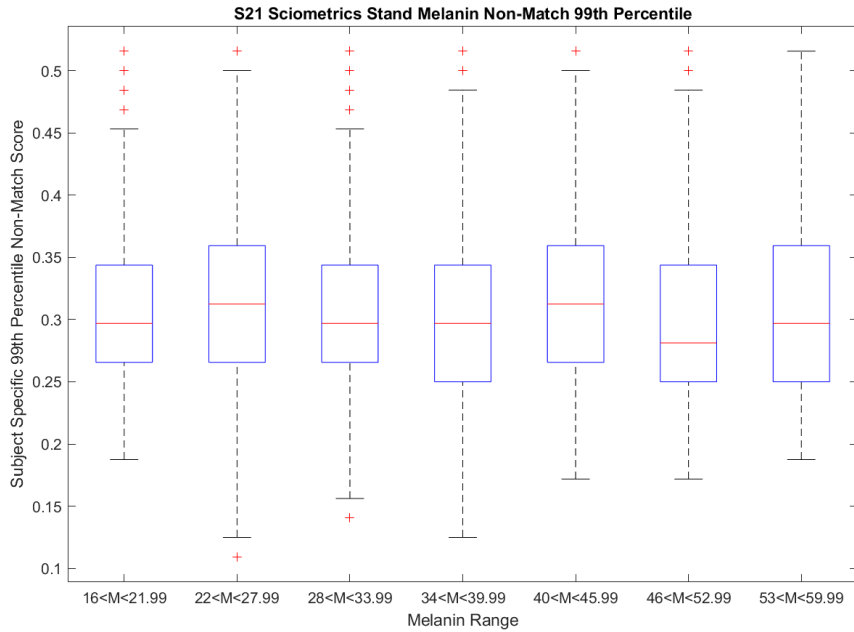


Figure 157 Bozorth3 99th non-match percentile binned into melanin ranges for S21 Sciometrics Stand.

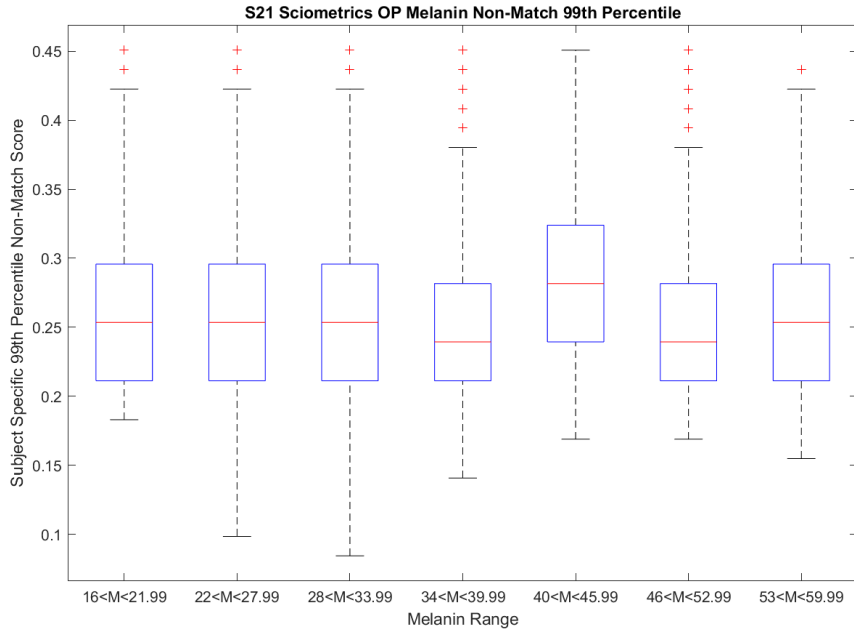


Figure 158 Bozorth3 99th non-match percentile binned into melanin ranges for S21 Sciometrics Op.

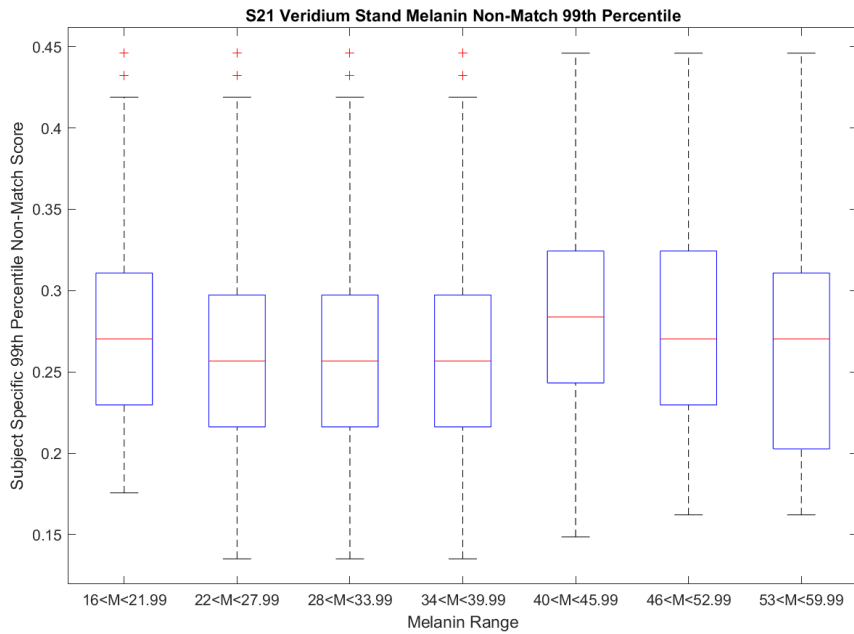
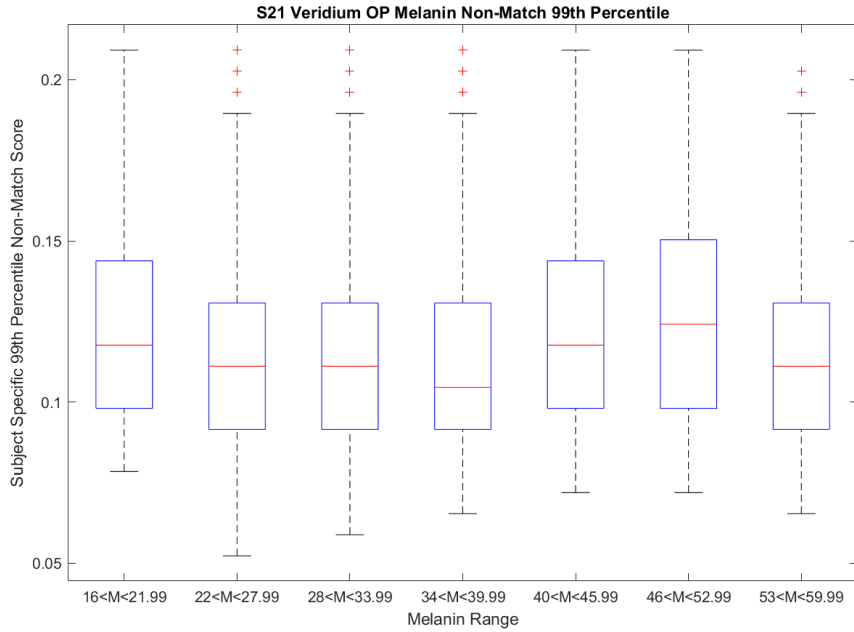


Figure 159 Bozorth3 99th non-match percentile binned into melanin ranges for S21 Veridium Stand.



*Figure 160 Bozorth3 99th non-match percentile binned into melanin ranges for S21 Veridium Op.*

The Bozorth3 melanin distributions using the 99<sup>th</sup> percentile non-match scores shown in Figure 148 through Figure 160 are similar to the Innovatrics melanin distributions. Though the distributions showing the exception are correlated towards the Stand setting since the S20 Sciometrics Stand, S20 Veridium Stand, and S21 Sciometrics Stand distributions all show the increased bin, though other cellphone operational distributions show a higher than average bin.



## 4.2.7.2 Erythema Distributions

### 4.2.7.2.1 Innovatrics

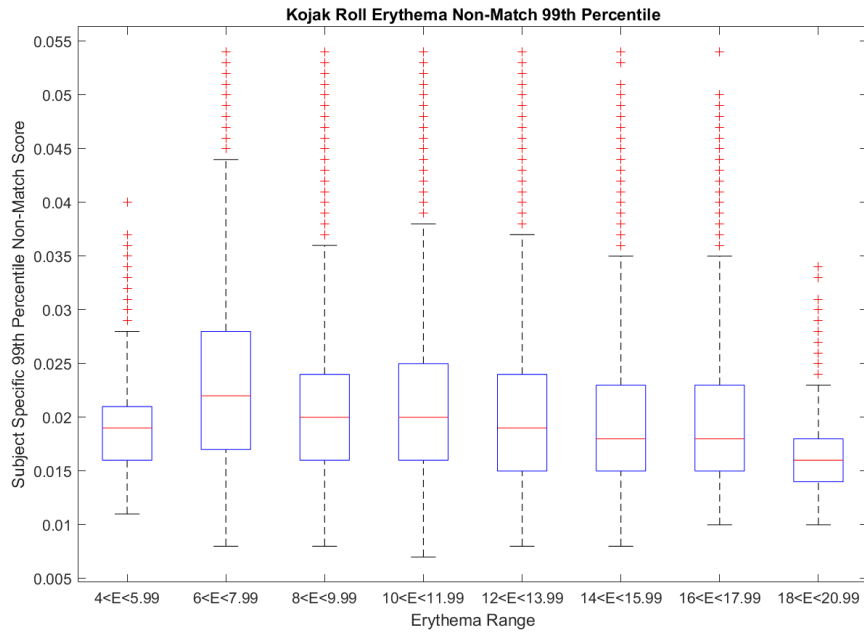


Figure 161 Innovatrics 99th non-match percentile binned into erythema ranges for Kojak Roll.

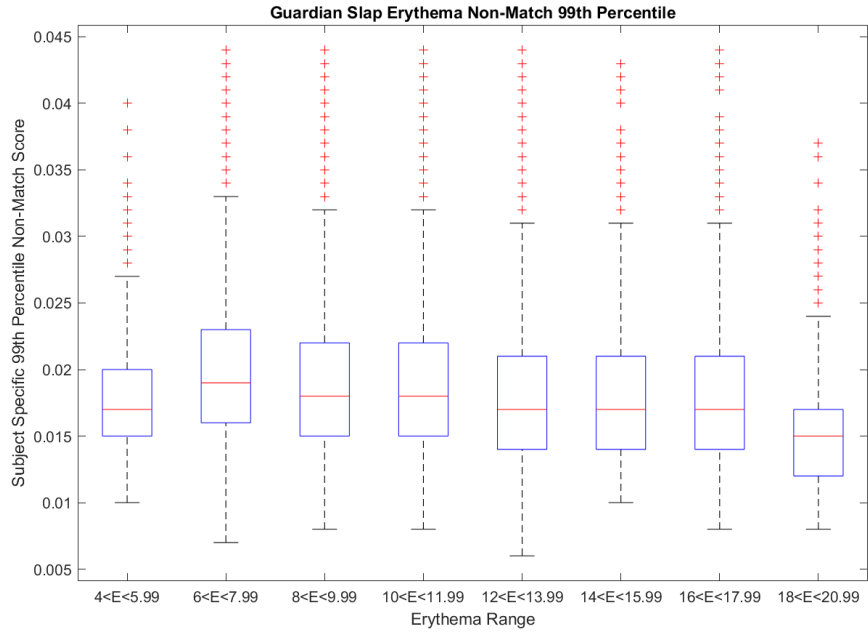


Figure 162 Innovatrics 99th non-match percentile binned into erythema ranges for Guardian Slap (Baseline).

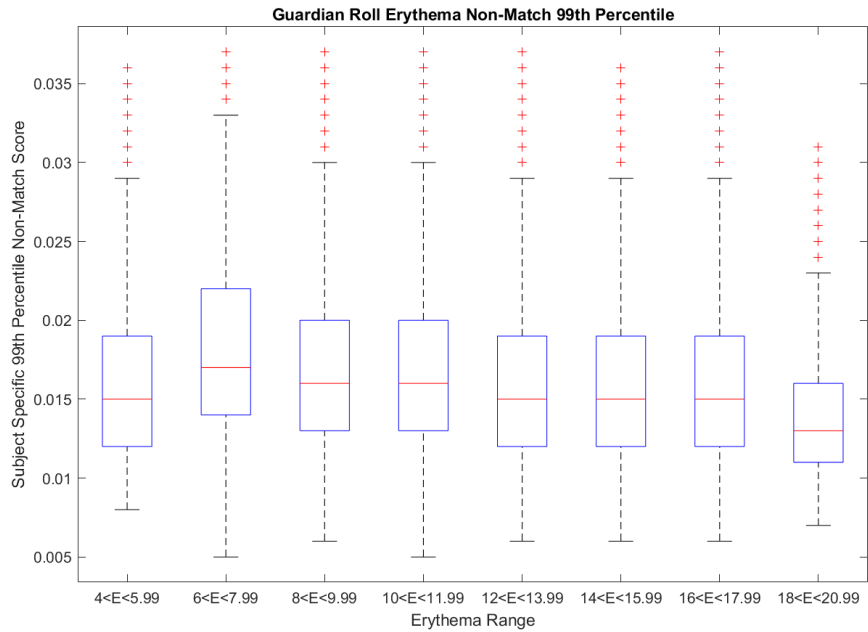


Figure 163 Innovatrics 99th non-match percentile binned into erythema ranges for Guardian Roll.

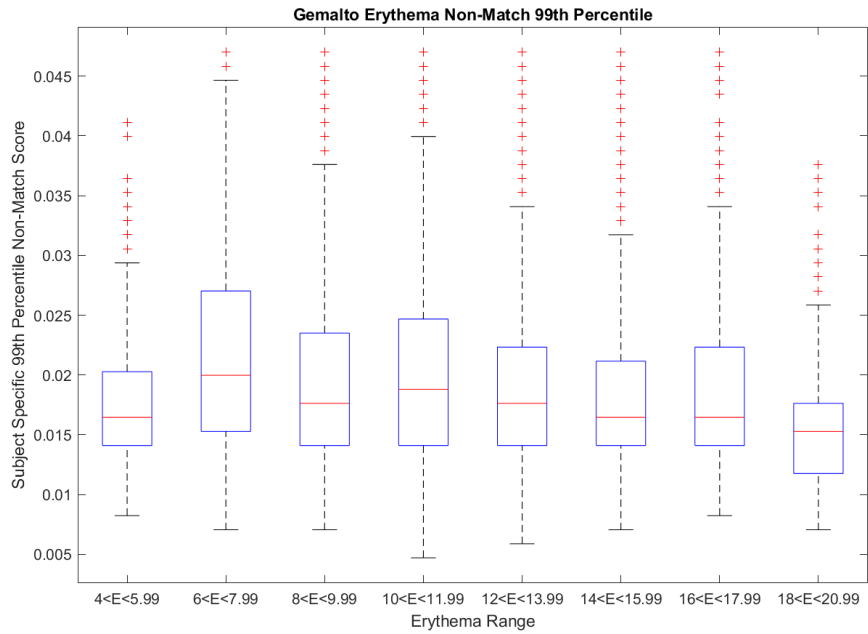


Figure 164 Innovatrics 99th non-match percentile binned into erythema ranges for Gemalto.

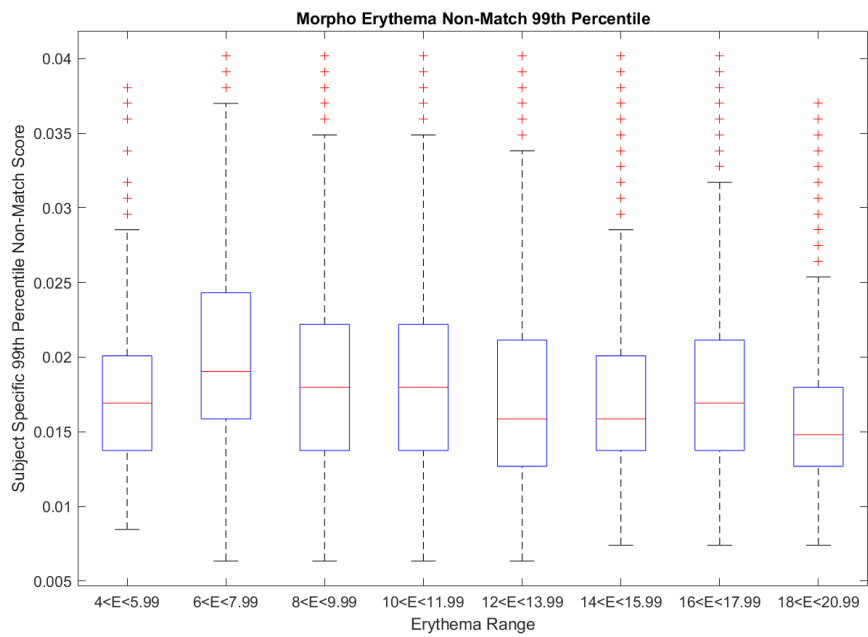


Figure 165 Innovatrics 99th non-match percentile binned into erythema ranges for MorphoWave.

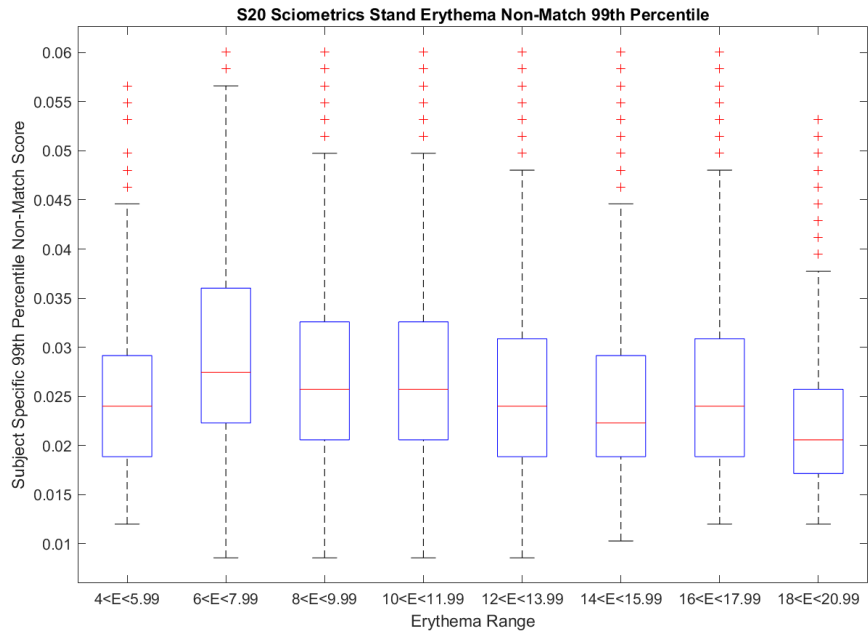


Figure 166 Innovatrics 99th non-match percentile binned into erythema ranges for S20 Sciometrics Stand.

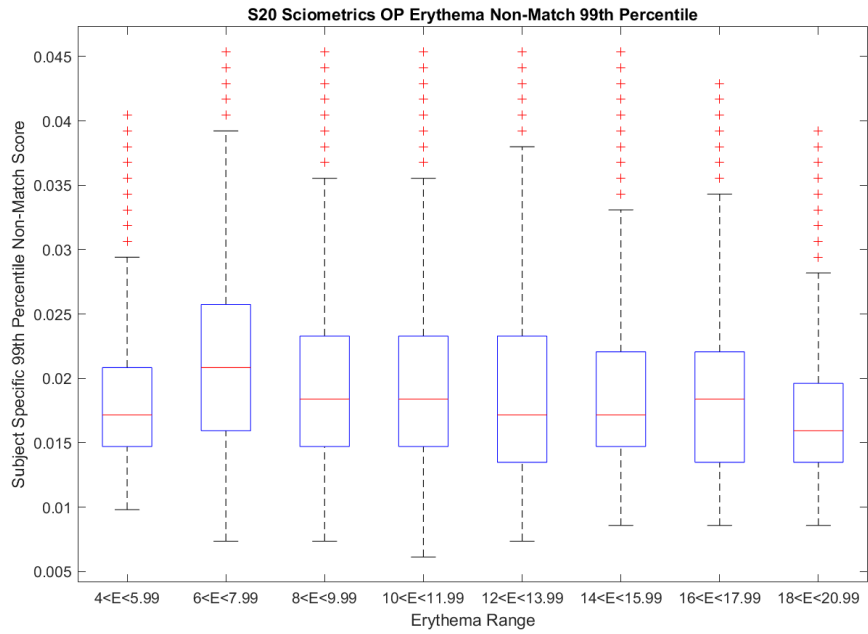


Figure 167 Innovatrics 99th non-match percentile binned into erythema ranges for S20 Sciometrics Op.

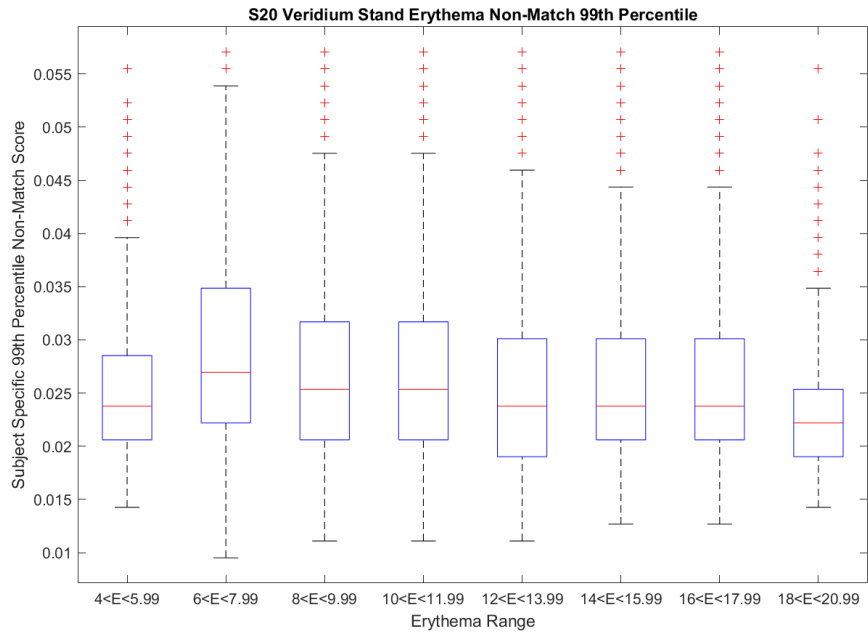


Figure 168 Innovatrics 99th non-match percentile binned into erythema ranges for S20 Veridium Stand.

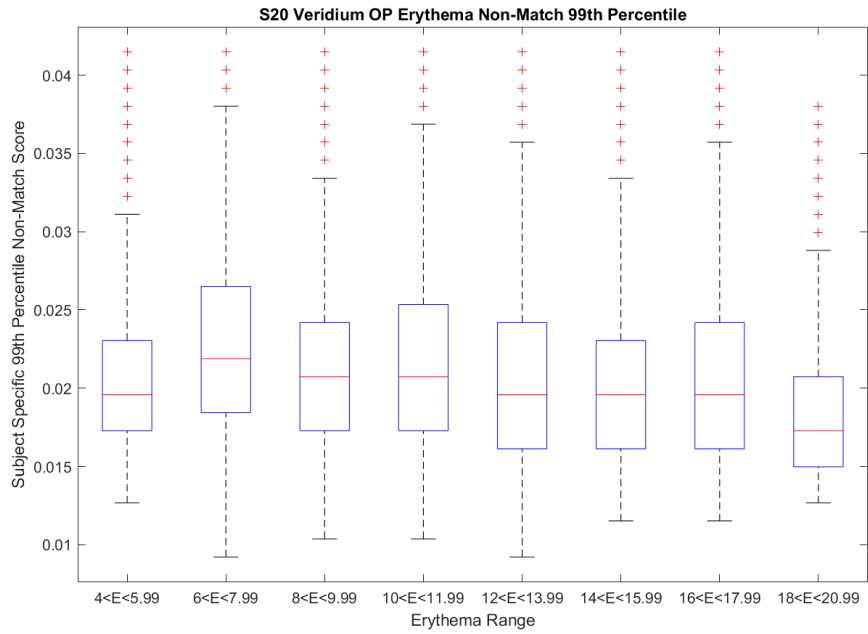


Figure 169 Innovatrics 99th non-match percentile binned into erythema ranges for S20 Veridium Op.

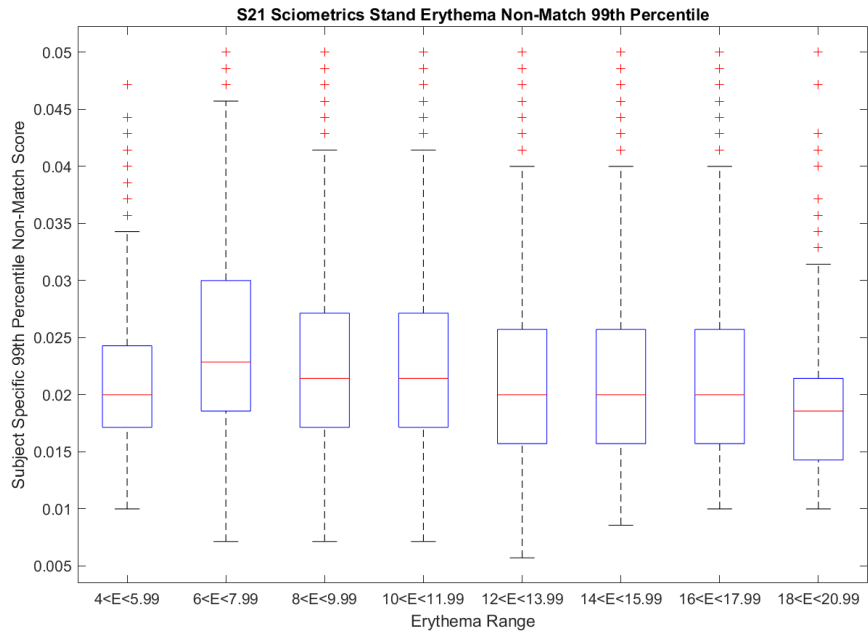


Figure 170 Innovatrics 99th non-match percentile binned into erythema ranges for S21 Sciometrics Stand.

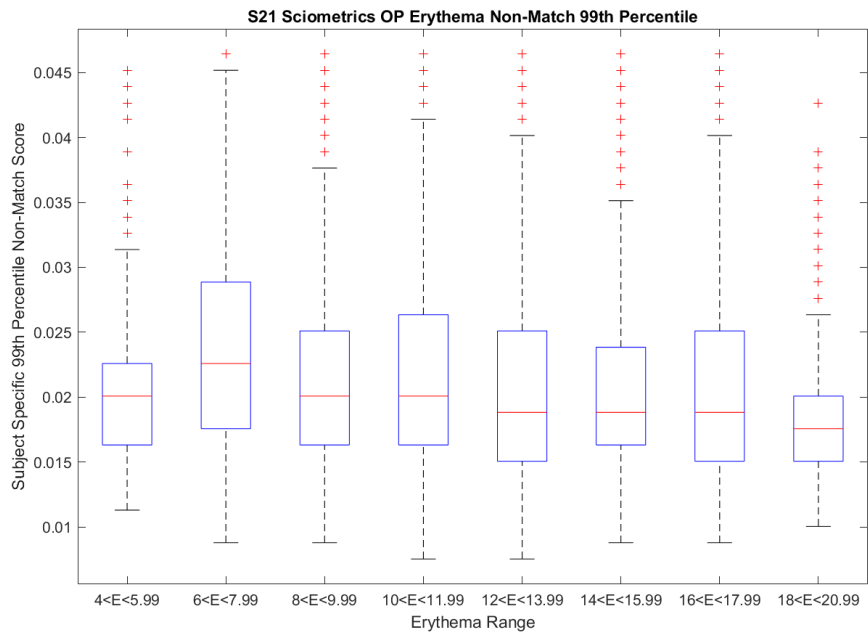


Figure 171 Innovatrics 99th non-match percentile binned into erythema ranges for S21 Sciometrics Op.

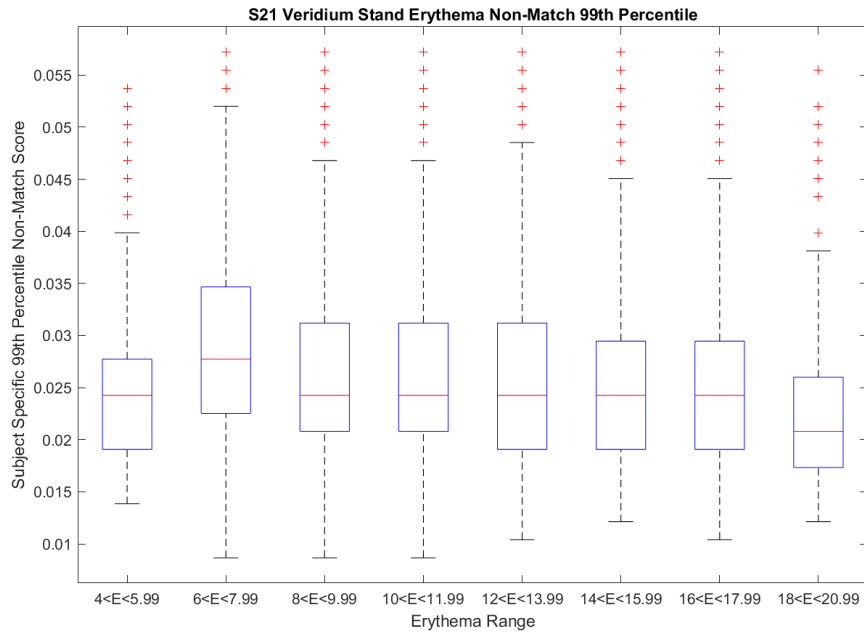


Figure 172 Innovatrics 99th non-match percentile binned into erythema ranges for S21 Veridium Stand.

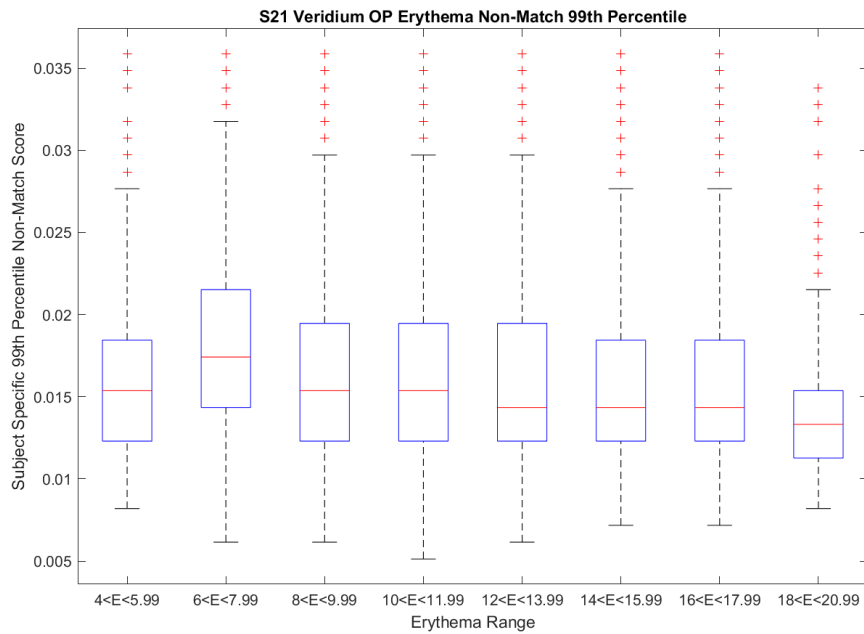


Figure 173 Innovatrics 99th non-match percentile binned into erythema ranges for S21 Veridium Op.

For Figure 161 through Figure 173, the erythema distributions using the 99th percentile non-match scores for the Innovatrics matches show a gradual downward trend from the lowest erythema bin to the highest. Similar to the previous pattern in the melanin distribution, all distributions show the pattern, though the downward trend is more consistent with the erythema distributions. In the Guardian slap distribution in Figure 162, the first bin has a lower interquartile range and median value, though moving to the second erythema bin, the interquartile range and median increase. Every few bins after the second then has a decrease in both the interquartile range and median value, with the highest erythema bin being the lowest interquartile range and the median value.

#### 4.2.7.2.2 VeriFinger

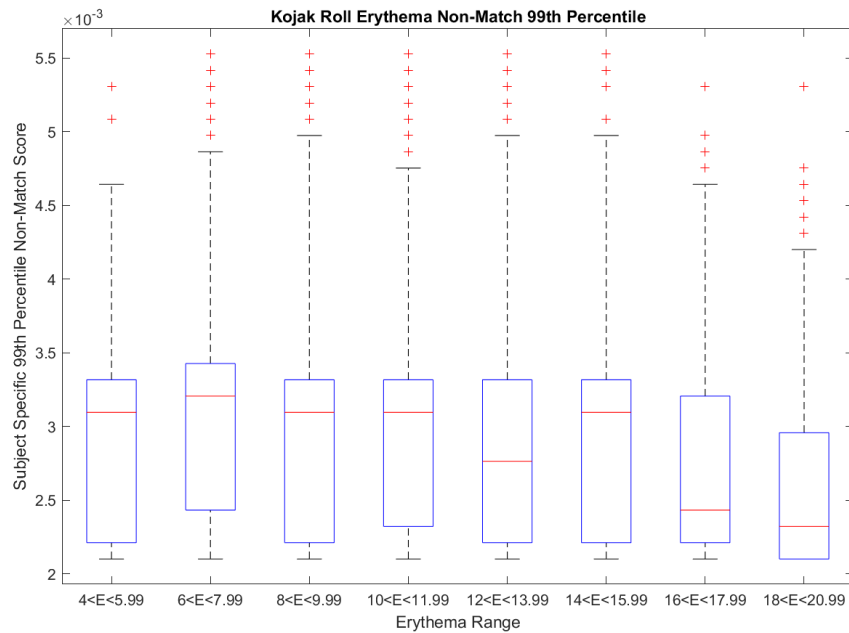


Figure 174 VeriFinger 99th non-match percentile binned into erythema ranges for Kojak Roll.



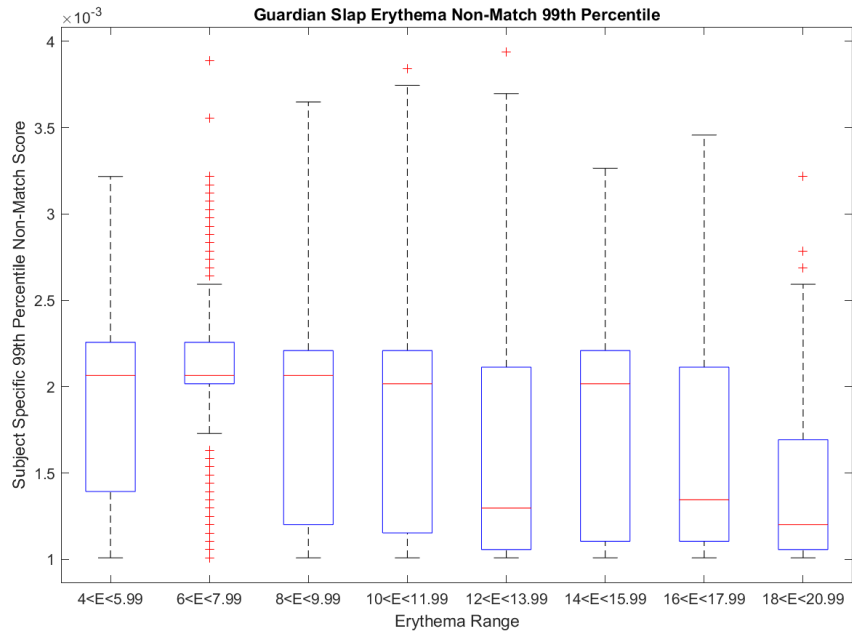


Figure 175 VeriFinger 99th non-match percentile binned into erythema ranges for Guardian Slap.

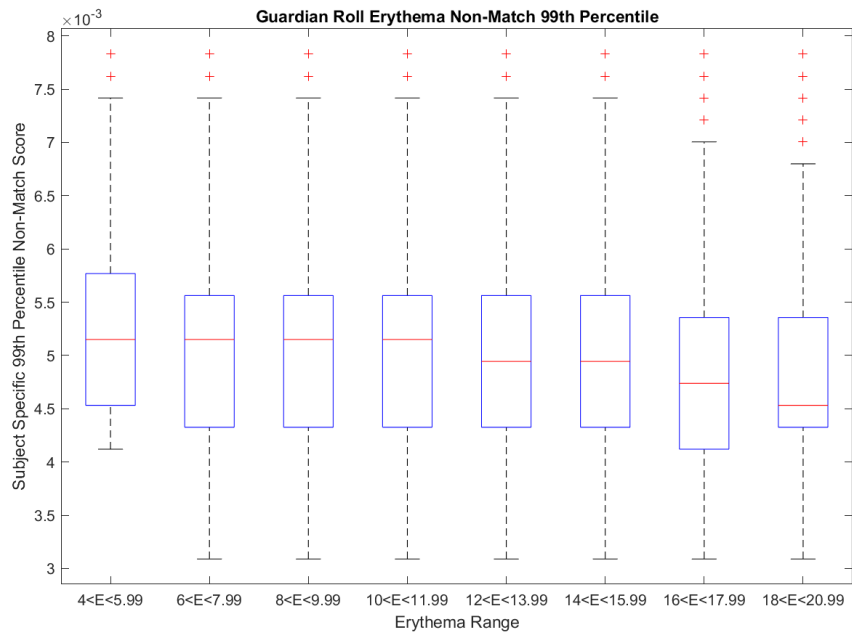


Figure 176 VeriFinger 99th non-match percentile binned into erythema ranges for Guardian Roll.

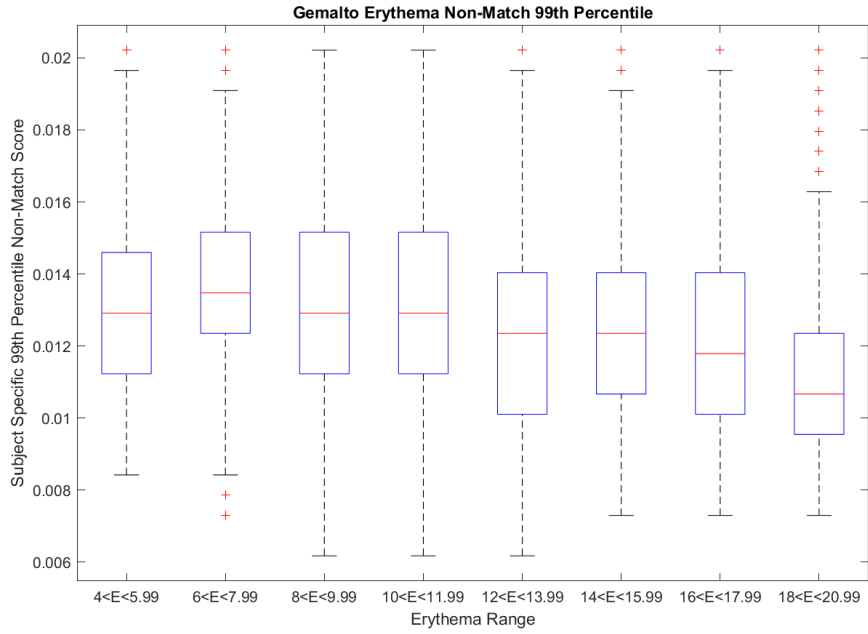


Figure 177 VeriFinger 99th non-match percentile binned into erythema ranges for Gemalto.

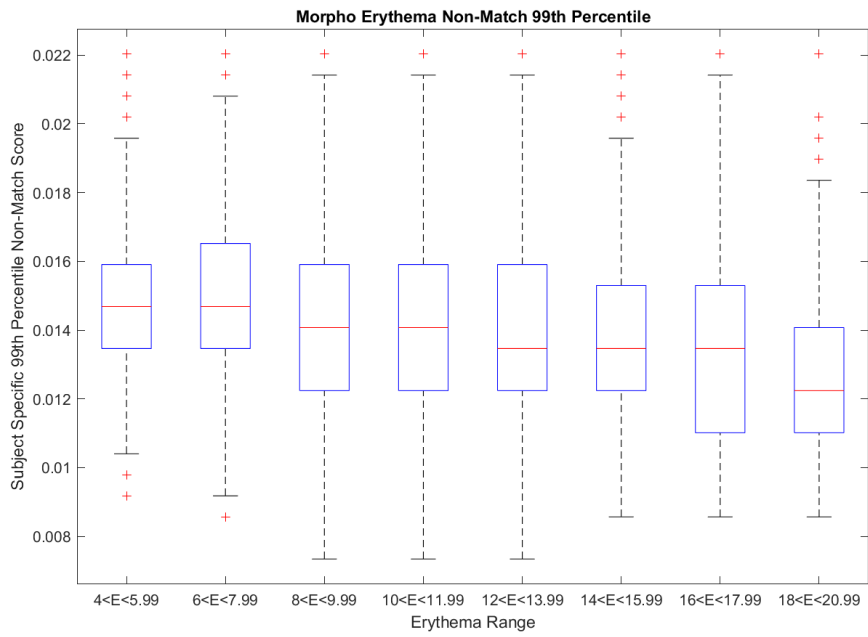


Figure 178 VeriFinger 99th non-match percentile binned into erythema ranges for MorphoWave.

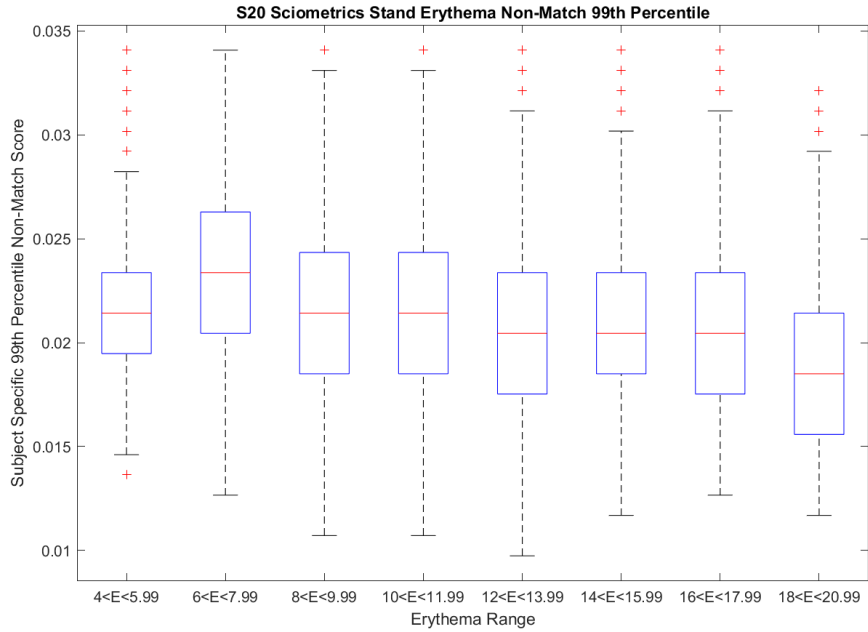


Figure 179 VeriFinger 99th non-match percentile binned into erythema ranges for S20 Sciometrics Stand.

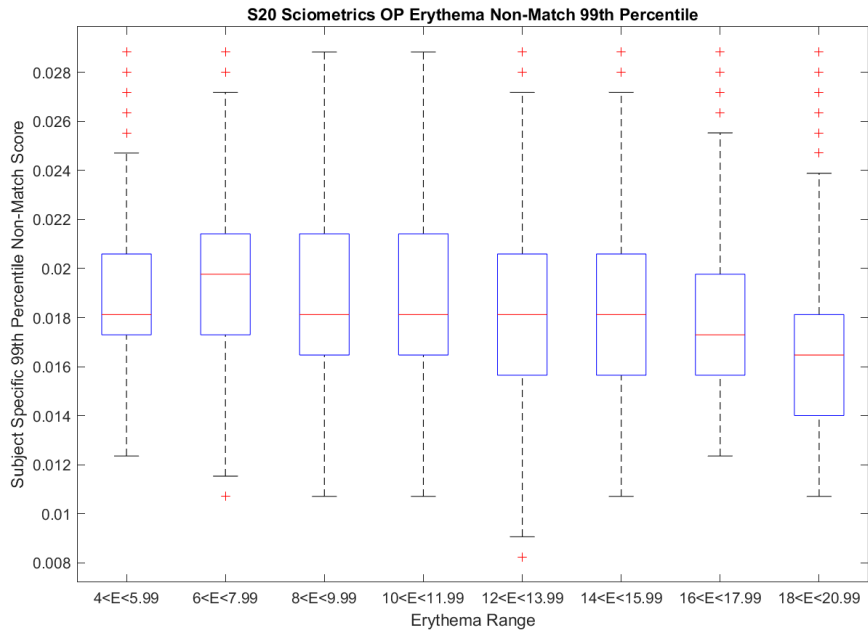


Figure 180 VeriFinger 99th non-match percentile binned into erythema ranges for S20 Sciometrics Op.

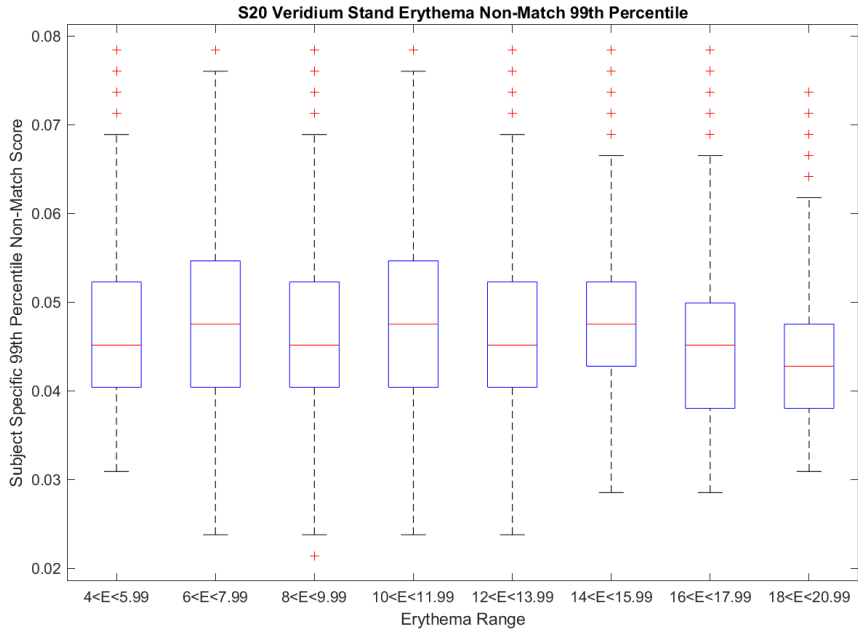


Figure 181 VeriFinger 99th non-match percentile binned into erythema ranges for S20 Veridium Stand.

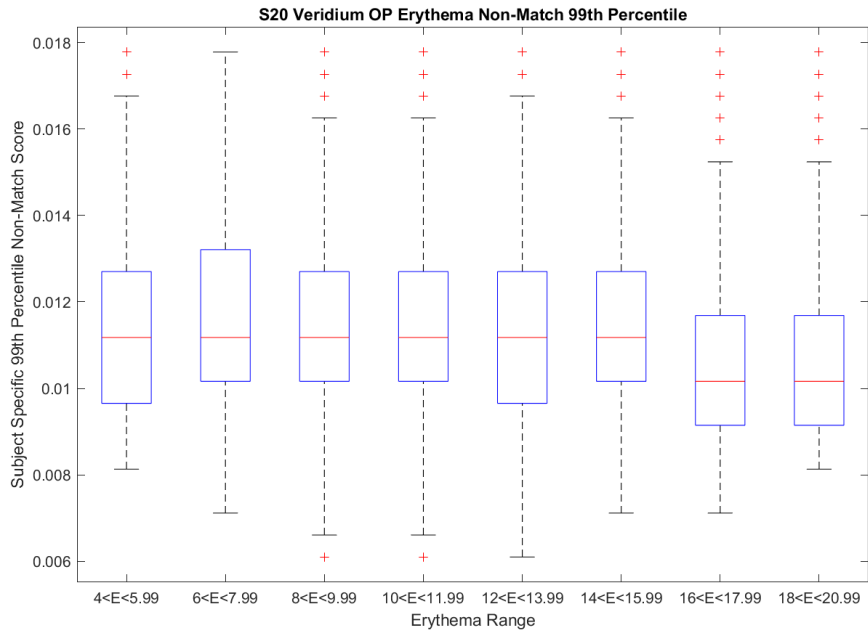


Figure 182 VeriFinger 99th non-match percentile binned into erythema ranges for S20 Veridium Op.

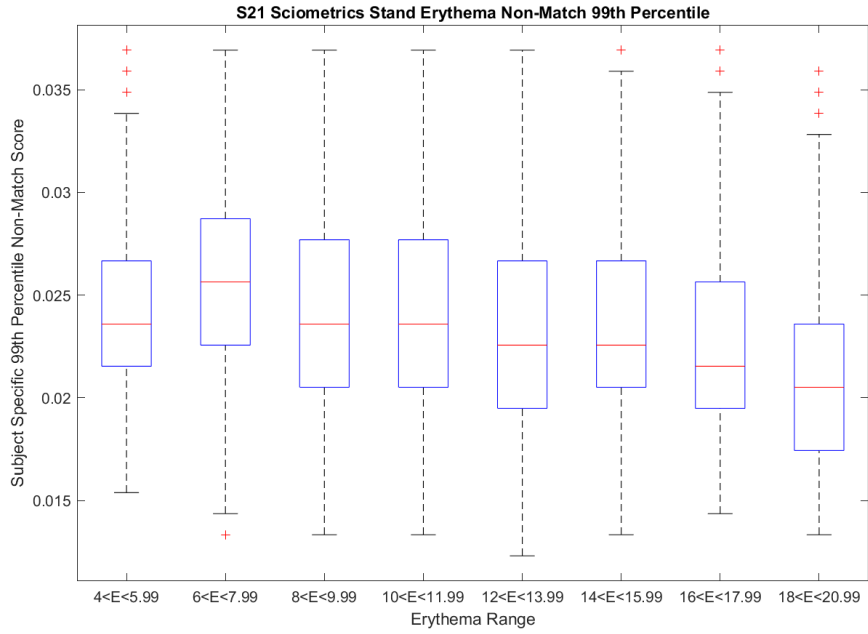


Figure 183 VeriFinger 99th non-match percentile binned into erythema ranges for S21 Sciometrics Stand.

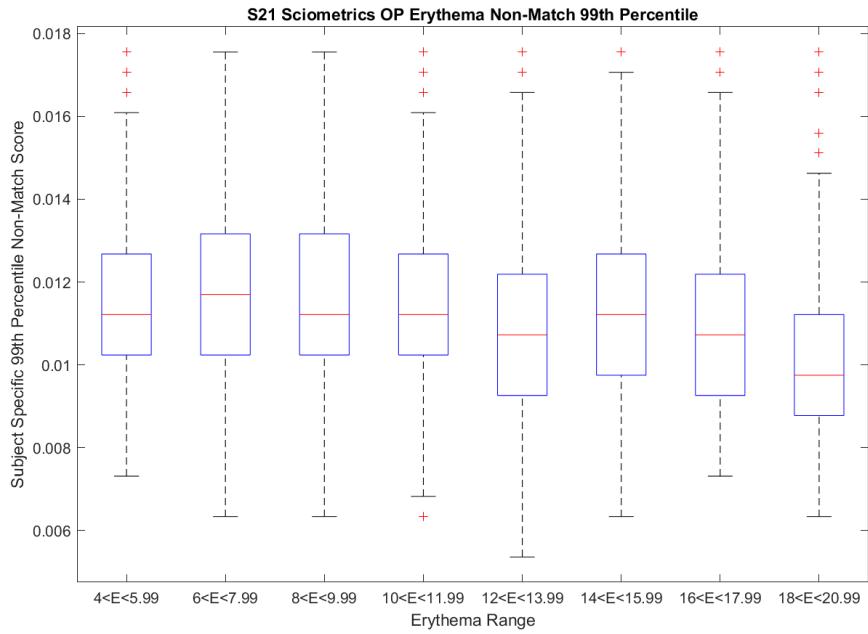


Figure 184 VeriFinger 99th non-match percentile binned into erythema ranges for S21 Sciometrics Op.

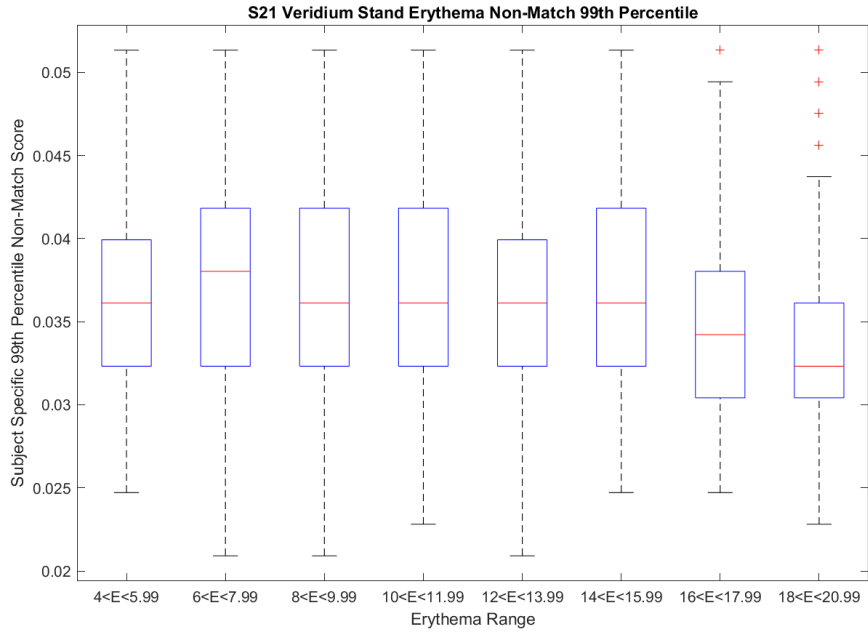


Figure 185 VeriFinger 99th non-match percentile binned into erythema ranges for S21 Veridium Stand.

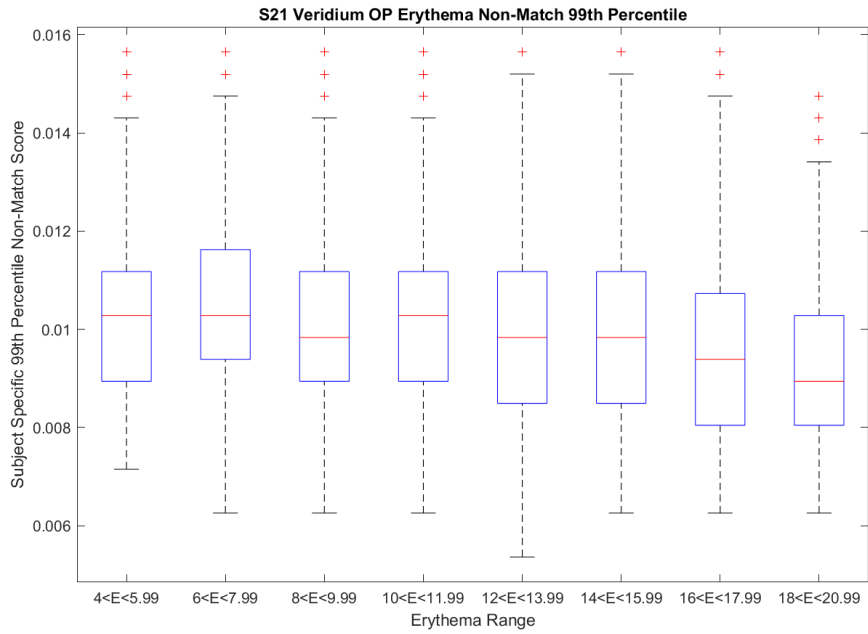


Figure 186 VeriFinger 99th non-match percentile binned into erythema ranges for S21 Veridium Op.

In the 99<sup>th</sup> percentile, non-match VeriFinger erythema distributions, both the Kojak Roll (Figure 174) and Guardian Slap (Figure 175) show varied median non-match scores for all ranges though generally even interquartile ranges. The Guardian Slap distribution's second bin appears differently, with a concise interquartile range and many outliers. The Guardian Roll, Gemalto, and MorphoWave distributions in Figure 176, Figure 177, and Figure 178 show a downward trend of the median non-match score as erythema increases. Though the interquartile ranges only trend downward for Gemalto and MorphoWave, the interquartile ranges remain similar for the Guardian Roll. In Figure 179 through Figure 186, the Sciometrics distributions show a downward trend in the median non-match score as erythema increases. The Veridium distributions show no trend or relatively similar results across all bins. However, the highest two bins have a lower median non-match score for each distribution except the S20 Veridium Stand.

#### 4.2.7.2.3 Bozorth3

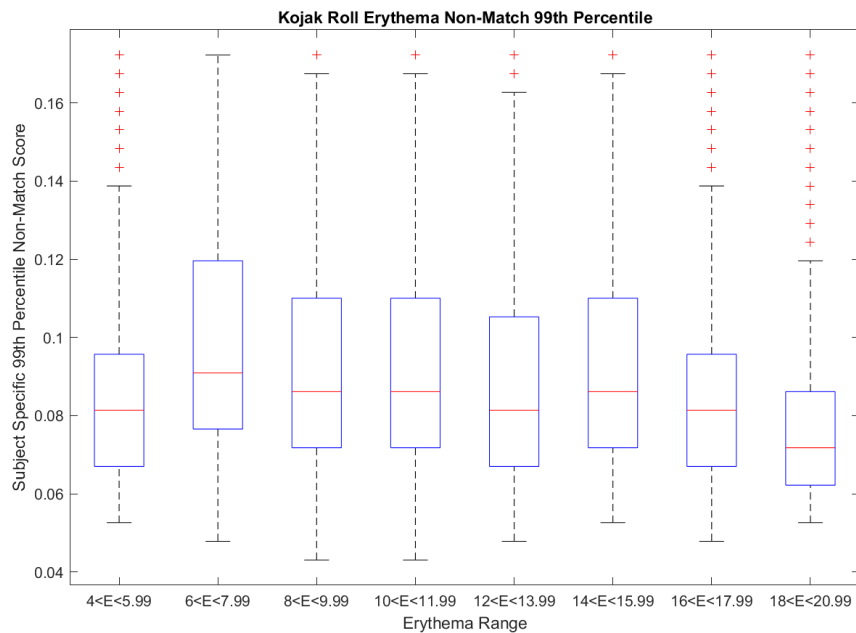


Figure 187 Bozorth3 99th non-match percentile binned into erythema ranges for Kojak Roll.

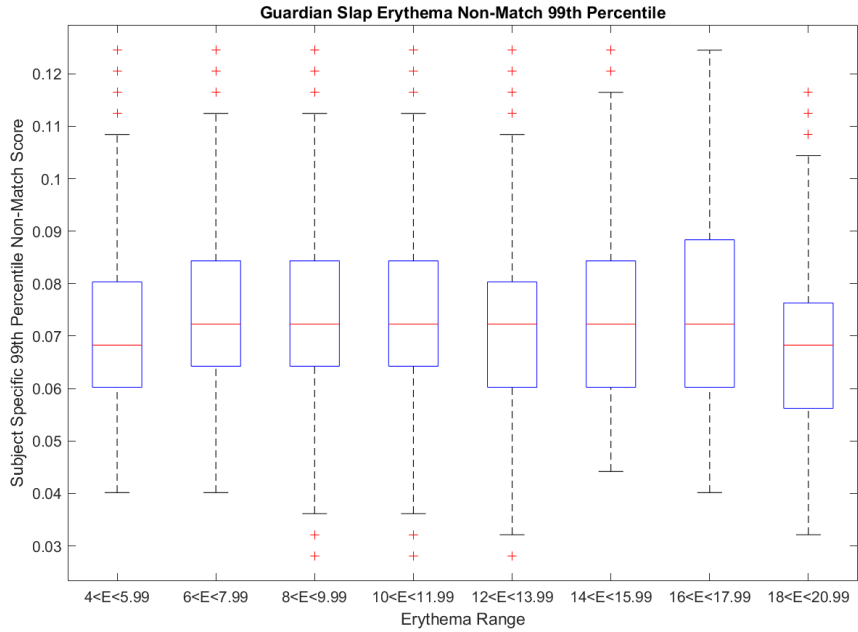


Figure 188 Bozorth3 99th non-match percentile binned into erythema ranges for Guardian Slap (Baseline).

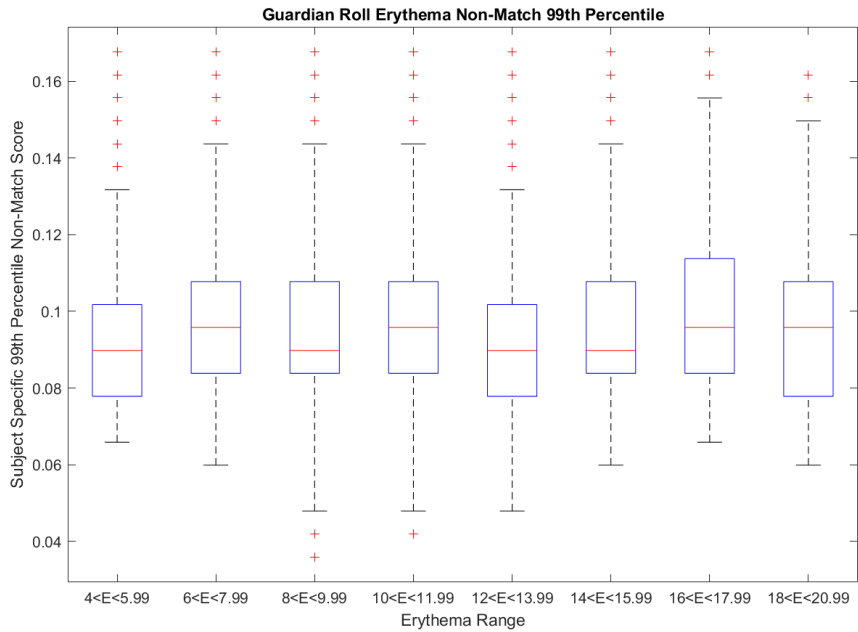


Figure 189 Bozorth3 99th non-match percentile binned into erythema ranges for Guardian Roll.



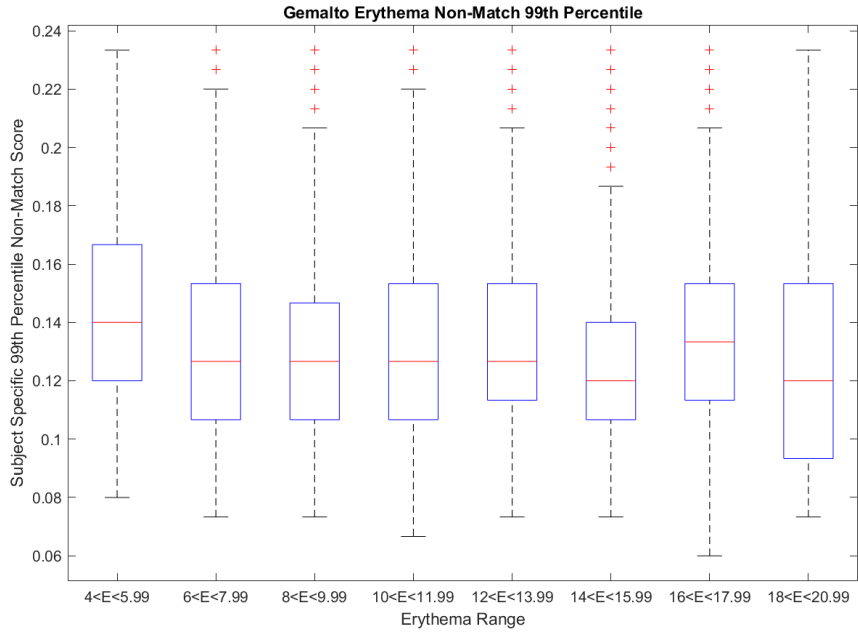


Figure 190 Bozorth3 99th non-match percentile binned into erythema ranges for Gemalto.

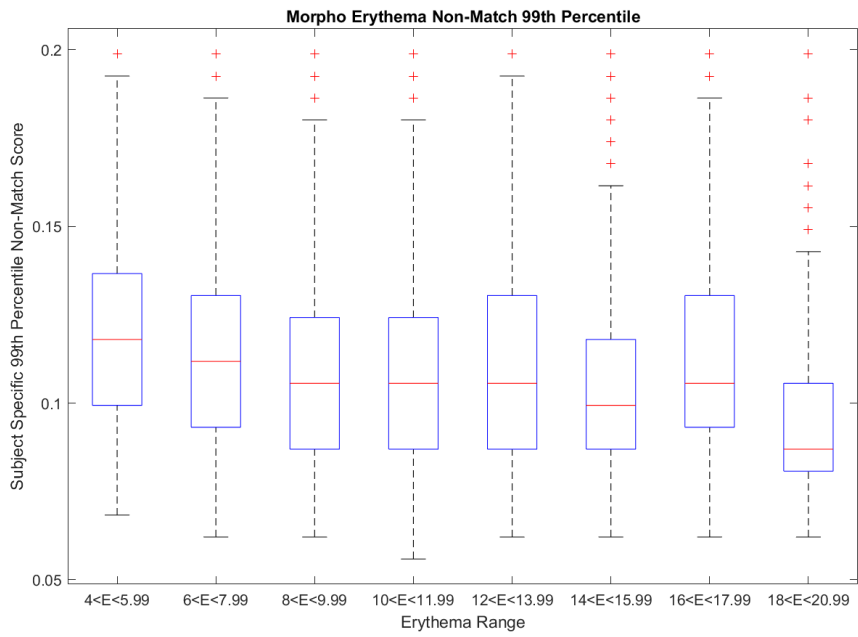


Figure 191 Bozorth3 99th non-match percentile binned into erythema ranges for MorphoWave.

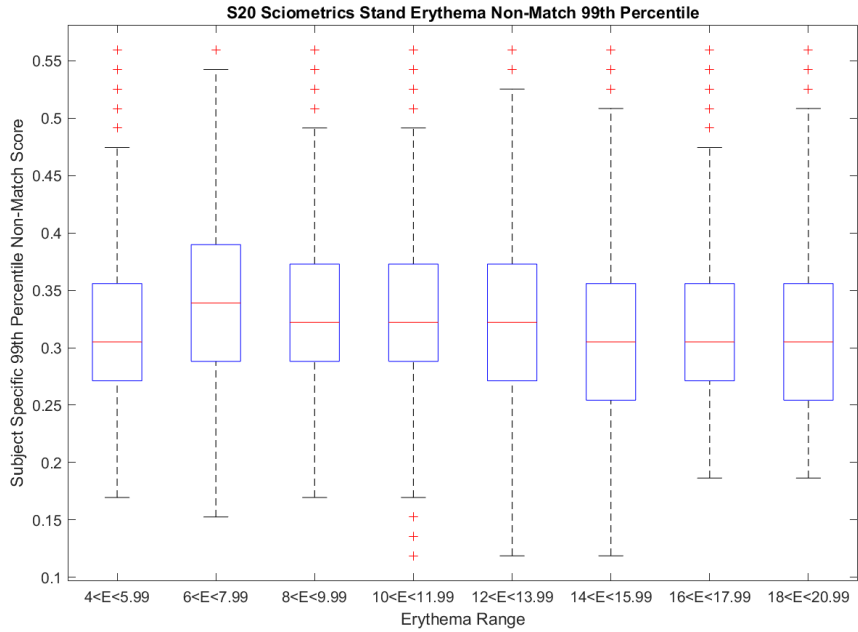


Figure 192 Bozorth3 99th non-match percentile binned into erythema ranges for S20 Sciometrics Stand.

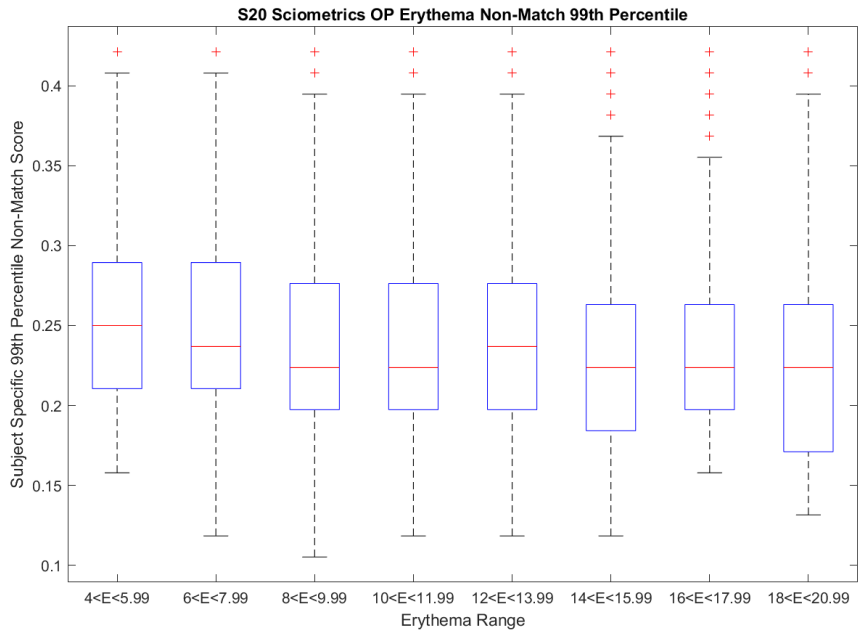


Figure 193 Bozorth3 99th non-match percentile binned into erythema ranges for S20 Sciometrics Op.

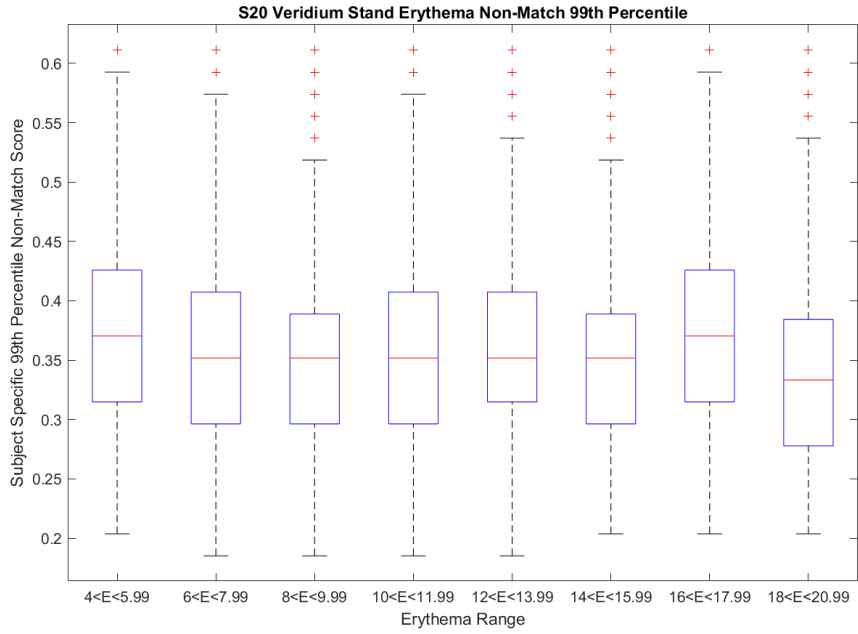


Figure 194 Bozorth3 99th non-match percentile binned into erythema ranges for S20 Veridium Stand.

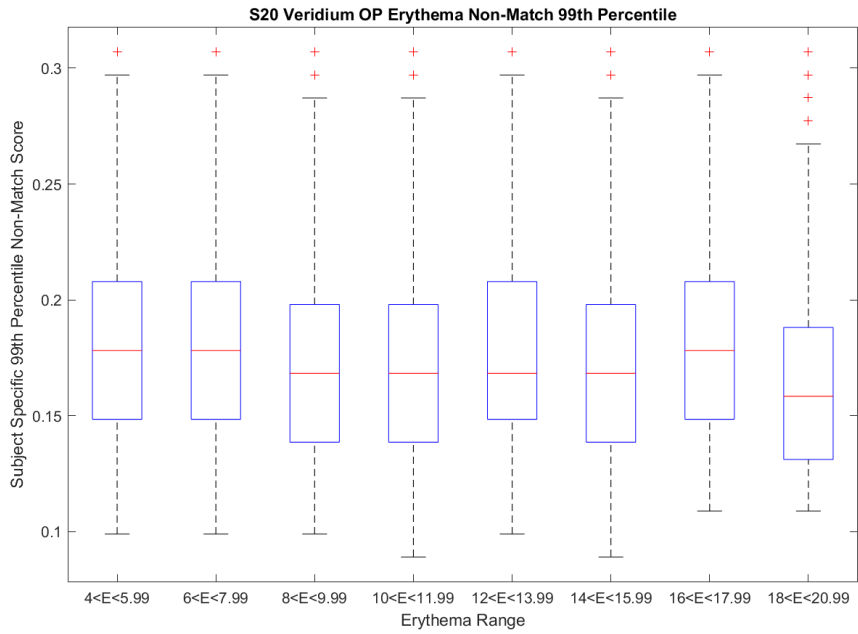


Figure 195 Bozorth3 99th non-match percentile binned into erythema ranges for S20 Veridium Op.

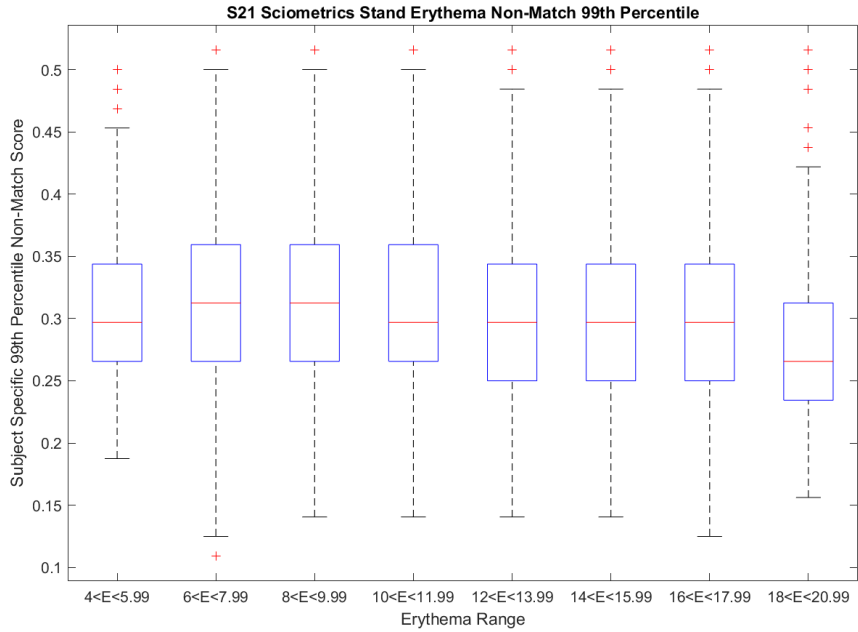


Figure 196 Bozorth3 99th non-match percentile binned into erythema ranges for S21 Sciometrics Stand.

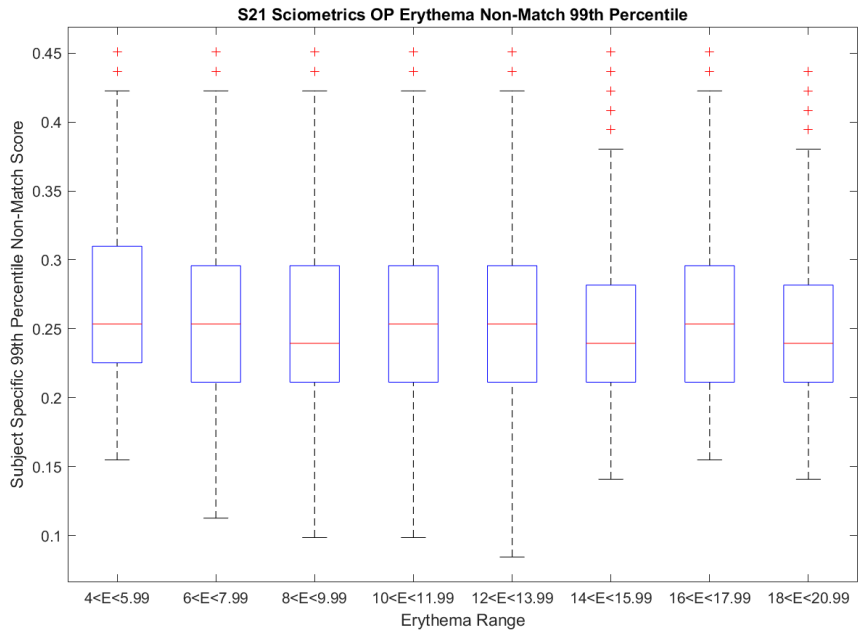


Figure 197 Bozorth3 99th non-match percentile binned into erythema ranges for S21 Sciometrics Op.

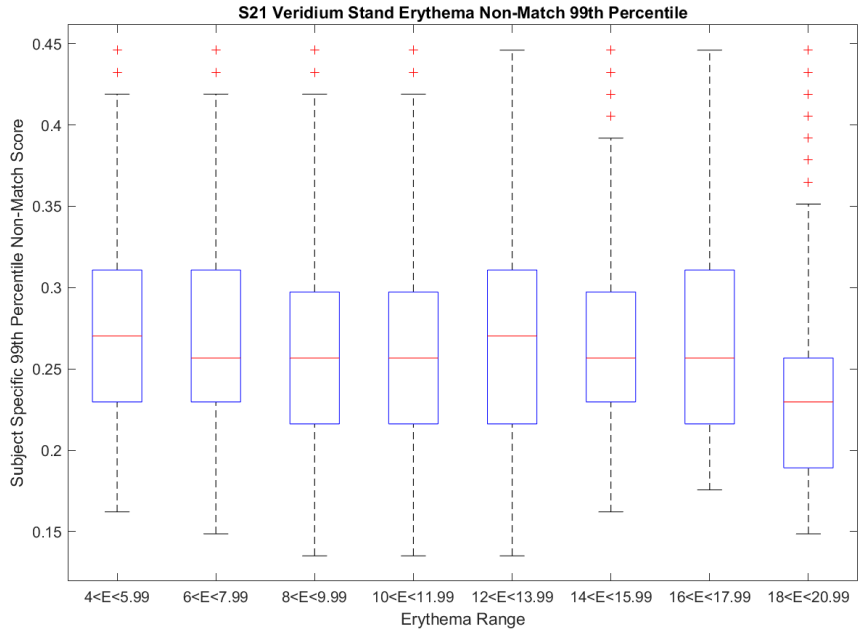


Figure 198 Bozorth3 99th non-match percentile binned into erythema ranges for S21 Veridium Stand.

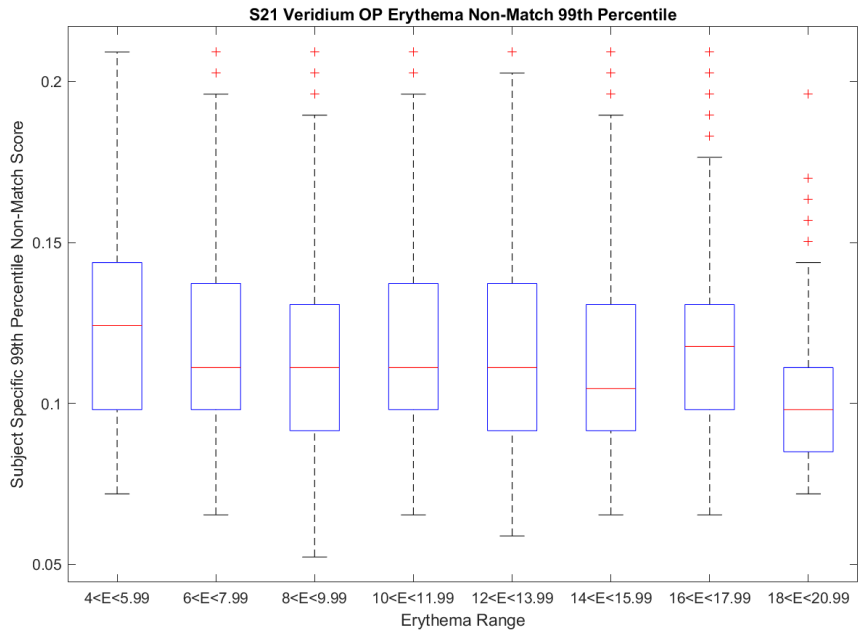


Figure 199 Bozorth3 99th non-match percentile binned into erythema ranges for S21 Veridium Op.

Similar to the Bozorth3 melanin distributions using the 99<sup>th</sup> percentile non-match scores results, the Bozorth3 erythema results shown in Figure 187 through Figure 199 show trends easily perceivable across all distributions, unlike both the Innovatrics melanin and erythema distributions. The Veridium erythema distributions show a trend for the highest erythema bin to have a lower interquartile range and median. The Sciometrics, contact, and contactless distributions otherwise show no trends and stay relatively steady, except for some distributions having a deviating bin that could range higher or lower.

### 4.2.7.3 Lightness Spectrum Distributions

#### 4.2.7.3.1 Innovatrics

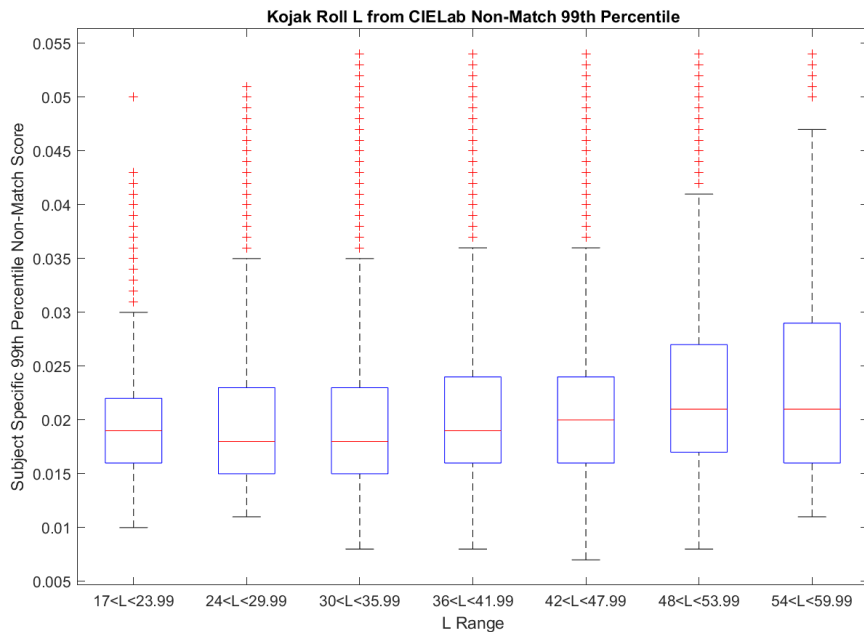


Figure 200 Innovatrics 99th non-match percentile binned lightness ranges Kojak Roll.

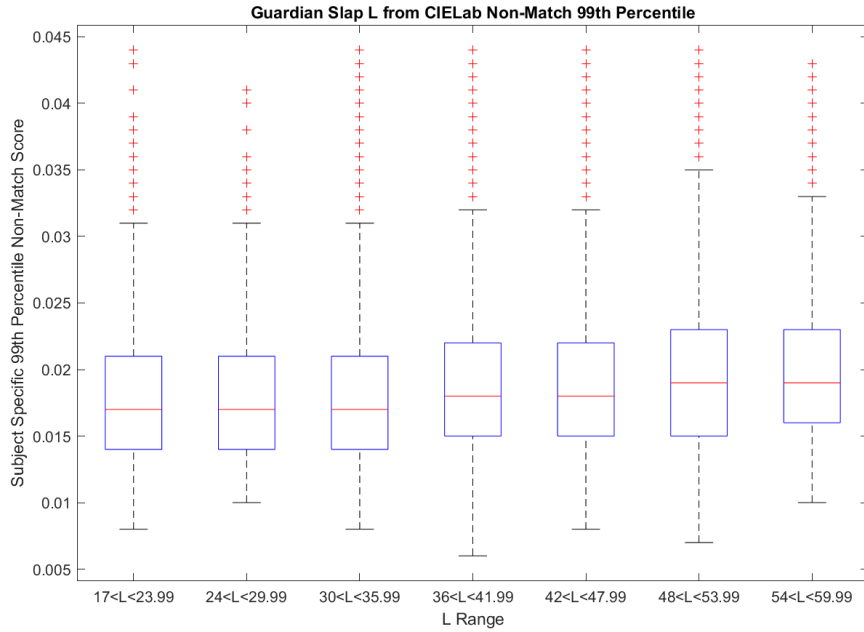


Figure 201 Innovatrics 99th non-match percentile binned lightness ranges Guardian Slap (Baseline).

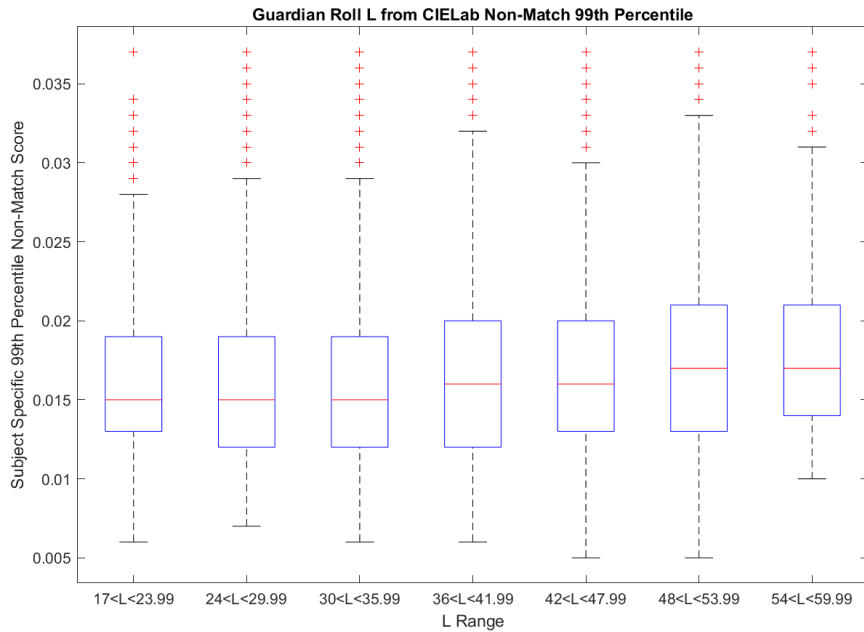


Figure 202 Innovatrics 99th non-match percentile binned lightness ranges Guardian Roll.

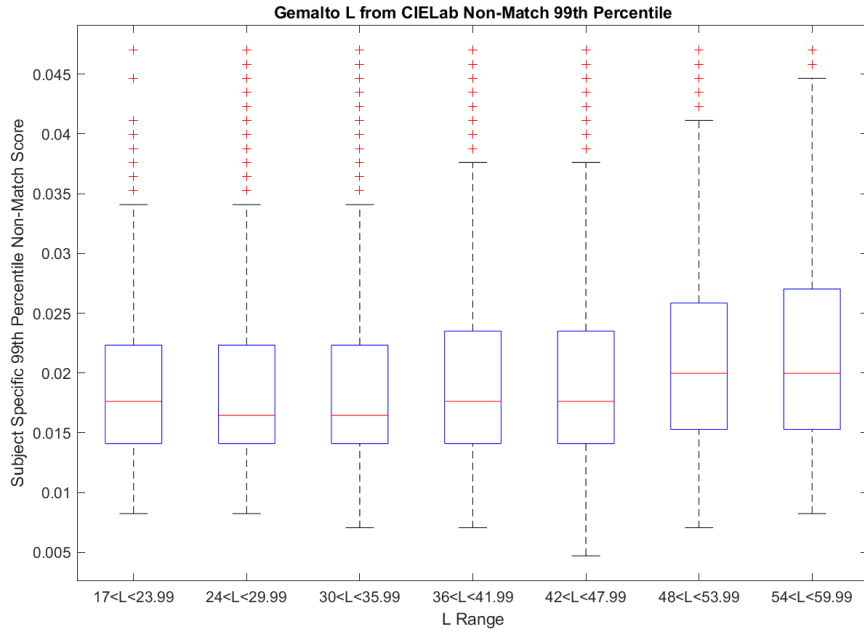


Figure 203 Innovatrics 99th non-match percentile binned lightness ranges Gemalto.

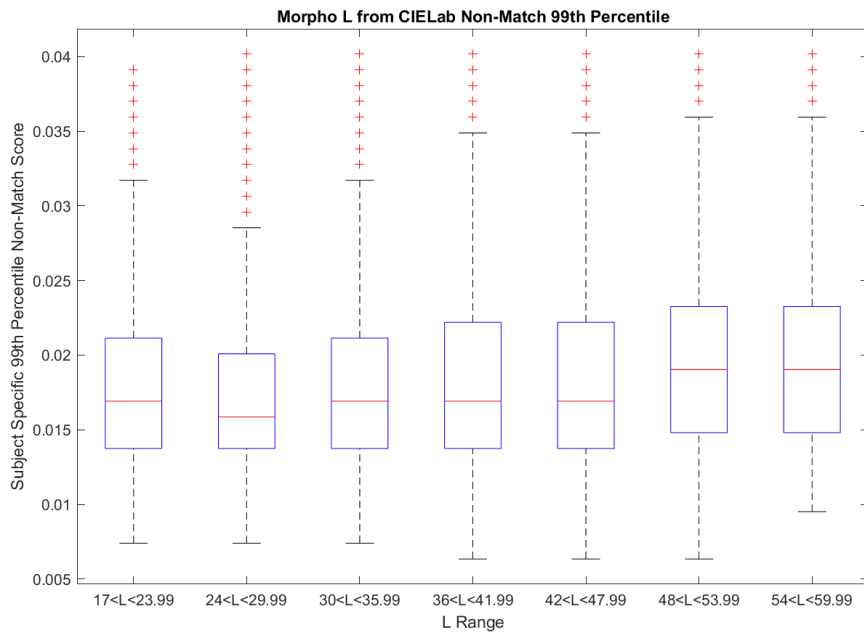


Figure 204 Innovatrics 99th non-match percentile binned lightness ranges MorphoWave.



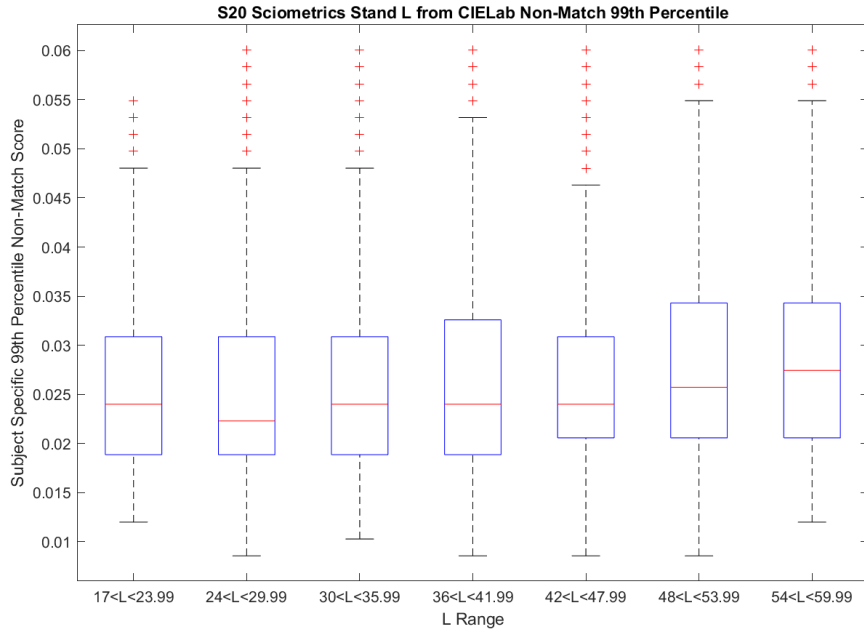


Figure 205 Innovatrics 99th non-match percentile binned lightness ranges S20 Sciometrics Stand.

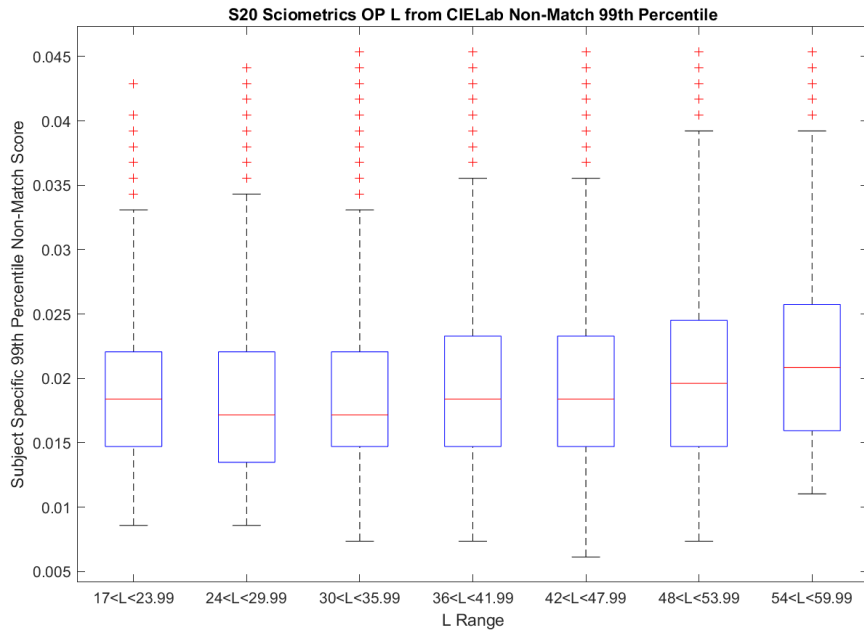


Figure 206 Innovatrics 99th non-match percentile binned lightness ranges S20 Sciometrics Op.

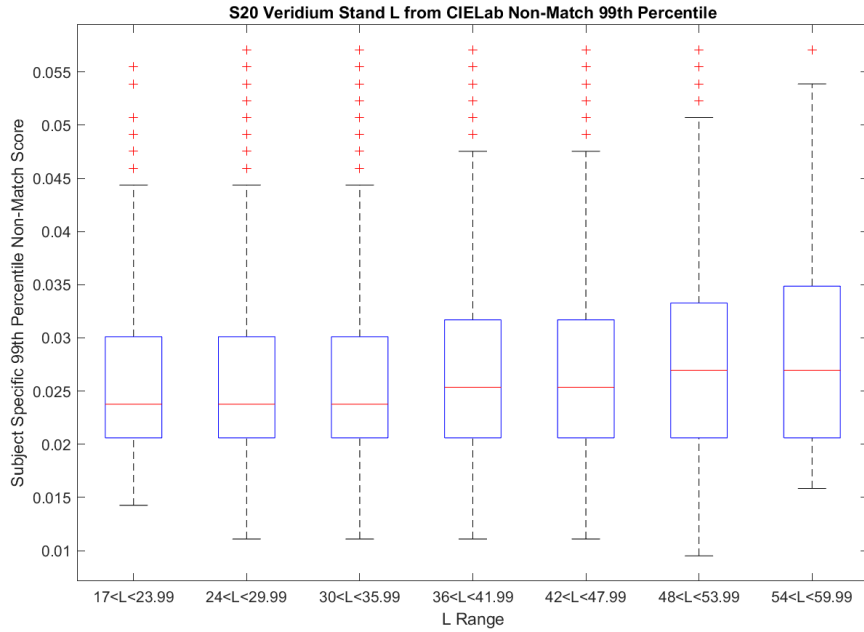


Figure 207 Innovatrics 99th non-match percentile binned lightness ranges S20 Veridium Stand.

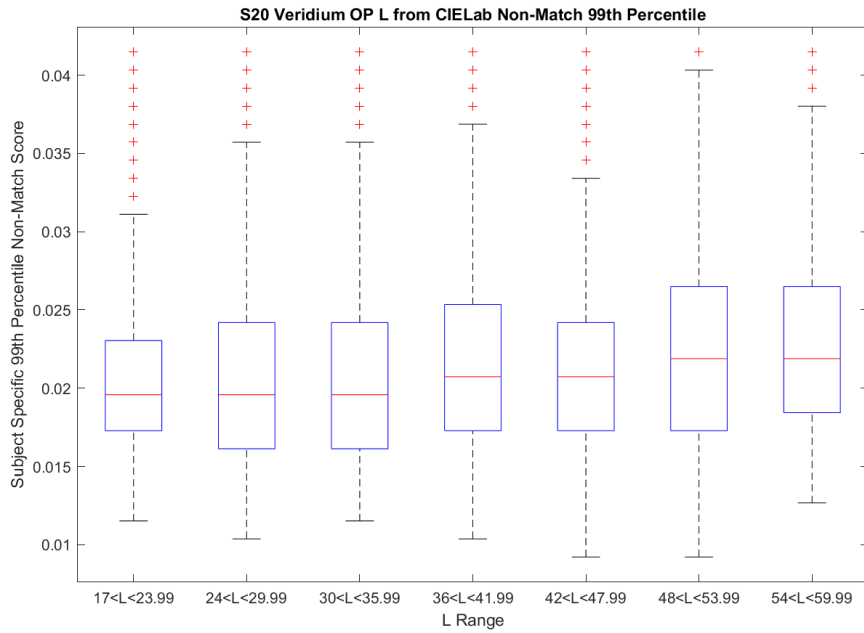


Figure 208 Innovatrics 99th non-match percentile binned lightness ranges S20 Veridium Op.

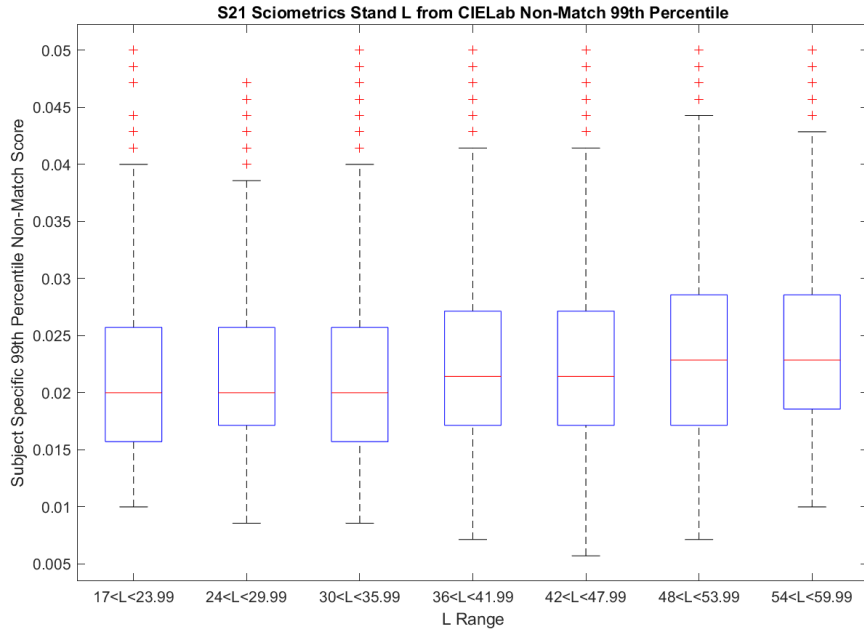


Figure 209 Innovatrics 99th non-match percentile binned lightness ranges S21 Sciometrics Stand.

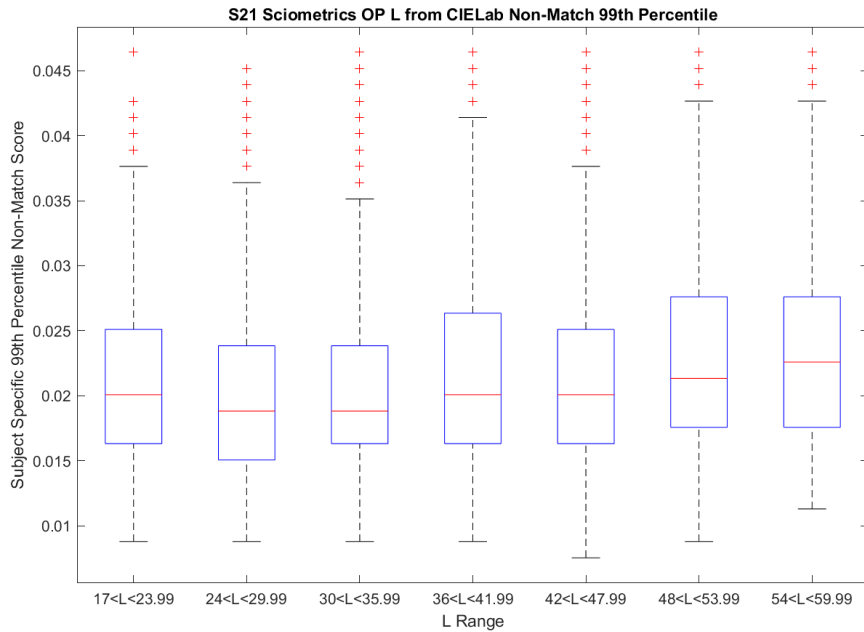


Figure 210 Innovatrics 99th non-match percentile binned lightness ranges S21 Sciometrics Op.

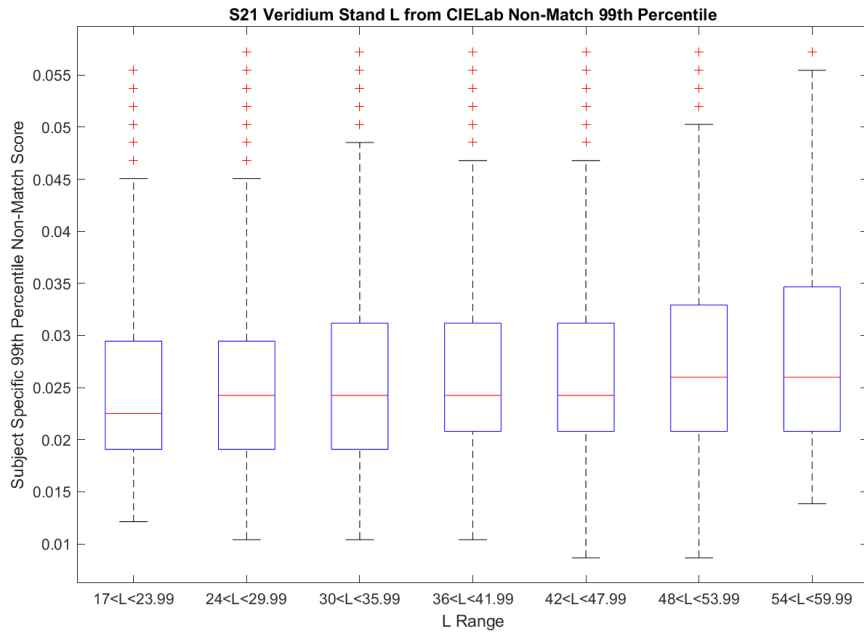


Figure 211 Innovatrics 99th non-match percentile binned lightness ranges S21 Veridium Stand.

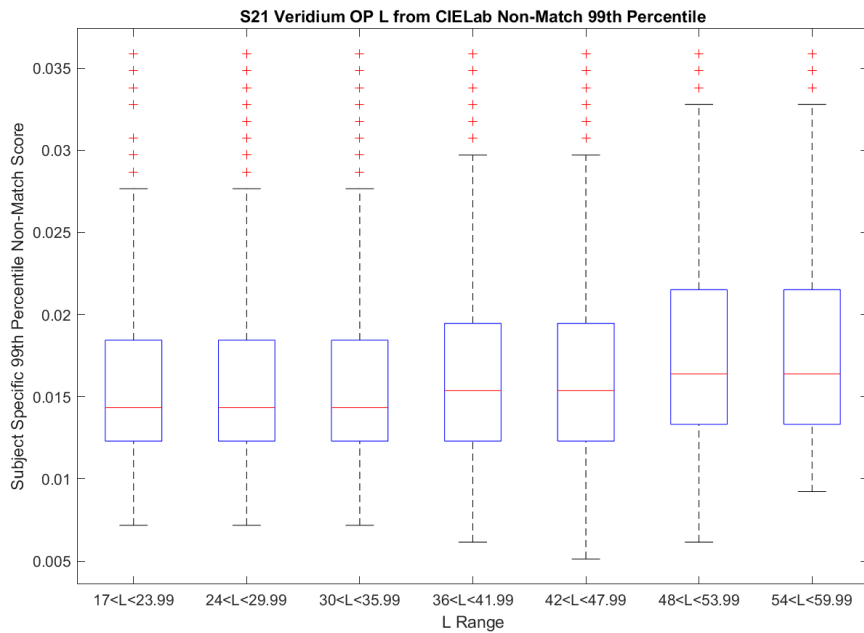


Figure 212 Innovatrics 99th non-match percentile binned lightness ranges S21 Veridium Op.

For Figure 200 through Figure 212, the Innovatrics 99<sup>th</sup> percentile non-match results are compared to the lightness ranges. All graphs show an upward trend in the median, interquartile

range, and whiskers. The upward trend shows that lighter skin values perform slightly worse than darker ones since the non-match score ranges are increasing. No individual trends are seen in any experiment.

#### 4.2.7.3.2 VeriFinger

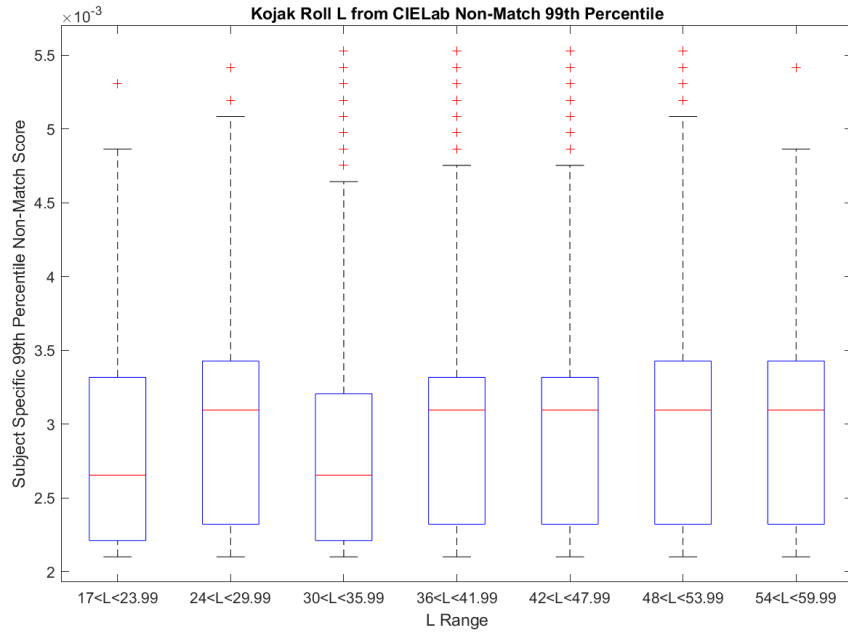


Figure 213 VeriFinger 99th non-match percentile binned lightness ranges Kojak Roll.

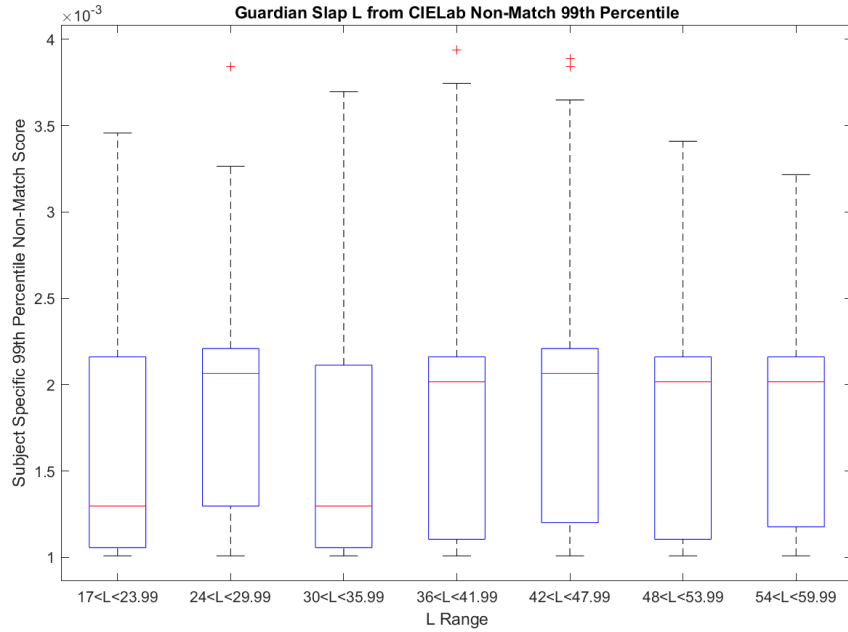


Figure 214 VeriFinger 99th non-match percentile binned lightness ranges Guardian Slap.

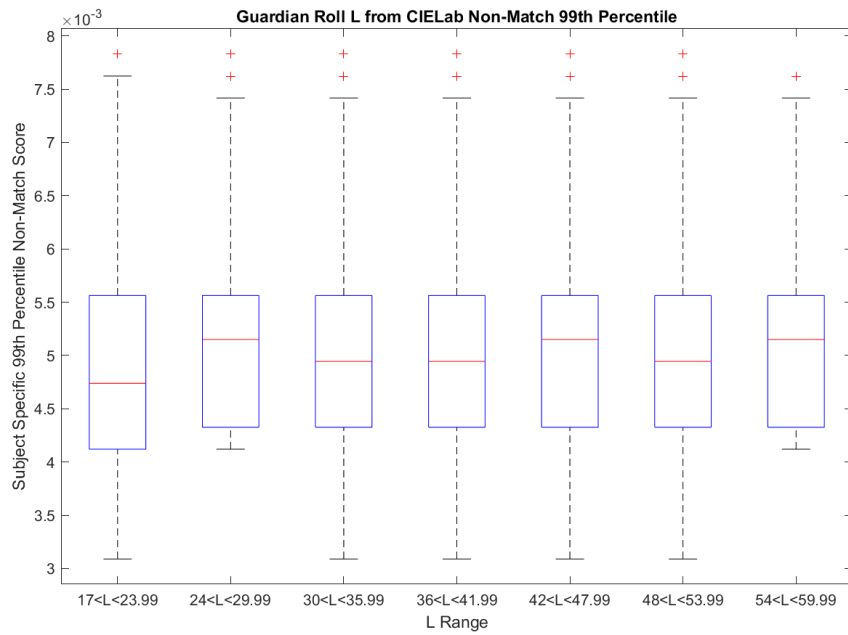


Figure 215 VeriFinger 99th non-match percentile binned lightness ranges Guardian Roll.

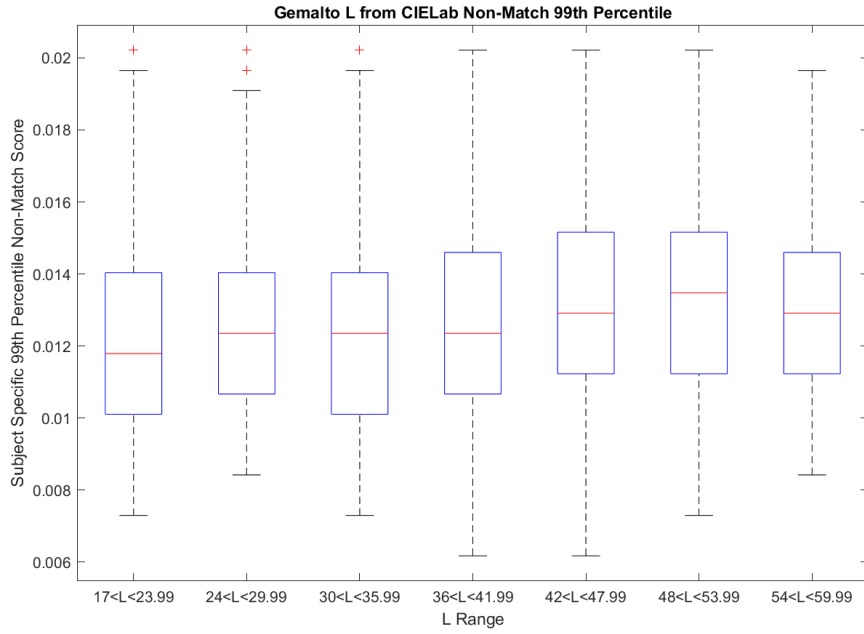


Figure 216 VeriFinger 99th non-match percentile binned lightness ranges Gemalto.

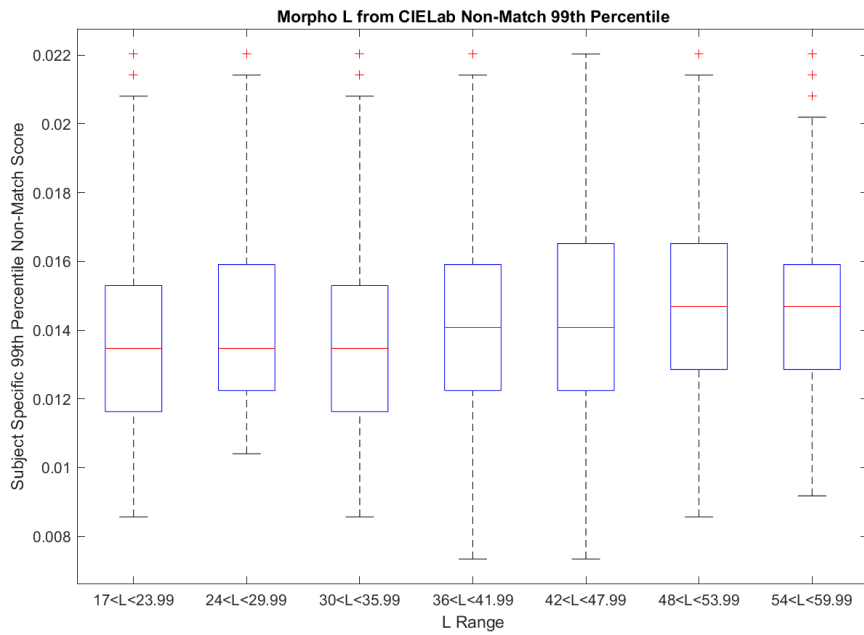


Figure 217 VeriFinger 99th non-match percentile binned lightness ranges MorphoWave.

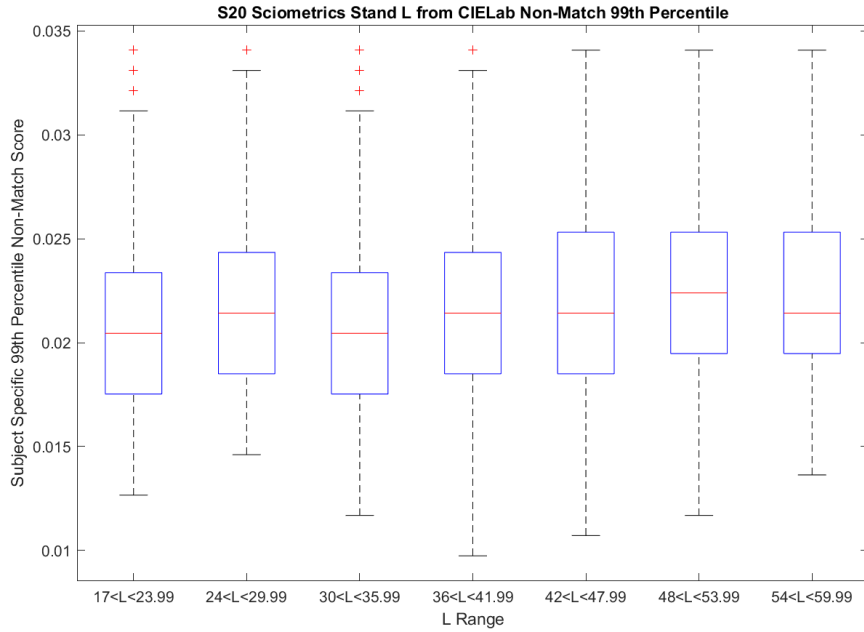


Figure 218 VeriFinger 99th non-match percentile binned lightness ranges S20 Sciometrics Stand.

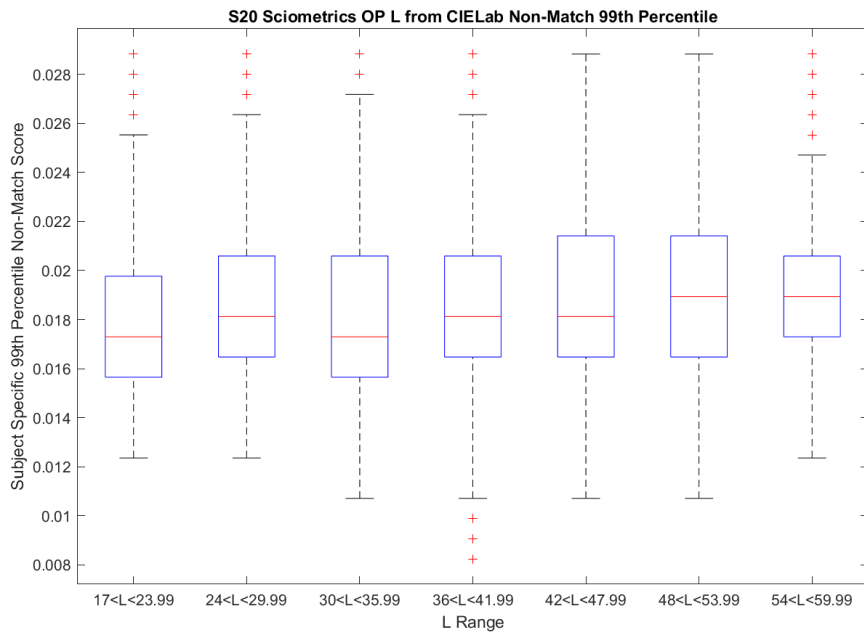


Figure 219 VeriFinger 99th non-match percentile binned lightness ranges S20 Sciometrics Op.



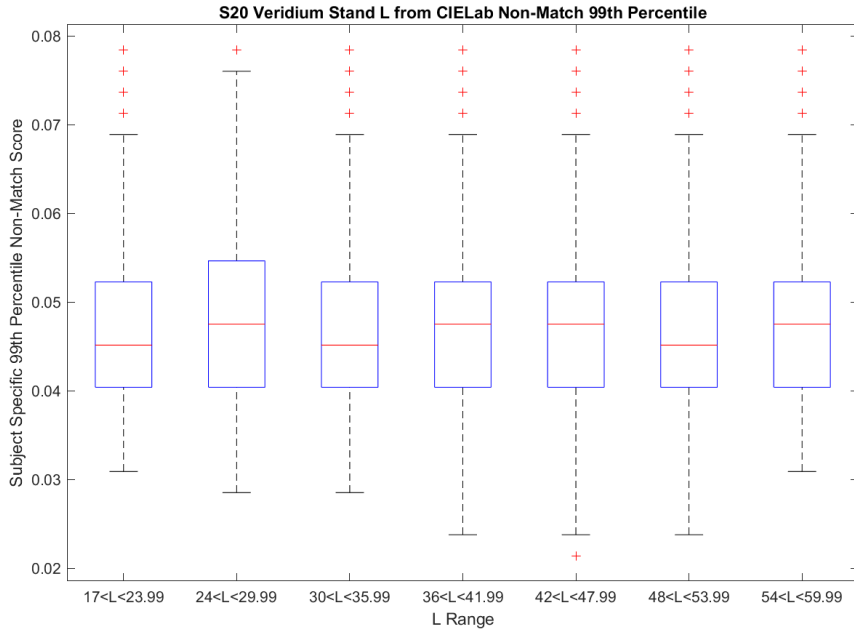


Figure 220 VeriFinger 99th non-match percentile binned lightness ranges S20 Veridium Stand.

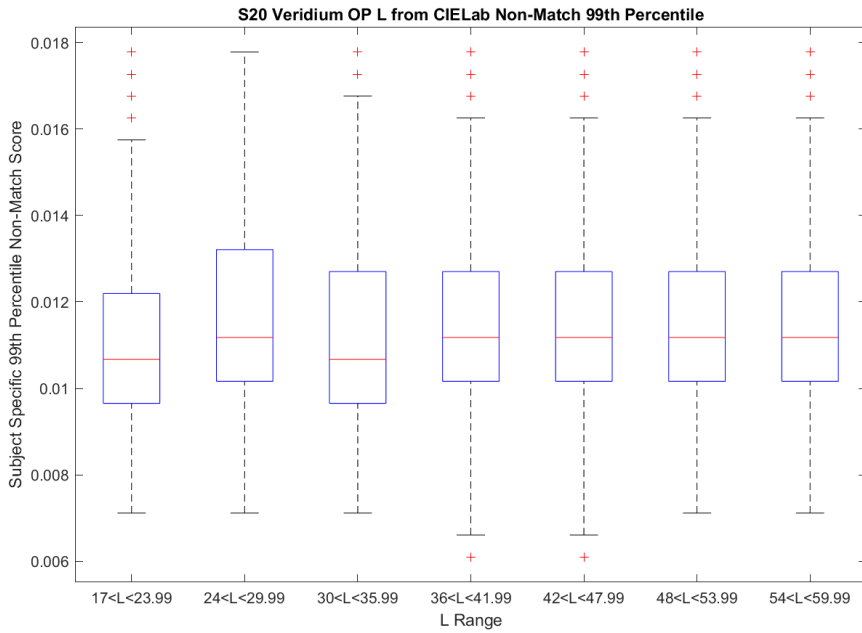


Figure 221 VeriFinger 99th non-match percentile binned lightness ranges S20 Veridium Op.

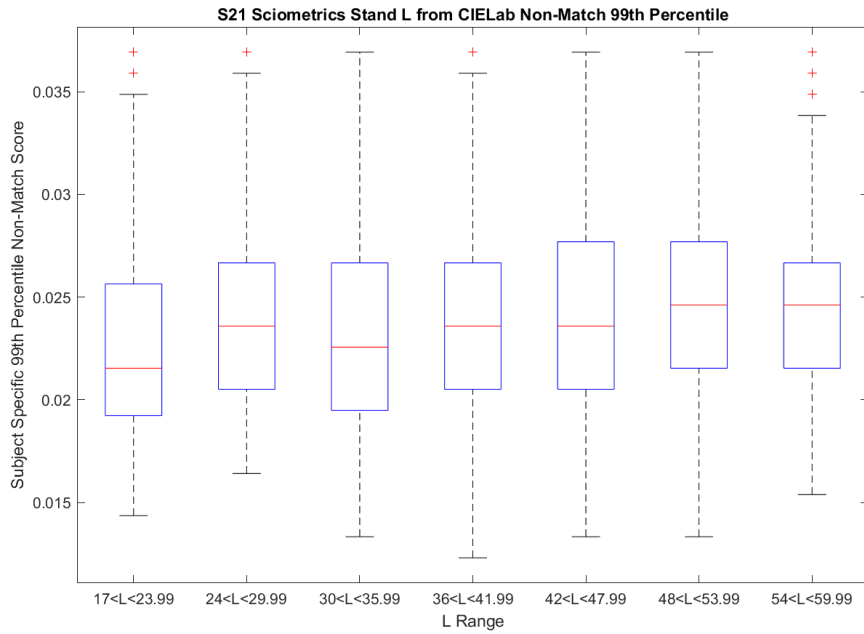


Figure 222 VeriFinger 99th non-match percentile binned lightness ranges S21 Sciometrics Stand.

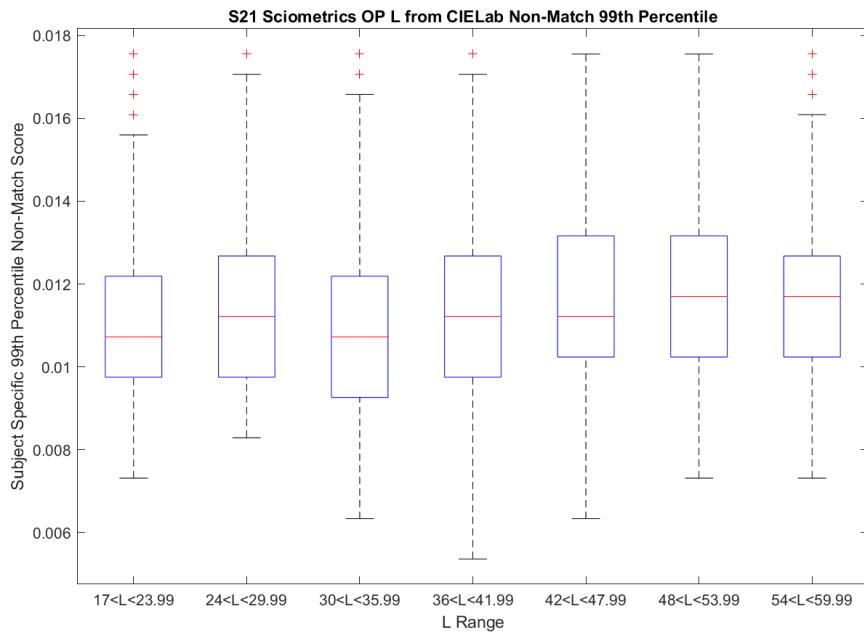


Figure 223 VeriFinger 99th non-match percentile binned lightness ranges S21 Sciometrics Op.

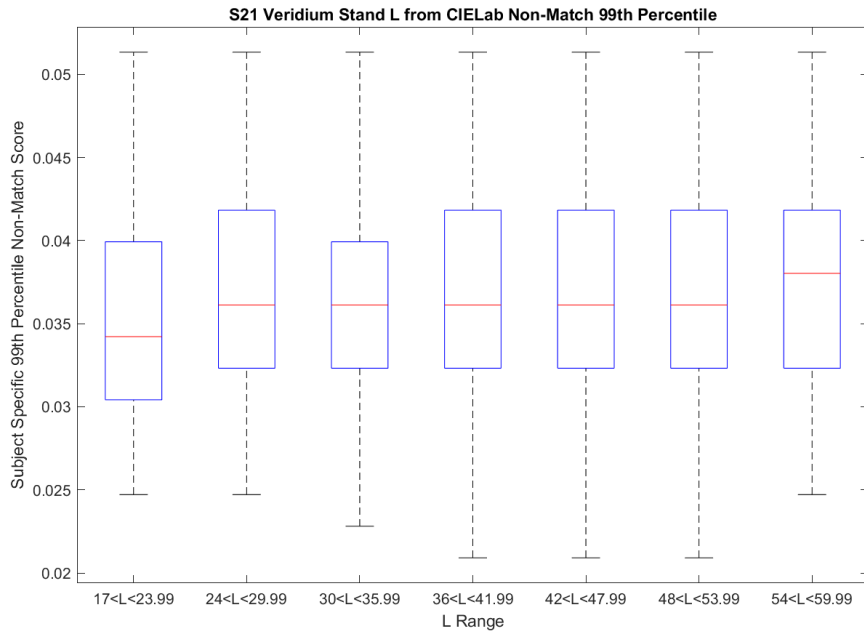


Figure 224 VeriFinger 99th non-match percentile binned lightness ranges S21 Veridium Stand.

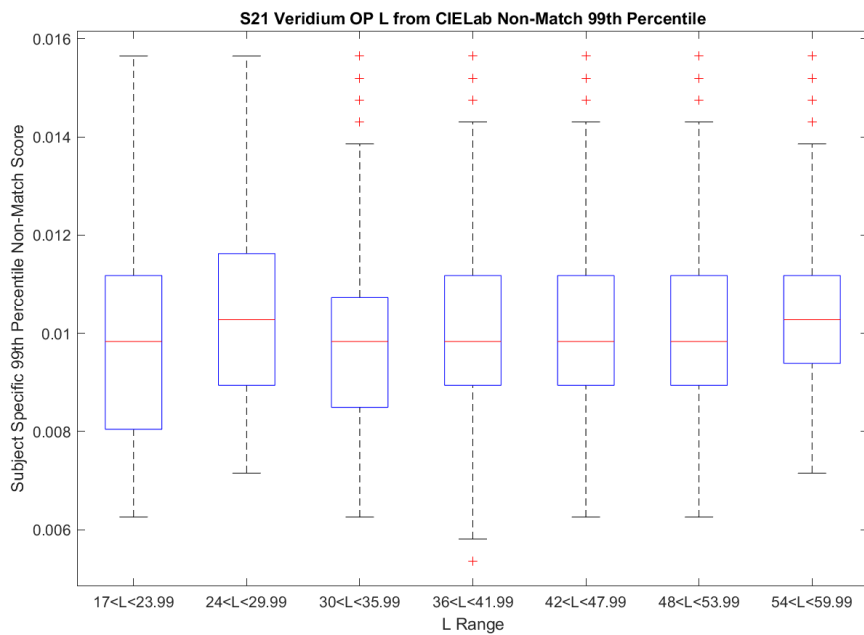


Figure 225 VeriFinger 99th non-match percentile binned lightness ranges S21 Veridium Op.

The 99<sup>th</sup> percentile non-match contact distributions in Figure 213 through Figure 215 all have steady interquartile ranges. However, the Kojak Roll and Guardian Slap distribution have a

first and third bin with a deviated median non-match score. The Guardian Roll distribution median non-match scores vary though they do not trend in any direction. The Gemalto and MorphoWave distributions (Figure 216 and Figure 217) have an upward trend for their interquartile ranges and median non-match scores. None of the cellphone distributions in Figure 218 through Figure 225 showed consistent trends outside some bins having seemingly random deviations. Otherwise, all median values and interquartile ranges remained steady.

#### 4.2.7.4 Red-Green Spectrum $a^*$ measurement Distributions

##### 4.2.7.4.1 Innovatrics

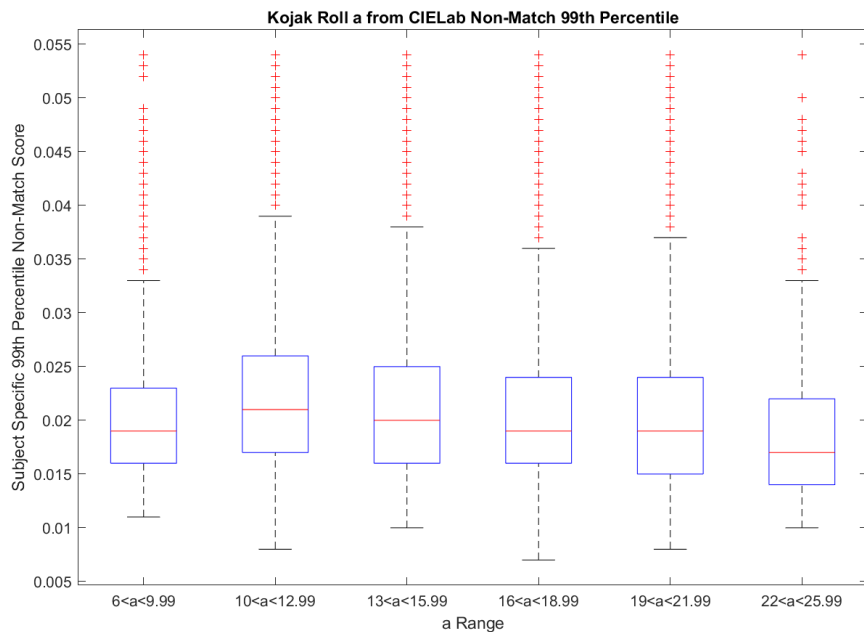


Figure 226 Innovatrics 99th non-match percentile binned red-green ranges Kojak Roll.

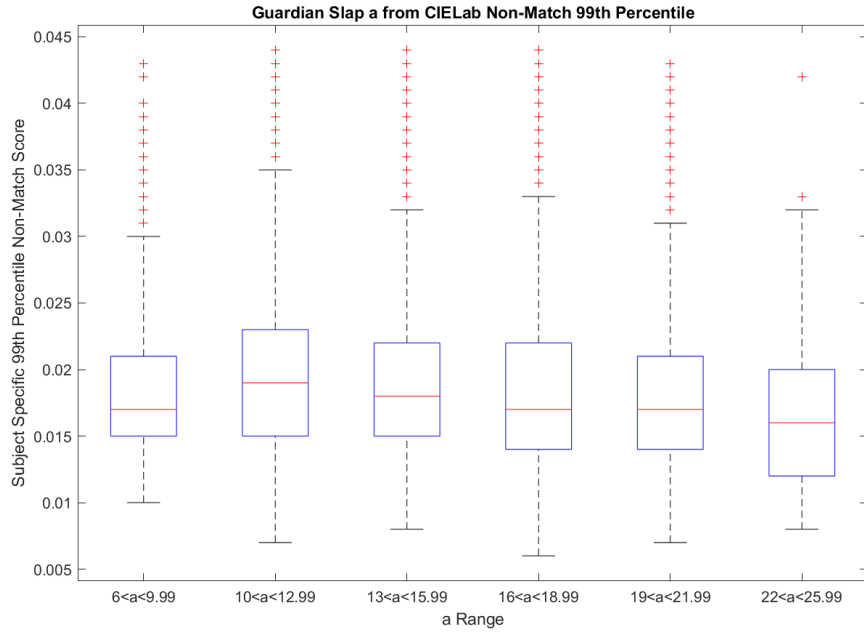


Figure 227 Innovatrics 99th non-match percentile binned red-green ranges Guardian Slap (Baseline).

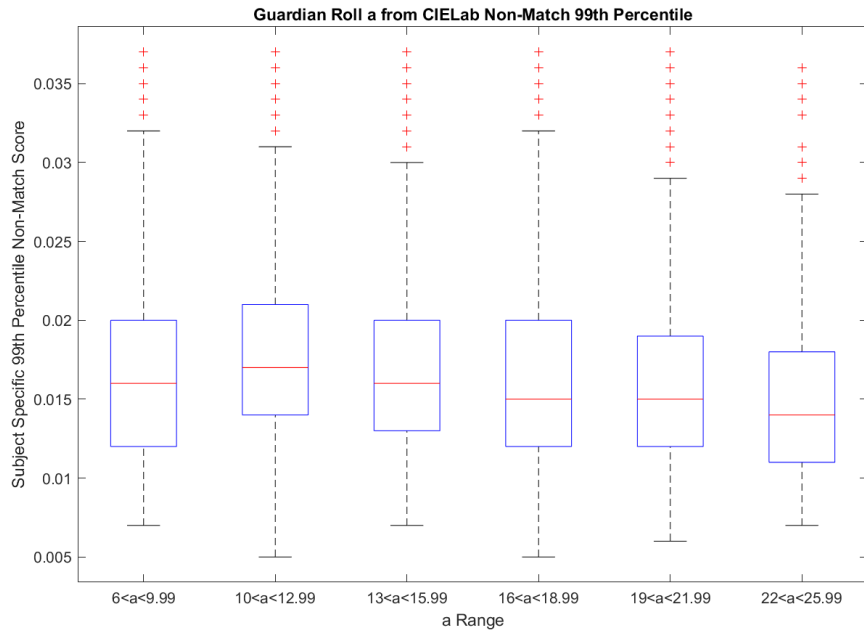


Figure 228 Innovatrics 99th non-match percentile binned red-green ranges Guardian Roll.

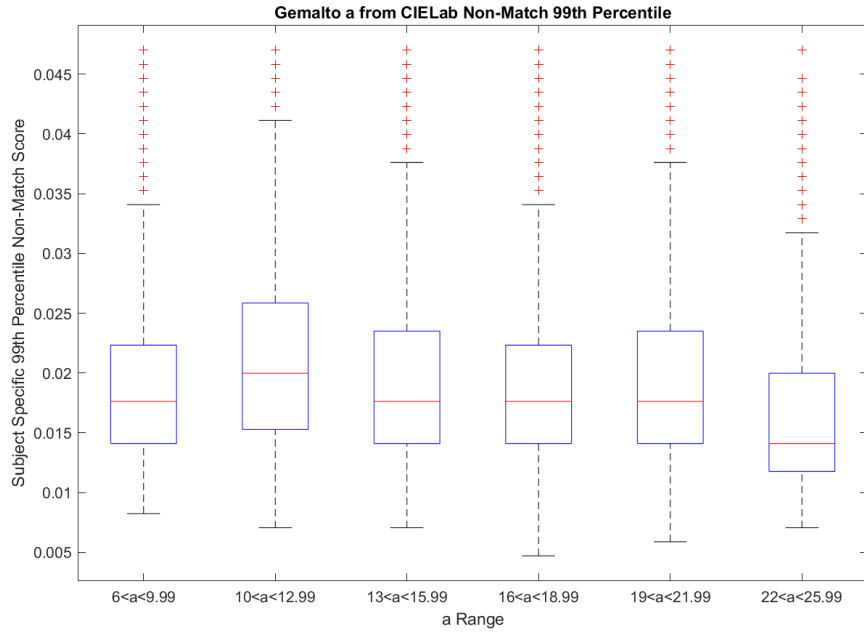


Figure 229 Innovatrics 99th non-match percentile binned red-green ranges Gemalto.

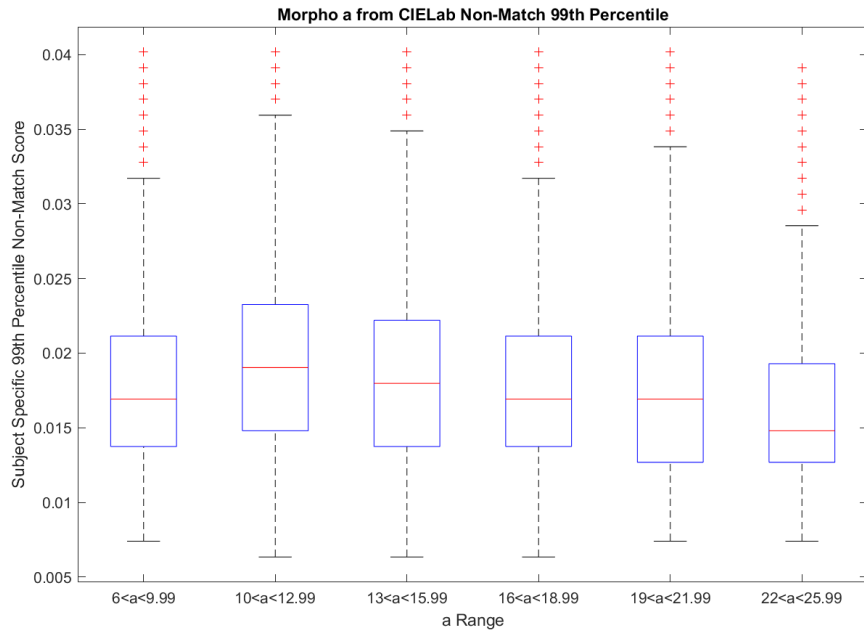


Figure 230 Innovatrics 99th non-match percentile binned red-green ranges MorphoWave.

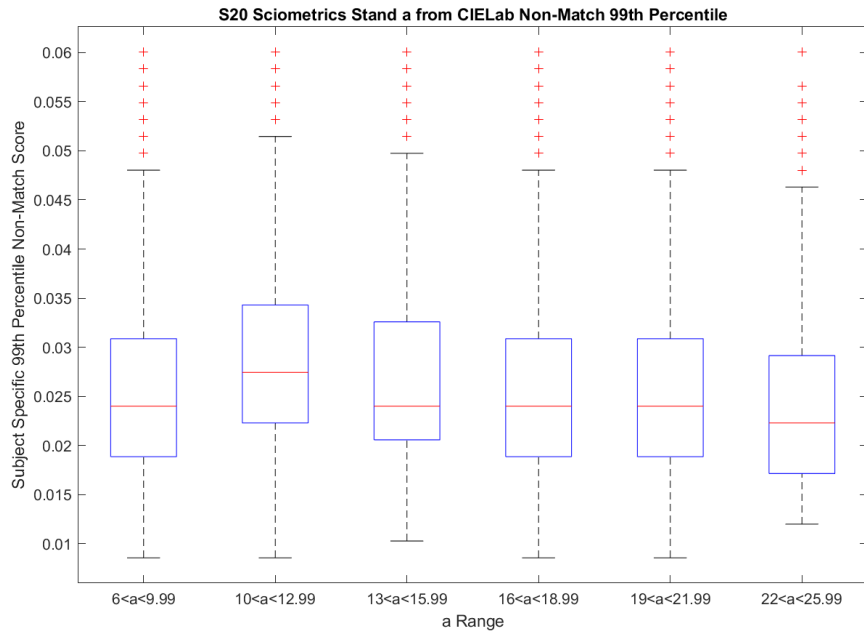


Figure 231 Innovatrics 99th non-match percentile binned red-green ranges S20 Sciometrics Stand.

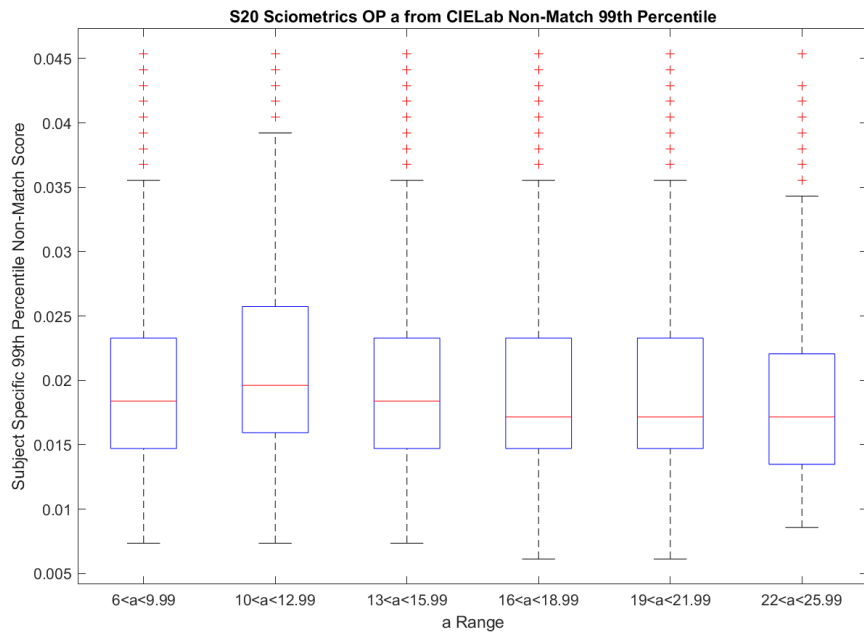


Figure 232 Innovatrics 99th non-match percentile binned red-green ranges S20 Sciometrics Op.

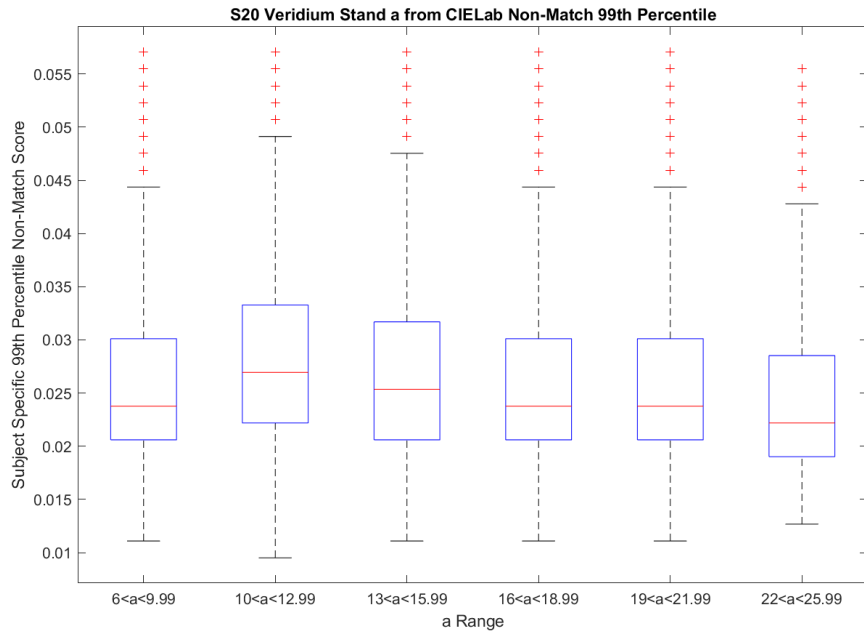


Figure 233 Innovatrics 99th non-match percentile binned red-green ranges S20 Veridium Stand.

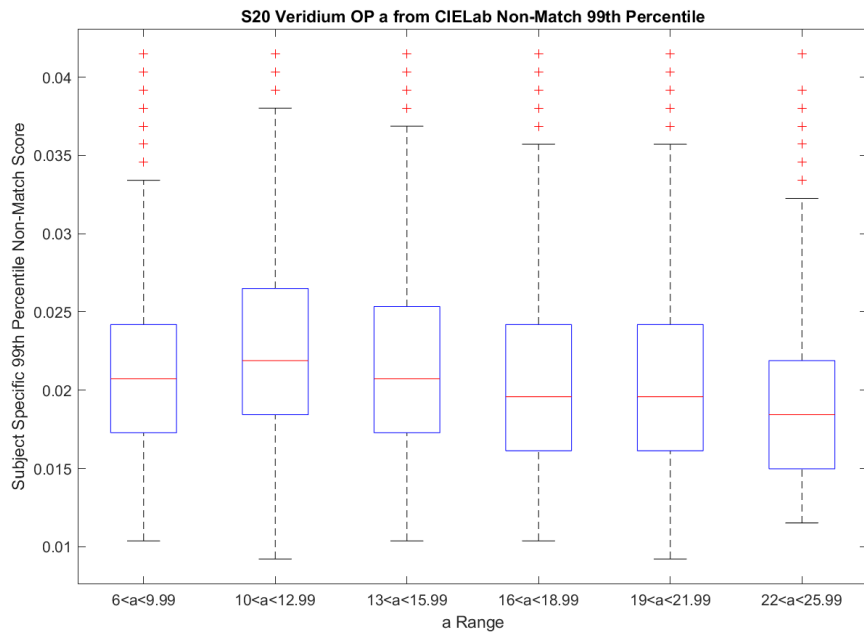


Figure 234 Innovatrics 99th non-match percentile binned red-green ranges S20 Veridium Op.



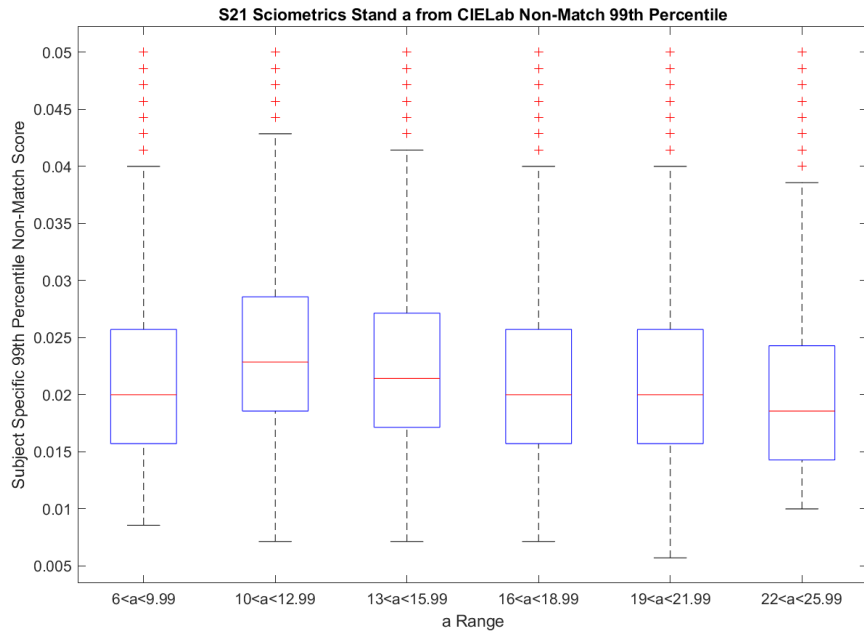


Figure 235 Innovatrics 99th non-match percentile binned red-green ranges S21 Sciometrics Stand.

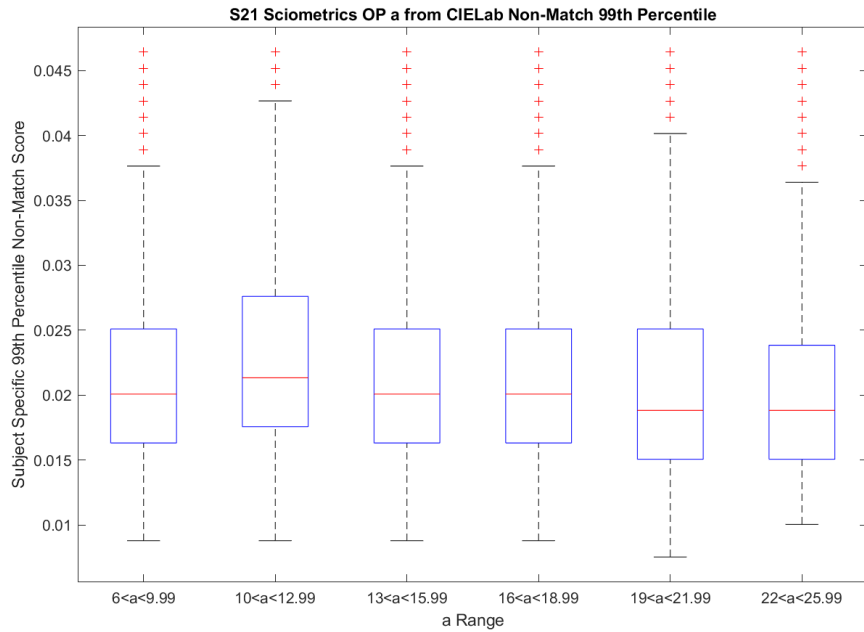


Figure 236 Innovatrics 99th non-match percentile binned red-green ranges S21 Sciometrics Op.

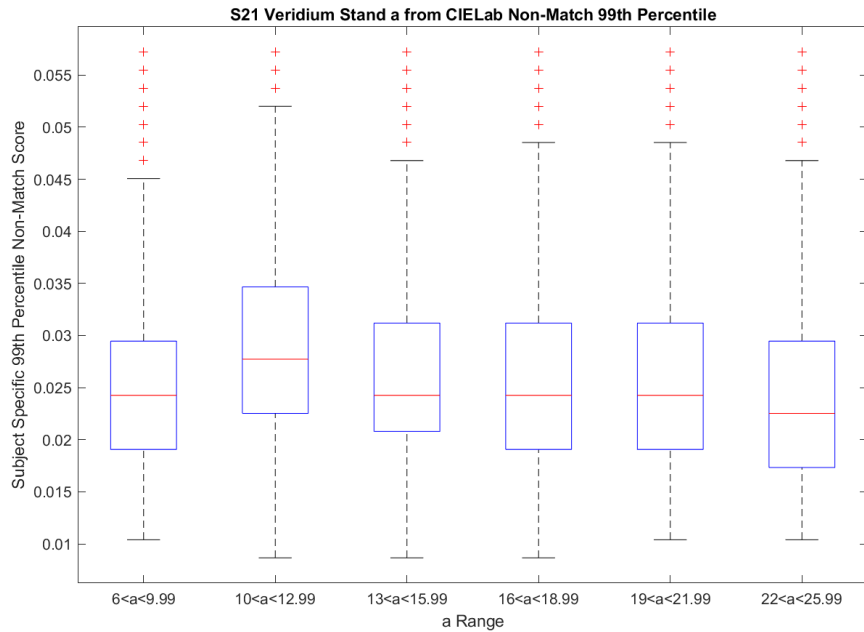


Figure 237 Innovatrics 99th non-match percentile binned red-green ranges S21 Veridium Stand.

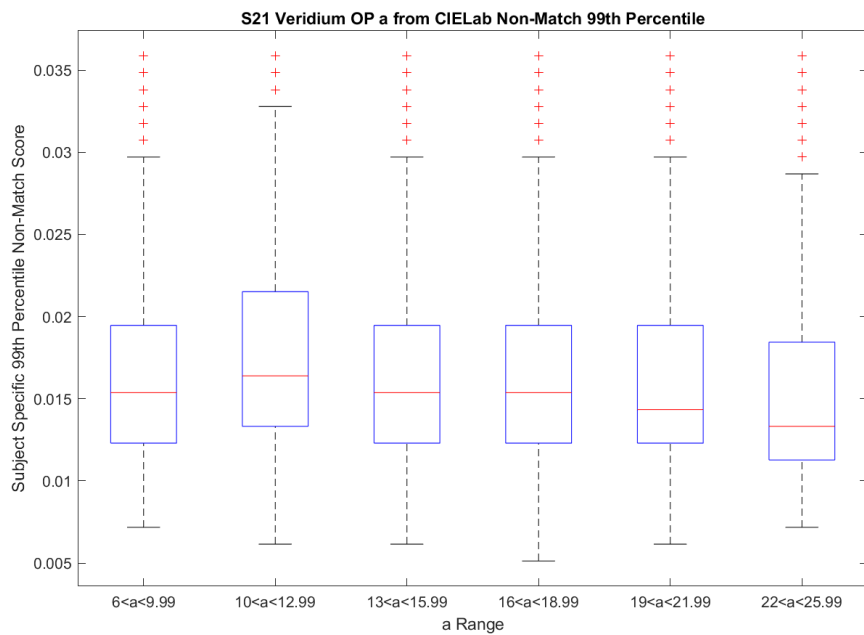


Figure 238 Innovatrics 99th non-match percentile binned red-green ranges S21 Veridium Op.

In Figure 226 through Figure 238, the Innovatrics 99<sup>th</sup> percentile non-match results are compared to the red-green spectrum ranges. A downward trend is seen in all experiments, similar to the

erythema experiments. The median and interquartile values reflect the trend, while the whiskers vary but generally also follow the downward trend. No other anomalies are visible for any individual experiments.

#### 4.2.7.4.2 VeriFinger

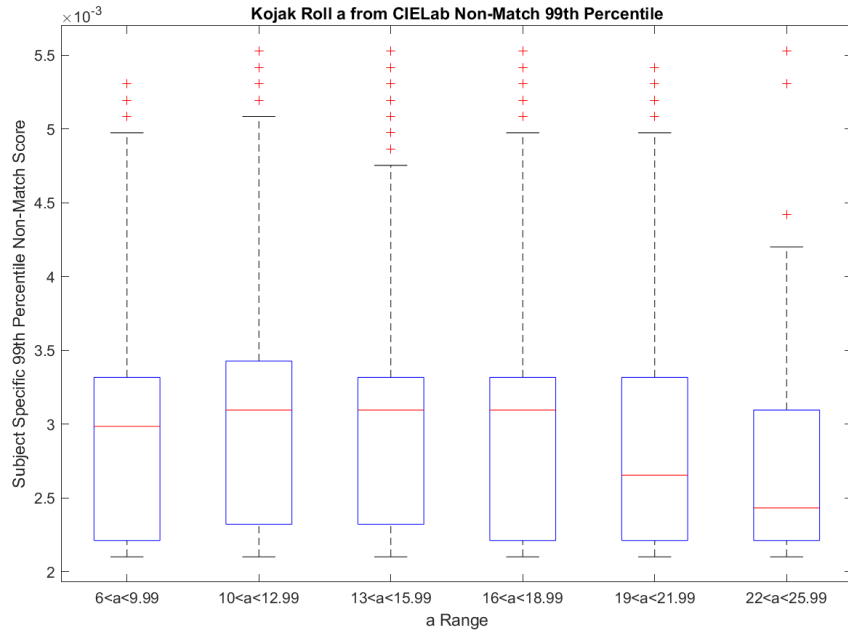


Figure 239 VeriFinger 99th non-match percentile binned red-green ranges Kojak Roll.

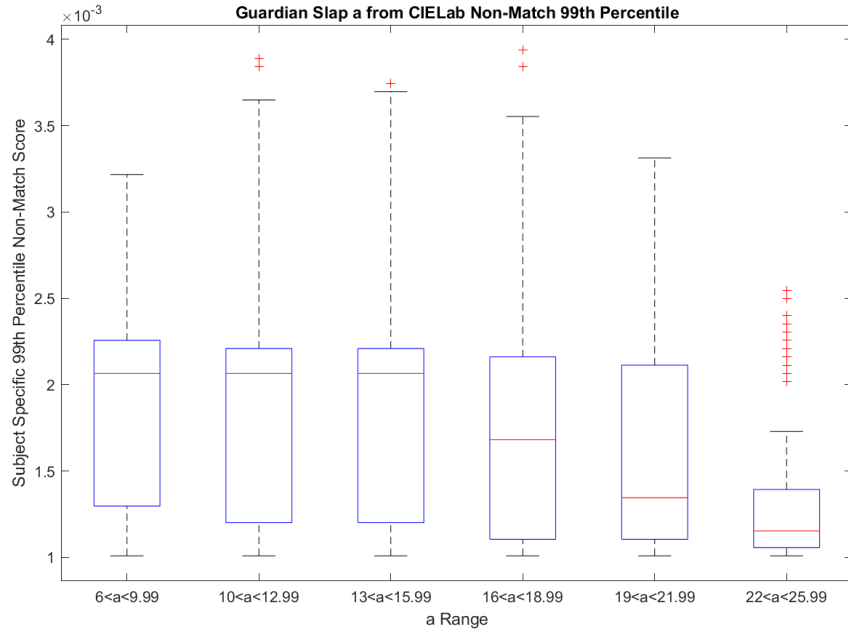


Figure 240 VeriFinger 99th non-match percentile binned red-green ranges Guardian Slap.

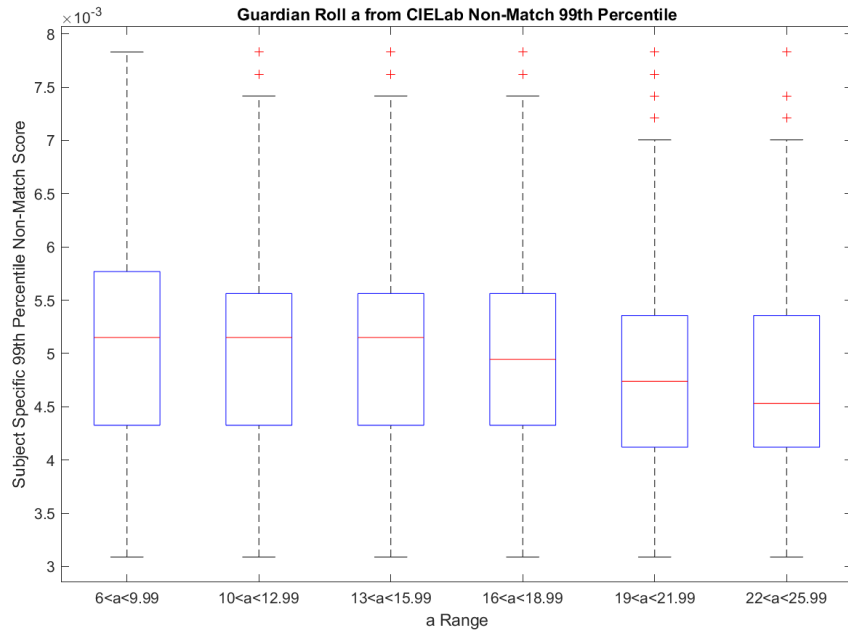


Figure 241 VeriFinger 99th non-match percentile binned red-green ranges Guardian Roll.

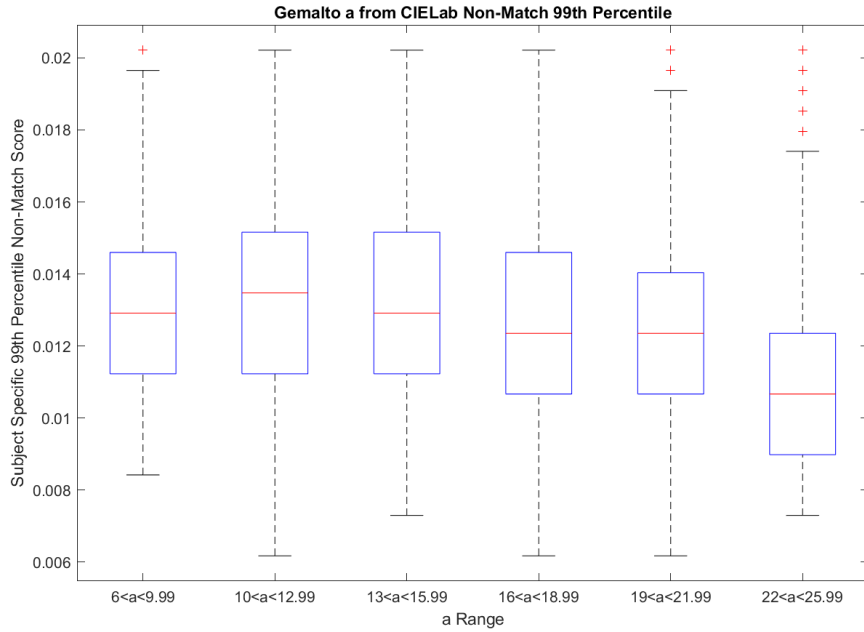


Figure 242 VeriFinger 99th non-match percentile binned red-green ranges Gemalto.

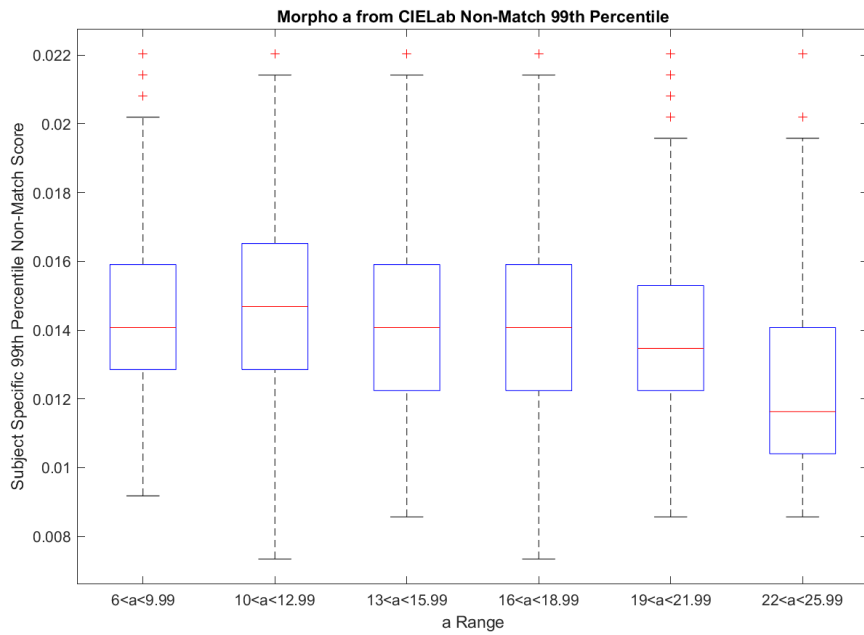


Figure 243 VeriFinger 99th non-match percentile binned red-green ranges MorphoWave.

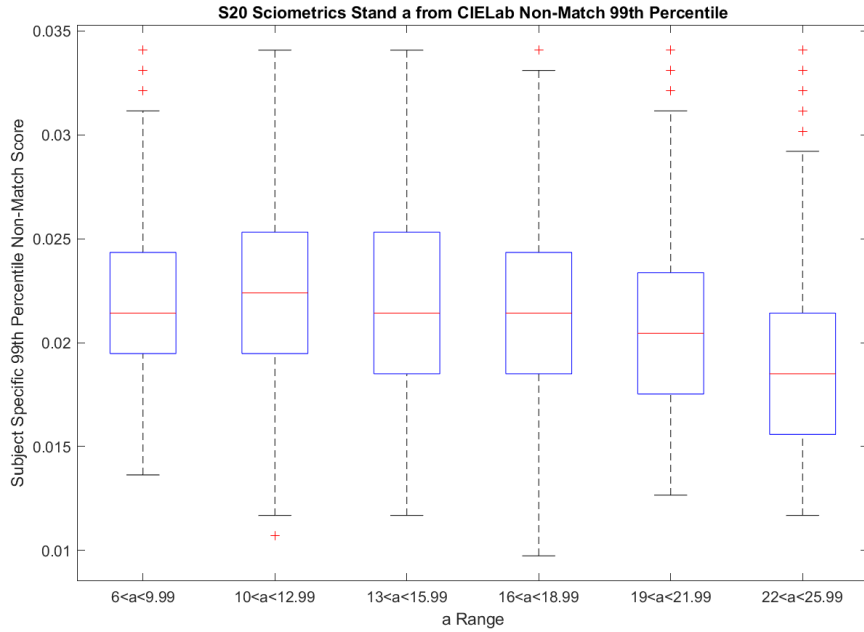


Figure 244 VeriFinger 99th non-match percentile binned red-green ranges S20 Sciometrics Stand.

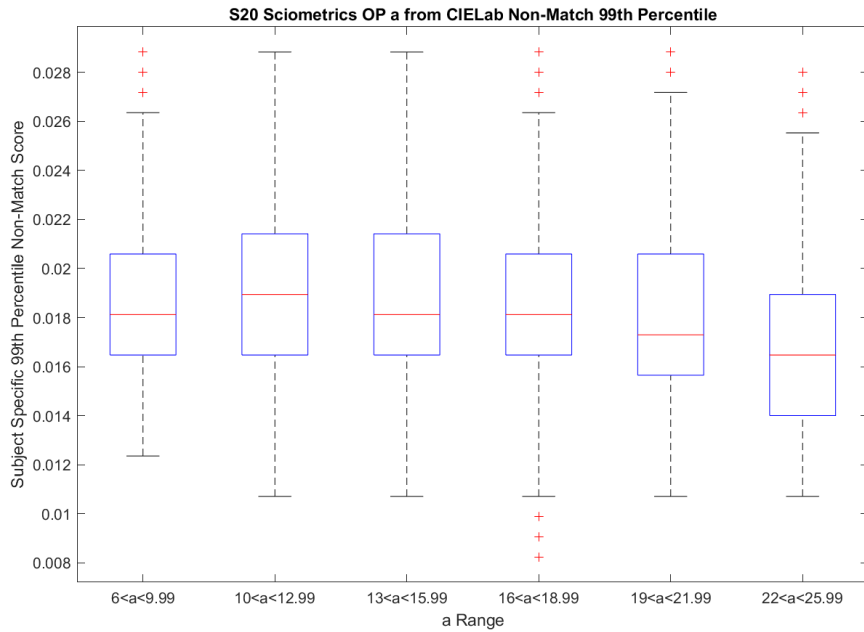


Figure 245 VeriFinger 99th non-match percentile binned red-green ranges S20 Sciometrics Op.

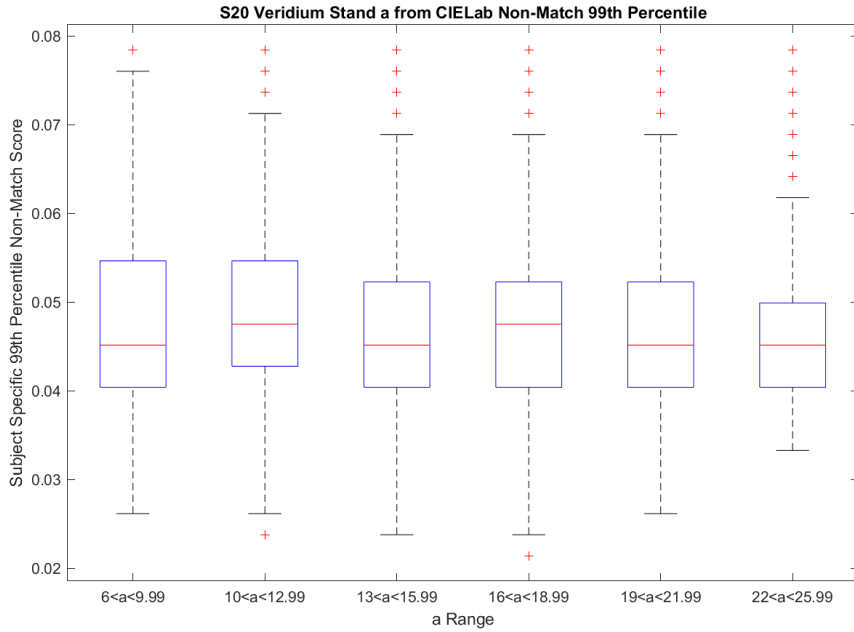


Figure 246 VeriFinger 99th non-match percentile binned red-green ranges S20 Veridium Stand.

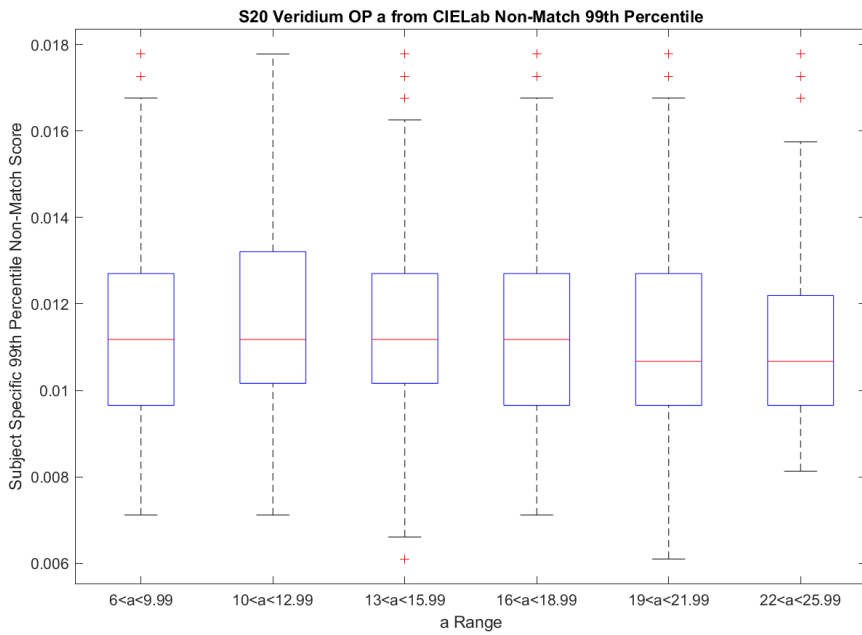


Figure 247 VeriFinger 99th non-match percentile binned red-green ranges S20 Veridium Op.

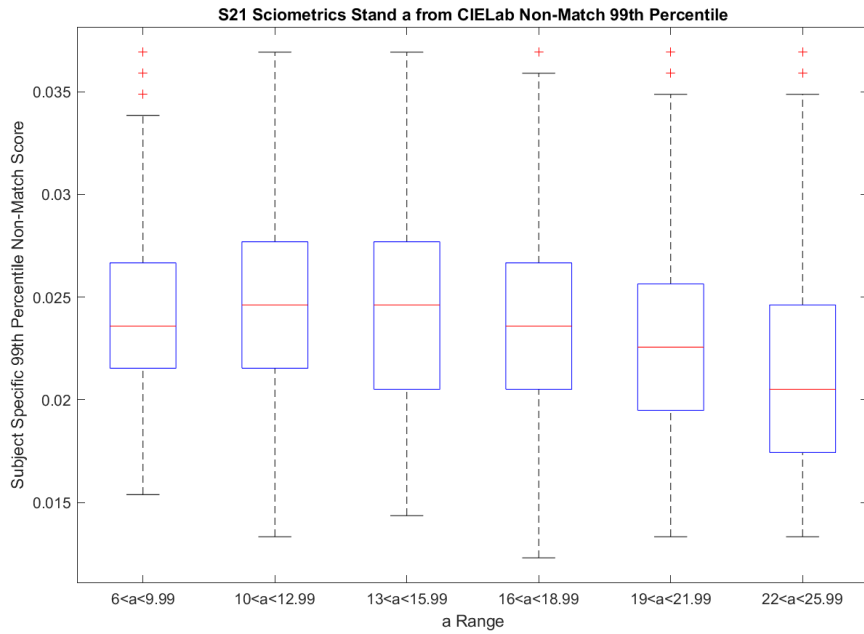


Figure 248 VeriFinger 99th non-match percentile binned red-green ranges S21 Sciometrics Stand.

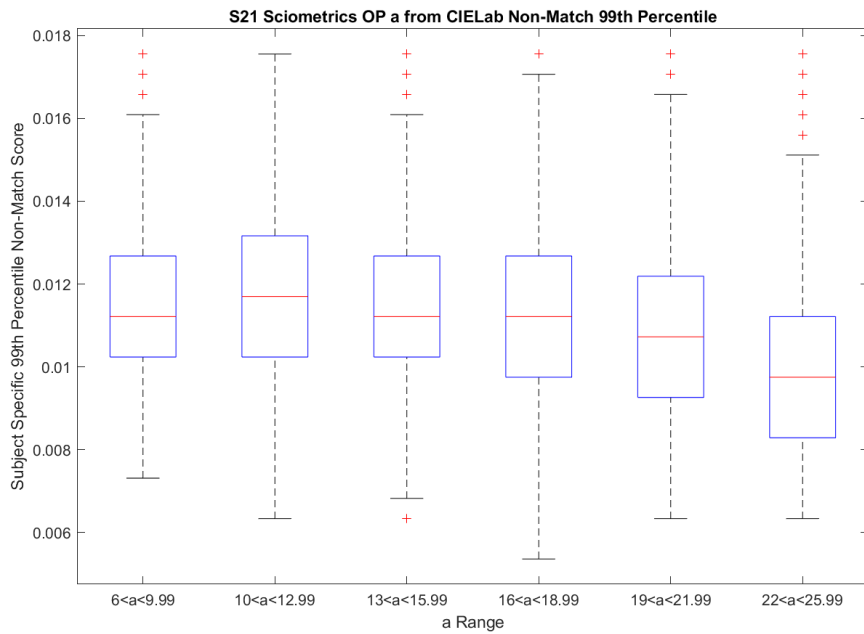


Figure 249 VeriFinger 99th non-match percentile binned red-green ranges S21 Sciometrics Op.



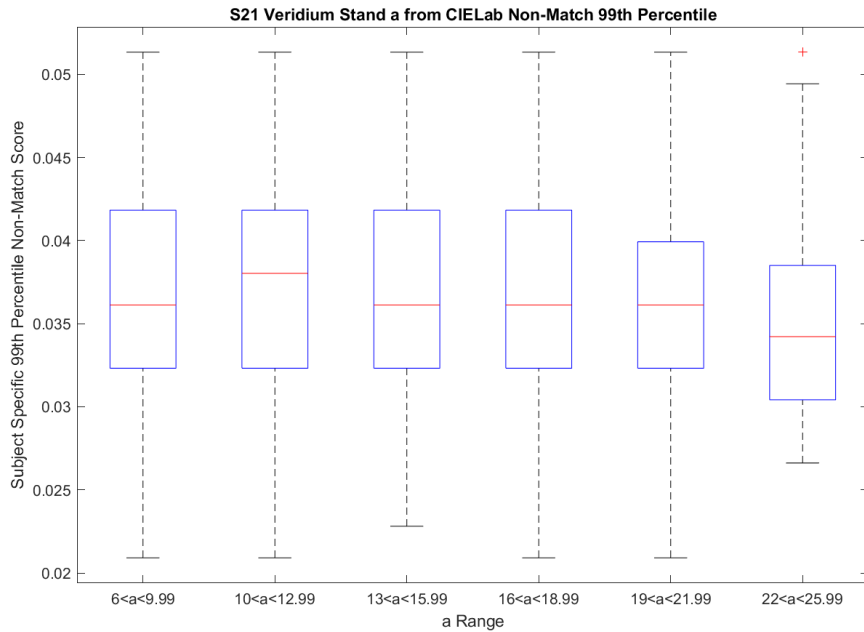


Figure 250 VeriFinger 99th non-match percentile binned red-green ranges S21 Veridium Stand.

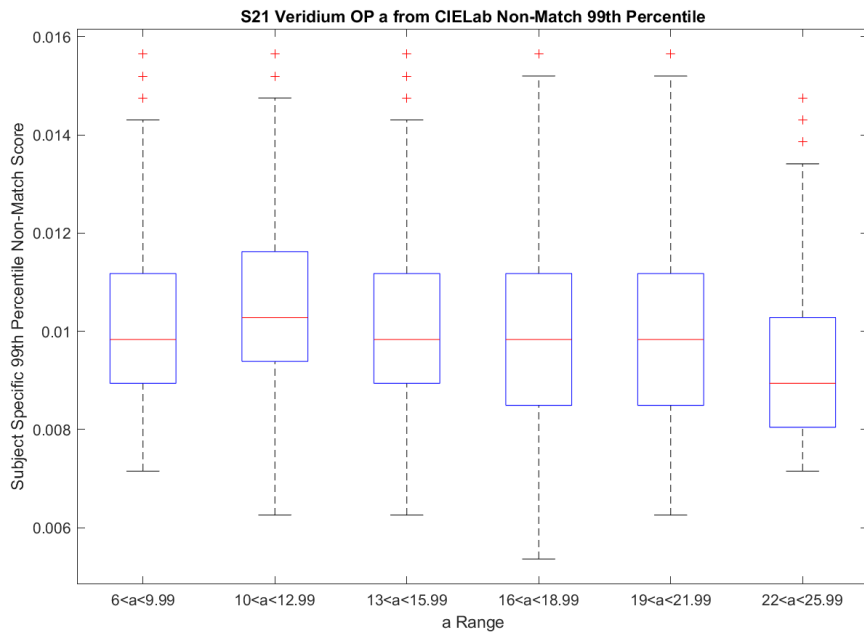


Figure 251 VeriFinger 99th non-match percentile binned red-green ranges S21 Veridium Op.

For the VeriFinger 99<sup>th</sup> percentile non-match red-green distributions, the Kojak Roll and Guardian Slap distributions (Figure 239 and Figure 240) both show a drop in median non-match

score in the upper red value bins with little to no change in the interquartile ranges except for the highest bin in the Guardian Slap distribution having a significant drop in the interquartile range. The Guardian Roll and contactless distributions (Figure 241 through Figure 243) and the Sciometrics distributions (Figure 244, Figure 245, Figure 248, and Figure 249) all show a trend of a decreased median non-match score and interquartile range as the red values increase. While the Veridium distributions (Figure 246, Figure 247, Figure 250, and Figure 251) show only slight deviations with no trend other than the highest bin for the S21 Veridium distributions having the lowest median non-match score. Figure 241

## 4.2.7.5 Blue-Yellow Spectrum $b^*$ measurement Distributions

### 4.2.7.5.1 Innovatrics

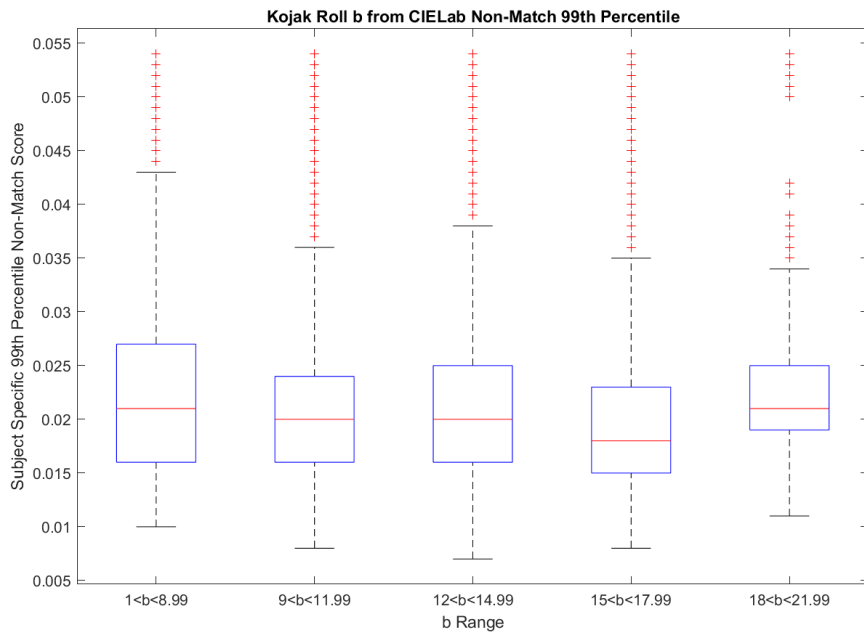


Figure 252 Innovatrics 99th non-match percentile binned blue-yellow ranges Kojak Roll.

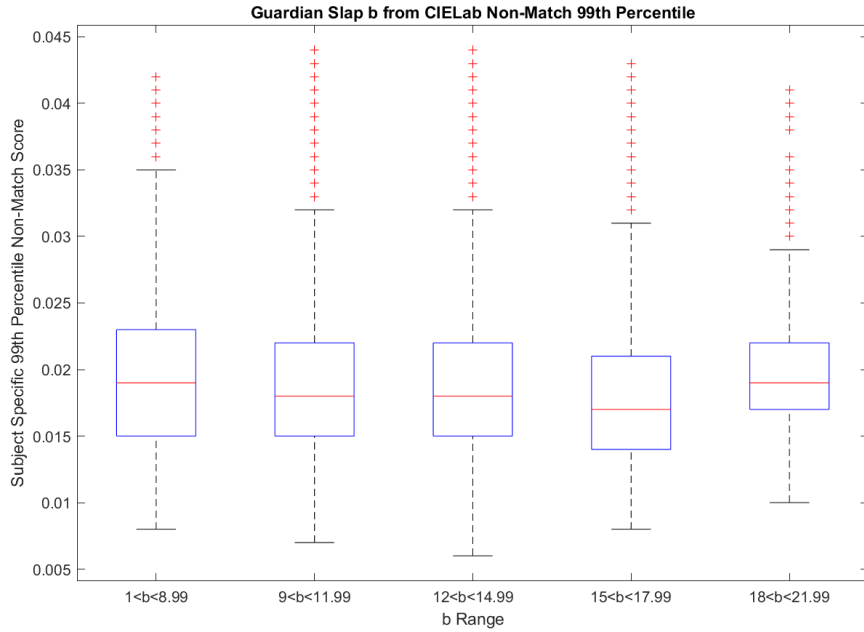


Figure 253 Innovatrics 99th non-match percentile binned blue-yellow ranges Guardian Slap (Baseline).

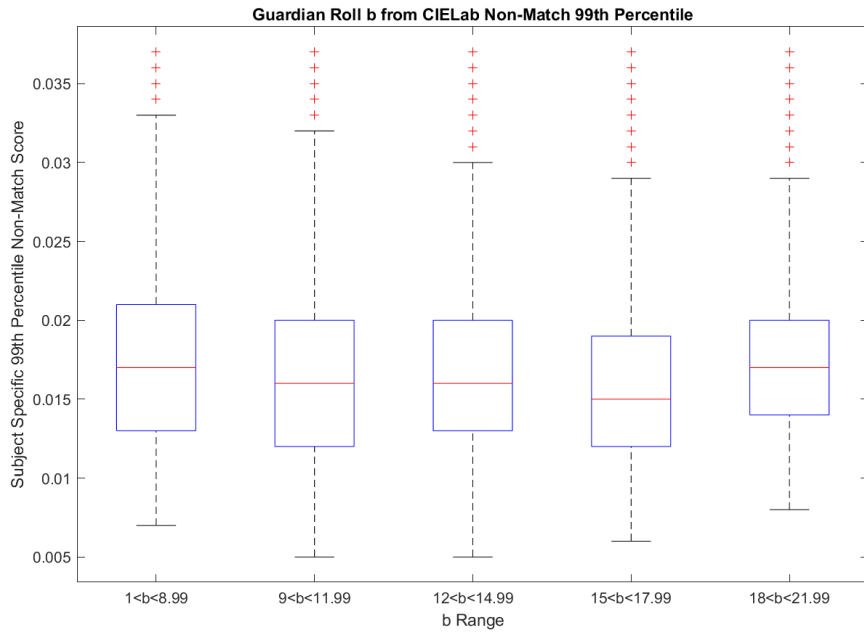


Figure 254 Innovatrics 99th non-match percentile binned blue-yellow ranges Guardian Roll

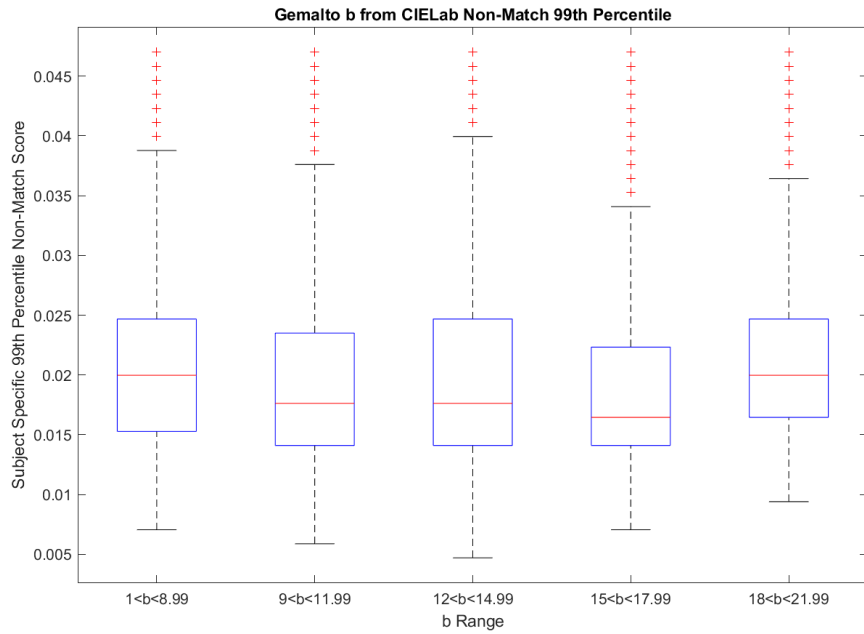


Figure 255 Innovatrics 99th non-match percentile binned blue-yellow ranges Gemalto.

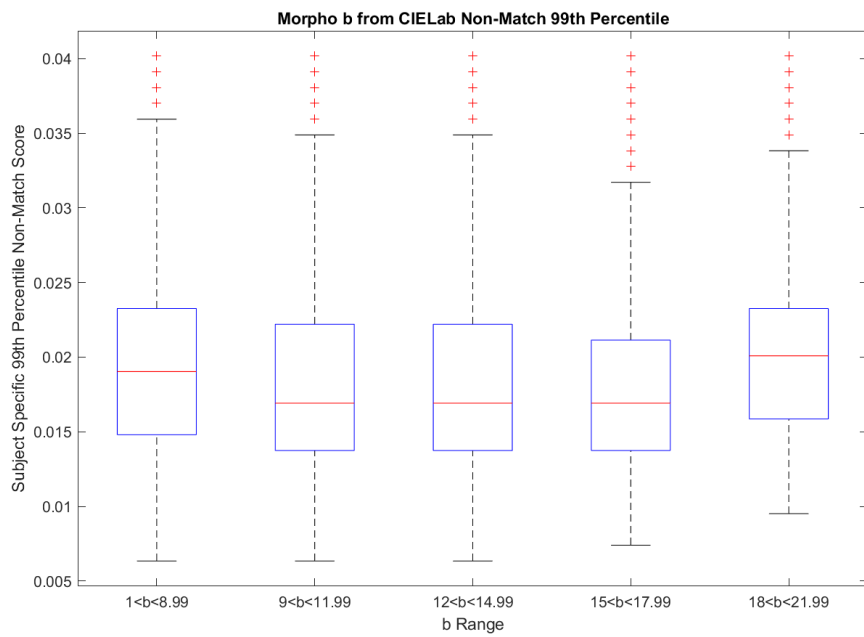


Figure 256 Innovatrics 99th non-match percentile binned blue-yellow ranges MorphoWave.

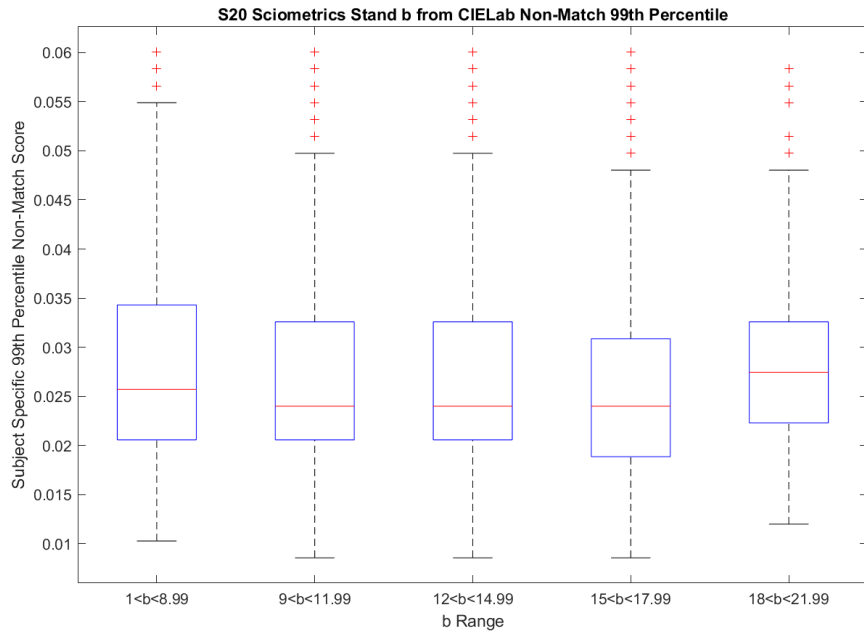


Figure 257 Innovatrics 99th non-match percentile binned blue-yellow ranges S20 Sciometrics Stand.

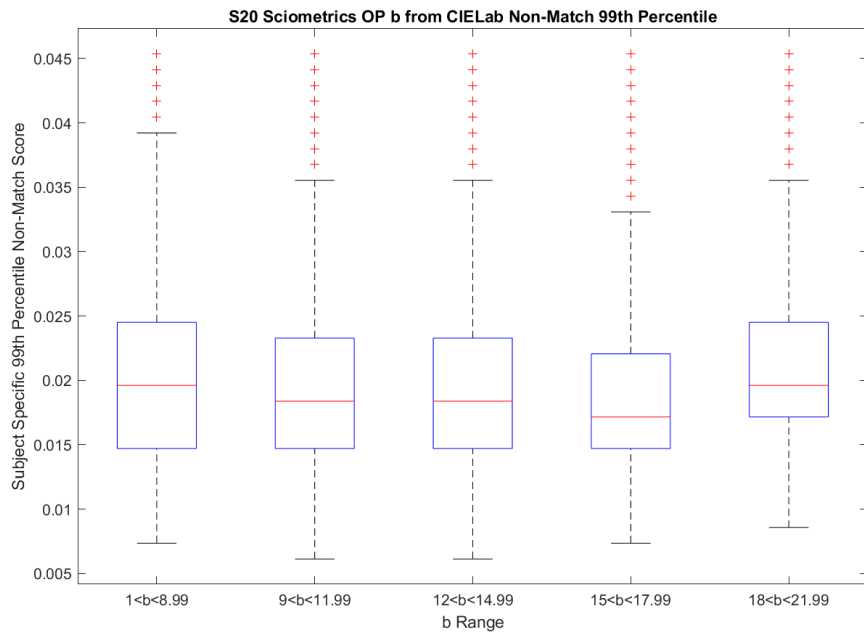


Figure 258 Innovatrics 99th non-match percentile binned blue-yellow ranges S20 Sciometrics Op.

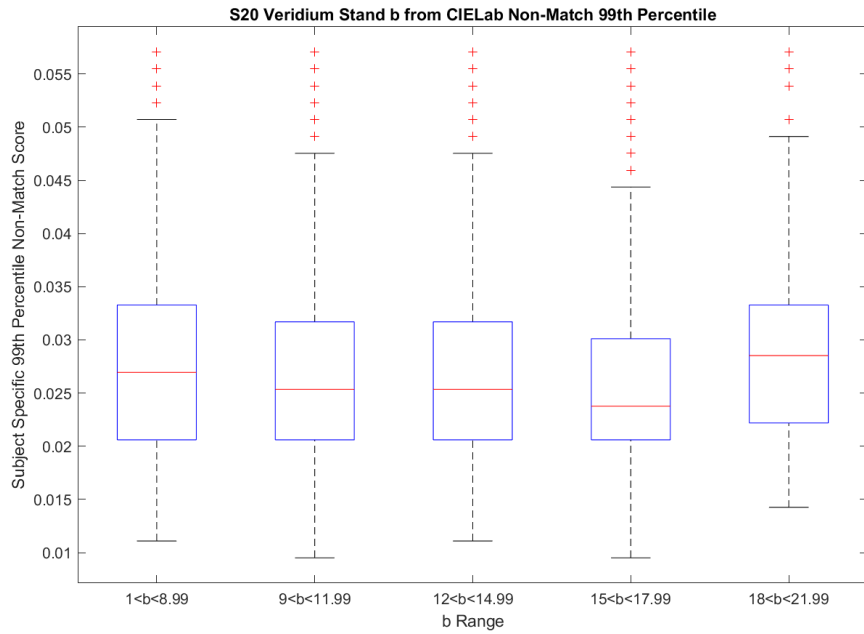


Figure 259 Innovatrics 99th non-match percentile binned blue-yellow ranges S20 Veridium Stand.

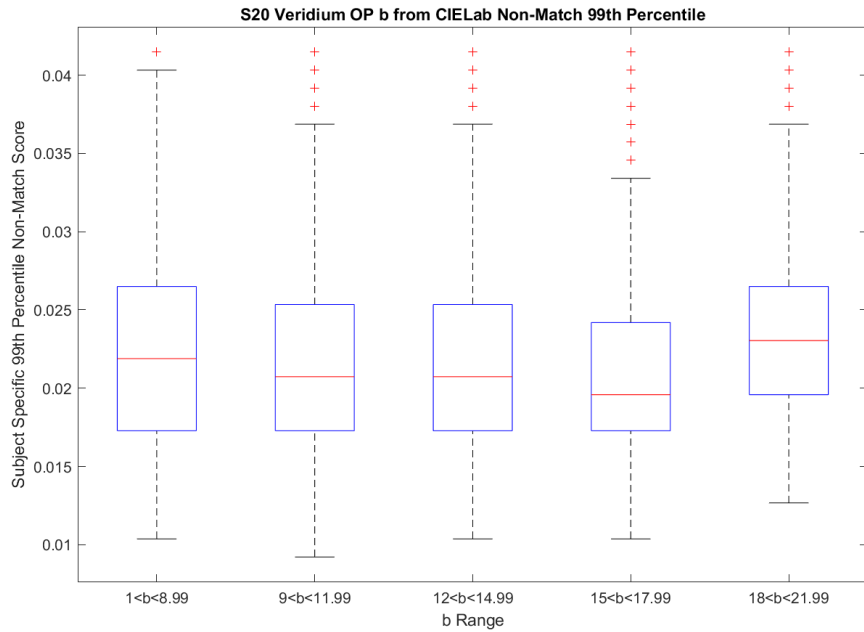


Figure 260 Innovatrics 99th non-match percentile binned blue-yellow ranges S20 Veridium Op.

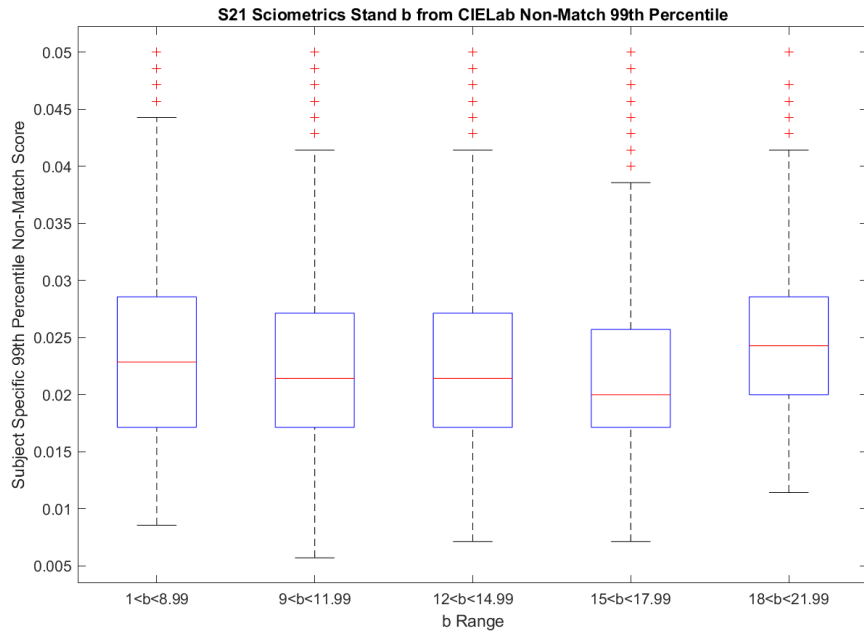


Figure 261 Innovatrics 99th non-match percentile binned blue-yellow ranges S21 Sciometrics Stand.

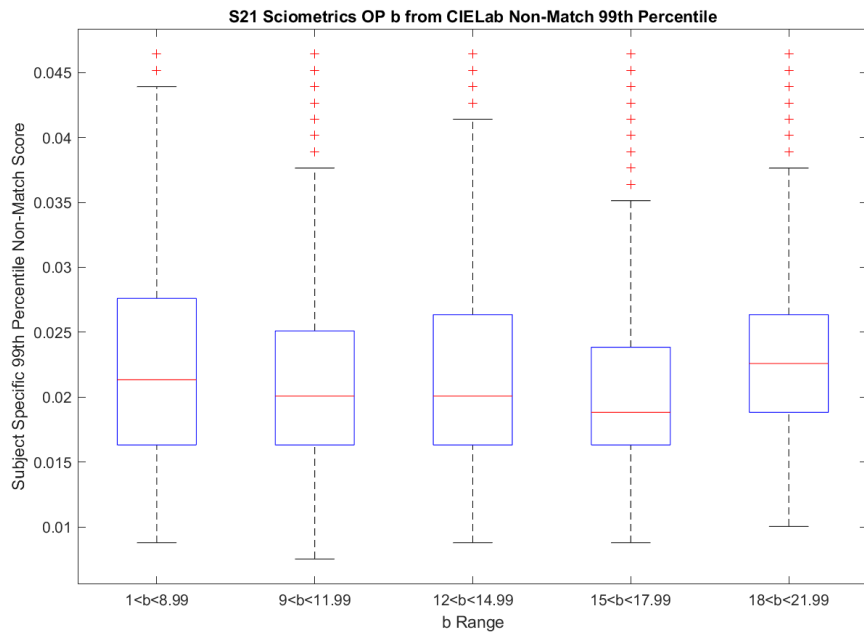


Figure 262 Innovatrics 99th non-match percentile binned blue-yellow ranges S21 Sciometrics Op.

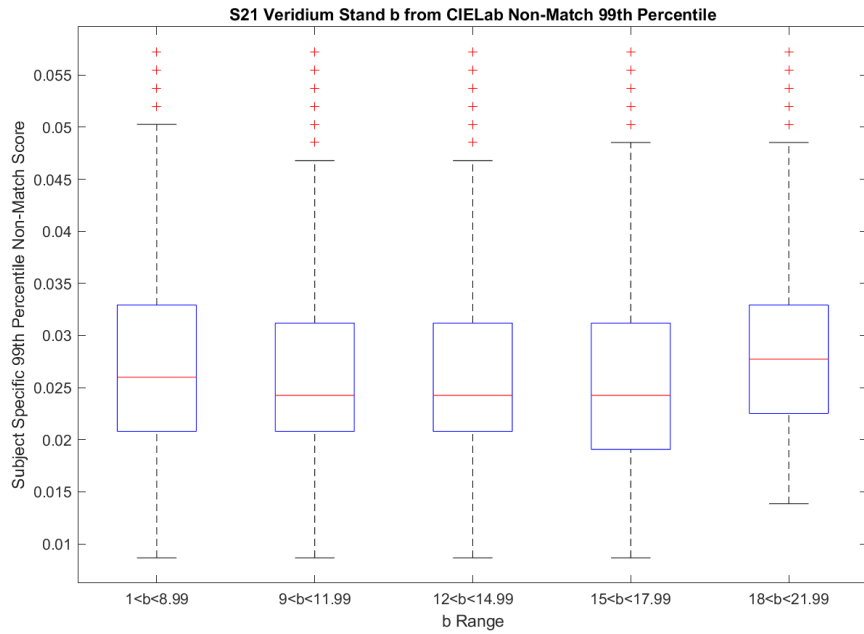


Figure 263 Innovatrics 99th non-match percentile binned blue-yellow ranges S21 Veridium Stand.

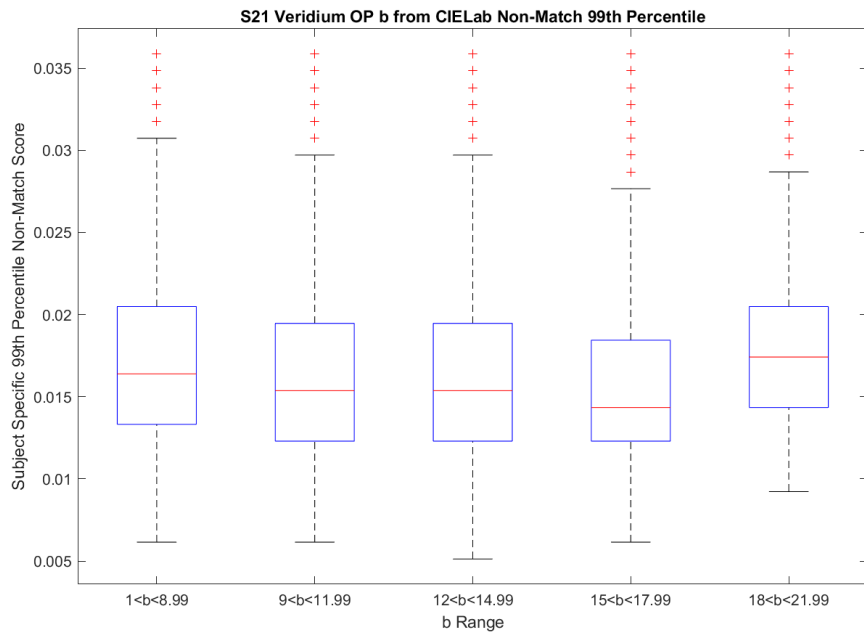


Figure 264 Innovatrics 99th non-match percentile binned blue-yellow ranges S21 Veridium Op.



Figure 252 through Figure 264 compare the Innovatrics 99th percentile non-match results to the blue-yellow spectrum ranges. The only notable information from the graphs is that the lowest and highest bin performed the worst for all experiments. The median value is always higher than the center three bin ranges. The second and third bins have the same median and interquartile range for all experiments, with the S21 Sciometrics Op in Figure 262 having the only exception. The fourth bin for each experiment is either the same as the second and third or is slightly lower. There is no trend in what experiments have a lower fourth bin, with occurrences appearing in the contact, contactless, and cell phone experiments.

#### 4.2.7.5.2 VeriFinger

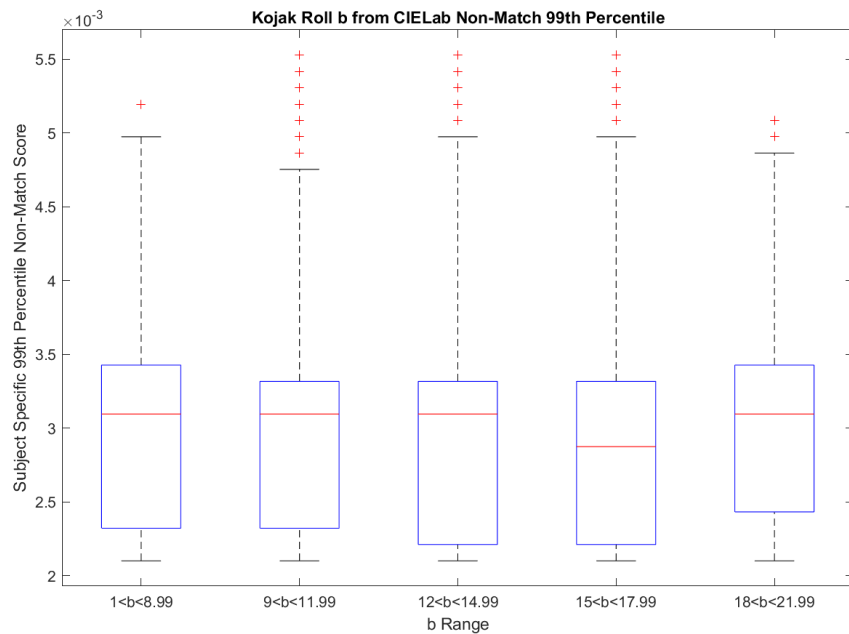


Figure 265 VeriFinger 99th non-match percentile binned blue-yellow ranges Kojak Roll.

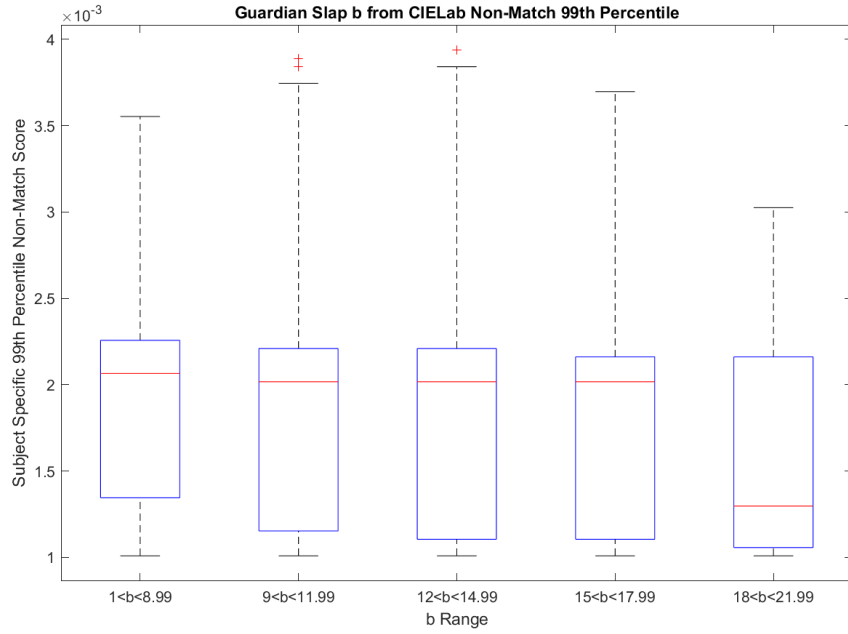


Figure 266 VeriFinger 99th non-match percentile binned blue-yellow ranges Guardian Slap.

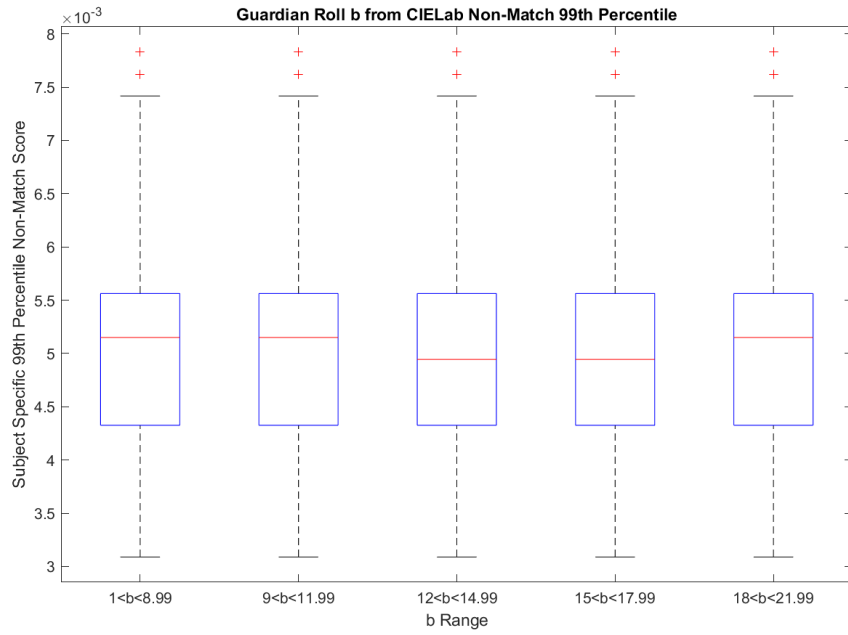


Figure 267 VeriFinger 99th non-match percentile binned blue-yellow ranges Guardian Roll.

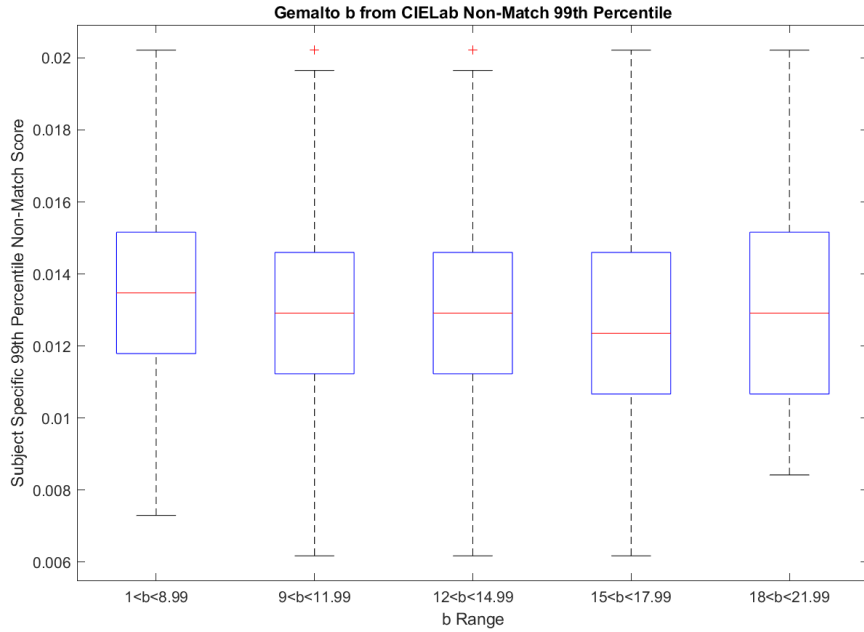


Figure 268 VeriFinger 99th non-match percentile binned blue-yellow ranges Gemalto.

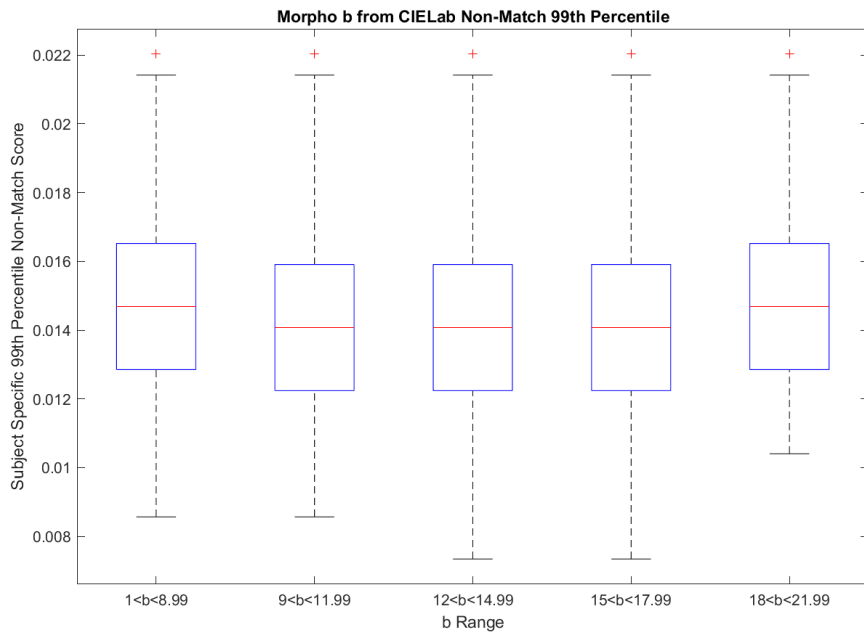


Figure 269 VeriFinger 99th non-match percentile binned blue-yellow ranges MorphoWave.

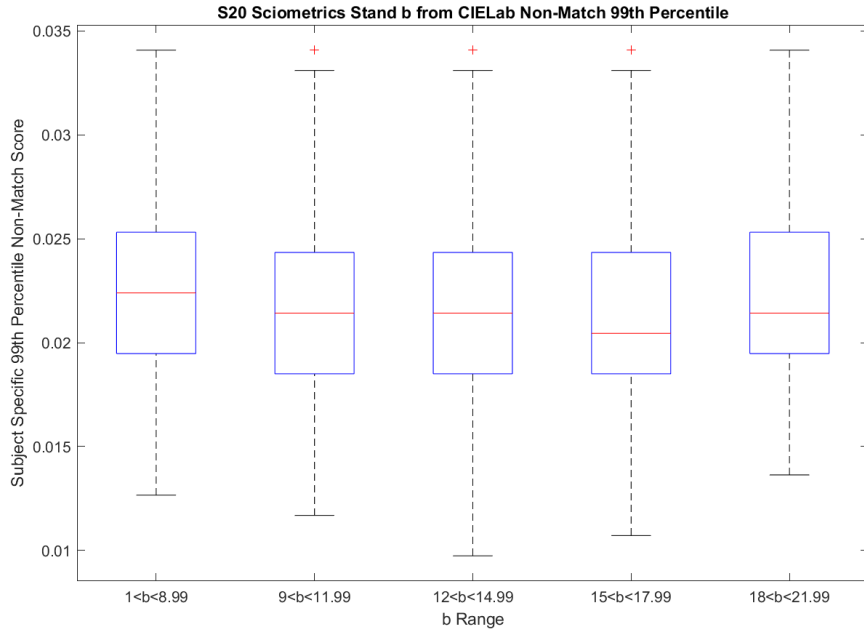


Figure 270 VeriFinger 99th non-match percentile binned blue-yellow ranges S20 Sciometrics Stand.

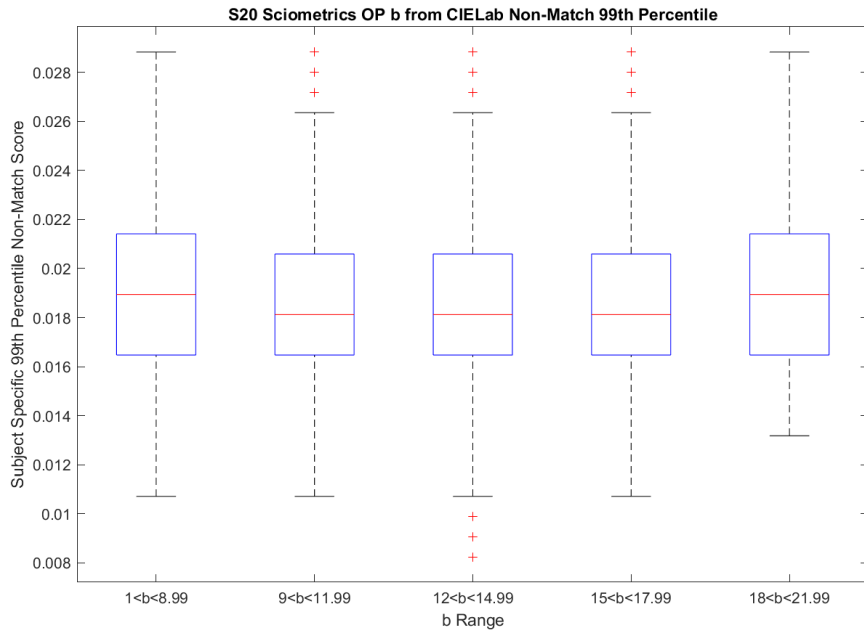


Figure 271 VeriFinger 99th non-match percentile binned blue-yellow ranges S20 Sciometrics Op.

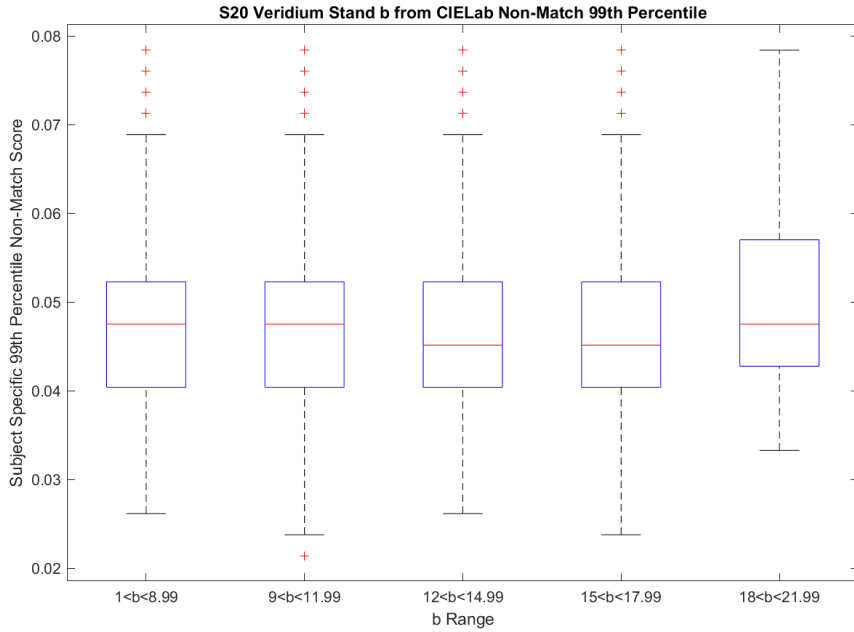


Figure 272 VeriFinger 99th non-match percentile binned blue-yellow ranges S20 Veridium Stand.

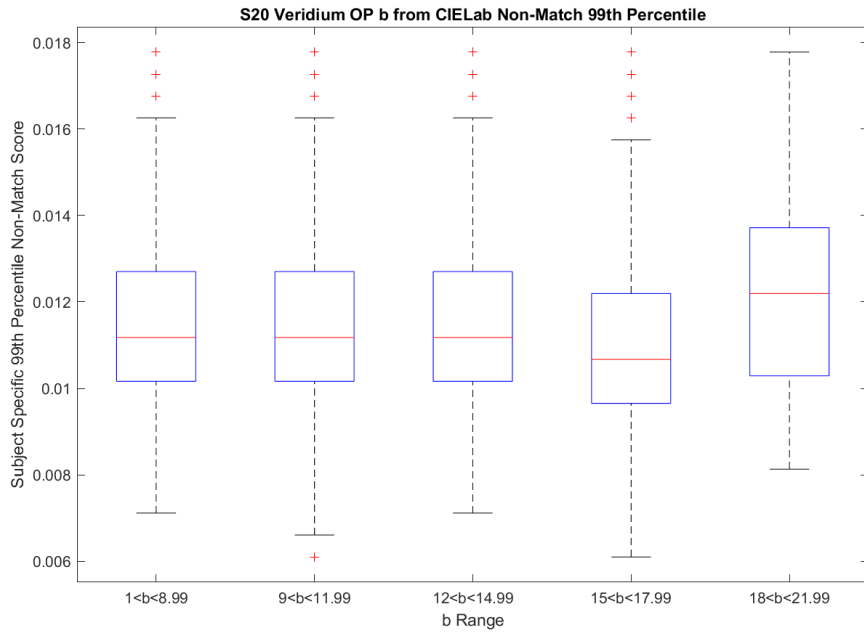


Figure 273 VeriFinger 99th non-match percentile binned blue-yellow ranges S20 Veridium Op.

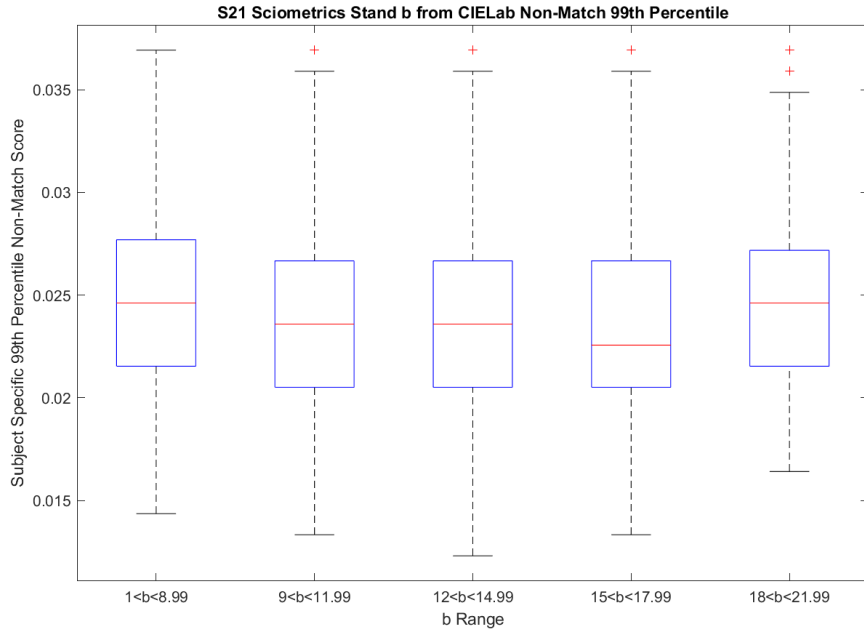


Figure 274 VeriFinger 99th non-match percentile binned blue-yellow ranges S21 Sciometrics Stand.

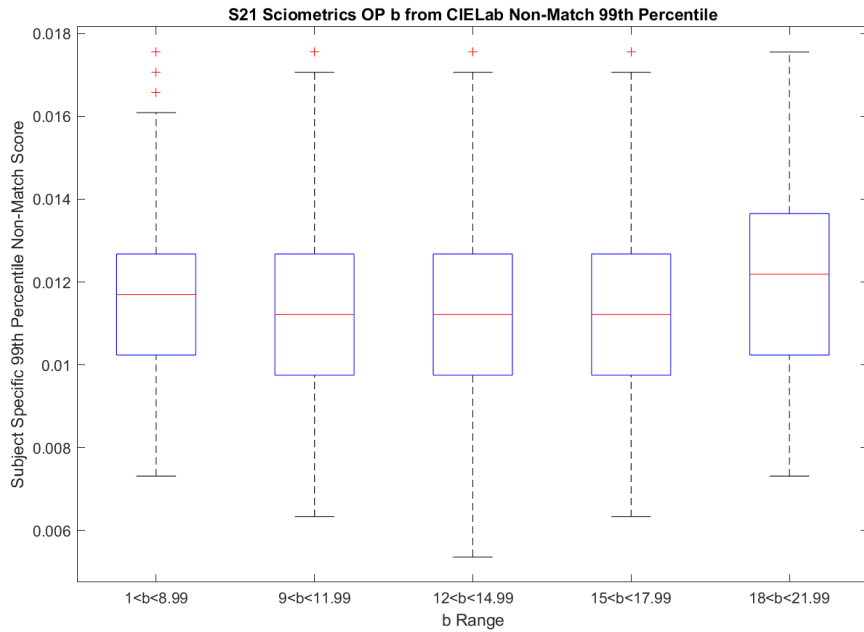


Figure 275 VeriFinger 99th non-match percentile binned blue-yellow ranges S21 Sciometrics Op.

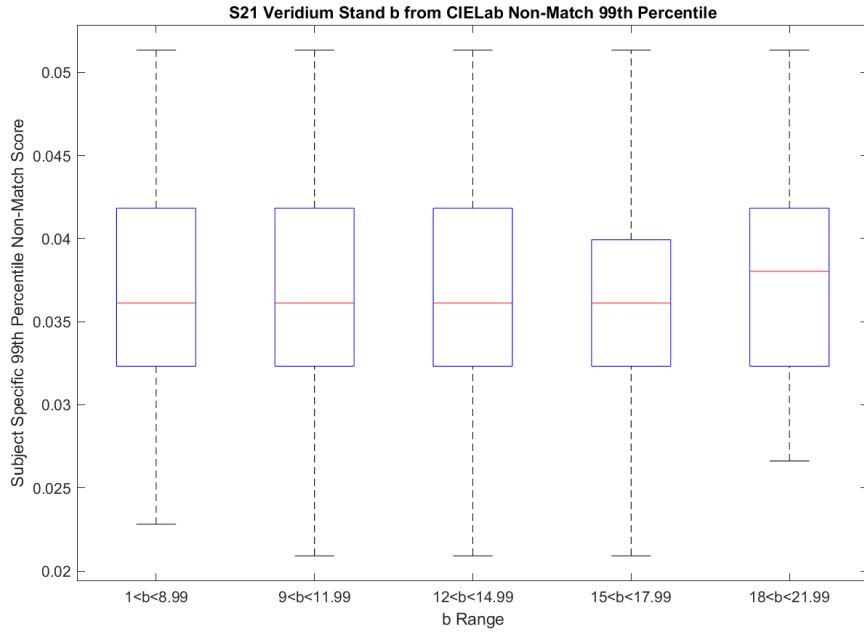


Figure 276 VeriFinger 99th non-match percentile binned blue-yellow ranges S21 Veridium Stand.

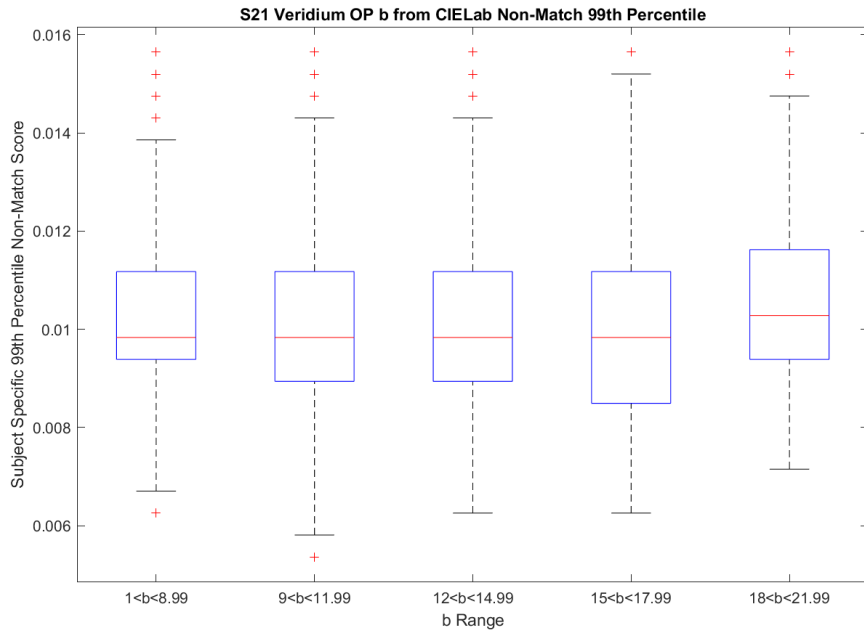


Figure 277 VeriFinger 99th non-match percentile binned blue-yellow ranges S21 Veridium Op.

In the 99<sup>th</sup> percentile non-match blue-yellow contact distributions, only the Guardian Slap distribution in Figure 266 has a bin that significantly deviates. The highest bin has a lower median non-match score though all the interquartile ranges are similar. The Kojak Roll (Figure 265) and Guardian Roll (Figure 267) have no significant distribution deviations or trends. The Gemalto distribution in Figure 268 has a slightly higher median and interquartile range for the lowest bin. The MorphoWave distribution in Figure 269 has a higher median and interquartile range for the lowest and highest bin, with the same seen in each Sciometrics distribution in Figure 270, Figure 271, Figure 274, and Figure 275. The S20 Veridium Stand distribution (Figure 272) has a lower median for the third and fourth bins with a higher interquartile range in the fifth bin. The rest of the Veridium distributions shown in Figure 273, Figure 276, and Figure 277 all have a higher median non-match score in the highest bin.



# Chapter 5: Summary and Conclusion

## 5.1 Contact Fingerprints

This thesis explored the current interoperability and viability of advancing contactless fingerprint capture devices and cellphone fingerprint capture applications. The evaluation of the overall interoperability was performed on three separate fingerprint matchers. For the contact experiments, aside from the baseline performing the best for all three matchers, the Crossmatch Guardian Roll experiment for Innovatrics performed almost as well as the baseline Crossmatch Guardian Slap vs. Kojak Slap with an AUC of 0.99373, which is less than a thousandth lower than the baseline at an AUC value of 0.99398. The Kojak Roll experiment always performed the worst of the contact experiments across all three matchers for both AUC and EER. The Crossmatch Guardian Roll experiment performed second of the three, with the margin of difference becoming wider in the VeriFinger Matching experiment and even wider in the Bozorth3 experiment. The interoperability between the Kojak Roll and Slap fingerprints is lower than that of the Crossmatch Guardian. Additionally, the quality score distributions, when compared to the match score, followed the expected trend for all contact fingerprint sets; as the quality score increase, so does the median match score.

## 5.2 Contactless Fingerprints

The contactless fingerprint sets had two very different behaviors. The MorphoWave performed very well with an AUC of 0.99337 for the Innovatrics matcher and 0.97872 for the VeriFinger matcher, respectively, and even had the highest AUC of all Bozorth3 matching experiments at 0.91062. The MorphoWave uses structured light for fingerprint acquisition, and at

least in this model of the morpho, there is high interoperability between the MorphoWave and the contact gallery. When the Morpho images were processed through the NFIQ2 software, many images were given very low-quality scores that were outliers in the Genuine match comparison showing that the NFIQ2 software assigned very low scores to fingerprints that otherwise matched very well. On the contrary, the Cogent Gemalto had a much lower performance than the MorphoWave, though it was fourth overall for AUC values with a high of 0.97004 for Innovatrics and a low of 0.83604 for Bozorth3. Only VeriFinger had the Gemalto in fifth place behind the S21 Sciometrics Operational setting by less than a thousandth AUC though the EER for the Gemalto was better by a slim margin. When looking at the quality score distribution for the Gemalto, the expected gradual increase of match scores with the quality score is apparent, though there are many outliers towards the center of the distribution, signaling that the NFIQ2 software is assigning suppressed scores that follow the expected trend but are lower than the contact fingerprints.

## 5.3 Cellphone Fingerprints

The performance of each of the cellphone applications follows a distinct pattern for the Innovatrics and VeriFinger results. The S21 model performs better than the equivalent matches on the S20. The operational setting always performed better than the controlled setting when the expected behavior suggests the stand or controlled setting would have better quality images and better performance. The NFIQ2 quality score distribution shows the same trend, with operational quality scores having a higher frequency of higher-quality images. Lastly, the Sciometrics phone application consistently outperformed the Veridium application for both AUC and EER, with some Veridium AUC values dropping into the 0.8 range. The Stand setting imposed the most significant performance impact on the Veridium application, with the lowest drop and AUC

being more than 0.06 for the S20 Innovatrics experiments. The most significant drop was 0.16 in the S20 VeriFinger experiment. The Bozorth3 results for the cellphone matching could have been better, with results only marginally better than a coin flip. When observing the quality vs. match score distribution, each cellphone fingerprint set follows the same pattern as the Gemalto quality vs. match score distribution for the Innovatrics results. However, the pattern is more compressed across the different distributions showing that the NFIQ2 software underscores the cellphone fingerprints even more than the Gemalto fingerprints. The Bozorth3 results are mostly noise, with little helpful information when observing the cellphone experiments. However, the Bozorth3 matcher is the oldest of the three software and does not see active development, unlike the Innovatrics and VeriFinger software which has continued development. The Bozorth3 software was not designed to be used with cellphone fingerprints, so the low performance is within expectation.

## 5.4 Melanin Analysis

For the Innovatrics experiments, the melanin distributions for all fingerprint sets had a similar pattern with no individual set showing any deviations, which could represent a bias existing in that bin's range. Instead, as discussed in the results, the lowest melanin bin tended to have a higher median non-match score. The lower edge of the melanin range contains the least number of samples, so the deviation is probably from the smaller sampling not showing an accurate representation of what the bin should be. Though the melanin bin for the range 34-39.99 consistently trended lower, the adjacent bin on either side had a similar median or higher non-match score. These center bins contain the largest number of samples so that the lower value could be a characteristic of the demographics of the dataset, or when the matchers were being designed and tested, these melanin ranges were oversampled and therefore showed a dip in the

non-match score for this specific range rather than a general trend in the ability for the Innovatrics matcher to match better or worse based on melanin.

In the VeriFinger melanin distributions, no consistent trend was seen across all experiments. Instead, the Guardian Slap distribution had bins that appeared significantly different from the other bins. The first and fifth bins had tiny interquartile ranges compared to the other bins, and the fifth bin is the only bin with an outlier to appear lower than the median. The VeriFinger software, when enrolling, will reject certain fingerprints that do not meet unknown criteria. The rejected prints could be concentrated in the two bins affected by the distribution leading to fewer samples for the two bins. The same is seen in the second bin of the Guardian Slap's erythema distribution. The only other trends seen in the VeriFinger melanin distributions were the Gemalto and MorphoWave having a slight trend with lower melanin bins having a higher median non-match score than higher melanin bins suggesting a specific issue with only the contactless fingerprint sets.

## 5.5 Lightness Analysis

While lightness could be compared to melanin with higher light values comparable to pale skin and low light values to darker melanin-rich skin, the light distribution showed a different trend to the melanin results for the Innovatrics distributions, with an apparent increase in the median non-match score as the lightness of the skin increased. The only exception was the lowest light value bin, always having a higher or equal median value to the second lowest bin. Otherwise, for all graphs, an upward movement for both the interquartile range and median occurred, showing an issue with the matcher having a bias against higher lightness values. Only the contactless

VeriFinger distributions had any trends for lightness. The Gemalto and MorphoWave distributions slightly increased the median non-match score as the lightness of the skin increased.

## 5.6 Erythema and Red-Green Spectrum Analysis

For the Innovatrics erythema and red-green spectrum distributions, a trend towards a gradual decrease in the non-match score as erythema and red increased was present in all fingerprint sets except for the Gemalto fingerprint set. The trend is always very slight and is primarily seen in the median, while the interquartile adjusts differently. An explanation for the occurrence could be an under-sampling similar to melanin, where the dataset does not have enough low erythema and red samples since most erythema and red samples are above ten. In contrast, only a few Caucasians have any erythema samples below 7.74. with the same seen for the red-green spectrum, with only Caucasians having the lowest value at 6.55. Most self-reported ethnicities have erythema and red-green spectrum samples in the upper two bins. Only Pacific Islanders and Native Americans did not have high erythema samples available. The same is seen for red values, though with the inclusion of Indians, with the highest red value being 18.26.

For VeriFinger Distributions, trends are seen in the contact, contactless, and Sciometrics distributions. The same trend occurs in both the erythema and red value. Showing a decrease in the median as the erythema or red values increases, though not seeing any trends in the Veridium distributions similar to the Sciometrics distributions, does raise a question about the differences between the two applications do not show the same trends. Even the contact distributions showed better performance for higher erythema and red value. However, the slight trends occur mainly in the median value and not the interquartile range. A possible explanation could be the lower performance for the Veridium experiments masking trends due to noisy results similar to the

Bozorth3 erythema distributions showing no trends. The contact distributions show a decrease in the median as the erythema or red values increase. However, there is little change to the interquartile range suggesting the distribution of the non-match scores has not changed.

## 5.7 Blue-Yellow Spectrum Analysis

The blue-yellow spectrum results through all of the Innovatrics graphs and the Contactless and Sciometrics VeriFinger graphs showed the highest and lowest value bins with higher median values than the center three bins VeriFinger Veridium graphs showed the highest bin with a higher median value. For all the graphs, the center three bins all performed about the same, with only the fourth bin with a value range of 15-17.99 performing lower for some experiments with no visible pattern of occurrence. The demographic range for the blue value spectrum was heavily concentrated towards the center range of the graph. The lowest value seen was in Caucasians, with a value of 1.62, while the second lowest ethnicity jumps to 8.61 for Middle Eastern. The highest bin is closely tied between Caucasian and Middle Eastern, with the values 20.92 and 21.03, respectively. However, the next highest ethnicity was Indian, with a value of 17.28. Based on the behavior of the center three bins and that both ends are likely underrepresented, leading to lower performance, there is most likely no bias occurring that can be seen in the blue-yellow spectrum.

## 5.8 Bozorth3

The Bozorth3 demographic distributions showed inconsistent trends for melanin, with even the different Crossmatch Guardian fingerprint sets having different distributions even though they use the same optical sensor. With the poor performance for each cellphone experiment, the distributions appear only noisy, with only the high and low bins showing any consistent

deviation. Some of the erythema distributions show a gradual decrease in non-match score as erythema increases, as seen in the Kojak Roll distribution, though otherwise, the distributions are steady and show no deviations other than what could be reasoned as noise from the poor match performance, especially when viewing the cellphone distributions.

## 5.9 Concluding Thoughts

Based on the results, the general performance of contactless fingerprints shows very high interoperability for the MorphoWave. In the case of the Cogent Gemalto, the performance is close but lower than the contact fingerprint experiments. The interoperability of cellphone fingerprint applications has room for improvement, with minor improvements in camera quality between the S20 and S21 having noticeable match performance improvements for lower-performing matching experiments. However, the higher-performing matching experiments had slight improvement. Most of the interoperability improvement is based on the fingerphoto ridge extraction performed by the application and any other finger quality assurance systems in place.

The demographic analysis showed no trend toward higher or lower melanin being favored. Only the middle melanin range showed better results for the Innovatrics experiments, suggesting a possible bias for specific melanin ranges. Though the lightness distributions showed otherwise, with a gradual decrease in performance as the light value increased, the matcher is most likely having issues detecting minutia points on increasingly light fingerprints. The VeriFinger showed no evidence of bias across the different fingerprint sets. The Guardian and Kojak Roll fingerprint distributions did show varying median non-match scores for melanin. However, the discrepancy is most likely a scaling issue with the data since the Guardian and Kojak Roll distributions have a slight variance in the interquartile range. The Guardian Slap distribution had two bins with a

drastically different appearances. The lowest melanin bin and the fifth bin had drastically different interquartile ranges. However, the median was similar, if only a bit higher than expected, and the same is seen in the second bin in the erythema distribution. As discussed earlier in the melanin analysis, the VeriFinger software will fail to enroll fingerprints that do not meet specific criteria. The software could be disproportionately disqualifying fingerprints of these specific melanin ranges. Only the baseline shows the discrepancy because the performance was the best overall with an AUC of 0.98525 vs. the next highest AUC being the Guardian Roll with 0.97987. So while VeriFinger's matching system does not show any bias, there could be issues with the enrolling system removing specific demographic ranges for melanin and erythema.

The Innovatrics and most of the VeriFinger distributions for erythema and red-green spectrum showed a gradual trend of better performance as they increased. However, most samples are in the middle to upper range, making an existing bias possible but less likely than the melanin bias. The VeriFinger Veridium distributions showed no trends for erythema and red-green spectrum. However, that could be due to the low performance since the Bozorth3 distributions showed little to no trends for melanin and erythema. The results for all Bozorth3 experiments were abysmally low, nullifying the purpose of observing the 99th percentile non-match scores. The blue-green results show no evidence of bias for both Innovatrics and VeriFinger since the center three bins were consistent for all graphs, even when the edges of the range showed slightly worse performance.



## 5.10 Future Work

Additional efforts into scrutinizing different fingerprinting technology must always be made with both continued usage and the introduction of new technologies. Exhaustive analysis of each different fingerprint set matched against each other fingerprint set to show the interoperability loss between contact and each technology rather than only the interoperability between contact fingerprints and other types to show potential tradeoffs in match performance. For example, if a matching experiment were conducted using the MorphoWave as the gallery and the Cogent Gemalto as the probes, the change in match performance between the Kojak Slap as the gallery and MorphoWave would show the opportunity cost of maintaining legacy contact fingerprint databases. Additionally, demographic analyses that were not covered in the thesis could be made, such as fused analysis of multiple skin reflectance measures or a gray level analysis comparing match performance to the amount of gray in a fingerprint. A higher quantity of gray could obscure ridges when the fingerprint is binarized for matching. The impact of finger size on match performance could also be looked into, and the correlation between finger size and gender could be explored. While reviewing different available demographics, some trends were visible in performance correlated with gender, so an additional review to see if specifically finger size could be affecting performance at all or if other factors could be at play.

# References

- [1] J. G. Barnes, "The Fingerprint Sourcebook Chapter 1," National Institute of Justice, Washington, 2011.
- [2] Federal Bureau of Investigation Criminal Justice Information Services Division, "ELECTRONIC BIOMETRIC TRANSMISSION (EBTS) Version 11.0," Federal Bureau of Investigation Criminal Justice Information Services Division, Clarksburg, 2021.
- [3] J. Libert, J. Grantham, B. Bandini, S. Wood, M. Garris, K. Ko, F. Byers and C. Watson, "Guidance for Evaluating Contactless," National Institute of Standards and Technology, Gaithersburg, 2018.
- [4] D. Söllinger and A. Uhl, "Optimizing contactless to contact-based fingerprint comparison using simple parametric warping models," in *2021 IEEE International Joint Conference on Biometrics*, Shenzhen, China, 2021.
- [5] S. Grosz, J. Engelsma, E. Liu and A. Jain, "C2CL: Contact to Contactless Fingerprint Matching," *IEEE Transactions on Information Forensics and Security*, vol. 17, pp. 196 - 210, 2021.
- [6] H. Tan and A. Kumar, "Minutiae Attention Network With Reciprocal Distance Loss for Contactless to Contact-Based Fingerprint Identification," *IEEE Transactions on Information Forensics and Security*, vol. 16, pp. 3299 - 3311, 2021.
- [7] C. Lin and A. Kumar, "A CNN-Based Framework for Comparison of Contactless to Contact-Based Fingerprints," *IEEE Transactions on Information Forensics and Security*, vol. 14, no. 3, pp. 662 - 676, 2019.
- [8] J. Libert, J. Grantham, B. Bandini, K. Ko, S. Orandi and C. Watson, "Interoperability Assessment 2019: Contactless-to-Contact Fingerprint Capture," National Institute of Standards and Technology, Gaithersburg, 2020.
- [9] M. O. O. B. C. B. A. F. G. F. O. H. J. M. T. R. C. S. M. S. Elham Tabassi, "NIST Fingerprint Image Quality 2," 13 07 2021. [Online]. Available: <https://www.nist.gov/publications/nist-fingerprint-image-quality-2>. [Accessed 08 03 2023].
- [10] D. Molina, L. Causa and J. Tapia, "Reduction of Bias for Gender and Ethnicity from Face Images using Automated Skin Tone Classification," in *2020 International Conference of the Biometrics Special Interest Group (BIOSIG)*, Darmstadt, Germany, 2020.

- [11] J. Howard, Y. Sirotin, J. Tipton and A. Vemury, "Reliability and Validity of Image-Based and Self-Reported Skin Phenotype Metrics," *IEEE Transactions on Biometrics, Behavior, and Identity Science*, vol. 3, no. 4, pp. 550 - 560, 2021.
- [12] C. Cook, J. Howard, Y. Sirotin, J. Tipton and A. Vemury, "Demographic Effects in Facial Recognition and Their Dependence on Image Acquisition: An Evaluation of Eleven Commercial Systems," *IEEE Transactions on Biometrics, Behavior, and Identity Science*, vol. 1, no. 1, pp. 32 - 41, 2019.
- [13] J. Howard, Y. Sirotin and A. Vemury, "The Effect of Broad and Specific Demographic Homogeneity on the Imposter Distributions and False Match Rates in Face Recognition Algorithm Performance," in *2019 IEEE 10th International Conference on Biometrics Theory, Applications and Systems*, Tampa, FL, 2019.
- [14] K. S. Krishnapriya, V. Albiero, K. Vangara, M. C. King and K. W. Bowyer, "Issues Related to Face Recognition Accuracy Varying Based on Race and Skin Tone," *IEEE Transactions on Technology and Society*, vol. 1, no. 1, pp. 8 - 20, 2020.
- [15] S. Gong, X. Liu and A. Jain, "Mitigating Face Recognition Bias via Group Adaptive Classifier," in *2021 IEEE/CVF Conference on Computer Vision and Pattern Recognition (CVPR)*, Nashville, TN, USA, 2021.
- [16] R. Hancock and S. Elliott, "Evidence of correlation between fingerprint quality and skin attributes," in *2016 IEEE International Carnahan Conference on Security Technology (ICCST)*, Orlando, FL, USA, 2016.
- [17] L. Lugini, E. Marasco, B. Cukic and J. Dawson, "Removing gender signature from fingerprints," in *2014 37th International Convention on Information and Communication Technology, Electronics and Microelectronics (MIPRO)*, Opatija, Croatia, 2014.
- [18] B. Williams, J. McCauley, J. Dando, N. Nasrabadi and J. Dawson, "Interoperability of Contact and Contactless Fingerprints Across Multiple Fingerprint Sensors," in *2021 International Conference of the Biometrics Special Interest Group (BIOSIG)*, Darmstadt, Germany, 2021.
- [19] A. Godbole, S. Grosz, K. Nandakumar and A. Jain, "On Demographic Bias in Fingerprint Recognition," 19 May 2022. [Online]. Available: <https://arxiv.org/abs/2205.09318>. [Accessed 30 June 2022].
- [20] M. Emanuela, H. Mengling, T. Larry and T. Yuanting, "Demographic Effects in Latent Fingerprint Matching and their Relation to Image Quality," in *2022 7th International Conference on Machine Learning Technologies*, New York, 2022.
- [21] S. Yoon and A. K. Jain, "Longitudinal study of fingerprint recognition," *Proceedings of the National Academy of Sciences*, vol. 112, no. 28, p. 8555–8560, 2015.

- [22] Integrated Biometrics, "LES Film Technology: Fingerprint Sensor Descriptions and Alternative Fingerprint Technologies," Integrated Biometrics, Spartanburg, n.d..
- [23] Integrated Biometrics, "LES Optical Direct Imaging Sensors: A Smarter Alternative to Prism-Based Scanners," Integrated Biometrics, Spartanburg, 2017.
- [24] D. L. L. H. G. D. Laurence G. Hassebrook, "System and method for 3d imaging using structured light illumination". International Patent WO2007050776A2, 25 10 2006.
- [25] F. Chen, "3D Fingerprint and palm print data model and capture devices using multi structured lights and cameras". United States of America Patent US20060120576A1, 05 11 2005.
- [26] D. M. ., A. K. J. ., S. P. Davide Maltoni, Handbook of Fingerprint Recognition, London : Springer, 2009.
- [27] G. V. T. V. G. I. Keith Antonelli, "Fingerprint image optical input apparatus". US Patent US6259108B1, 09 10 1998.
- [28] S. a. P. A. a. M. J. Mehta, "CCD or CMOS Image sensor for photography," in *2015 International Conference on Communications and Signal Processing (ICCSP)*, Melmaruvathur, 2015.
- [29] K. G. H. Q. H. S. M. M. G. C. A. N. Gil Abramovich, "Method and system for contactless fingerprint detection and verification". United States of America Patent US8406487B2, 27 01 2010.
- [30] P. Favaro, "Depth from focus/defocus," 25 06 2002. [Online]. Available: [https://homepages.inf.ed.ac.uk/rbf/CVonline/LOCAL\\_COPIES/FAVARO1/dfdtutorial.html](https://homepages.inf.ed.ac.uk/rbf/CVonline/LOCAL_COPIES/FAVARO1/dfdtutorial.html). [Accessed 08 03 2023].
- [31] A. Sharma, "Fingerprint matching Using Minutiae Extraction Techniques," *Journal of Advances in Electrical Devices*, vol. 2, no. 1, pp. 1-20, 2016.
- [32] M. Y. A. S. M. A. S. Mahdi Jampour, "A new fast technique for fingerprint identification with fractal and chaos game theory," *Fractals-complex Geometry Patterns and Scaling in Nature and Society*, vol. 18, 2010.
- [33] S. S. J. S. Arun Ross, "Image versus feature mosaicing: A case study in fingerprints," in *SPIE - The International Society for Optical Engineering*, Bellingham, 2006.
- [34] J. T. X. Y. Xinjian Chen, "A new algorithm for distorted fingerprints matching based on normalized fuzzy similarity measure," *IEEE transactions on image processing: a publication of the IEEE Signal Processing Society*, vol. 15, pp. 767-776, 2006.

- [35] R. K. B. V. K. R. J. Ravi, "Fingerprint Recognition Using Minutia Score Matching," *International Journal of Engineering Science and Technology*, vol. 1, pp. 35-42, 2010.
- [36] J. F. K. N. Anil K. Jain, "FINGERPRINT," *COMPUTER*, vol. 44, no. 2, pp. 36-44, 2010.
- [37] M. D. G. E. T. C. L. W. R. M. M. S. J. K. K. Craig I. Watson, "User's Guide to Export Controlled Distribution of NIST Biometric Image Software (NBIS-EC)," [Online]. Available: <https://nvlpubs.nist.gov/nistpubs/Legacy/IR/nistir7391.pdf>. [Accessed 10 03 2023].
- [38] M. M. ARAT, "How to plot ROC curve and compute AUC by hand," Mustafa Murat ARAT, 01 10 2019. [Online]. Available: <https://mmuratarat.github.io/2019-10-01/how-to-compute-AUC-plot-ROC-by-hand>. [Accessed 08 03 2023].
- [39] T. G. Tape, "The Area Under an ROC Curve," University of Nebraska Medical Center, [Online]. Available: <https://darwin.unmc.edu/dxtests/roc3.htm>. [Accessed 08 03 2023].
- [40] T. G. Tape, "Plotting and Intrepretating an ROC Curve," University of Nebraska Medical Center, [Online]. Available: <https://darwin.unmc.edu/dxtests/roc2.htm>. [Accessed 08 03 2023].
- [41] M. E. S. Andy Adler, "Calculation of a Composite DET Curve," [Online]. Available: <https://citeseerx.ist.psu.edu/document?repid=rep1&type=pdf&doi=c7b16e46179f17802d436aef2ccfa5ebd8a2d495>. [Accessed 08 03 2023].
- [42] G. D. M. O. M. P. A. Martin, "THE DET CURVE IN ASSESSMENT OF DETECTION TASK PERFORMANCE," 17 09 2008. [Online]. Available: <https://ccc.inaoep.mx/~villasen/bib/martin97det.pdf>. [Accessed 08 03 2023].
- [43] "Equal Error Rate (EER)," Innovatrics, [Online]. Available: [https://www.innovatrics.com/glossary/equal-error-rate-eer/#:~:text=Equal%20Error%20Rate%20\(EER\)%20definition&text=The%20EER%20is%20the%20location,accuracy%20of%20the%20biometric%20system..](https://www.innovatrics.com/glossary/equal-error-rate-eer/#:~:text=Equal%20Error%20Rate%20(EER)%20definition&text=The%20EER%20is%20the%20location,accuracy%20of%20the%20biometric%20system..) [Accessed 08 03 2023].
- [44] A. R. S. P. Anil K. Jain, "An introduction to biometric recognition," *IEEE Transactions on Circuits and Systems for Video Technology*, vol. 14, no. 1, pp. 4-20, 2004.
- [45] Sappi, "Defining and Communicating Color: The CIELAB System," 2013. [Online]. Available: <https://cdn-s3.sappi.com/s3fs-public/sappietc/Defining%20and%20Communicating%20Color.pdf#:~:text=Published%20in%201976%20by%20the,making%20and%20graphic%20arts%20industries..> [Accessed 08 03 2023].

- [46] The National Center for Biotechnology Information, "Biochemistry, Melanin," U.S. National Library of Medicine, [Online]. Available: <https://www.ncbi.nlm.nih.gov/books/NBK459156/>. [Accessed 22 03 2023].
- [47] The National Center for Biotechnology Information, "Erythema," U.S. National Library of Medicine, [Online]. Available: <https://www.ncbi.nlm.nih.gov/medgen/11999>. [Accessed 22 03 2023].
- [48] Neurotechnology, "CROSS MATCH GUARDIAN USB / FW FAMILY," Neurotechnology, [Online]. Available: <https://www.neurotechnology.com/fingerprint-scanner-cross-match-l-scan-guardian.html>. [Accessed 20 June 2022].
- [49] Integrated Biometrics, "KOJAK SMALL. FLEXIBLE. EFFICIENT," Integrated Biometrics, [Online]. Available: <https://integratedbiometrics.com/products/fbi-certified-fingerprint-scanners/kojak>. [Accessed 20 June 2022].
- [50] Idemia, "MorphoWave™ Desktop Take a Step Beyond Touch User Guide Version 1.3," Idemia, 2017.
- [51] Cortex Technology, "SKIN ANALYSIS — SKIN COLORMETER," Cortex Technology, 2022. [Online]. Available: <https://cortex.dk/skin-color-meter-dsm-iii/>. [Accessed 25 June 2022].
- [52] P. Ganesan, V. Rajini and R. Rajkumar, "Segmentation and edge detection of color images using CIELAB color space and edge detectors," in *INTERACT-2010*, Chennai, 2010.
- [53] W. J. S. Kenneth Ko, "NIST Biometric Image Software (NBIS)," National Institute of Standards and Technology (NIST), 10 02 2010. [Online]. Available: <https://www.nist.gov/services-resources/software/nist-biometric-image-software-nbis>. [Accessed 09 03 2023].
- [54] L. C. L. B. Saleh Mosaddegh, "Digital (or touch-less) fingerprint lifting using structured light," in *Computer Vision and Pattern Recognition*, Boston, 2015.
- [55] O. K. M. D. Jan Svoboda, "Biometric recognition of people by 3D hand geometry," in *The International Conference on Digital Technologies 2013*, Zilina, 2013.
- [56] A. G. V. P. F. S. Ruggero Donida Labati, "Fast 3-D fingertip reconstruction using a single two-view structured light acquisition," in *2011 IEEE Workshop on Biometric Measurements and Systems for Security and Medical Applications (BIOMS)*, Milan, 2011.